TID
[illegible]
SEP 13 1971

~~SECRET~~
~~SECURITY INFORMATION~~

AEC RESEARCH AND DEVELOPMENT REPORT

ORNL
MASTER COPY

ORNL 1592
Special

DECLASSIFIED
Classification changed to:
By authority of: [illegible] – Doc.
By: M. Day 11-4-73 [illegible]

LABORATORY RECORDS
1954

INV 70

CHEMICAL METHODS FOR THE SEPARATION OF LITHIUM ISOTOPES

V. D. Allred
Ivan B. Cutler

INV.
53

CLASSIFICATION CANCELLED
DATE JUL 12 1979 (DOE Review Order)

DECLASSIFICATION OFFICER
OAK RIDGE NATIONAL LABORATORY
AUTHORITY DELEGATED BY ERDA 8-15-77

OAK RIDGE NATIONAL LABORATORY
OPERATED BY
CARBIDE AND CARBON CHEMICALS COMPANY
A DIVISION OF UNION CARBIDE AND CARBON CORPORATION
UCC
POST OFFICE BOX P
OAK RIDGE, TENNESSEE

~~RESTRICTED DATA~~
This document contains Restricted Data as defined in the Atomic Energy Act of 1946. Its transmittal or the disclosure of its contents in any manner to an unauthorized person is prohibited.

~~SECRET~~
~~SECURITY INFORMATION~~

[redacted]

ACCESS LIMITED TO
AUTHORIZED PERSONNEL

ORNL- 1592
Special

This document consists
of 176 pages. Copy 68
of 77 copies. Series A.

ALLOY DEVELOPMENT PROJECT

CHEMICAL METHODS FOR THE SEPARATION OF LITHIUM ISOTOPES

V. Dean Allred and Ivan B. Cutler
(of the Catalytic Construction Company assisting
the Oak Ridge National Laboratory under the
terms of AEC Contract AT (40-1) 1520)

MATERIALS CHEMISTRY DIVISION

G. H. Clewett, Director

July 10, 1953

Date Issued

AUG 18 1953

OAK RIDGE NATIONAL LABORATORY
Operated by
CARBIDE AND CARBON CHEMICALS COMPANY
A DIVISION OF UNION CARBIDE AND CARBON CORPORATION
Oak Ridge, Tennessee

Contract No. W-7405-eng-26

[redacted]

[redacted]

Internal Distribution

1. V. D. Allred
2. T. A. Arehart
3. M. D. Barringer
4. G. M. Begun
5. R. E. Blanco
6. E. G. Bohlmann
7. W. H. Brand
8. F. R. Bruce
9. W. L. Carter
10. C. E. Center
11. G. H. Clewett
12. F. L. Culler
13. W. DeLany
14. M. L. Drabkin
15. J. S. Drury
16. G. A. Eaton
17. W. K. Eister
18. L. B. Emlet
19. D. E. Ferguson
20. H. H. Garretson
21. H. E. Goeller
22. R. M. Healy
23. W. B. Humes
24. E. D. Innes
25. H. K. Jackson
26. A. C. Jealous
27. W. N. Johnson
28. K. O. Johnsson
29. C. P. Johnston
30. M. T. Kelley
31. H. T. Kite
32. B. B. Klima
33. W. B. Lanham
34. L. Landau
35. C. E. Larson
36. D. A. Lee
37. W. J. Lilley
38. R. B. Lindauer
39. A. C. Martinsen
40. H. M. McLeod
41. R. P. Milford
42. D. J. Oriolo
43. A. A. Palko
44. F. S. Patton
45. R. H. Powell
46. G. A. Ropp
47. A. D. Ryon
48. A. C. Rutenberg
49. J. Shacter
50. G. A. Strasser
51. J. W. Strohecker
52. E. H. Taylor
53. L. P. Twichell
54. W. E. Unger
55. A. M. Weinberg
56. H. O. Weeren
57. J. J. Williams
58. C. E. Winters
59. L. B. Yeatts

60-63. Y-12 Central Files
64-67. X-10 Central Files
68. ORNL-RC

External Distribution

69-70. R. W. Cook, c/o A. J. Vander Weyden, AEC, Washington
71. Brigadier General K. E. Fields, D.M.A., AEC, Washington
72. Jane Hall, L.A.S.L., Los Alamos
73. T. H. Johnson, AEC, Washington
74-75. K. Kasschau, AEC, Oak Ridge
76. J. H. Rushton, Illinois Institute of Technology, Chicago
77. W. W. Weinrich, Catalyti[redacted]
Philadelphia, Pa.

PREFACE

This report has been prepared by personnel of the Catalytic Construction Company (Philadelphia, Pa.) under technical supervision of the Oak Ridge National Laboratory for ADP development under the terms of AEC Contract AT-(40-1)-1520. Many members of the ORNL staff and Catalytic Construction Company personnel in Oak Ridge have made contributions and aided in making corrections to the preliminary draft. Special acknowledgement should be given to G. M. Begun, R. E. Blanco, G. H. Clewett, J. S. Drury, H. H. Garretson, K. O. Johnsson, and D. J. Oriolo for their assistance.

CONTENTS

PART ONE. PROCESS CHEMISTRY

PART TWO. CHEMICAL AND PHYSICAL DATA

III. MAGNESIUM AND MAGNESIUM COMPOUNDS

IV. POTASSIUM AND POTASSIUM COMPOUNDS

V. SODIUM AND SODIUM COMPOUNDS

VI. LIQUID SOLVENTS

FIGURES

~~**RESTRICTED DATA**~~

~~This document contains restricted data as defined in the Atomic Energy Act of 1946. Its transmittal or the disclosure of its contents in any manner to an unauthorized person is prohibited.~~

INTRODUCTION

By the first part of 1953, the program for the separation of lithium isotopes by chemical methods had expanded and matured to such a point that it was believed an interim report condensing the chemistry under one cover would be advantageous. Consequently, under the direction of the project director, G. H. Clewett, the task of compiling this report was undertaken with the following original objectives:

(1) Organize all chemical and physical data under one cover.

(2) Make data readily available with logical presentation, visual representation, and cross indexing.

(3) Evaluate data to give clear understanding and stimulate research activity.

Although these objectives were not attained in their entirety, they guided the assembly of this material.

This report is divided into two parts. The first part is an evaluation of the data pointed toward an understanding of some of the current problems. It is expected that this section will rapidly become out of date as a better understanding of underlying principles is obtained. The second part contains physical and chemical data that should be of more lasting value to those who continue development of separation processes for lithium isotopes. The data presented are largely those available from classified information available as weekly, biweekly, monthly, quarterly, etc., reports from the divisions of the Oak Ridge National Laboratory. In addition, several excellent topical reports and handbooks issued by this laboratory have been drawn upon heavily.

The ideas and methods utilized in the correlation and evaluation of the data are not original with the authors. The ideas of many of the chemists and engineers associated with the project have been used freely. Special acknowledgement should be given to the chemists in the Materials Chemistry and Chemical Technology Divisions.

To the uninitiated, it may be well to illustrate briefly the main features of a chemical system for the separation of isotopes employing chemical reflux. It may be seen in Figure 1 that the heart of the process is an isotopic exchange and enrichment section which in most instances is a column in which lithium amalgam flows countercurrent to a lithium salt dissolved in a suitable solvent. Next in importance are two reflux sections which remove the lithium from the phase flowing from the column and insert it into the phase flowing to the column. A certain number of auxiliary processes, of course, are necessary for continuous operation. The product in the separation of lithium isotopes is enriched in lithium six (Li^6) and the waste is enriched in lithium seven (Li^7).

Experimental data from all of the systems investigated for the chemical separation of lithium isotope have shown the separation factor to be a marked function of temperature. For this reason it is possible to consider a unique method of achieving reflux known as the dual temperature process. A simplified sketch of a dual temperature system for the separation of lithium isotopes is presented in Figure 2. This process has maximum utility when it is possible to operate an exchange system between two widely separated temperatures. The theory of the dual temperature process is not given in this report but may be found in the work of Spivack (114), Eidinoff (115), and Demarcus (116).

FIGURE 1

~~SECRET~~
~~DWG. 20289~~

SIMPLIFIED CHEMICAL REFLUX SYSTEM FOR LITHIUM ISOTOPIC OPERATIONS

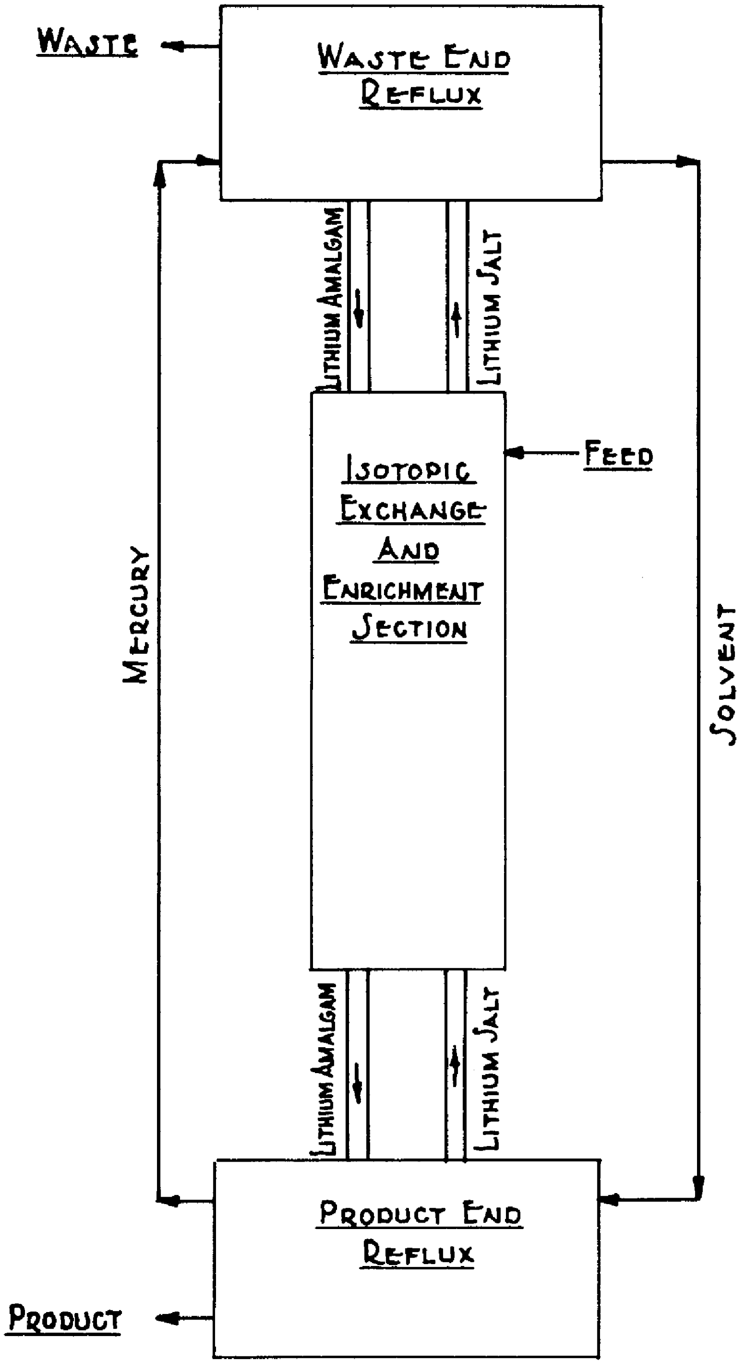

FIGURE 2

~~SECRET~~
~~DWG. 20290~~

SIMPLIFIED DUAL TEMPERATURE PROCESS FOR LITHIUM ISOTOPE SEPARATION

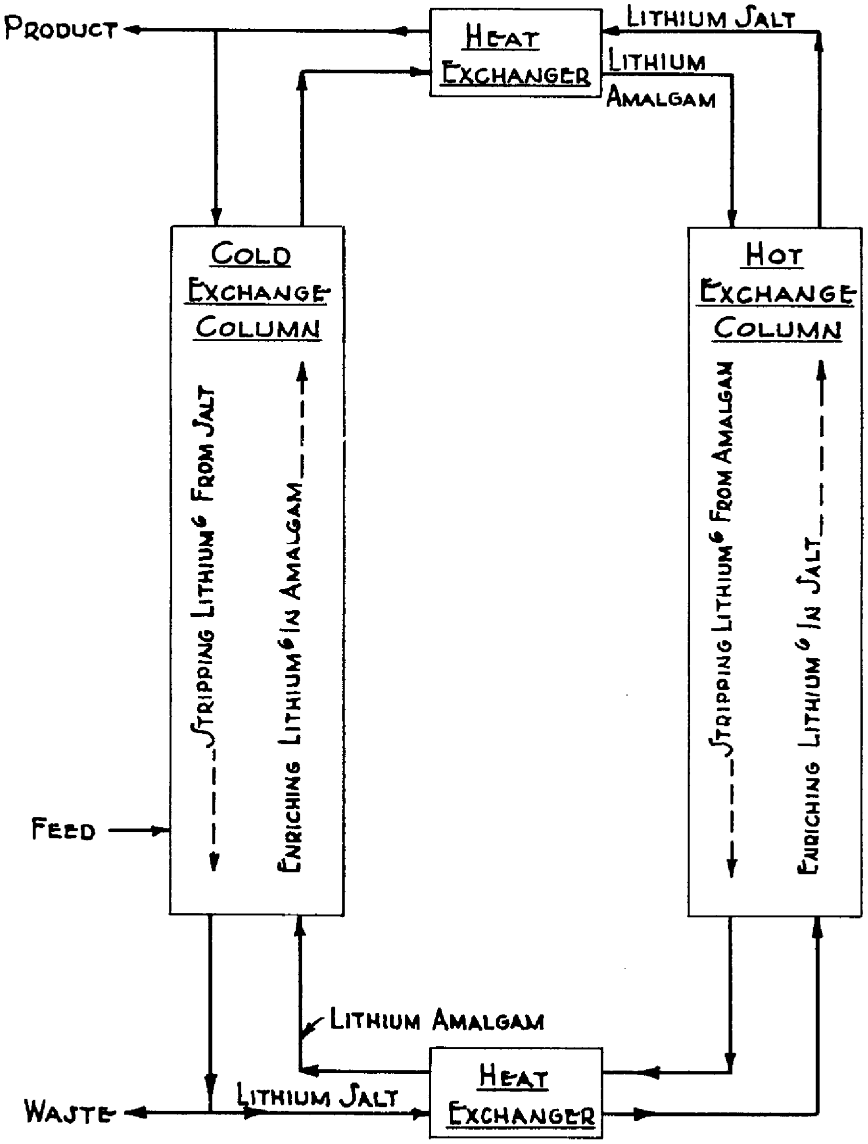

PART ONE

PROCESS CHEMISTRY

I: CHEMICAL EQUILIBRIUM METHODS

A. INTRODUCTION

Theoretically, the energy requirements for the separation of isotopes of the same element need not be any larger than that needed to overcome the entropy of mixing of the isotopes provided a thermodynamically reversible system is employed. In addition to being slow at times, thermodynamically reversible processes are difficult to obtain; however, it is desirable from an economic point of view to approach these ideal conditions within engineering limits. Processes carried out at chemical equilibrium offer this opportunity.

The separation of isotopes by chemical equilibrium methods is possible with two phase systems such as a gas and a liquid, two immiscible liquids, a liquid and a solid, or a gas and a solid. Since compounds of lithium which remain gaseous at room temperature are unknown, the separation of lithium isotopes by chemical methods has been limited to liquid-liquid and liquid-solid systems. At present, all of the systems which have plant production feasibility are liquid-liquid systems in which one of the liquids is lithium amalgam. If lithium isotopic separation could be extended to a gaseous-liquid system by discovery of a volatile lithium compound, perhaps some improvements over present systems could be realized.

Separation of lithium isotopes in a system of lithium amalgam in contact with lithium chloride dissolved in ethyl alcohol was described by Lewis and MacDonald (110) in 1936. This important contribution indicated that isotopic exchange took place with astonishing rapidity, that the separation factor (α) per stage was at least 1.025, and that the heavier isotope was found preferentially in the alcohol phase indicating that chemical bonding of lithium in the solvent was stronger than it was in the amalgam.

The separation factor, α, may be defined by the equation

$$\alpha = \frac{(\mathrm{Li}^6/\mathrm{Li}^7) \text{ - amalgam}}{(\mathrm{Li}^6/\mathrm{Li}^7) \text{ - light phase}}$$

where the ratios shown are atomic ratios.

Systems involving lithium amalgam in contact with lithium hydroxide in aqueous solution have been reported in the literature (111) but confusion as to whether the separation factors were due to equilibrium or to kinetic effects developed because potentials were applied to these systems to prevent lithium depletion through decomposition of the amalgams. The isotopic separation systems for lithium under current investigation may be classified according to the stability of lithium amalgam in contact with an organic or aqueous solution. Reactive solvents such as water and various alcohols decompose lithium amalgam to form lithium hydroxide or lithium alcoholate and hydrogen gas. These solvents depend on a slow rate of amalgam decomposition for their usefulness. Much more research and development has been applied to aqueous solution of lithium hydroxide in contact with lithium amalgam than any other reactive system. Stable solvent systems employ lithium chloride dissolved in amines or unreactive ethers in contact with lithium amalgam. In this latter class of solvents, propylenediamine (1,2, diamine propane) has received the most attention.

B. EXCHANGE EQUILIBRIA

The reasons for expecting separation factors for systems at chemical equilibrium aredue to the difference in chemical properties of isotopes of the same element. These differences are accentuated with isotopes of elements of low atomic weight; consequently, chemical methods of separation have proved to be the most efficient methods available for separating isotopes of hydrogen, nitrogen, carbon, boron, etc.

One method of representing the chemical separation of lithium isotopes is illustrated in Figure 3. The heavier isotope is found preferentially in the organic or water phase indicating that the chemical stability of the lithium in this phase is higher than the stability of the lithium in the amalgam phase. Since chemical stability is associated with low free energy content, lithium in the propylenediamine phase, for example, is at a lower free energy level than lithium in the amalgam phase. For the energy changes indicated in Figure 3, we have

$$Li^7 \text{ (amalgam)} \longrightarrow (Li^7)^+ \text{ (PDA)} + e, \Delta F^o = -A \qquad (1)$$

$$Li^6 \text{ (amalgam)} \longrightarrow (Li^6)^+ \text{ (PDA)} + e, \Delta F^o = -B \qquad (2)$$

where $|A|$ is larger than $|B|$, but $-A$ is smaller than $-B$. Subtracting equation (2) from (1),

$$Li^7 \text{ (amalgam)} + (Li^6)^+ \text{ (PDA)} \longrightarrow Li^6 \text{(amalgam)} + (Li^7)^+ \text{ (PDA)} \qquad (3)$$

$$\Delta F^o = -A + B = -C \qquad (4)$$

Since our illustration is greatly exaggerated, $-C$ does not represent a very large free energy change ($\Delta F^o \cong - 31$ cal. at 25°C for the system in question).

The separation factor (α) and equilibrium constant for equation (3) are identical since α is defined as the Li^6/Li^7 ratio in the amalgam phase divided by the Li^6/Li^7 ratio is the amine phase. The dependence of α on temperature may be given by the equations

$$\log_e \alpha = \frac{-\Delta F^o}{RT} = \frac{\Delta H^o}{RT} + \frac{\Delta S^o}{R} \qquad (5)$$

and

$$\alpha - 1 \cong -\frac{\Delta H^o}{RT} + \frac{\Delta S^o}{R} \qquad (6)$$

where ΔH^o and ΔS^o are assumed to be independent of temperature over small temperature changes. The binomial approximation that $\alpha - 1$ is equal to $\log_e \alpha$ contains an error of less than 3% up to $\alpha = 1.06$. The assumption that ΔH^o and ΔS^o are independent of temperature over the range of temperature in which isotopic separation factors have been measured (0 - 100°C) appears to be as accurate as the analytical methods available for the determination of isotopic abundance. Other ideas concerning the dependence of separation factors on temperature have been given by Begun, Drury and Palko (111).

The temperature dependence of the separation factor for three systems having approximately the same degree of chemical stability is shown in Figure 4. The agreement with theory is within the accuracy of the data. Furthermore, it

FIGURE 3

[redacted]

ENERGIES OF LITHIUM ISOTOPES

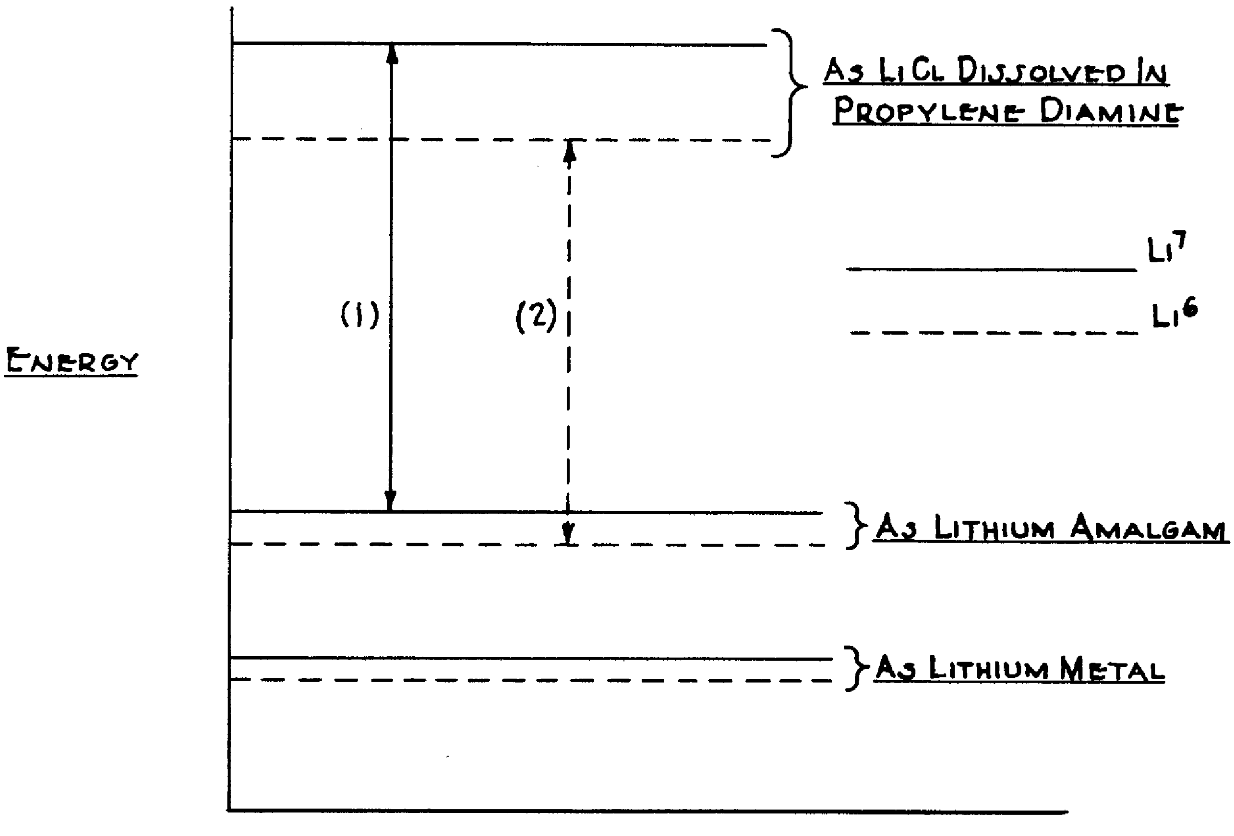

[redacted] 20292

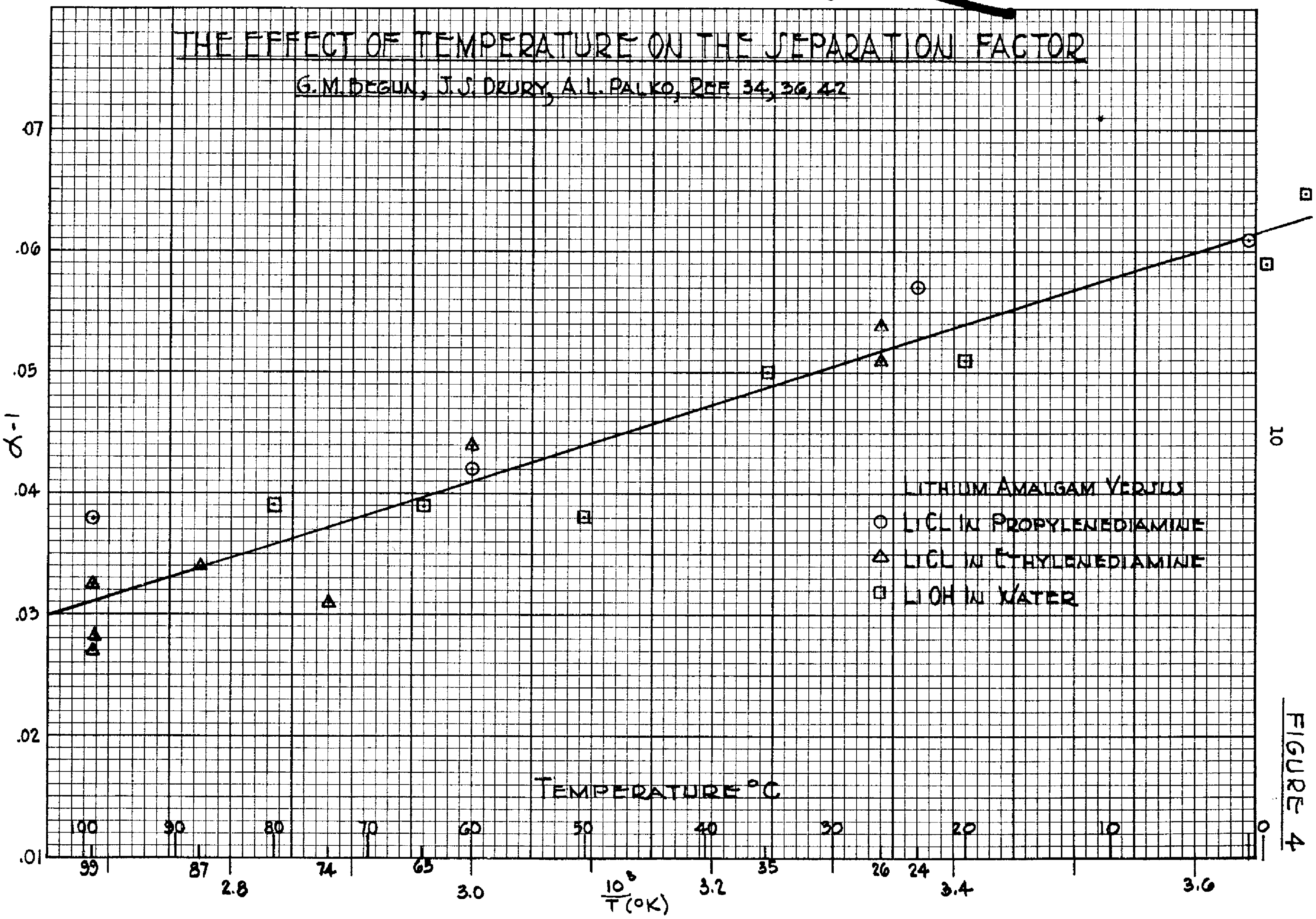

FIGURE 4

should be noted that one of the systems investigated was an aqueous solution of lithium hydroxide in contact with amalgam in which a variable holding current was necessary, yet the agreement with the other systems indicates the rate of electrolysis and decomposition has little or no effect on the separation factor.

Not all solvents for lithium salts in contact with lithium amalgams yield similar results to those shown in Figure 4. Table 1 illustrates the results obtained with solvent of markedly different properties. Evidently, both the salt and the solvent determine the separation factor obtained in contact with lithium amalgam. This is explainable on the basis that different solvents have varying affinities for lithium ions and that different salts dissociate in varying degrees to produce lithium ions.

Table 1

Separation Factors* for Solvent Systems in Contact with Lithium Amalgam**

Salt	Solvent		
	Dimethyl-cellosolve	Tetra-hydrofuran	Propylene diamine
Lithium chloride	1.023 ± 0.013	1.036 ± 0.006	1.057 ± 0.021
Lithium benzophenone	1.056 ± 0.008	1.045 ± 0.008	1.055 ± 0.016
Lithium benzophenone anil	1.037 ± 0.008	1.046 ± 0.012	1.047 ± 0.012

---

* Precision given for 95% confidence interval.

** Data by G. M. Begun, ref. 40.

In a liquid-liquid method for chemical separation of lithium isotopes, one of the difficulties encountered in the development of economical systems is the limited number of solvents for lithium salts and lithium metal that are available. Three factors limit the selection of an organic solvent; limited solubility of lithium salts, rapid reactivity of some solvents toward lithium amalgam, and emulsifying characteristics of some organic solvents toward lithium amalgam. The emulsification of amalgams has received very little attention. Probably very few of the amalgam "emulsions" described as such are true emulsions, but appear to be insoluble reaction products containing chemically bonded or physically adsorbed mercury.

Solvents for ionic salts as a rule have large dielectric constants which are a measure of their ion separating and isolating power. Other effects, however, appear to be more important in the case of lithium chloride solubility. Ethylenediamine which has a rather low dielectric constant of 12.9 compared to 81.7 for water shows low solubility for sodium and potassium chlorides, but high solubility for lithium chloride. It is expected that propylenediamine would have an even lower dielectric constant for it shows only one-tenth the solubility for sodium and potassium chloride, yet lithium chloride is four times as soluble in propylenediamine than in ethylenediamine.

The logical conclusion to these results is that a specific interaction exists between lithium and some solvents. At least part, if not all, of this specific interaction effect is the result of the coordination demanded by lithium ion. With a coordination number of four, two ethylenediamine or two propylenediamine molecules could be tightly bound to a lithium ion. Because of steric effects due to the methyl group, propylenediamine probably has a greater chance of accomplishing the desired coordination.

The cyclic ether series gives even stronger indication of this coordinating effect. Six membered rings are apparently too large and any additional groups on a five membered ring (tetrahydrofuran) also presents a molecule too large for four-coordination. Tetrahydrofuran itself is the borderline size for four-coordination as indicated by the inverse solubility of lithium chloride with temperature. Table 2 illustrates these conclusions.

Table 2

Specific Interaction Effects of Selected Solvents I

Solvent	Dielectric Constant	Solubility in moles/liter at 25°C					
		LiCl		NaCl		KCl	
Ethylenediamine	12.9 (25°C) (17)	0.27	(48)	0.045	(11)	0.0017	(11)
Propylenediamine	12.9	1.0	(47)	0.0048	(60)	0.0001	(43)
Water	81.7 (18°C) (17)	14.0	(56)	5.43	(4)	4.13	(4)

Specific Interaction Effects of Selected Solvents II

(105)

Solvent	Structure	Solubility of LiCl (moles/liter at 25°C)
Propylene oxide	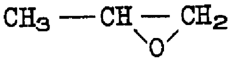	0.22
Trimethylene oxide	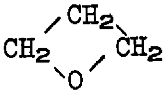	6.0
Tetrahydrofuran	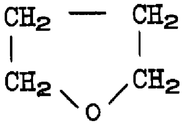	0.78
2-Methyltetrahydrofuran	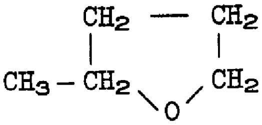	0.07
Tetrahydropyran	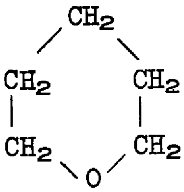	0.08

Mercury as a solvent for lithium metal has many advantages and disadvantages for a liquid-liquid system. Unfortunately, there are no alternate solvents for lithium metal that remain liquid down to room temperature that have been brought to the attention of the research groups.

C. EXCHANGE KINETICS

One property of alkali metal amalgams which deserves particular attention is their high surface activity since it may account, at least in part, for the rapid exchange of isotopes. The application of Gibbs adsorption thermodynamics to data obtained by Convers (26) and by Johnston and Ubbelohde (112) indicates adsorption (surface excess) of alkali metals at amalgam surfaces. Qualitatively, amalgams have been observed to disperse much more readily in propylenediamine than mercury indicating the amalgam interface has lower interfacial tension than the mercury interface. The lowering of surface or interfacial tension upon the addition of another component to a system is the result of adsorption of the added component at the interface.

The limitations of analytical techniques for isotopes and the extremely rapid exchange reaction (even at room temperature) have made the direct observation of reaction kinetics very difficult.

It is quite possible that with a rapid continuous method of isotopic analysis, such as the neutron adsorption technique, a system could be devised which would prove satisfactory for such an investigation.

Theoretical stage heights obtained from operation of isotopic exchange columns reflect the kinetics of the exchange reaction. If the reaction is diffusion controlled, the following factors appear to be important to the amalgam phase or solvent phase which ever is rate controlling: (1) agitation, (2) concentration, (3) viscosity, and (4) temperature. Of these factors, agitation is the most important since better agitation would produce larger interfacial areas as well as thinner diffusion films. If the adsorption of lithium of the amalgam interface produces a rigid film, the rate of formation of fresh surfaces may be a rate controlling step. Temperature has only a slight effect on diffusion controlled reactions.

If diffusion is not the rate controlling step in the isotopic exchange reaction, the following factors appear to be important: (1) interfacial area and (2) temperature. An increase in interfacial area or temperature should increase the rate of the reaction and decrease the stage height; however, these two factors are difficult to vary independent of each other in the system employing propylenediamine because interfacial tension increases with increased temperatures resulting in poorer dispersions and lower interfacial areas. If the rate of the exchange reaction shows first order dependence on the lithium concentration in the amalgam (similar to the waste end reaction), then the stage height should be independent of lithium concentration in the amalgam.

II: REFLUX PROCESSES

A. INTRODUCTION

A major consideration in large scale isotopic separation by equilibrium exchange is the reflux process. Refluxes may be achieved by either physical or chemical processes and many alternate schemes are possible.

No attempt will be made in this report to differentiate between reflux methods with regard to economics and with the exception of the dual temperature system discussion will be limited to chemical reflux processes. Further, only those schemes which appeared to have engineering adaptation to existing systems have been considered.

The degree and rate at which the inversion (refluxes) are attained are prime considerations in evaluating the reflux processes since the systems involved require recycling of solvents.

The degree of inversion or removal of enriched lithium from the amalgam phase (product reflux) is important in that this material not only represents a valuable product but also either its loss or its cycling to the waste end would greatly affect the cascade equilibrium. On the waste end the last traces of lithium must be removed prior to cycling the solvent stream to the product end for even small amounts of material are capable of reducing the enrichment to a point where the desired product could not be attained.

The rate at which the reflux processes proceed is equally important. It must be very rapid not only to yield the desired degree of inversion, but also to prevent a large holdup of material which would greatly influence the length of time required to reach isotopic steady state conditions.

B. THE DUAL TEMPERATURE PROCESS

The dual temperature process is applicable to any of chemical isotopic exchange system employing nonreactive substances and in which the separation factor is a function of temperature. It may be seen from Figure 4 that the separation factor in several lithium systems is a function of temperature.

The operability of the dual temperature process has been demonstrated by the Materials Chemistry Division (See ORNL reports 1238, 1306, 1401, YB 35-12, and ORNL CF 53-4-299). The extremely rapid isotopic exchange noted in the laboratory was confirmed by pilot plant data. Both ethylenediamine and propylenediamine were utilized as solvents for lithium chloride in contact with lithium amalgam. Propylenediamine appears to have the widest useful temperature range of from room temperature to 100°C; however, the stability of propylenediamine above 100°C in the presence of an alkali amalgam has not been well established.

A schematic representation of the dual temperature process is shown in Figure 2. Since the effective separation factor for a dual temperature system is dependent upon the difference between the factors in the hot and cold columns and is generally less than either one, many more stages are required for this method than for a chemical reflux system (to effect the same overall separation).

C. CHEMICAL REFLUX PROCESSES

Although chemical reflux schemes are classified in this report according to which end of the isotopic exchange system they are applicable, this is not entirely satisfactory since many of the waste end refluxes can be tied together into desirable overall processes. Two such processes are illustrated in Figure 5 to indicate how reflux at one end may supplement reflux at the other end.

1. Waste End Reflux

a. Electrolytic Reflux

Four reactions have been considered for the electrolysis of lithium salts to form lithium amalgam: aqueous electrolysis of lithium hydroxide with a mercury cathode, aqueous electrolysis of lithium chloride with a mercury cathode, electrolysis of an organic solution of lithium chloride, and electrolysis of fused salts with a liquid lithium product from the cathode. These may be illustrated in the following equations:

$$2LiOH_{aq} + (\text{potential}) \rightarrow 2\,Li(Hg) + 1/2\,O_{2\,gas} + H_2O \quad (7)$$

$$LiCl_{aq} + (\text{potential}) \rightarrow Li(Hg) + 1/2\,Cl_{2\,gas} \quad (8)$$

$$LiCl_{org} + Na(Hg) + (\text{potential}) \rightarrow Li(Hg) + NaCl_{(\text{insoluble})} \quad (9)$$

$$LiCl(\text{fused salt with KCl}) + (\text{potential}) \rightarrow Li(\text{metal}) + 1/2\,Cl_2 \quad (10)$$

Industrial equipment and methods are available for the processes utilizing reactions (7), (8), and (10). Current efficiencies of 90% or higher have been reported for such installations. Reaction (9) which has a mercury cathode and a sodium amalgam anode would require an extensive cell development program for successful application as a plant reflux method.

Under completely thermodynamically reversible conditions reactions (7) and (8) would be impossible as only hydrogen would be produced at the cathode. Under actual operating conditions hydrogen ion develops an over-potential which prevents the electrolysis of water. Certain impurities in the electrolysis systems catalyze the formation of hydrogen by lowering the over-voltage. Possibilities of minimizing this

FIGURE 5

~~SECRET~~
~~DWG. 20293~~

CLOSED REFLUX SYSTEMS

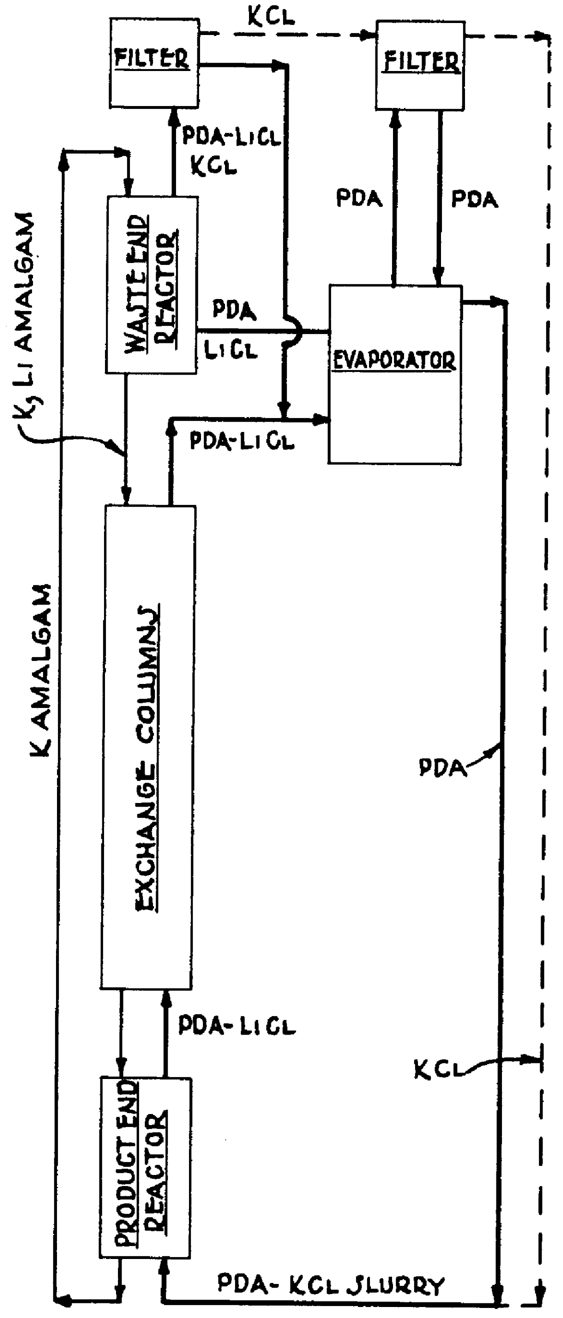

POTASSIUM CLOSED REFLUX SYSTEM

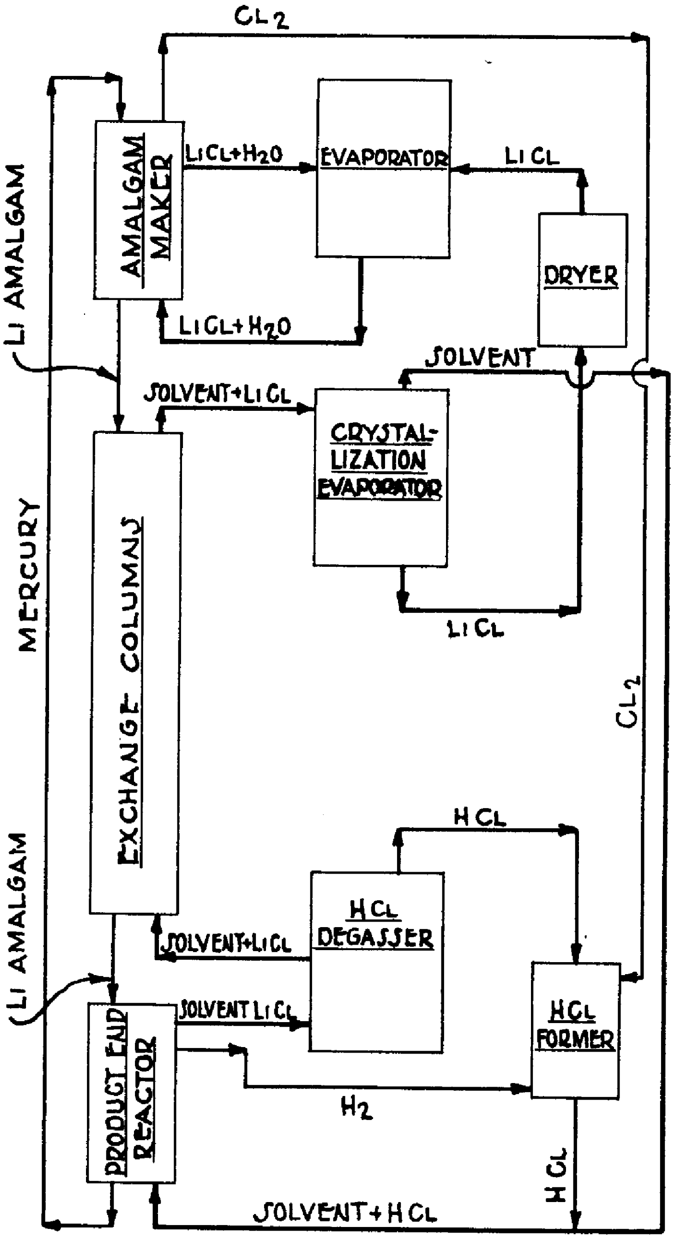

ELECTROLYTIC CLOSED REFLUX SYSTEM

important side reaction are: (1) purification of cell feed, (2) addition of inhibiting agents that complex the catalyzing impurities, and (3) removal of oxygen and other depolarizing agents.

Reactions (8) and (10) if applied to organic systems require the desolvation of the lithium chloride. This is no problem with tetrahydrofuran or isopropanol according to preliminary scanning experiments (see Part II - Lithium Chloride-Isopropanol and Lithium Chloride - Tetrahydrofuran); however, with ethylenediamine and propylenediamine the problem becomes significant. At the time of the writing of this report, a research program was well under way for the determination of vapor pressures of lithium chloride solvates with propylenediamine. Preliminary scanning experiments have demonstrated the engineering applicability of several methods of thermal decomposition to this material with success.

Reaction rates for systems involving electrolysis are not generally defined in the same sense as those of the usual chemical reaction. The kinetics are usually studied from the single electrode standpoint*. They are complicated for the usual type of rate study in that there are an increased number of variables not strictly chemical in nature which may be rate controlling or else have an effect on the rate controlling step. Further, electrolytic reactions often have complicating side or decomposition reactions which proceed spontaneously.

From a viewpoint that the applied potential only overcomes the driving force (free energy) tending to keep the reactants in their present low energy state it is possible, at least qualitatively, to look at electrolytic reactions as though they were only simple chemical reactions with an additional energy term involved. One such method of looking at the rate process for an electrolytic reaction is as follows. The equation:

$$(E) + 2LiOH + (Hg) \xrightarrow{k'} 2Li(Hg) + H_2O + 1/2\ O_2$$

represents a process that produces liquid lithium amalgam Li(Hg). The rate of formation of amalgam may be represented by:

$$d\,\frac{[Li(Hg)]}{dt} = k'\ f\ [(E),\ LiOH,\ Li(Hg),\ O_2,\ T] \qquad (11)$$

---

* For a detailed and quantitative approach the reader is referred to the work of H. H. Garretson (109) and W. E. Clark (107).

where the items inside the brackets are variables which are probably involved in the rate. The effects of these variables have not been elucidated at this time. However, for a given cell operating under steady state conditions the reaction can be represented by the equation:

$$d\frac{[Li(Hg)]}{dt} = k' f(E) \qquad (12)$$

where k' is not a true rate constant but is dependent upon operation at steady state condition with fixed current density, temperature, concentrations, etc.

For the case under consideration the most important side reaction is decomposition which proceeds as follows:

$$Li(Hg) + H_2O \xrightarrow{k_2} [LiOH]\ aq + 1/2\ H_{2\,(gas)} + Hg$$

The rate of disappearance of amalgam is given by the equation:

$$-d\frac{[Li(Hg)]}{dt} = k_2 f\left\{[Li(Hg)]\ ,\ LiOH,\ S,\ T\right\} \qquad (13)$$

where 'S' is the interfacial surface area between phases, 'T' the temperature: [Li(Hg)] the amalgam concentration, and LiOH the hydroxide concentration. These variables are known to effect the rate [29,30]. In addition, this reaction rate may be greatly affected by the catalytic action of certain impurities which have low hydrogen over-voltages. For example, the presence of oxygen is considered to greatly accelerate the decomposition rate. Other variables not well defined, such as, rate of agitation are incorporated into the rate constant 'k_2' by operating under fixed condition.

The function, $f[Li(Hg)]$, has been shown to depend upon the one-half power of the amalgam concentration [29,30,108]. For constant conditions of lithium hydroxide concentration, interfacial area, and temperature, equation 13 becomes:

$$-d\frac{[Li(Hg)]}{dt} = k_2' [Li(Hg)]^{1/2} \qquad (14)$$

or

$$k' = \frac{[Li(Hg)]_o^{1/2} - [Li(Hg)]_f^{1/2}}{t} \qquad (15)$$

The effect of hydroxide concentration has not been clearly established, but available data tends to show that the rate constant decreases in direct proportion to the increase in hydroxide concentration [29]. The pronounced effect of temperature is shown by Figure 6. The effect of the interfacial area per unit of amalgam volume upon the rate apparently is directly proportional (1st order), but methods of completely elucidating the actual area of the surface involved have not been devised at this time.

By combining the electrolytic rate (equation 12) and the decomposition rate (equation 14), one obtains an expression for the net rate of amalgam formation for steady state conditions as follows:

$$d \frac{[Li(Hg)]}{dt} = k_1' f(E) - k_2' [Li(Hg)]^{1/2} \qquad (16)$$

Equation 16 qualitatively defines the kinetics of the "Elex" process. For example, if $k_1' f(E)$ is greater than $k_2' [Li(Hg)]^{1/2}$, the reaction rate is positive and lithium is transferred from the aqueous to the amalgam phase. This corresponds to the waste end reflux. When the two terms are equal the rate is zero, and no net lithium transfer takes place; however, the exchange reaction between isotopes proceeds uninhibited. This corresponds to conditions maintained in the exchange section. Finally, when $k_1' f(E)$ is less than $k_2' [Li(Hg)]^{1/2}$ the rate is negative and net decomposition of the amalgam occurs to provide a product end reflux.

Similar treatment could be extended to the reactions represented by equations 8-10; however, little is to be gained by such a generalized development. It is important, however, to recognize that these electrolytic refluxes are complex and that the presence of traces of impurity can greatly alter the rates especially by influencing the decomposition reactions.

b. Magnesium Amalgam Reflux

Magnesium amalgam as a reflux agent is of importance in systems using the amine solutions of lithium chloride. The details of the reaction,

$$\text{Mg amalgam} + 2\ \text{LiCl(PDA sol'n)} \rightarrow \text{Li amalgam} + MgCl_2 \cdot 3PDA \qquad (17)$$

FIGURE 6

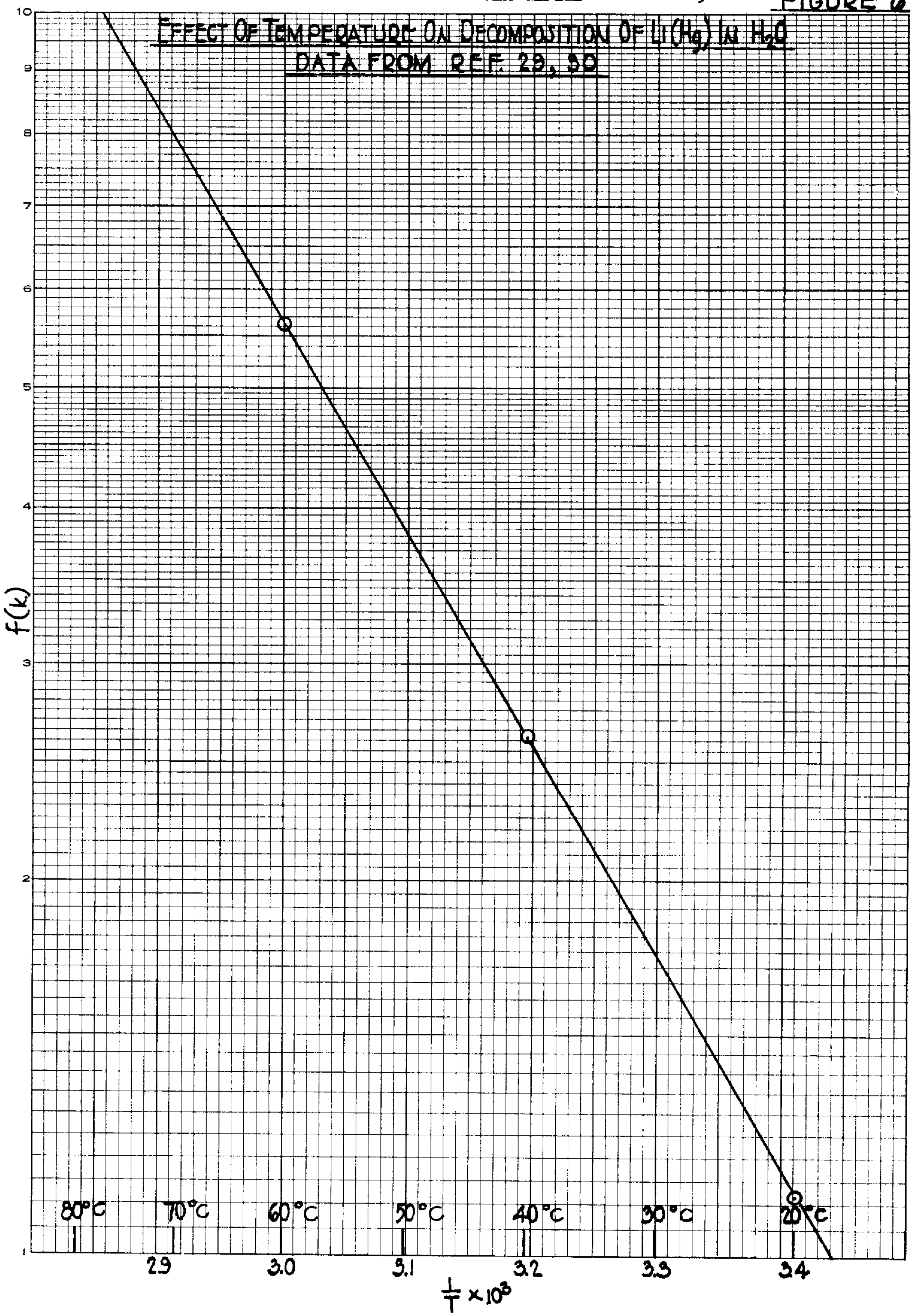

EFFECT OF TEMPERATURE ON DECOMPOSITION OF Li(Hg) IN H_2O

DATA FROM REF. 29, 30

have been worked out for propylenediamine solutions, but they should apply equally as well to ethylenediamine solutions. Reaction (17) proceeds very near completion because of the high stability and insolubility of the magnesium chloride solvate with propylenediamine. However, the equilibrium ratio of lithium to magnesium in the amalgam as a function of temperature or amine concentration has not been fully investigated (57).

Laboratory batch data (90, 91, 92 and 100) indicate that the conversion of magnesium amalgam to lithium amalgam follows a first order rate with respect to magnesium in the amalgam and to be independent of lithium chloride concentration in the amine phase as long as it was in stoichiometric excess. The rate may be defined as follows:

$$- d \frac{[Mg(Hg)]}{dt} = k [Mg(Hg)] \qquad (18)$$

or

$$\ln \frac{[Mg(Hg)]_o}{[Mg(Hg)]_f} = kt \qquad (19)$$

where $[Mg(Hg)]_o$ and $[Mg(Hg)]_f$ are the initial and final concentration of the magnesium in the amalgam.

In addition to the effect of magnesium concentration in the amalgam, the reaction rate is greatly influenced by the degree of dispersion (interfacial contact area) of the two phases. The optimum rate of agitation has not been established but will probably vary considerably from one type of equipment to another.

Increasing the temperature also increases the reaction rate. However, the optimum rate is likely to be determined by the maximum temperature for which the organic solvent will remain stable in the presence of the amalgam phase rather than by decreasing the holdup time to a point where a further increase of rate would not be economical from an equipment standpoint.

An important side reaction of the magnesium amalgam reflux is the chemical combination of trace amounts of water with magnesium amalgam to form magnesium hydroxide and hydrogen as follows:

$$\text{Mg amalgam} + 2\ H_2O \rightarrow Mg(OH)_2 + H_2 \qquad (20)$$

Although propylenediamine is a very hydroscopic solvent, reaction (20) is likely to contribute heavily to preventing any buildup of water in the solvent.

The favorable equilibrium conditions resulting from reaction (17) making it an excellent reflux reaction for the waste end of the exchange system are largely due to the stability of the complex salt, $MgCl_2 \cdot 3PDA$. The chemical stability, however, has prevented the utilization of simple thermal methods for complete desolvation of the magnesium chloride and recovery of the propylenediamine. (See Part II, Magnesium Chloride - Propylenediamine System for Vapor Pressure Data).

Chemical methods for recovery of propylenediamine by cleavage of the $MgCl_2 \cdot 3PDA$ structure fall into two classes: (1) replacement of the propylenediamine with a cheaper chemical having the ability of forming a more stable solvate and (2) chemical reaction to form new salts that do not have stable solvates with propylenediamine. Successful methods have utilized ammonia in the first classification and sodium hydroxide in the second.

Reaction of the solvate, $MgCl_2 \cdot 3PDA$ with ammonia may be illustrated as follows:

$$MgCl_2 \cdot 3PDA + 6NH_3 \longrightarrow MgCl_2 \cdot 6NH_3 + 3PDA \qquad (21)$$

This reaction may be carried out either at room temperature under pressure or below the boiling point of liquid ammonia at atmospheric pressure. Research is currently under way to disclose the details of this reaction.

The same reaction has been studied using methanol as a solvent for the solvate, $MgCl_2 \cdot 3PDA$. (See Part II, Magnesium Chloride - Ammonia - Methanol - Propylenediamine Systems). In this instance, the amount of excess propylenediamine accompanying the solvate, $MgCl_2 \cdot 3PDA$, limits the solubility of the solvate. Apparently, lithium chloride dissolved in the accompanying propylenediamine also limits the solvate, $MgCl_2 \cdot 3PDA$, solubility (see Figure 55). The degree of completion of the precipitation of $MgCl_2 \cdot 6NH_3$ from a methanol solution, $MgCl_2 \cdot 3PDA$ is highly dependent upon the concentration of ammonia. Some propylenediamine has been found in the precipitate, $MgCl_2 \cdot 6NH_3$, as may be seen in Figure 57. From the data available, it is impossible to predict whether this propylenediamine content is the result of mechanical occlusion or chemical interaction.

The reaction with sodium hydroxide may be carried out in aqueous or nonaqueous media. The reaction is essentially the same and may be illustrated as follows:

$$2\ NaOH + MgCl_2 \cdot 3PDA \longrightarrow Mg(OH)_2 + 2\ NaCl + 3PDA \quad (22)$$

The released propylenediamine must be separated from the solvent (water or alcohol) before it can be considered as completely recovered. Although the propylenediamine can be chemically released by reaction (22), because of the nature of the magnesium hydroxide precipitate, physical recovery of propylenediamine is difficult. Evaporation from the slurry has been effective where water and 2-ethyl hexanol have been used as solvents. Advantage may be taken of the two phase immiscibility with excess aqueous caustic. With methanol as solvent for sodium hydroxide, the magnesium hydroxide was found to be filterable. These propylenediamine recovery problems have been largely engineering in nature.

Regardless of the solvent used for reaction (22) the rate of reaction and equilibrium are very favorable for the release of propylenediamine. The reaction under agitation proceeds more rapidly than measurements can be taken. The propylenediamine remaining with the magnesium hydroxide is held there by physical entrainment as the chemical reaction apparently goes quantitatively to the right within the limits of analytical measurements. Some decomposition of the propylenediamine has been noted at high temperatures and high caustic concentrations and constitutes a disadvantage of this desolvation method. In alcohol solutions some dehydration of the magnesium hydroxide may take place due to the great affinity propylenediamine shows towards water. If this dehydration is appreciable, wet propylenediamine will result and the advantages of using an alcohol solvent will be lessened.

c. Potassium and Sodium Amalgam Refluxes

Both potassium and sodium amalgam reactions have been shown to have application to the waste end reflux utilizing propylenediamine as solvent. The reactions do not proceed to virtual completion as they do in the case of magnesium amalgam, and a mixed amalgam is the result in both cases. The reactions are as follows:

$$K(\text{amalgam}) + LiCl(\text{PDA sol'n}) \rightleftharpoons LiK(\text{amalgam}) + KCl(\text{ppt.}) \quad (23)$$

$$\text{Na(amalgam)} + \text{LiCl(PDA sol'n)} \rightleftharpoons \text{LiNa(amalgam)} + \text{NaCl(ppt.)} \quad (24)$$

The conditions under which the mixed amalgam is produced is that of high temperatures and high lithium chloride concentration in the amine phase. These conditions are also ideal for the reactivity of any trace amounts of water in the amine phase with the mixed amalgam to produce insoluble lithium hydroxide and hydrogen gas.

Reaction rates for these types of inversion (similar to isotopic exchange) are extremely rapid (93, 101). For this reason the reaction mechanism has not been elucidated to this date. It may be inferred, however, that the rate determining step will be similar to that of the magnesium inversion reaction and probably shows first order dependence upon the amalgam concentration.

An indication of why potassium or sodium amalgams reflux at the waste end at high temperature, and yet at low temperature form very stable amalgams can be shown qualitatively from thermochemical considerations.

Table 3 gives a series of idealized reflux reactions involving alkali amalgams and alkali halide salts. The heats and free energies are computed from data presented in Table 4. These equations represent reactions in which no interaction (solvation) of the halide salts would be involved, however, the effect of solvation will be discussed in a following paragraph.

From Table 3 it is observed that for these reactions under ideal conditions at room temperature the formation of lithium amalgam is slightly favored over sodium or potassium amalgam. The tendency being much more pronounced with increasing atomic weight of either the anion or the cation in the salt.

Experimental data (See Part II: Lithium - Mercury - PDA - NaCl - KCl) show that at room temperature lithium amalgam in contact with amine solution of sodium or potassium chloride is unstable and an inversion to sodium or potassium amalgam proceeds rapidly and to virtual completion (this is discussed under product end refluxes). These data indicate that the behavior of the halide salts in amine solution deviate widely. This behavior can be best understood by examining the solvation energies involved since a difference in

Table 3

Thermochemistry of Idealized Reflux Reactions

		ΔH^{o}_{298}	ΔF^{o}_{298}
1.	$LiCl_{(s)} + Na(Hg)_{100} \rightleftharpoons NaCl_{(s)} + Li(Hg)_{100}$	-0.3	-0.05
	$LiBr_{(s)} + Na(Hg)_{100} \rightleftharpoons NaBr_{(s)} + Li(Hg)_{100}$	-2.6	-1.9
	$LiI_{(s)} + Na(Hg)_{100} \rightleftharpoons NaI_{(s)} + Li(Hg)_{100}$	-3.9	-3.3
2.	$LiCl_{(s)} + K(Hg)_{100} \rightleftharpoons KCl_{(s)} + Li(Hg)_{100}$	-0.2	-1.5
	$LiBr_{(s)} + K(Hg)_{100} \rightleftharpoons KBr_{(s)} + Li(Hg)_{100}$	-3.8	-4.8
	$LiI_{(s)} + K(Hg)_{100} \rightleftharpoons KI_{(s)} + Li(Hg)_{100}$	-7.3	-8.1

solvation energy between lithium and potassium or sodium halide as small as 6 k cal could account for the observed reactions.

It is well known that neither sodium or potassium chlorides solvate to any great extent with PDA or EDA. It is equally well established that lithium chloride solvates readily with these amines. Solvation is accompanied by the evolution of an appreciable quantity of heat as follows: (53) (47)

$$LiCl_{(s)} + (345)\ PDA_{(l)} \longrightarrow LiCl\cdot(345)\ PDA_{(l)}$$

$$\Delta H \cong -19.41 \text{ k cal/g mole} \qquad (25)$$

$$LiCl_{(s)} + (10)\ PDA_{(l)} \longrightarrow LiCl\cdot(10)\ PDA_{(l)}$$

$$\Delta H \cong -13.5 \text{ k cal/g mole} \qquad (26)$$

$$LiCl\cdot 2PDA_{(s)} + (8)\ PDA_{(l)} \longrightarrow LiCl\cdot(10)\ PDA_{(l)}$$

$$\Delta H \cong -7 \text{ k cal/g mole} \qquad (27)$$

Table 4

Selected Thermodynamic Properties

$T = 288.16^{o}K$ Kcal/g mole

Component	State	ΔH_f	ΔF_f	Reference
LiCl	c	-97.7	-92.2	6
LBr	c	-87.4	-82.3	6
LiI	c	-72.5	-67.5	6
NaCl	c	-98.3	-91.9	6
NaBr	c	-90.3	-83.9	6
NaI	c	-76.7	-70.5	6
KCl	c	-104.4	-97.8	6
KBr	c	-97.7	-91.2	6
KI	c	-86.3	-79.7	6
$ZnCl_2$	c	-99.6	-88.4	7
$ZnBr_2$	c	-78.2	-	7
ZnI_2	c	-50.0	-	7
$ZnCl_2 \cdot EDA$	c	-138	-	7
$ZnCl_2 \cdot 3EDA$	c	-179.4	-	7
$ZnBr_2 \cdot EDA$	c	-112.5	-	7
$ZnBr_2 \cdot 3EDA$	c	-157.1	-	7
$ZnI_2 \cdot EDA$	c	86.9	-	7
$ZnI_2 \cdot 3EDA$	c	133.7	-	7
EDA	l	-8.8	-	11
$Li(Hg)_{100}$	l	-19.6	(-20.3)*	7,13
$Na(Hg)_{100}$	l	-19.9	(-19.95)*	7,13
$K(Hg)_{100}$	l	-26.08	(-24.4)*	7,13

---

* Free energy data from single electrode potentials (13).

In the absence of any free energy data it is assumed that they will be in the order of magnitude of the heats of reaction. In this event the reactions shown in Table 3 will have lower free energy in the direction which yields stable sodium or potassium amalgam.

In order to appreciate the magnitude of the energy involved in solvation more fully the system zinc halide versus ethylenediamine is presented. Thermochemical data are available and are presented in Table 4. The solvation reactions are presented in Table 5.

In addition to the magnitude of the heats of formation of these solvates another fact becomes quite evident from Table 5, i. e., apparently the anion contributes little to the heat of formation. If this observation holds true for systems involving lithium halides solvated with EDA or PDA then it is expected that solvation energy would have a less pronounced effect upon the inversion reaction in going from sodium to potassium and especially from sodium chloride to potassium iodide systems.

Table 5

Solvation of Zinc Halides with Ethylenediamine

Reaction	ΔH^o_{298}
$ZnCl_2 + EDA \longrightarrow ZnCl_2 \cdot EDA$	-29.8
$ZnBr_2 + EDA \longrightarrow ZnBr_2 \cdot EDA$	-25.0
$ZnI_2 + EDA \longrightarrow ZnI_2 \cdot EDA$	-28.1
$ZnCl_2 + 3EDA \longrightarrow ZnCl_2 \cdot 3EDA$	-53.6
$ZnBr_2 + 3EDA \longrightarrow ZnBr_2 \cdot 3EDA$	-52.0
$ZnI_2 + 3EDA \longrightarrow ZnI_2 \cdot 3EDA$	-56.9

Lithium chloride may be desolvated from EDA or PDA by heating to a moderately high temperature (113). From this it can be concluded that the degree (energy) of solvation is greatly affected by temperature. Such being the case at high temperature the effect of solvation energy upon the reaction given by equations 23 and 24 would be largely overcome and the more idealized reactions (Table 3) proceed to yield lithium or mixed amalgams. These conclusions are borne out by examination of figures 43, 44 and 46 (Part II) where the effect of temperature and lithium chloride concentration upon the inversion of potassium and sodium amalgams to lithium amalgam is shown.

2. Product End Reflux

a. Decomposition Reflux

Product end reflux with lithium amalgam in the water system appears to be comparatively simple upon first inspection. During isotopic exchange the decomposition of lithium amalgam takes place all the time that the amalgam and the aqueous solution are in contact. An applied potential in the exchange system does not prevent decomposition but replaces the amount decomposed. Thus reflux may be obtained by discontinuation of an applied potential and/or an increase in temperature of the system to increase the rate of the reaction. The kinetics of this reflux have been previously discussed as a complicating or side reaction to the Electrolytic Waste End Reflux Section, Page 17. Decomposition is illustrated as:

$$\text{Li(amalgam)} + H_2O \longrightarrow \text{LiOH} + 1/2\ H_{2\,(gas)} + \text{Hg} \qquad (28)$$

The similar type decomposition has application to systems utilizing the simple alcohols as a solvent to replace water.

$$\text{Li(amalgam)} + \text{ROH} \longrightarrow \text{LiOR} + 1/2\ H_{2\,(gas)} + \text{Hg} \qquad (29)$$

The rate of reaction is expected to decrease with the series of solvents - water, methanol, ethanol, propanol, etc., with water having the highest rate of reaction; however, solubility of the decomposition product decreases as the series increases in molecular weight.

b. Hydrogen Chloride Reflux

Product end reflux with hydrogen chloride has promise in exchange systems containing lithium chloride dissolved in a solvent in contact with lithium amalgam. At the product end where lithium amalgam is to be decomposed and the lithium sent back to the isotopic exchange system as lithium chloride, the reaction with hydrogen chloride is perhaps the fastest and most complete of all product end refluxes.

$$\text{Li amalgam} + \text{HCl} \longrightarrow \text{LiCl} + 1/2\ \text{H}_2 + \text{Hg} \qquad (30)$$

One of the problems encountered in utilizing this reaction is decreasing the rate of the reaction rather than in increasing it as with other reflux reactions. The reaction appears to go entirely to completion and at a rate far too rapid for measurement under conditions applied to date.

Two methods are available for application of this reaction: (1) solution of the hydrogen chloride gas in the solvent and subsequent contact with the amalgam phase and (2) contact of the hydrogen chloride gas with the amalgam with subsequent contact with the organic solvent. Only the first method has been investigated to date. This has proved to be successful with propylenediamine and isopropanol as solvents. With tetrahydrofuran, some reaction of the solvent with hydrogen chloride was noted.

c. Sodium and Potassium Chloride Refluxes

Product end reflux with sodium and potassium chlorides has been extensively studied in amine solutions, especially propylenediamine solution. The reactions involved are the reverse of reactions (23) and (24). As previously discussed, it is evident that solvated conditions of lithium chloride contributes greatly to the reversal of these reactions at low temperature.

Several so-called equilibrium constants have been given for the reflux reactions. This method of reporting data may have many advantages but the fact that the equilibrium constants are greatly different for the forward reaction compared to the reverse reaction points to the conclusion that the given constants are not applicable beyond the range of concentrations and temperatures in which they were measured. It is quite evident that activities of the constituents are markedly different from their concentrations and have unusual temperature coefficients.

The rate determining steps in these reactions are markedly different from those of the forward reaction given by equation 23 and 24. Laboratory data (89 - 94) indicate that the rate determining step is independent of (zero order with respect to) the amalgam concentration and may be interpreted to follow a rate:

$$-\,d\frac{[\mathrm{Li(Hg)}]}{dt} = k f\,[S,\ I_A] \tag{31}$$

(I_A) is the interfacial area between phases. The quantity (S) involves the surface area of the salt particles in the slurry and is not well-defined. However, when a large excess of finely divided salt is used (S) is constant and under conditions of fixed agitation (I_A) is approximately constant.

For these conditions, equation 31 becomes:

$$-\,d\frac{[\mathrm{Li(Hg)}]}{dt} = k' \tag{32}$$

and

$$k' = \frac{[\mathrm{Li(Hg)}]_1 - [\mathrm{Li(Hg)}]_2}{t_1 - t_2} \tag{33}$$

These data indicate that the rate determining (slow) step is the rate of solution of the salt particles. This is further substantiated by the observation that the relative magnitude of the rate constant is consistent with the relative solubility of sodium and potassium chlorides in propylenediamine. (See Pages 69, 70 for evaluation of rate constants). Furthermore, the rate constant does not increase as an exponential function of temperature which would be expected if a chemical reaction were the slow step.

Figure 26, (Part II) shows the results of laboratory investigation on the rate for sodium chloride inversion as a function of the temperature, size and amount of sodium chloride particles in the amine phase. These data indicate that size of the particles is more important than the temperature in the rate determining step. The effect of agitation on the rate constant has not been fully investigated.

As pointed out in the section on waste end refluxes for the potassium or sodium amalgam systems, temperature and lithium chloride concentration have marked effects upon the final degree of inversion. If the general behavior predicted by the equations given in Table 3 holds then from equilibrium considerations a sodium chloride system should yield a better reflux than bromide or iodide in that a lower concentration of lithium remaining the amalgam per given stage would result. However, the rate at which equilibrium is achieved will probably change in the opposite order due to increased solubility of bromide and iodide.

III: SOLVENT AND FEED PURIFICATION

A. SOLVENT PURIFICATION

As chemical technology advances, chemical specifications become more difficult to meet and engineering complications increase. Certainly isotope separation is no exception to this trend. For successful separation of lithium isotopes by present chemical methods, exceptionally low impurity levels are required that have and will continue to demand chemical research and engineering development.

Impurities in the aqueous-amalgam system for lithium isotope separation are: (1) those that cannot be tolerated because of the catalytic effect they have on the rate of decomposition of lithium amalgam and (2) those that preferentially build up in some part of the system or dilute the product. Quantitative knowledge of tolerances for impurities in the first class is unknown indicating the necessity of further research. Having determined the catalyzing impurities and their concentration effects, at least two different avenues of approach should be investigated; i. e., solvent purification by such means as filtration and ion exchange, and the use of additives to poison or complex the catalyzing impurities. The second class of impurities may be controlled through feed purification.

Impurities in the organic-amalgam system for lithium isotope separation are little understood except for the system employing propylenediamine as the organic solvent. Even with propylenediamine, the impurity problem is only partially understood because pilot plant data for extended operation are not available as yet. The tolerance for water in propylenediamine is believed to be at least as low as methods of analysis (less than 0.01% by weight) for propylenediamine systems utilizing a waste end reflux with magnesium, potassium, or sodium amalgam. No quantitative data is available on the thermal stability of propylenediamine or of the nature and effects of the decomposition products.

Methods of drying propylenediamine consist of distillation and chemical reaction methods. Benzene azeotropic distillation (See Part II: Benzene-Propylenediamine and

Propylenediamine-Water Systems) has received engineering attention. Some data on an alternate system are available (See Part II: Ethylene Glycol-Propylenediamine-Water System). Chemical reaction of water in the propylenediamine with calcium carbide which produces calcium oxide and acetylene gas constitutes a successful chemical method of drying propylenediamine.

Mercury, like propylenediamine may be purified by distillation or chemical reaction. In this case, however, the serious impurities are contaminating metals and not water. Chemical reaction with an aqueous solution of dilute nitric acid under oxidizing conditions has long been used as a satisfactory method of removing base metals from mercury and need not be discussed here.

B. FEED PURIFICATION

Purification of lithium amalgam feed in the aqueous-amalgam system has been investigated and it is understood that partial decomposition of the amalgam has been successfully used to control sodium and potassium impurities; however, published data are not available as yet to substantiate the extent of the purification.

Among the systems using propylenediamine as a solvent, lithium feed purification is most important to the closed reflux system employing potassium chloride and potassium amalgam as reflux reagents. Impurities introduced with the feed are likely to build up in one of the reflux ends if the solubilities of the impurities are exceeded. Since it is possible to feed either lithium amalgam or lithium chloride solution to the exchange columns, a feed purification section could be designed for either situation. Data on the solubilities of the major impurities as metals in the amalgam phase and as chlorides in the amine phase are needed as a function of temperature. Assuming withdrawal of product and waste and introduction of feed are made in the same phase, predictions could be made with solubility data as to the extent of impurity build-up. In the absence of experimental data it appears that amalgam feed and amine feed are equivalent provided either feed stream is equilibrated against the opposite phase in a clean-up section prior to introduction into the exchange columns.

Generally the drying of salts and metals utilized as reflux reagents and isotopic exchange feeds can be accomplished by using a dry air except for lithium chloride which forms a hydrate which is stable at room temperatures. (See Part II: Lithium Chloride - Water System). In order to obtain anhydrous lithium chloride drying at temperatures above 100°C is required. Fortunately, little if any decomposition to form hydrogen chloride takes place in the drying operation (55).

Dry, inert atmospheres are required in all organic-amalgam systems. Nitrogen and helium when properly purified have shown no reactivity toward amalgams (13,28,67).

PART TWO

CHEMICAL AND PHYSICAL DATA

I. INTRODUCTION

A. ARRANGEMENT OF DATA

Systemization of information often leads to complexities in presentation. The attempted arrangement of chemical and physical properties presented here is organized in a somewhat complex but ordered manner. All information falls under the general headings:

Lithium and Lithium Compounds
Magnesium and Magnesium Compounds
Potassium and Potassium Compounds
Sodium and Sodium Compounds
Liquid Solvents

Under each of the above-mentioned headings, technical information is classified according to the initial chemical components of the reactions or equilibrium systems under consideration. While this method of presentation requires a knowledge of the initial components of the chemical reactions involved, it has an advantage of being self-indexing to those who are aware of the method of arrangement. For example, in the product end reflux with sodium chloride, lithium and mercury are reacted with a slurry of sodium chloride in propylenediamine to produce a solution of lithium chloride in propylenediamine and sodium amalgam. Lithium, mercury, sodium chloride and propylenediamine are the initial components, and the physical and chemical data for this reaction can be found with the system "Lithium - Mercury - Sodium Chloride - Propylenediamine". This system is listed with other four component systems under "Lithium" which is found under "Lithium and Lithium Compounds" since this is the first general heading that contains any of the four initial components.

In some systems the initial components are identical with the chemical species present at equilibrium. Such is the case with magnesium and mercury. The information concerning solubility, density, viscosity, etc., is to be found among the two component systems under "Magnesium" which is under the general heading "Magnesium and Magnesium Compounds".

The compilation of all chemical and physical data on the Orex process (as of April 1953) was one of the objectives that guided the writing of this report. Much of the data has been plotted or replotted in an attempt to obtain a correlation and, consequently, allow for extrapolation beyond the area of experimental results. Justification of this procedure may be questionable in several cases where limited precision or small number of data are available; however, in the majority of cases, theoretical considerations were utilized as a basis for this "best guess".

All data appearing in this report have been referenced for easy access to the original publication and to give credit to those who have derived the data. Some confusion was encountered in the ORNL literature over the use of the term "molarity". In many instances, molarity appeared to be the number of moles per liter of solution regardless of the temperature of the solution. In other reports, molarity referred to the number of moles per unit weight of solution corresponding to a liter at room temperature. When these differences were recognized, they were tabulated in this report accordingly.

The convention utilized in previous reports to indicate liquid amalgam has been followed here; for example, liquid lithium amalgam is designated as Li(Hg).

Missing from Part Two, Section VI, of this report are the chemical and physical properties of water. These data are tabulated in the usual handbooks of chemistry, and consequently, they have been omitted in this report.

B. CONTENTS

III. MAGNESIUM AND MAGNESIUM COMPOUNDS

IV. POTASSIUM AND POTASSIUM COMPOUNDS

V. SODIUM AND SODIUM COMPOUNDS

VI. LIQUID SOLVENTS

II. LITHIUM AND LITHIUM COMPOUNDS

A. LITHIUM

Atomic Weight	6.94	
Normal Isotopic Abundance	7.5% Li^6, 92.5% Li^7	(2)
Melting Point	179°C, 354°F	(1)
Boiling Point	1317°C, 2403°F (1640°C from vapor pressure data)	(1)
Latent Heat of Fusion	158 cal/g, 284 Btu/lb, 1100 cal/g mole, 1970 Btu/lb mole	(1)
Latent Heat of Vaporization	4680 cal/g, 8430 Btu/lb, 32500 cal/g mole, 58500 Btu/lb mole	(1)
Vapor Pressure	$\text{Log}_{10}\ P\ \text{(mm)} = \frac{-8143}{T(^{o}K)} + 8.00$	(20)
	Accuracy - 10% (1100-1400°K) 30% (700-1100°K)	
	See Figure 7	
Density	0.534 g/ml at 20°C, 0.507 g/ml at 200°C, 0.441 g/ml at 1000°C	
	34.4 lbs/ft^3 at 68°F	(2)
Heat Capacity	1.0 cal/g C (200°C to 1000°C) 1.0 Btu/lb °F	(1)
Thermal Conductivity	0.09 cal/sec - cm - °C (218 - 233°C) 23 $\frac{Btu}{hr\ ft^{o}F}$	(1)
Viscosity	See Figure 8	(1)
Electrical Resistivity	45.25 μohms at 230°C	(1)

UNCLASSIFIED DWG. 20295

FIGURE 7

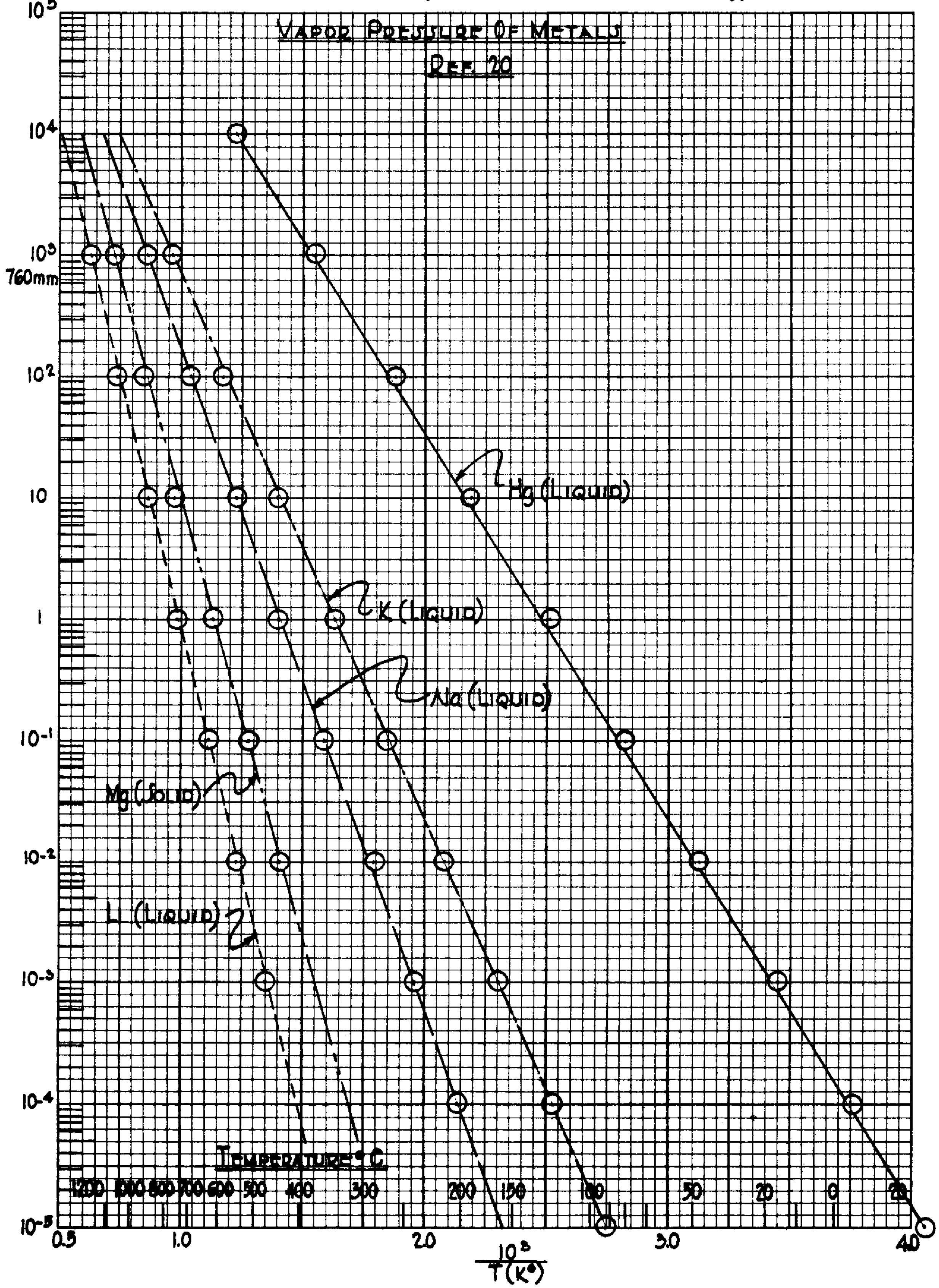

FIGURE 8

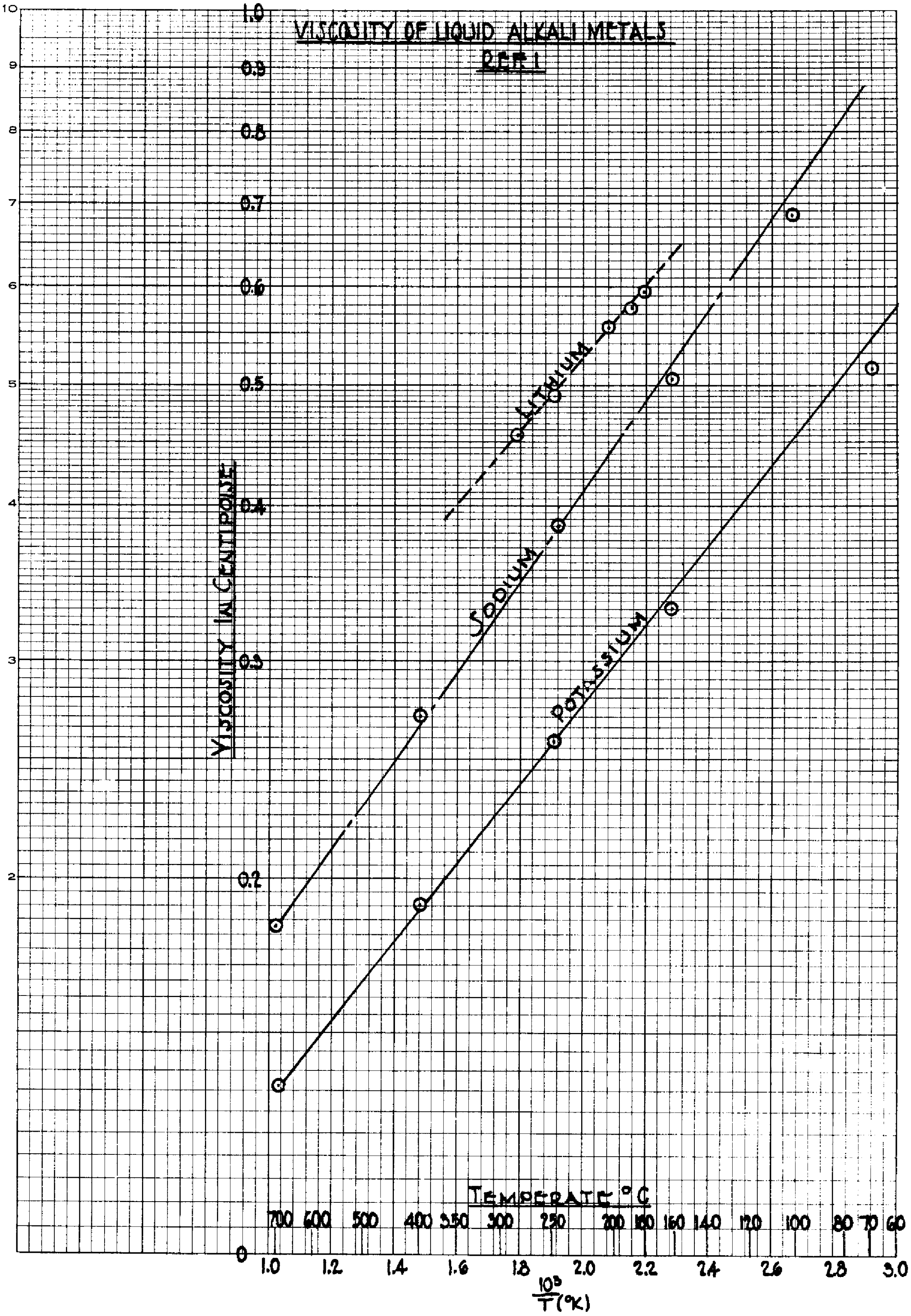
VISCOSITY OF LIQUID ALKALI METALS
REF 1
VISCOSITY IN CENTIPOISE
1.0
0.9
0.8
0.7
0.6
0.5
0.4
0.3
0.2
0
LITHIUM
SODIUM
POTASSIUM
TEMPERATURE °C
700
600
500
400
350
300
250
200
180
160
140
120
100
80
70
60
1.0
1.2
1.4
1.6
1.8
2.0
2.2
2.4
2.6
2.8
3.0
$\frac{10^3}{T(°K)}$

Volume Change on Fusion (% of solid volume)	1.5%	(1)

Lithium - Mercury

Density	See Figures 9, 10	(21)
Heat Capacity	0.0340 cal/g at 25°C and 0.0336 cal/g at 75°C	(106)
Viscosity	See Figure 11	(21)
Electrical Conductivity	See Figure 12	(13,29)
Surface Tension	See Figure 13	(13,26)
Phase Diagram	See Figure 14	(22)
Solubility of Lithium in Mercury	See Figures 15, 16	(13,23 24,25)
Chemical Reactions		
With O_2	Rate of reaction is appreciable at room temperature	(28)
With N_2	Apparently stable against dry N_2 at temperatures from 20°C beyond 165°C and atmospheric pressures	(28)
With H_2O	See Lithium - Mercury - Water System	
Heat of Solution	$(Li)_s + 99\ (Hg)_l \rightarrow Li(Hg)_{99}$ $\Delta H^o_{298^oK} = -19.6$ k cal/g mole	(5)
Activity Coefficient	$\text{Log}_{10} \gamma = 0.1428M$ (15°C to 55°C) Where $\gamma =$ activity coefficient and M = g-atoms Li per 13,534 g Hg at 25°C	(54)

[redacted] DWG. 20297

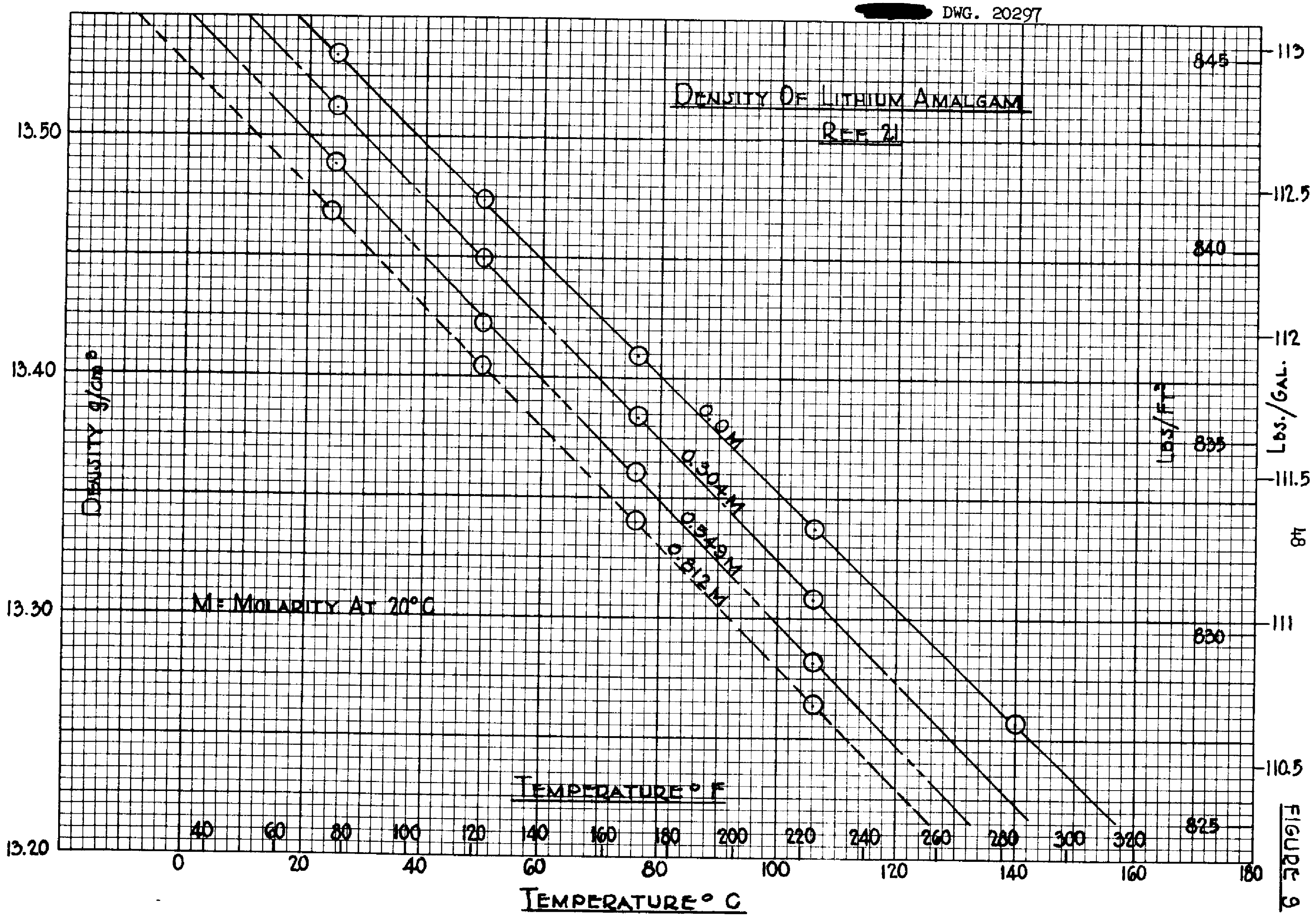

FIGURE 9

[redacted]
DWG. 20298

FIGURE 10

DENSITY OF LI AND MG AMALGAMS

DATA BY E.L. COMPERE REF. 65,67
C.M. BOYD REF. 21

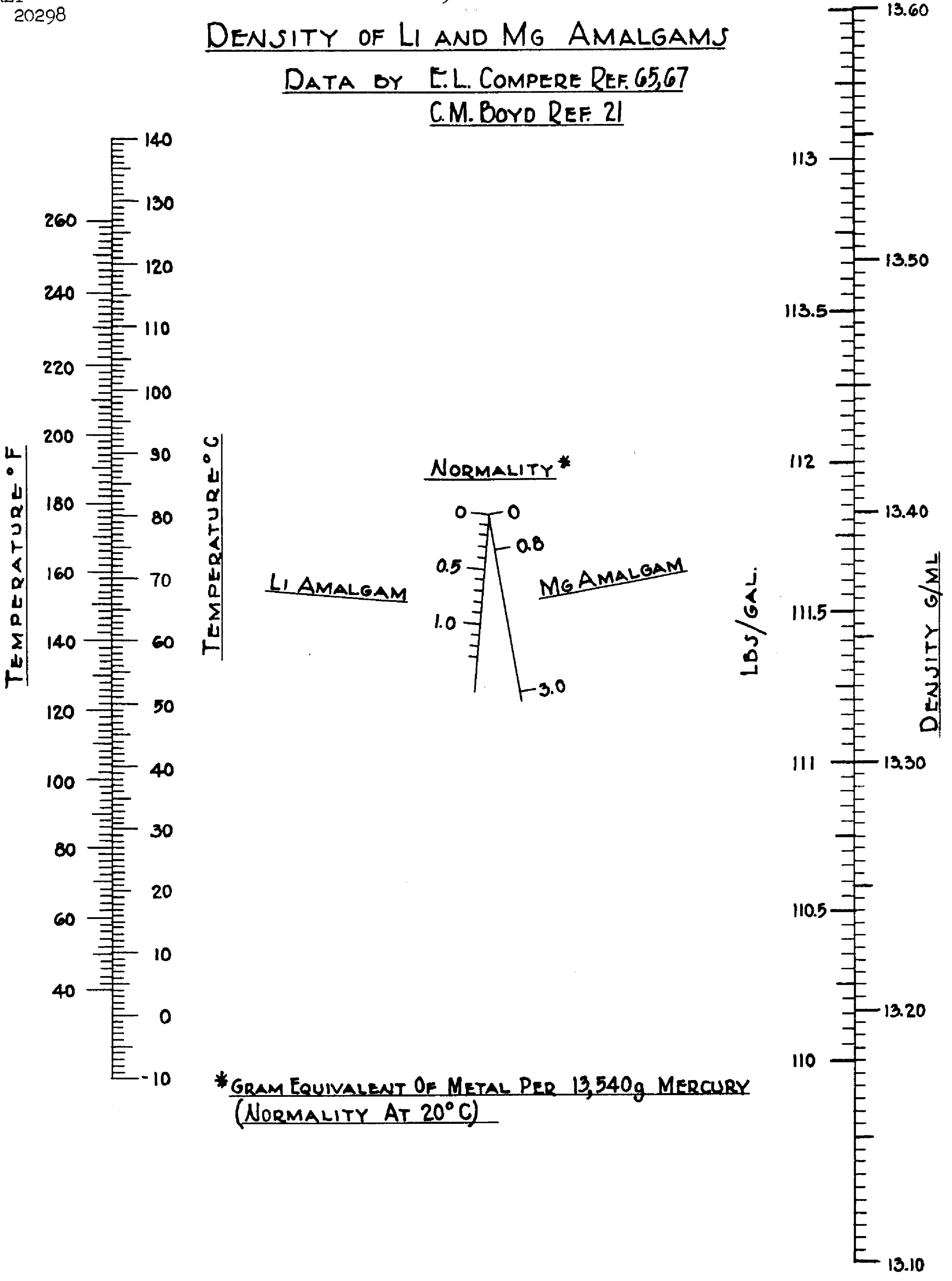

*GRAM EQUIVALENT OF METAL PER 13,540g MERCURY
(NORMALITY AT 20°C)

VISCOSITY OF LITHIUM AMALGAMS

REF. 21

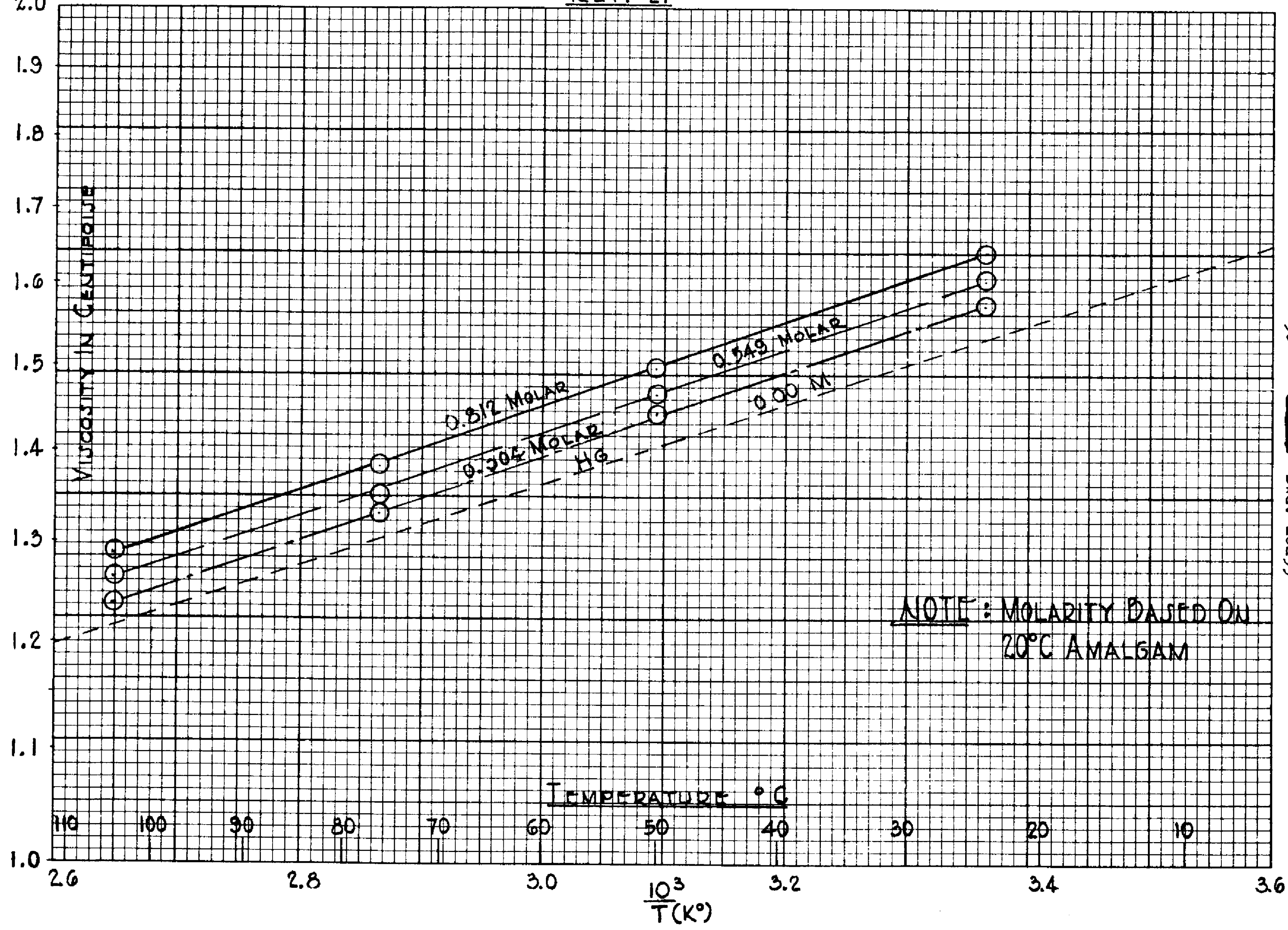

DWG. 20299

FIGURE 11

UNCLASSIFIED DWG. 20300

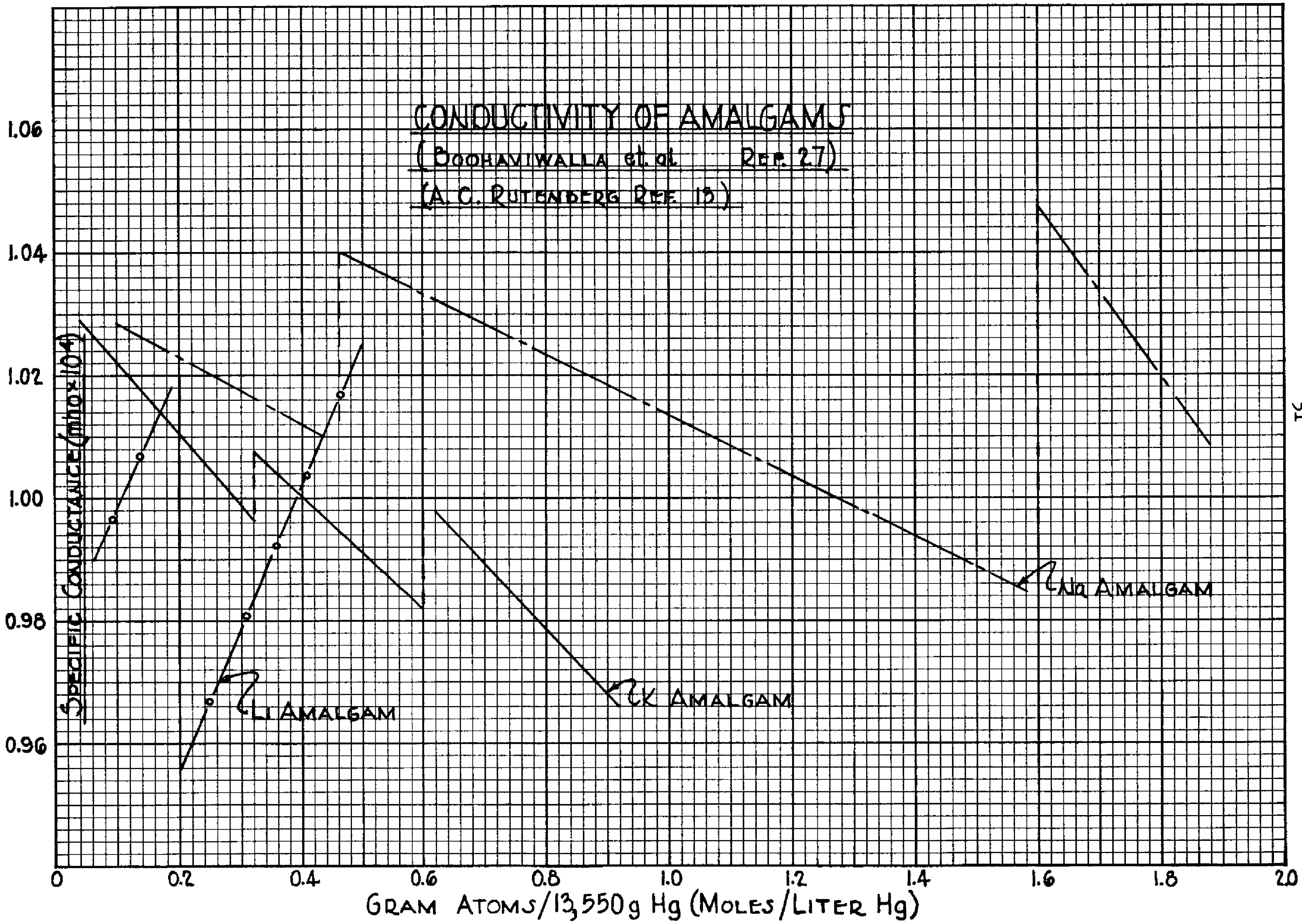

FIGURE 12

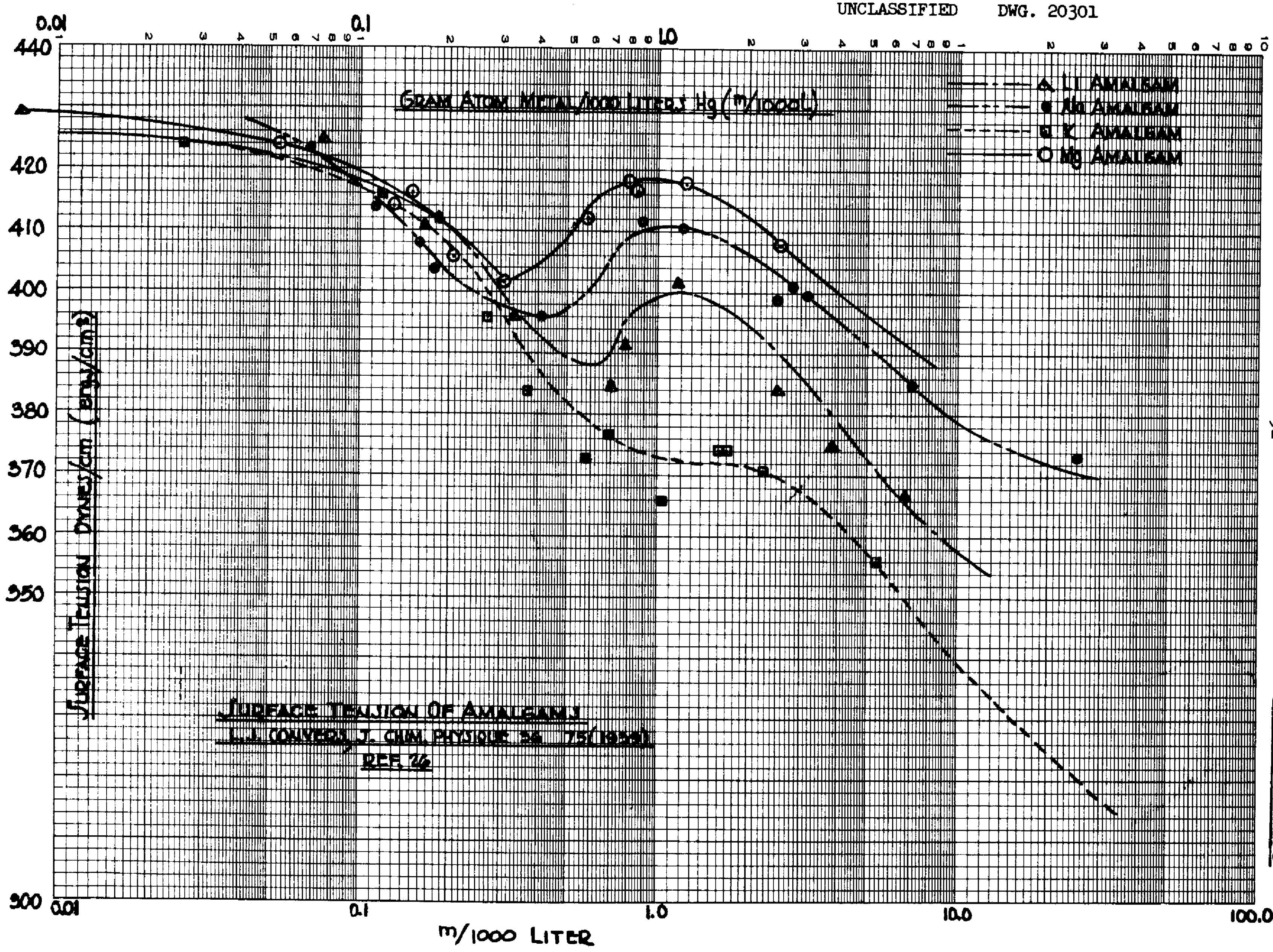

SURFACE TENSION OF AMALGAMS
L.J. CONVERS, J. CHIM. PHYSIQUE 56 75(1959)
REF. 26

FIGURE 13

UNCLASSIFIED DWG. 20373

FIGURE 14

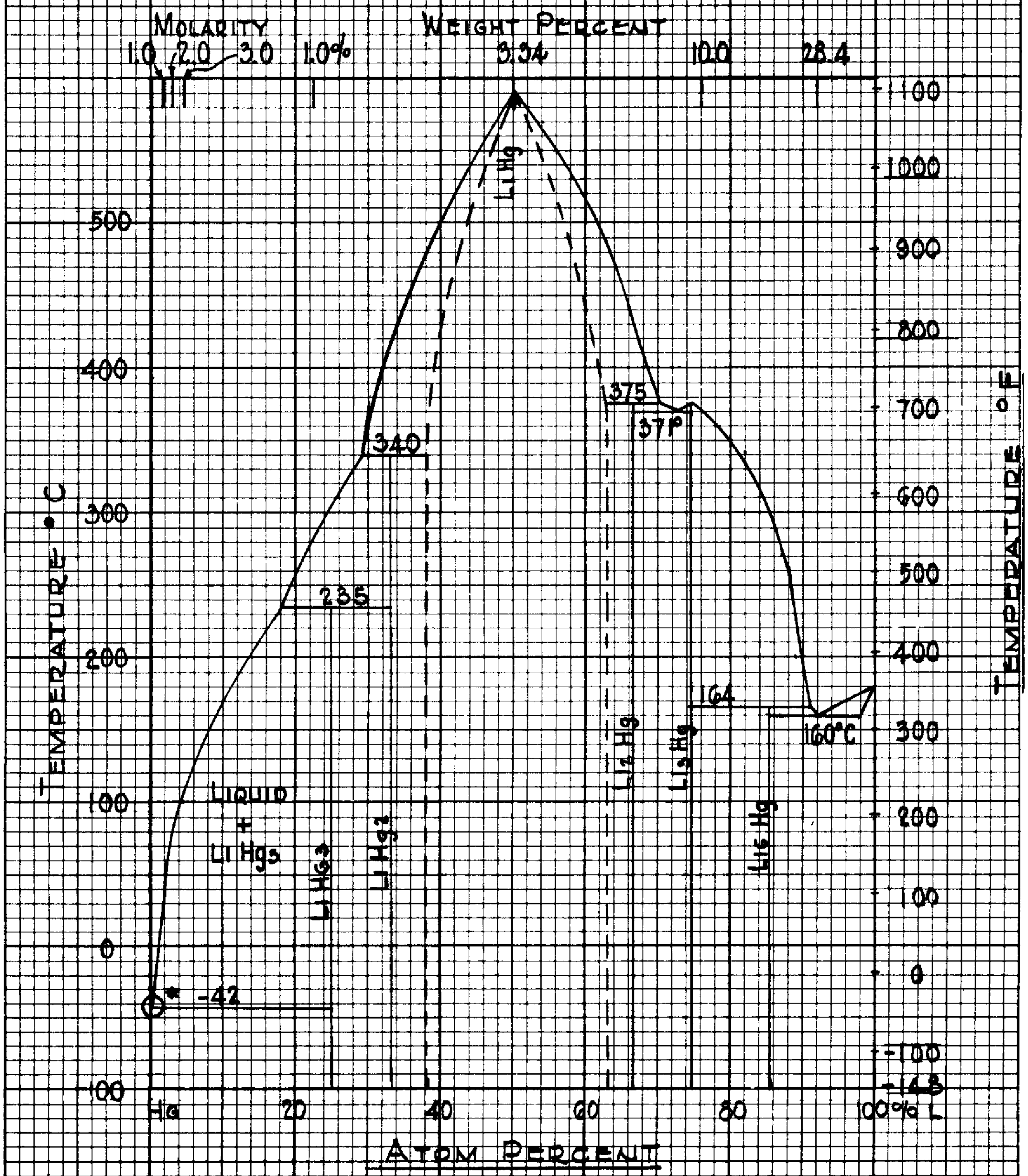

* ~ 0.4 MOLAR AT -42° C (EUTECTIC)

LITHIUM-MERCURY PHASE DIAGRAM

REF. 22

FIGURE 15

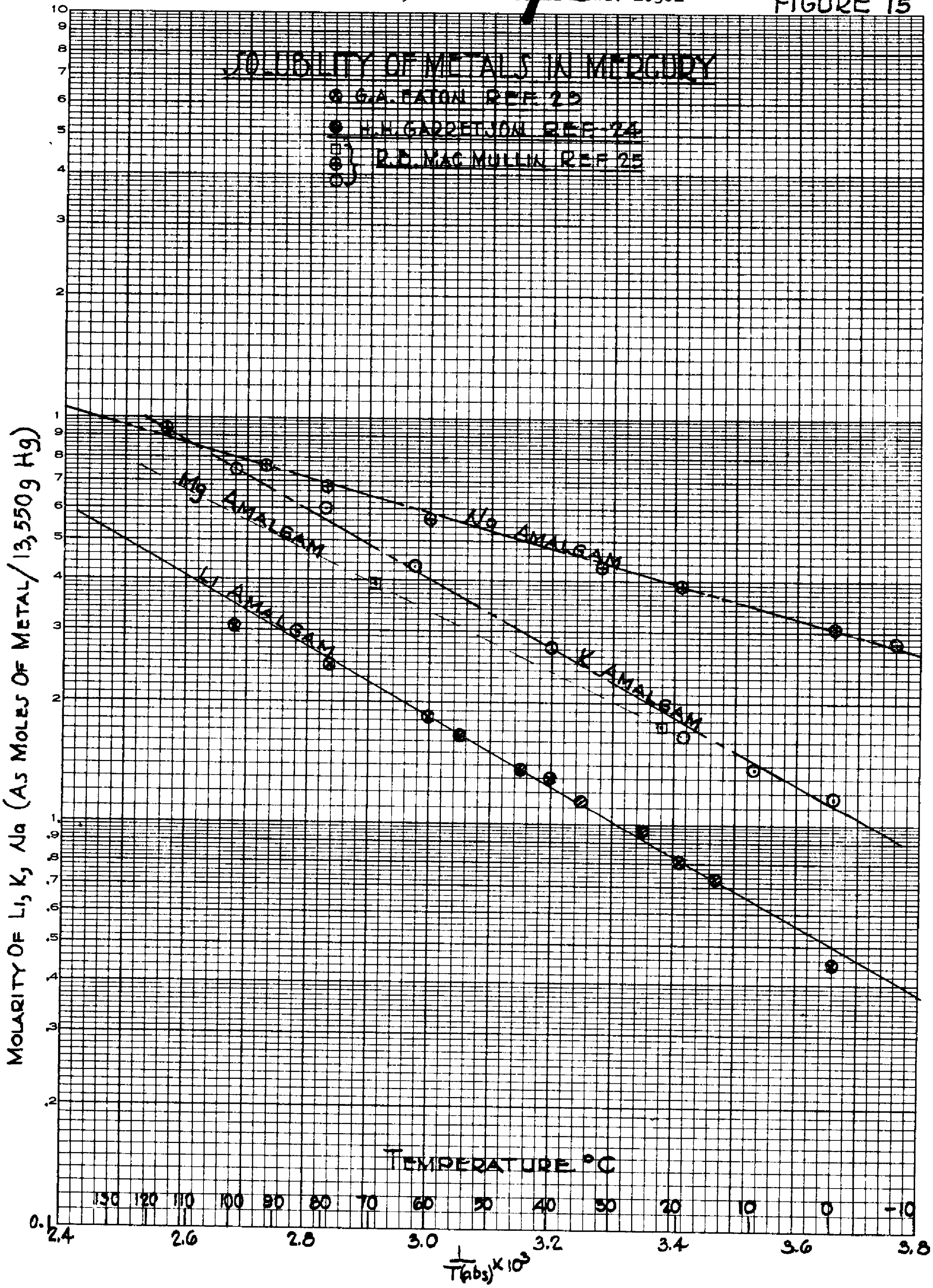
SOLUBILITY OF METALS IN MERCURY
⊗ G.A. EATON REF 23
● H.H. GARRETSON REF 24
□ ⊕ ○ } R.E. MAC MULLIN REF 25
Na AMALGAM
Mg AMALGAM
K AMALGAM
Li AMALGAM
MOLARITY OF Li, K, Na (AS MOLES OF METAL/13,550 g Hg)
TEMPERATURE °C
130 120 110 100 90 80 70 60 50 40 30 20 10 0 -10
1/T(abs) ×10³
2.4 2.6 2.8 3.0 3.2 3.4 3.6 3.8
0.1 .2 .3 .4 .5 .6 .7 .8 .9 1 2 3 4 5 6 7 8 9 1 2 3 4 5 6 7 8 9 10

SOLUBILITY OF ALKALI METALS AND SALTS IN SELECTED SOLVENTS

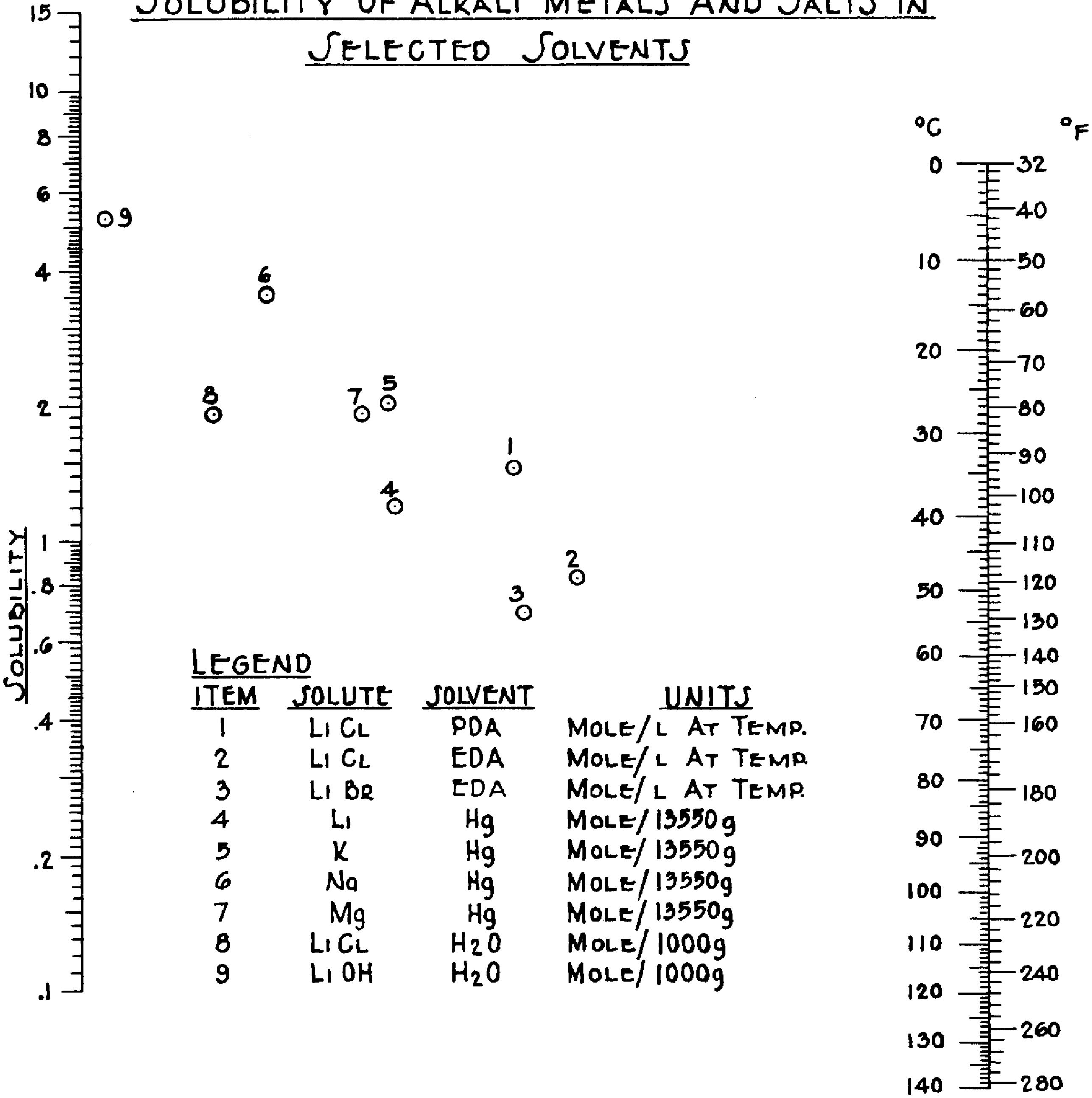

LEGEND

ITEM	SOLUTE	SOLVENT	UNITS
1	LiCl	PDA	MOLE/L AT TEMP.
2	LiCl	EDA	MOLE/L AT TEMP.
3	LiBr	EDA	MOLE/L AT TEMP.
4	Li	Hg	MOLE/13550g
5	K	Hg	MOLE/13550g
6	Na	Hg	MOLE/13550g
7	Mg	Hg	MOLE/13550g
8	LiCl	H_2O	MOLE/1000g
9	LiOH	H_2O	MOLE/1000g

DWG. 20303

FIGURE 16

Lithium - Potassium

See phase diagram	Figure 17	

Lithium - Sodium

See phase diagram	Figure 18	

Lithium - Potassium - Mercury

Solubility Curve	See Figure 19	(38)

Lithium - Sodium - Mercury

Solubility Curve	See Figure 20	(38)

Lithium - Mercury - Water

Reversible Electrode	$Li(Hg) \parallel Li^+ (aq)$ $E^o_{298^oK} = 2.079$ volts	(107)
Chemical Reaction	$Li(Hg) + xs\ H_2O \longrightarrow$ $(LiOH)aq + Hg + 1/2\ H_2$ $\Delta H_{298^oK} = -33.5$ k cal/g mole $\Delta F_{298^oK} = -28.75$ k cal/g mole	(107)
Rate of Reaction	$k = \frac{2(C_o^{1/2} - C_f^{1/2})}{st}$ for weak acids and water solution	(29,30, 108)
	Appears to have following dependence in LiOH solution: $k^1 = \frac{ks}{2} = \frac{(C_o^{1/2} - C_f^{1/2})(C_{OH})}{t}$	

FIGURE 18

LITHIUM SODIUM PHASE DIAGRAM
REF. 14

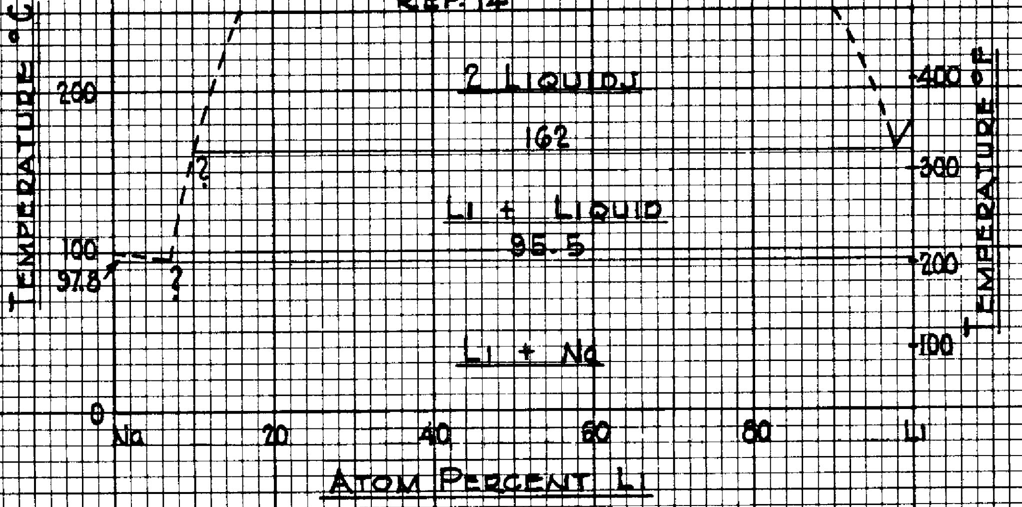

FIGURE 17

LITHIUM - POTASSIUM PHASE DIAGRAM
REF. 14

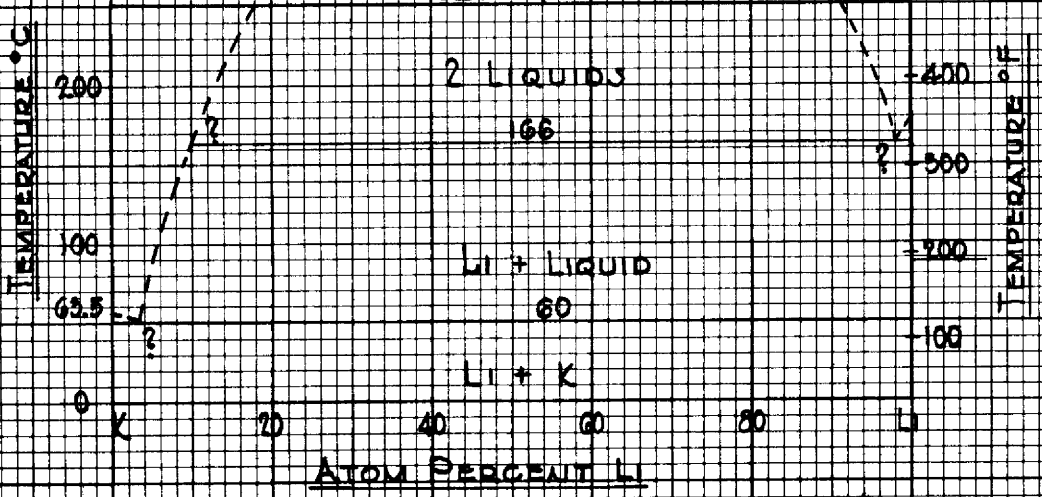

LI - K - HG
SOLUBILITY CURVE
TEMPERATURE 23°C
•TEMPERATURE 48°C•
REF. 38

NOTE:
MOLARITY IS APPROXIMATELY
= K × MOLE % AT <5 MOLAR SOLUTIONS

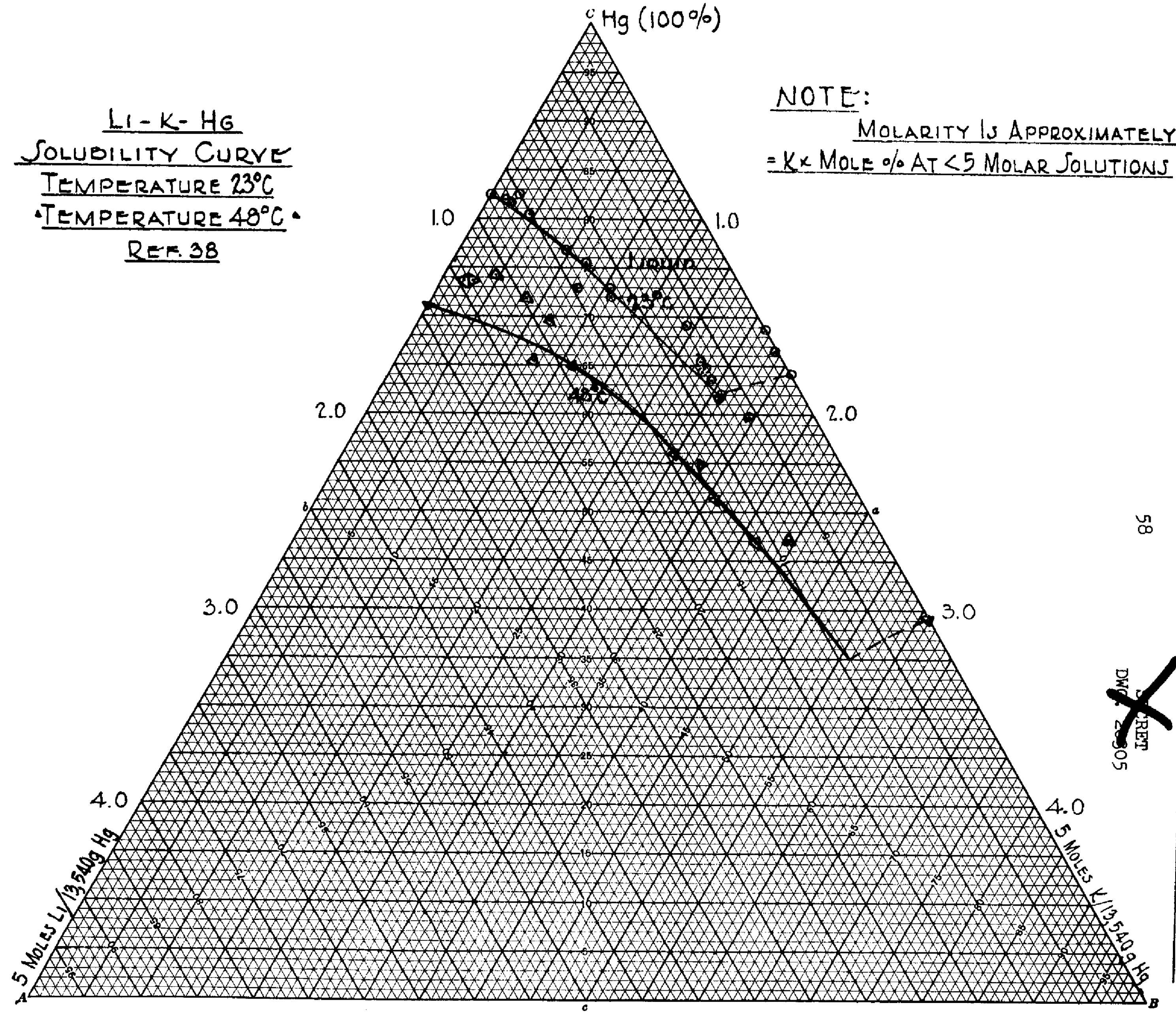

FIGURE 19

~~SECRET~~
DWG 20305

Li - Na - Hg
Solubility Curve
Temperature 23°C
Ref. -38

NOTE:
Molarity Is Approximately Proportional To Mole % At <5 Molar Solutions

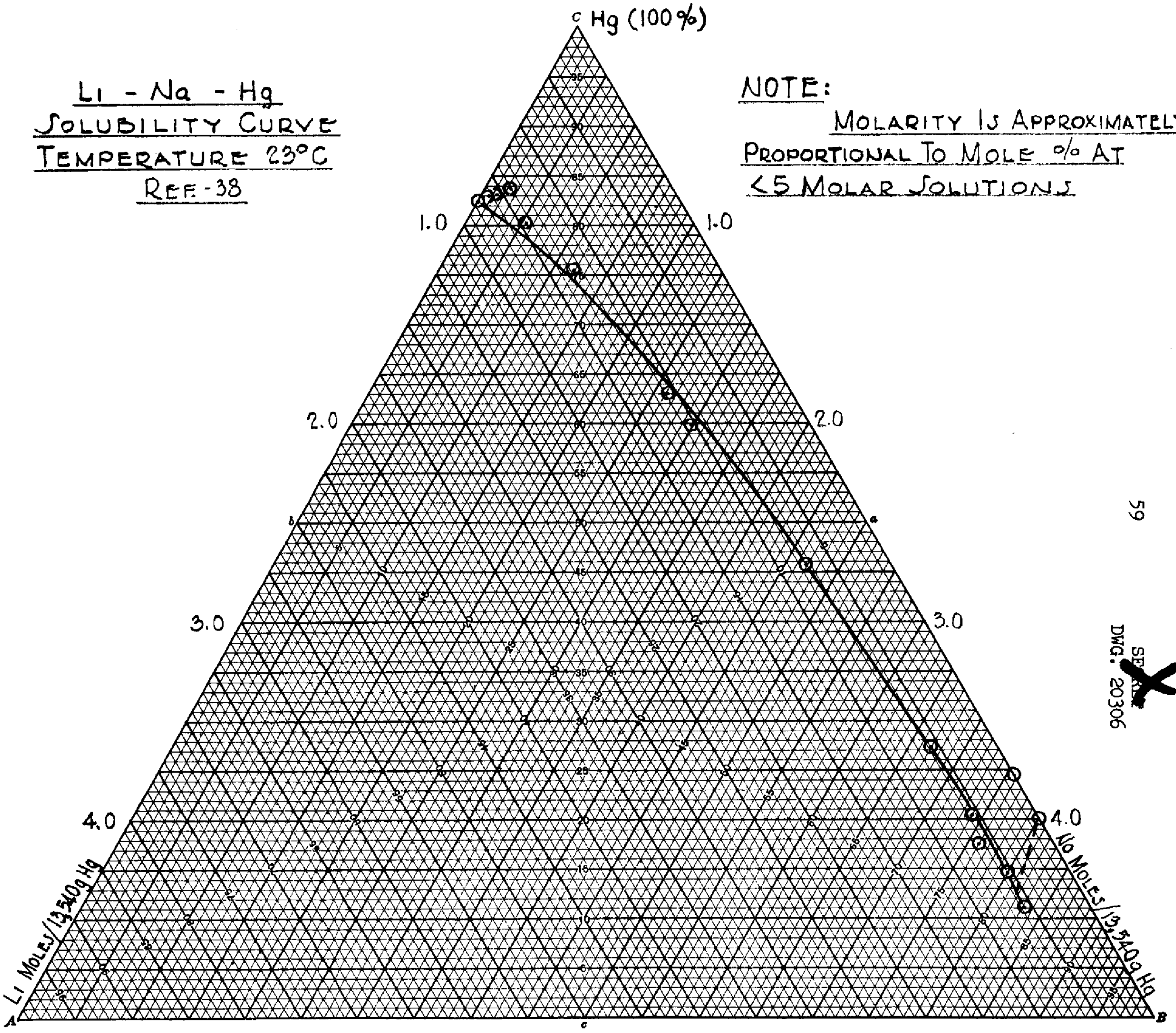

SEE DWG. 20306

FIGURE 20

	Where k is the specific rate constant, s the interfacial area, C_o and C_f the initial and final concentration of Lithium in the amalgam, t is the time corresponding to C_f, and (C_{OH}) is the LiOH concentration
Activation Energy	$E^{\ddagger} \cong 7.75$ k cal/g-mole (See Figure 6).

Lithium - Mercury - Ammonium Chloride - Tetrahydrofuran

Chemical Reaction	$Li(Hg) + NH_4Cl_{(solid)} + THF \rightarrow LiCl_{(dissolved)} + THF + Hg + 1/2H_2 + NH_3$
Rate of Reaction	Apparently limited by solubility of NH_4Cl in THF (31)

Lithium - Mercury - Lithium Anthracene - Dimethylcellosolve

Isotopic Exchange System	Li(Hg) vs Li Anthracene dissolved in Dimethylcellosolve (33)
Separation Factor	$\alpha = 1.042 \pm 0.012$ (95% CI) at 27°C (32)

Lithium - Mercury - Lithium Benzophenone - Dimethylcellosolve

Isotopic Exchange System	Li(Hg) vs Li-Benzophenone dissolved in Dimethylcellosolve (33)
Separation Factor	First Run - $\alpha = 1.057 \pm 0.012$ (95% CI) at 27°C (32)
	Second Run - $\alpha = 1.056 \pm 0.008$ (95% CI) at 27°C (40)

Lithium - Mercury - Lithium Benzophenone anil - Dimethylcellosolve

Isotopic Exchange System	Li(Hg) vs Li-Benzophenone anil dissolved in Dimethylcellosolve	(33)
Separation Factor	First Run - $\alpha = 1.038 \pm 0.011$(95% CI) at 27°C	(32, 34)
	Second Run - $\alpha = 1.037 - 0.008$(95% CI) at 26.5°C	

Lithium - Mercury - Lithium Chloride - Dimethylcellosolve

Isotopic Exchange System	Li(Hg) vs LiCl dissolved in Dimethylcellosolve	
Separation Factor	$\alpha = 1.023 \pm 0.013$(95% CI) at 26°C	(34)
	Low solubility of LiCl in Dimethylcellosolve made this run difficult.	

Lithium - Mercury - Lithium Benzophenone - Propylenediamine

Isotopic Exchange	Li(Hg) vs Li-Benzophenone dissolved in Propylenediamine	
Separation Factor	$\alpha = 1.055 \pm 0.016$(95% CI) at 27°C	

Lithium - Mercury - Lithium Benzophenone anil - Propylenediamine

Isotopic Exchange System	Li(Hg) vs Li-Benzophenone anil dissolved in Propylenediamine	
Separation Factor	$\alpha = 1.047 \pm 0.012$(95% CI) at 26.5°C	(40)

Lithium - Mercury - Lithium Benzophenone - Tetrahydrofuran

Isotopic Exchange System	Li(Hg) vs Li-Benzophenone dissolved in THF	
Separation Factor	$\alpha = 1.045 \pm 0.008$(95% CI) at 27°C	(40)

Lithium - Mercury - Lithium Benzophenone anil - Tetrahydrofuran

Isotopic Exchange System	Li(Hg) vs Li-Benzophenone anil dissolved in TFH	
Separation Factor	$\alpha = 1.046 \pm 0.012$(95% CI) at 27°C	(40)

Lithium - Mercury - Lithium Chloride - Ethylenediamine

Isotopic Exchange System	Li(Hg) vs LiCl dissolved in EDA	
Separation Factor	See Figures 21, 22	(36)
Isotopic Exchange Rate	≦ 30 seconds required to reach isotopic equilibrium according to shakeout tests.	(35)

Mass Transfer

	Before	After Equilibration
Amalgam phase	3.7g Li/l	3.4g Li/l
Amine phase	1.8 g Li/l	1.9g Li/l

(35)

Stability of System	Temperature and metallic contact increase decomposition of EDA as indicated by color change.	(36)
Interfacial (Surface) Tension	Dispersion in pulse column inversely proportional to temperature. This indicates interfacial tension increases with temperature.	(37)

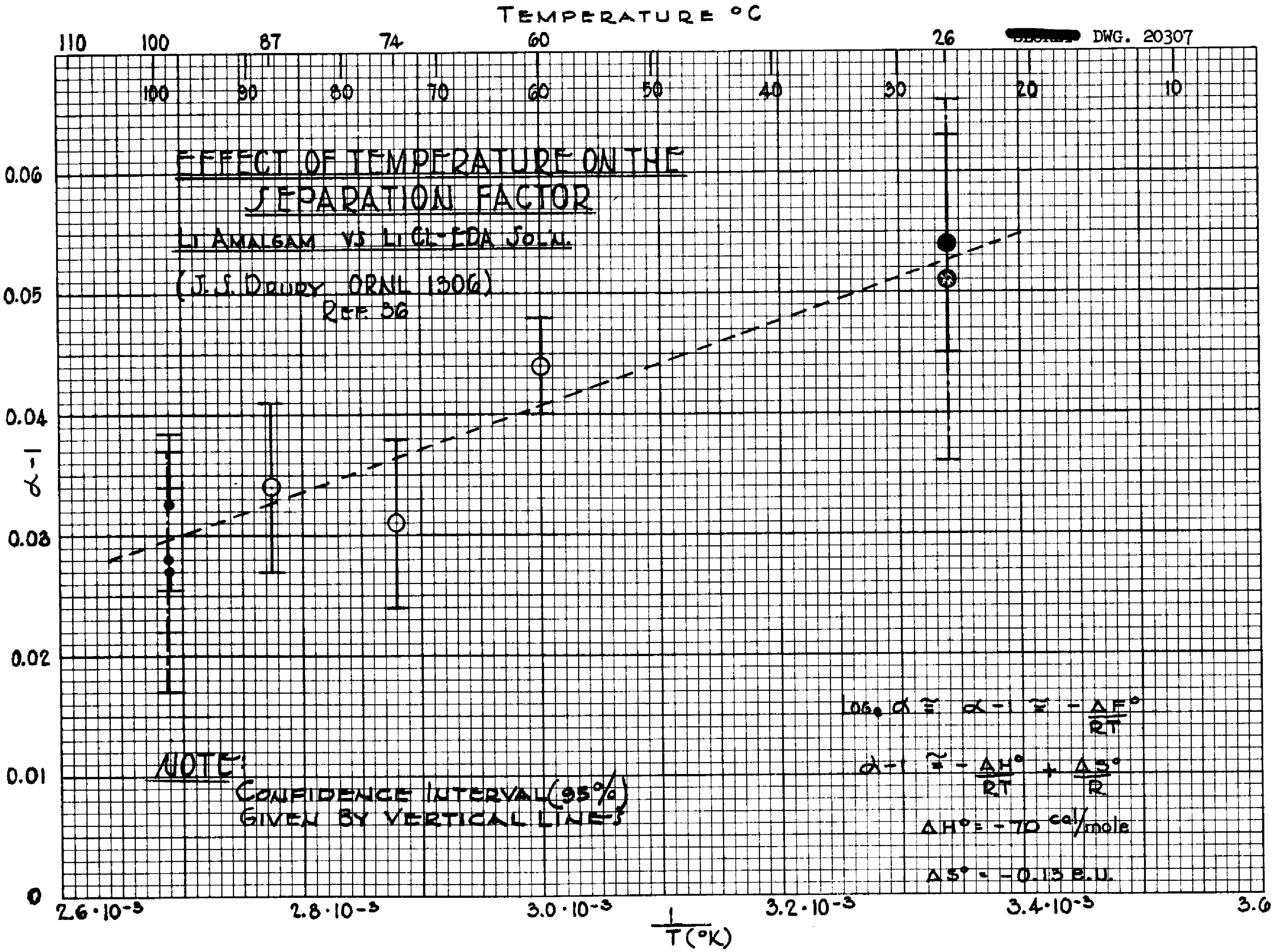

EFFECT OF TEMPERATURE ON THE SEPARATION FACTOR

LI AMALGAM VS LI CL-EDA SOL'N.

(J. S. DRURY ORNL 1306)
REF 36

NOTE: CONFIDENCE INTERVAL (95%) GIVEN BY VERTICAL LINES

$\log_e \alpha \cong \alpha - 1 \cong -\frac{\Delta F^\circ}{RT}$

$\alpha - 1 \cong -\frac{\Delta H^\circ}{RT} + \frac{\Delta S^\circ}{R}$

$\Delta H^\circ = -70$ cal/mole

$\Delta S^\circ = -0.13$ E.U.

FIGURE 21

[redacted]
DWG. 20308

SEPARATION FACTOR FOR LITHIUM ISOTOPE AS A FUNCTION TEMPERATURE

REF. (34) (36) (40) (42)

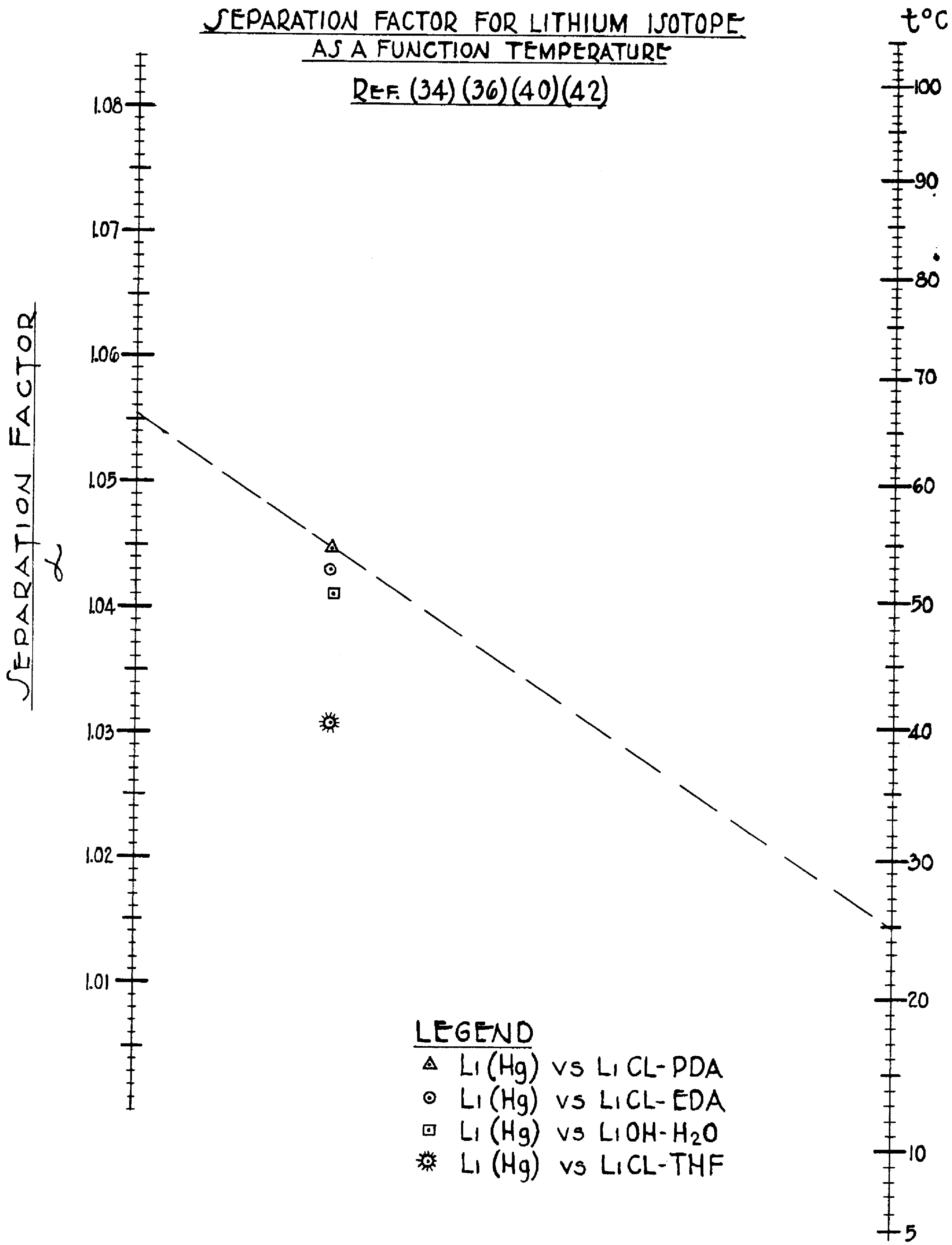

Lithium - Mercury - Lithium Chloride - Isopropanol

Isotopic Exchange System	Lithium amalgam vs LiCl dissolved in Isopropanol	
Separation Factor	$\alpha = 1.055 \pm 0.009$ (95% CI) at 26.5°C	(40)

Lithium - Mercury - Lithium Chloride - Propylenediamine

Isotopic Exchange System	Li(Hg) vs LiCl dissolved in PDA	
Separation Factor	See Figures 22, 23	(34,40)

Lithium - Mercury - Lithium Chloride - Tetrahydrofuran

Isotopic Exchange System	Li(Hg) vs LiCl dissolved in THF	
Separation Factor	See Figures 22, 24	(34)
Rate of Reaction	Isotopic exchange was reported complete in less than 5 minutes in laboratory shakeout tests.	(41)

Lithium - Mercury - Lithium Hydroxide - Water

Isotopic Exchange System	Li(Hg) vs LiOH dissolved in H_2O (Chemical reaction $Li(Hg) + H_2O \rightarrow LiOH + 1/2H_2\uparrow + Hg$ minimized by applied potential and/or low temperature.)	
Separation Factor	See Figures 22, 25	(42)
Stability of System (Reaction Rate)	See Li-Hg-H_2O system	

~~SECRET~~ DWG. 20372

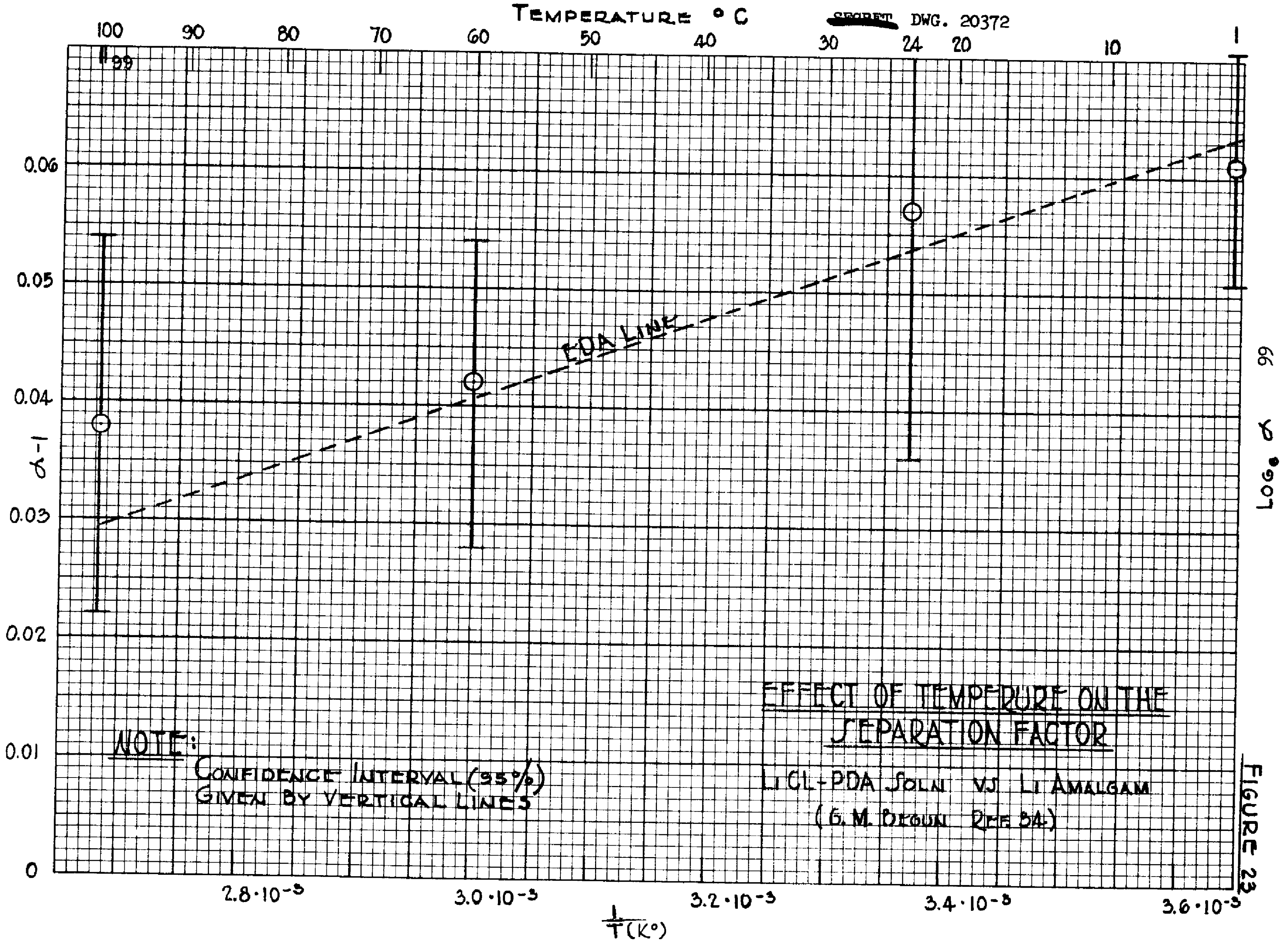

EFFECT OF TEMPERURE ON THE SEPARATION FACTOR

LiCL-PDA SOLN VS LI AMALGAM
(G. M. BEGUN REF 34)

NOTE:
CONFIDENCE INTERVAL (95%)
GIVEN BY VERTICAL LINES

FIGURE 23

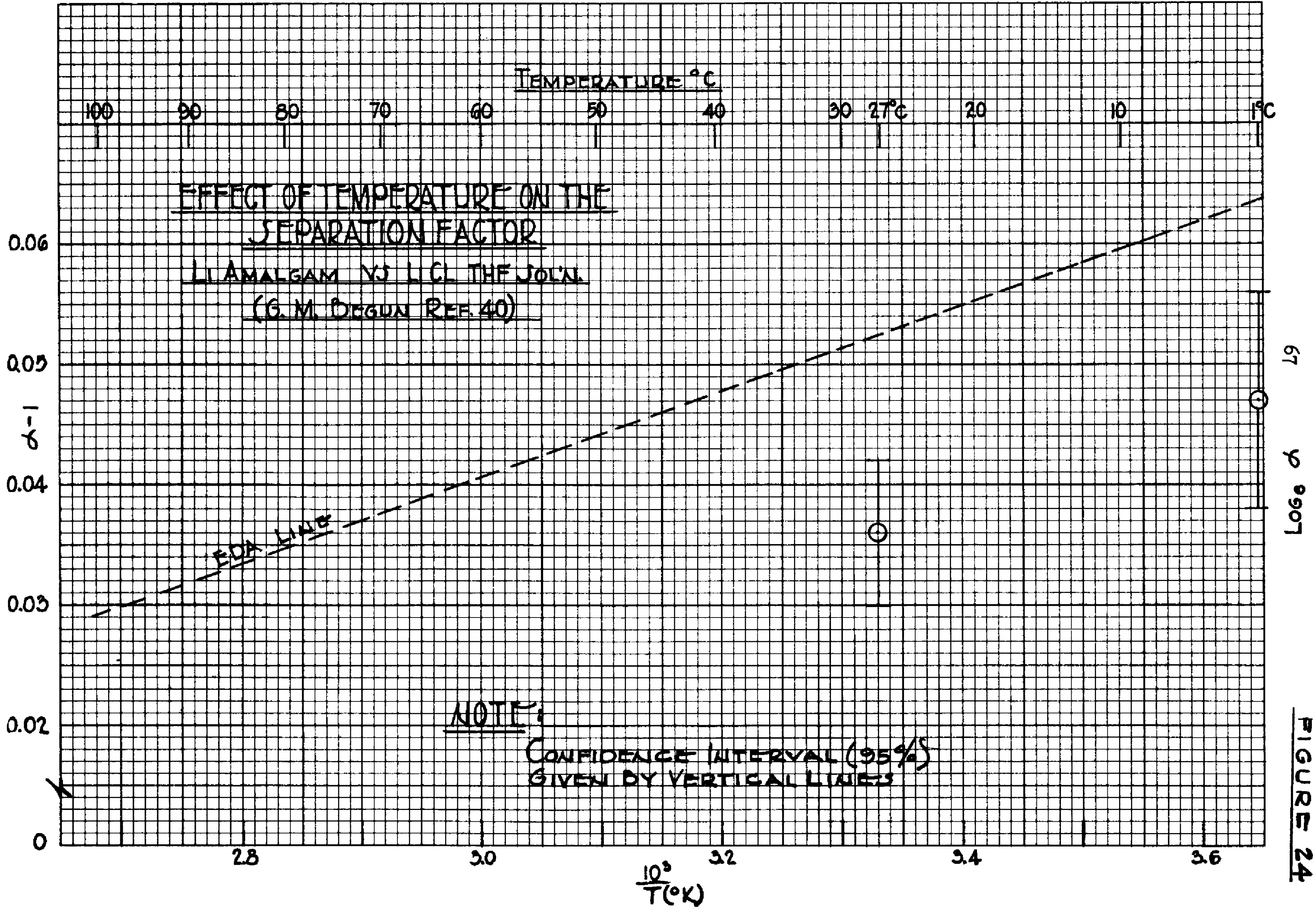

EFFECT OF TEMPERATURE ON THE SEPARATION FACTOR
LI AMALGAM VS LICL THF SOL'N.
(G. M. BEGUN REF. 40)

NOTE:
CONFIDENCE INTERVAL (95%)
GIVEN BY VERTICAL LINES

FIGURE 24

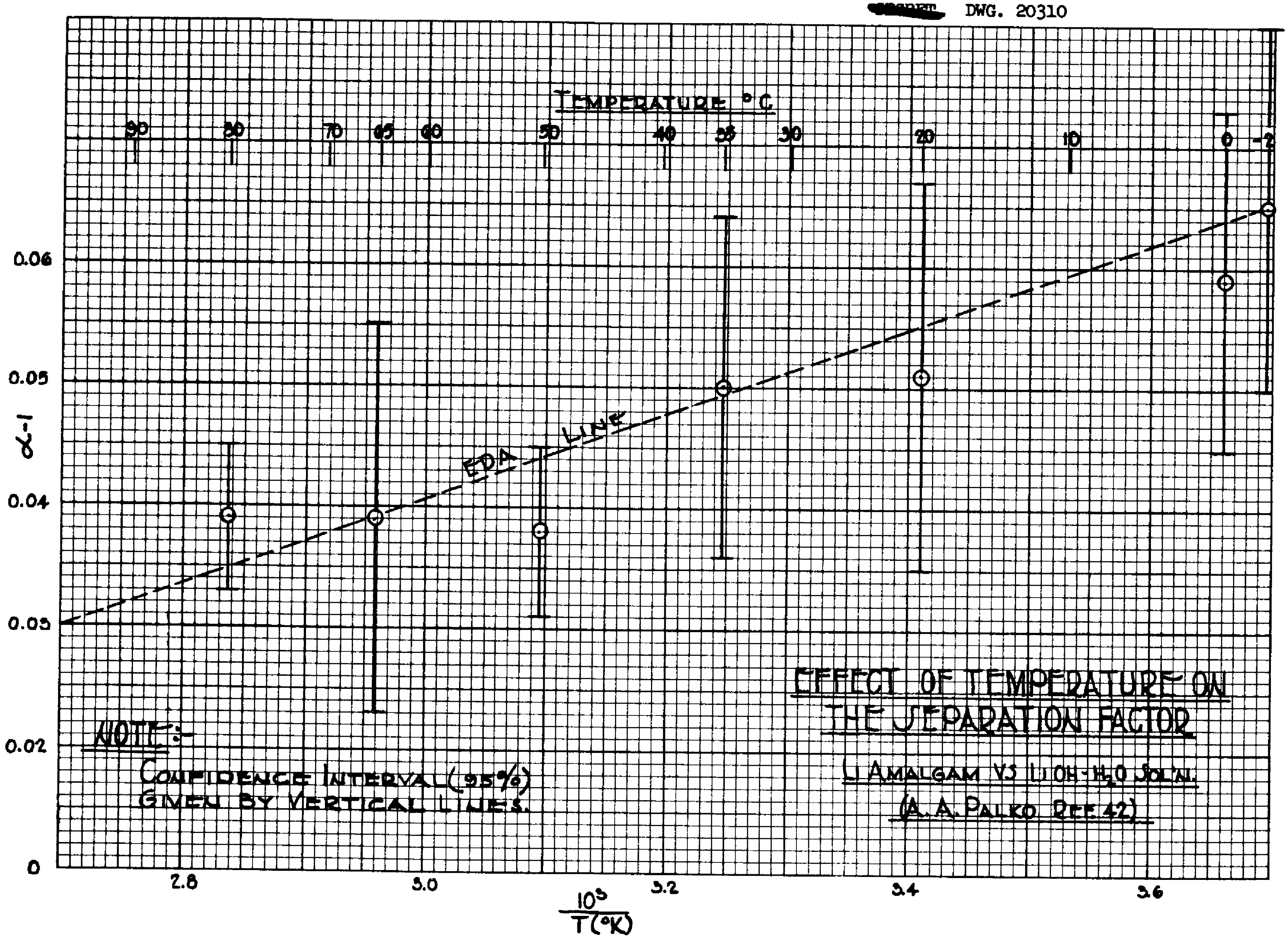

EFFECT OF TEMPERATURE ON THE SEPARATION FACTOR

Li AMALGAM VS LiOH-H_2O SOL'N.
(A. A. PALKO REF 42)

FIGURE 25

Lithium - Mercury - Potassium Chloride - Propylenediamine

Chemical Reaction	$Li(Hg) + KCl_{(solid)} + PDA \rightleftharpoons LiCl_{(PDA)} + K(Hg)$
Reaction Kinetics	Laboratory data indicate that the rate determining step is independent of the amalgam concentration, but is a function of available surface area of KCl when both phases are well dispensed by rapid agitation. (93,94) $-d\frac{[Li(Hg)]}{dt} \approx k \quad f(KCl)$ $k \cong 0.06 \frac{moles/l\text{-}Hg}{min}$ at temperature of $25^{o}C$ and 3 molar (325 mesh) KCl slurry in a laboratory sized mixing unit.
Equilibrium Data	$K_{eq} \cong \frac{[KCl][Li(Hg)]}{[LiCl][K(Hg)]}$ (39) $K_{eq} \cong 1.6 \times 10^{-5}$ at room temperature ($\sim 25^{o}C$) (These data are valid when starting with 0.4M K-amalgam and 0.7M LiCl - PDA solution).

Lithium - Mercury - Propylenediamine - Propylenediamine-Hydrochloride

Chemical Reaction	$2\ Li(Hg) + PDA \cdot 2HCl$ (solution in PDA) $\rightarrow 2LiCl + Hg + PDA + H_2$
Rate of Reaction	Rapid; decomposition of a lithium amalgam was complete within 10 minutes with inefficient laboratory agitation. (39)

Lithium - Mercury - Sodium Chloride - Propylenediamine

Chemical Reaction

$$Li(Hg) + NaCl_{(solid)} + PDA \rightleftharpoons LiCl\ (solution\ in\ PDA) + Na(Hg)$$

Reaction Kinetics

Laboratory tests show rate determining step is a function of the particle size of solid NaCl when both phases are well dispersed by rapid mixing. (89-92)

$$\frac{-d\,[Li(Hg)]}{dt} = k\ \ f_{(NaCl)}$$

where $f_{(NaCl)}$ is some function of the total surface area of salt particles.

Data shown in Figure 26 indicate that

$k_{(max)} \cong 1.2\ \frac{moles}{l\text{-}Hg}/min.$ where the NaCl (PDA-slurry) is 3 molar (-325 mesh) and rate of mixing is 578 rpm in a laboratory sized mixing unit.

Temperature (25 - 100^{o}C) appears to have a negligible effect upon the rate of reaction.

Equilibrium Data

$$K_{eq} = \frac{[Na(Hg)][LiCl]}{[Li(Hg)][NaCl]} \qquad (97)$$

$K \cong 2.8 \times 10^{4}$ at 25^{o}C

$K \cong 1.6 \times 10^{4}$ at 58^{o}C

(These data are valid when starting with 0.7M. Li-amalgam and excess NaCl in PDA).

KINETICS OF SODIUM CHLORIDE INVERSION

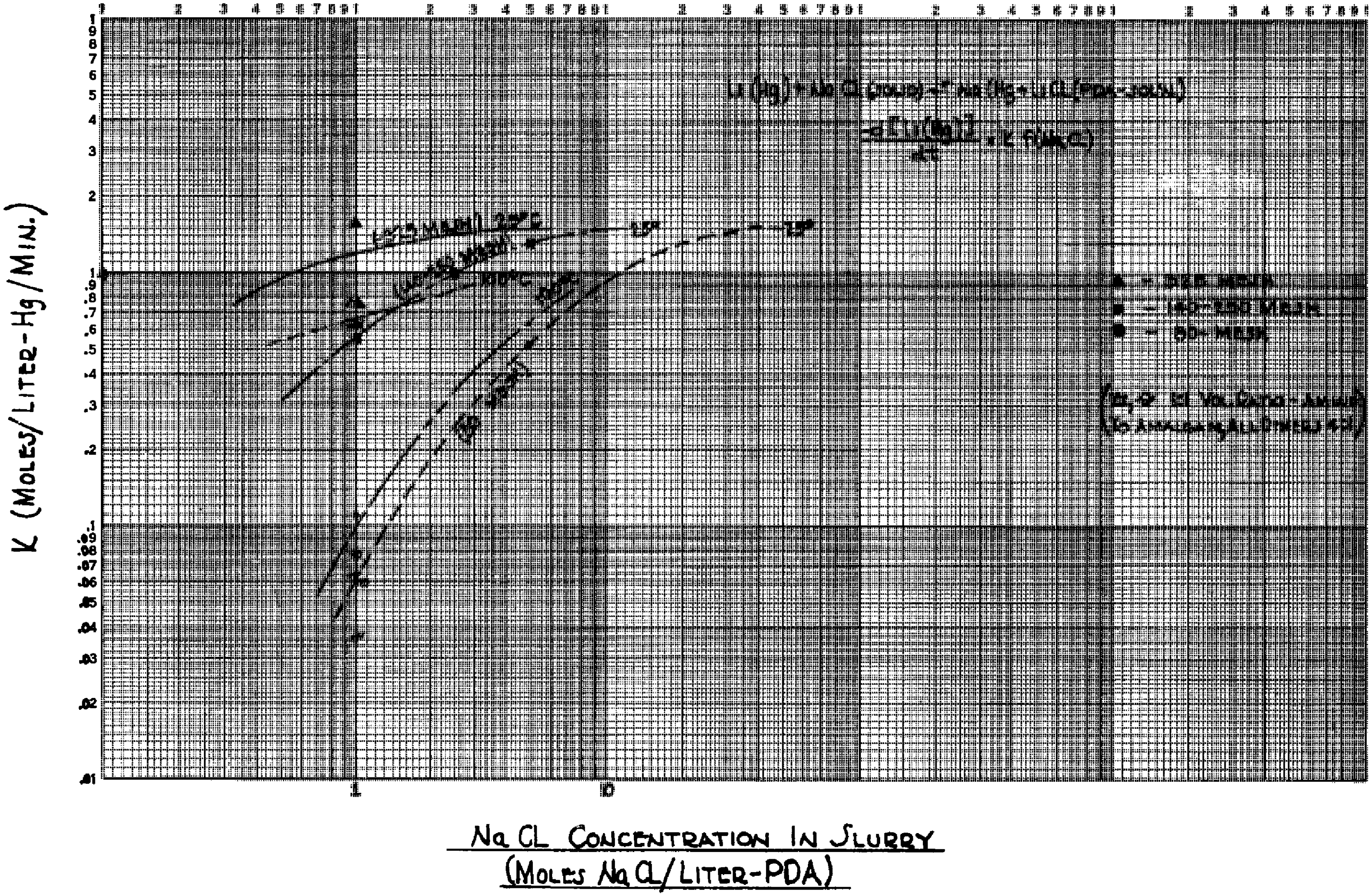

DWG. 20311

FIGURE 26

Lithium - Potassium - Mercury - Lithium Chloride - Propylenediamine

Isotopic Exchange System	Li(Hg) + K(Hg) vs LiCl dissolved in PDA	
Separation Factor	$\alpha = 1.045 \pm 0.008$(95% CI) at 23°C (K/Li in amalgam varied from 2 to 1)	(38)

Lithium - Sodium - Mercury - Lithium Chloride - Propylenediamine

Isotopic Exchange System	Li(Hg) + Na(Hg) vs LiCl dissolved in PDA	
Separation Factor	$\alpha = 1.051 \pm 0.05$ (95% CI) at 23°C (Na/Li in amalgam = 1)	(38)

B. LITHIUM CHLORIDE

Formula Weight	42.40	(3)
Melting Point	614°C, 1137°F	(6)
Boiling Point	1382°C, 2520°F	(6)
	1360°C, 2480°F	(3)
Latent Heat of Fusion	3200 cal/g mole, 75.5 cal/g, 5760 Btu/lb mole, 136 Btu/lb	(6)
Latent Heat of Vapor	36,000 cal/g mole, 850 cal/g, 65,000 Btu/lb mole, 153 Btu/lb	(6)
Vapor Pressure	10^{-4} atm at 663°C, 10^{-3} atm at 769°C, 10^{-2} atm at 911°C	(6)
Density	2.068 g/ml at 25°C	(3)

Heat Capacity	0.288 cal/°C g(Btu/°F lb) at 25°C, 12.2 cal/°C g mole (Btu/°F lb mole) at 25°C	
Refractive Index	1.662	(3)
Structure	Cubic - NaCl type	(3)
Purity of Reagent Grade	$<$0.01% Basic constituents in Baker and Adamson reagent grade LiCl	(43)
Solubility in Anhydrous Solvents	See "Experimental Solubilities of Salts in Anhydrous Solvents" by G. M. Begun	(44)

Lithium Chloride - Ethylenediamine

Thermal Conductivity	5.78 x 10^{-4} cal/sec °C cm, 0.140 Btu/hr ft °F for 0.2M LiCl solution	(45)
Viscosity	See Figure 27	(11)
Conductivity	1.73 x 10^{-4} mho for 0.227M LiCl at 25.2°C	(46)
Solubility	See Figures 16, 28, 29	(47)
Phase Diagram	See Figure 30	(48,49)

Lithium Chloride - 2 Ethylhexanol

Solubility (approx.)	Temp. °C	LiCl mole/liter	(50)
	Rm	1.1	
	165	0.23	
	184	0.09	

Lithium Chloride - Propylenediamine

Boiling Point Rise Constant	3.5°C/mole LiCl in PDA solution	(51)
Latent Heat of Vaporization	129.5 cal/gm (79-119°C)	(51)

[redacted] DWG. 20312

FIGURE 27

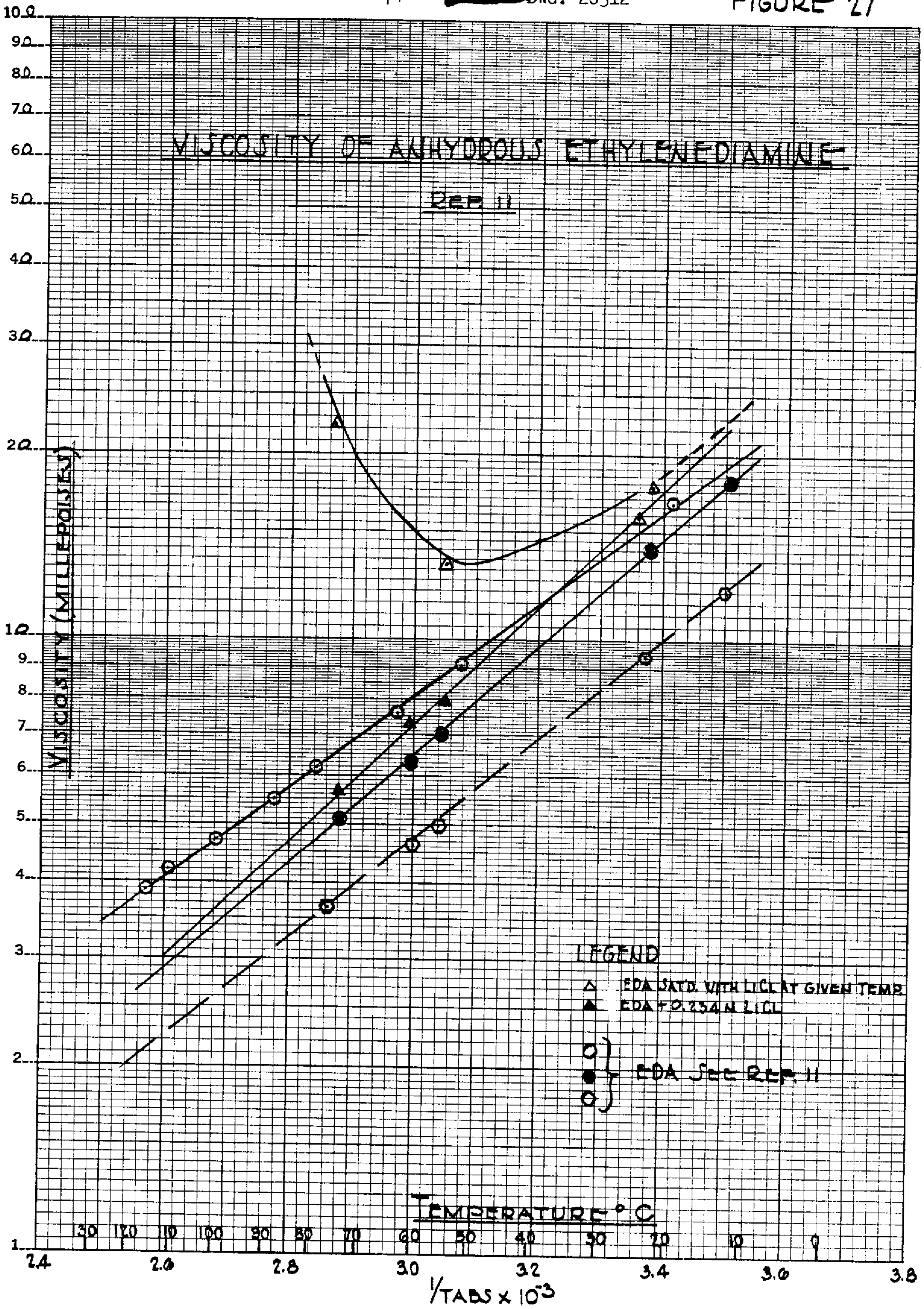

FIGURE 28

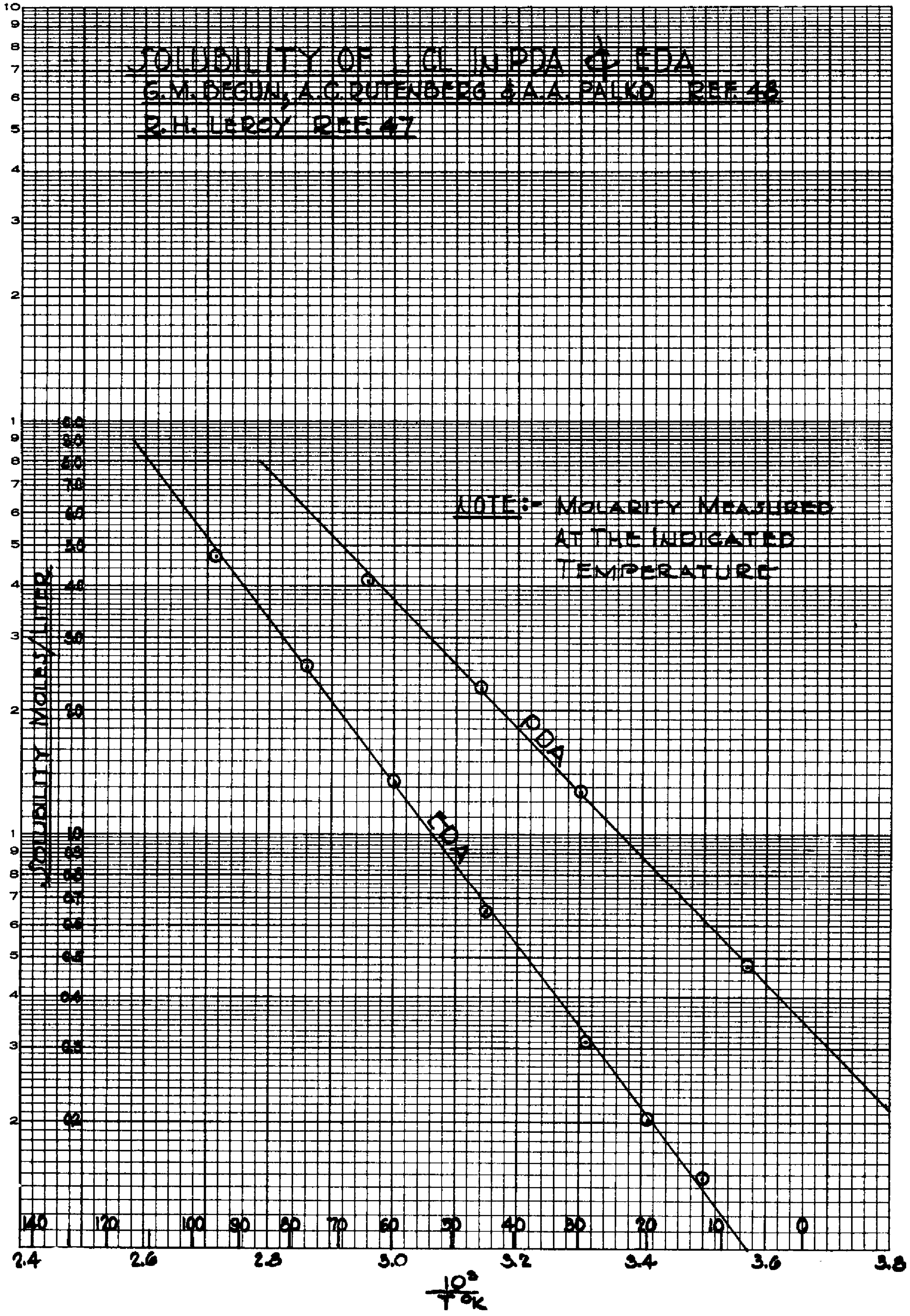

SOLUBILITY OF LiCl IN PDA & EDA
G.M. BEGUN, A.C. RUTENBERG & A.A. PALKO REF. 48
R.H. LEROY REF. 47

NOTE:- MOLARITY MEASURED AT THE INDICATED TEMPERATURE

FIGURE 29

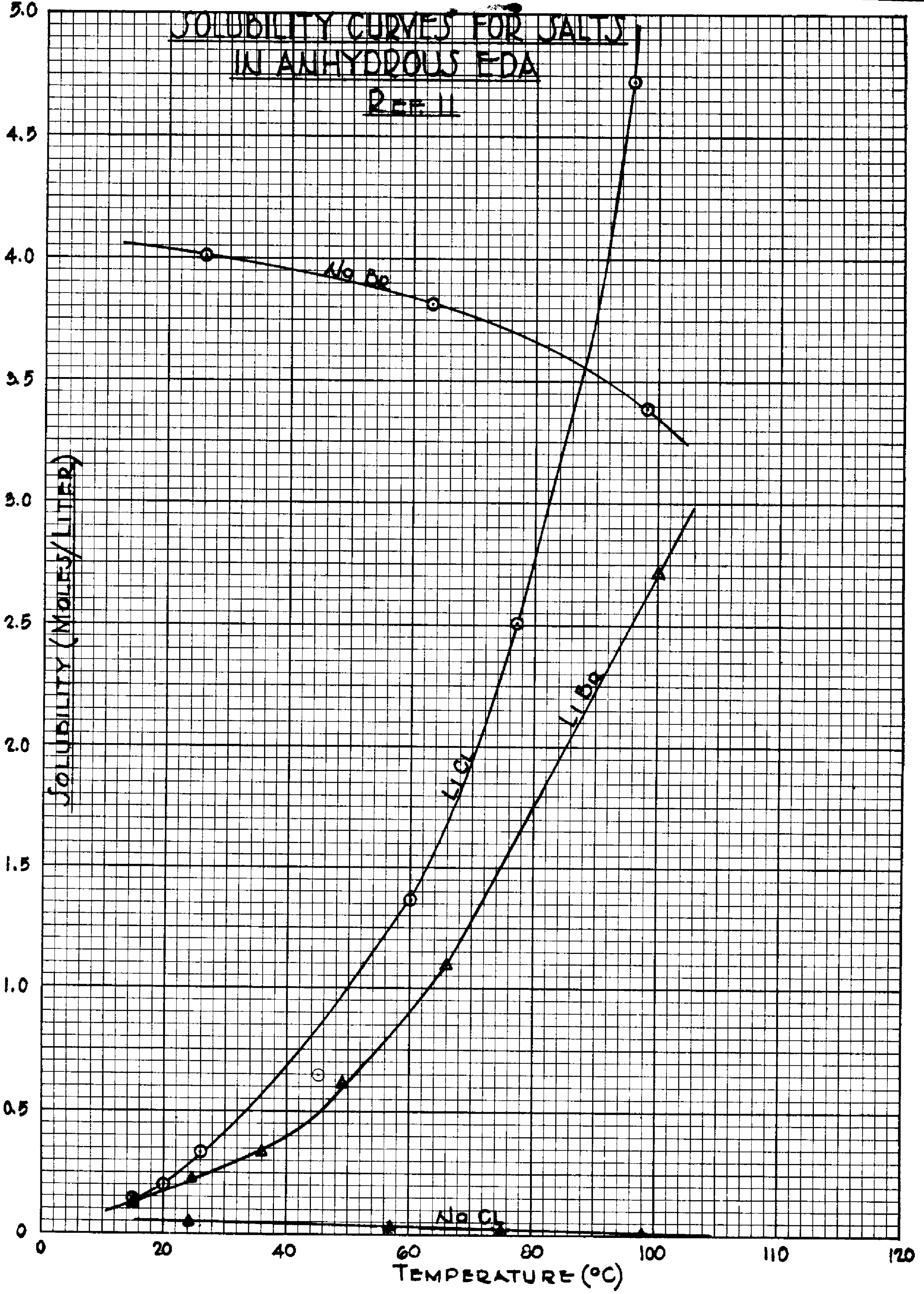

SOLUBILITY CURVES FOR SALTS IN ANHYDROUS EDA

REF. 11

FIGURE 30

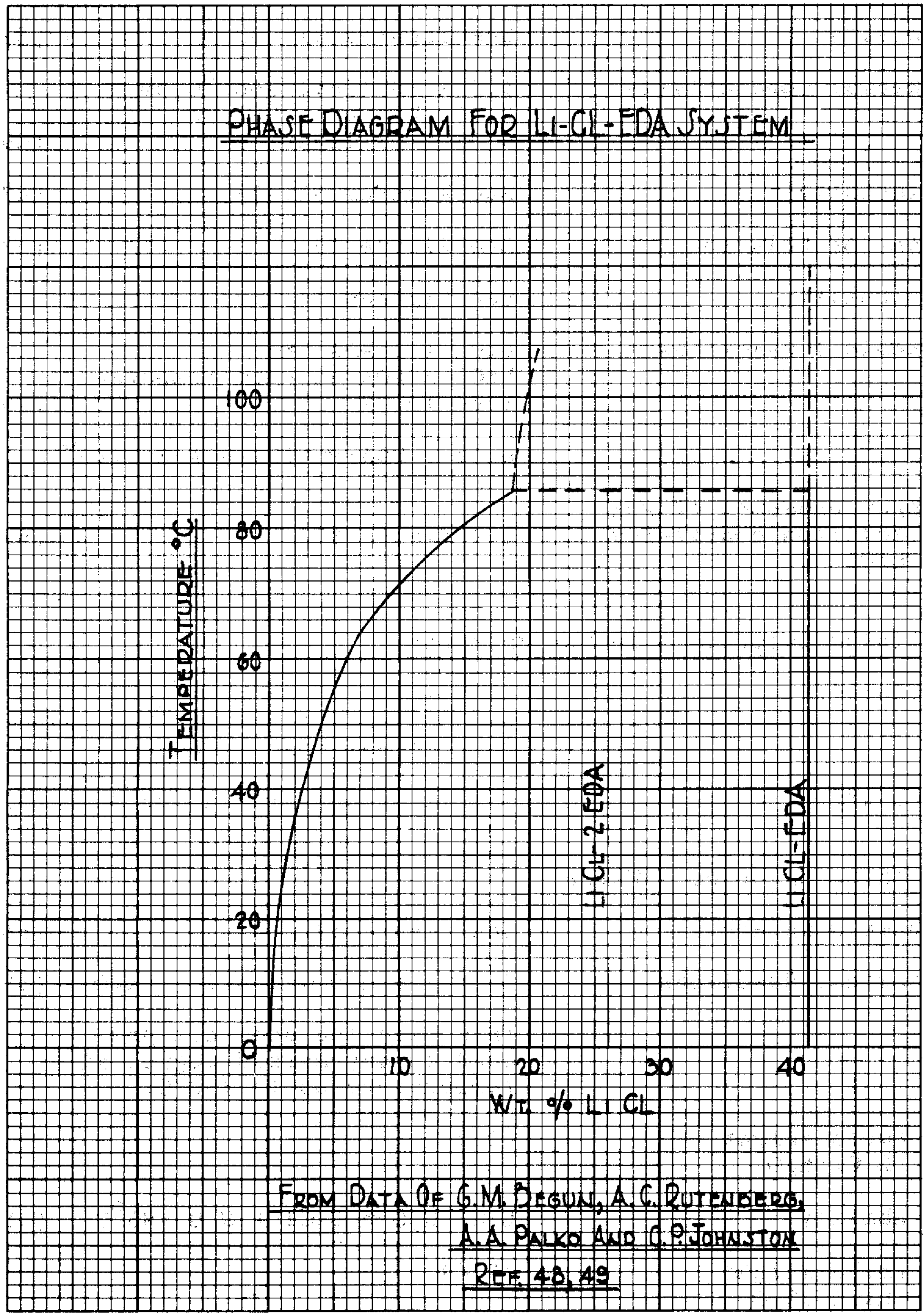

PHASE DIAGRAM FOR LI-CL-EDA SYSTEM

FROM DATA OF G.M. BEGUN, A.C. RUTENBERG, A.A. PALKO AND C.P. JOHNSTON REF. 48, 49

Density	See Figures 31, 32	(47,52)
Thermal Conductivity	5.5×10^{-4} cal/sec °C cm, 0.133 Btu/hr °F ft for 0.8M LiCl/liter	(45)
Viscosity	See Figures 33, 34	(47)
Heat of Solution	See Figure 35	(53)
Solubility	See Figures 16, 28	
Chemical Reactions	$\mathrm{LiCl} + 2\ \mathrm{PDA} \rightarrow \mathrm{LiCl}\cdot 2\ \mathrm{PDA}$ at room temperature to ?	(49)
	$\mathrm{LiCl} + \mathrm{PDA} \rightarrow \mathrm{LiCl}\cdot\mathrm{PDA}$ at 120°C	
Vapor Pressure of PDA solution containing LiCl	See Figure 36	(51)

Lithium Chloride - Tetrahydrofuran

Solubility	1.67 moles/liter at 1°C 0.8 moles/liter at 27°C 0.2 moles/liter at 60°C	(31,32)
Solvation	No stable solvate at 100°C	(31)

Lithium Chloride - Water

Phase Diagrams	See Figure 37	(56)
Chemical Reactions	$2\ \mathrm{LiCl} + \mathrm{H_2O} \rightarrow 2\ \mathrm{HCl} + \mathrm{Li_2O}$	(55)
	This reaction does not proceed to any marked degree at temperature up to 150°C.	
Formula Weight $\mathrm{LiCl}\cdot\mathrm{H_2O}$	60.41	
Stability	$\mathrm{LiCl}\cdot\mathrm{H_2O} \rightarrow \mathrm{LiCl} + \mathrm{H_2O}$ ~96°C	(56)
Formula Weight $\mathrm{LiCl}\cdot 2\mathrm{H_2O}$	78.43	

FIGURE 51

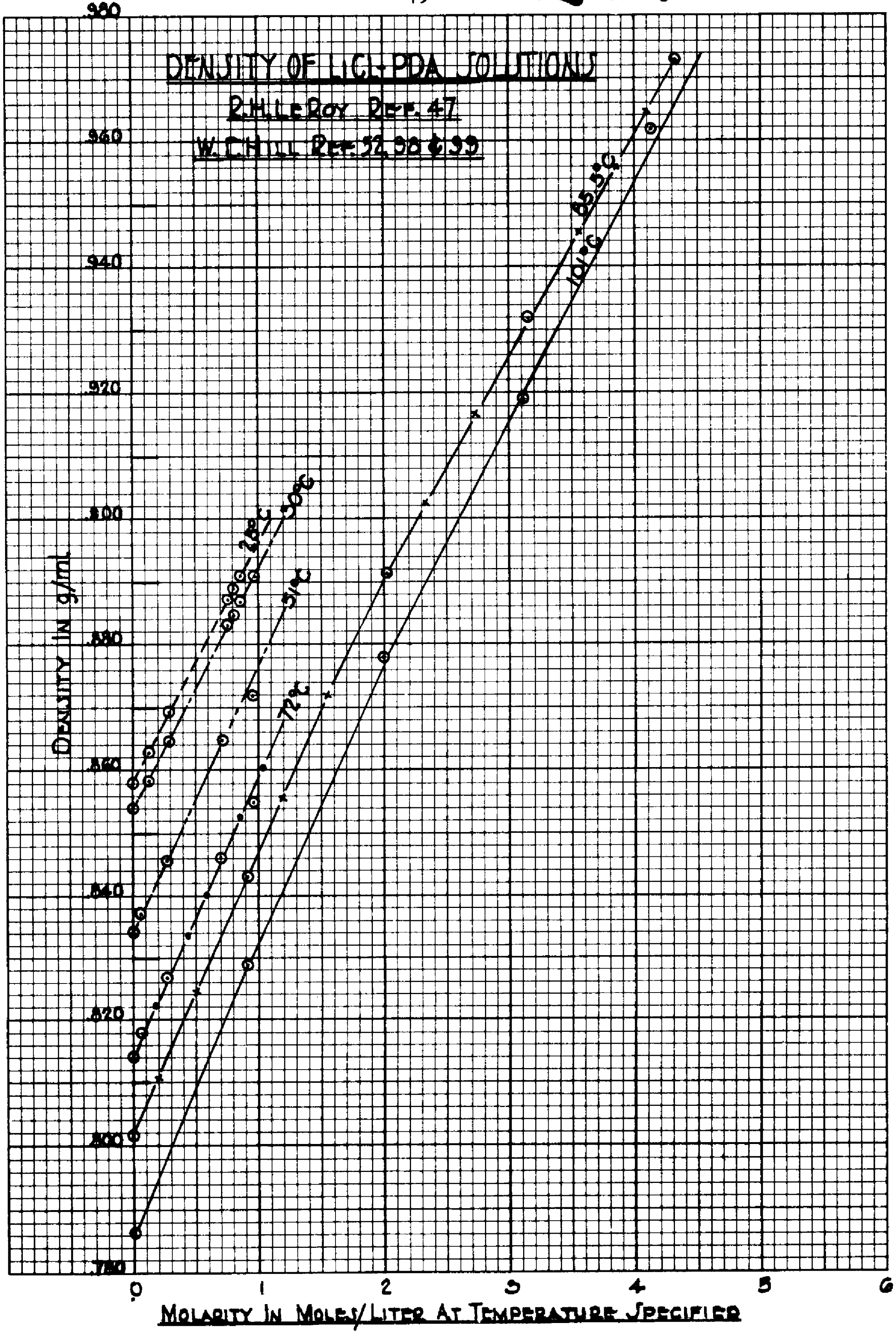
DENSITY OF LiCl-PDA SOLUTIONS
R.H. LeRoy Ref. 47
W.C. Hill Ref. 52, 98 & 99
.980
.960
.940
.920
.900
.880
.860
.840
.820
.800
.780
DENSITY IN g/ml.
25°C
30°C
51°C
72°C
85.5°C
101°C
0
1
2
3
4
5
6
MOLARITY IN MOLES/LITER AT TEMPERATURE SPECIFIED

[redacted]. 20317

FIGURE 32

DENSITY NOMOGRAPH
LiCl- PDA SOLUTIONS

DATA BY R.H. LEROY REF. 47
W.E. HILL REF. 52,98,99

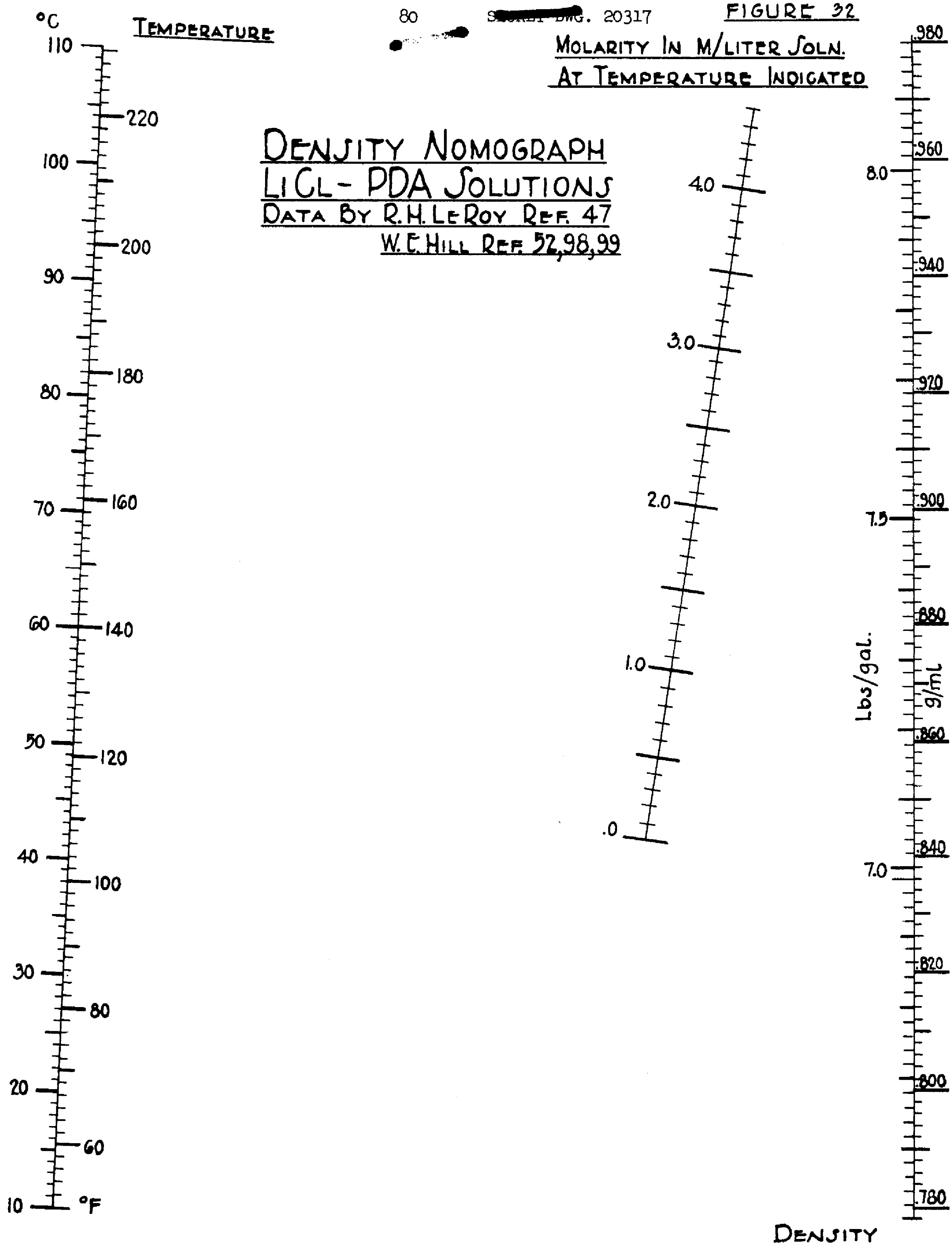

FIGURE 33

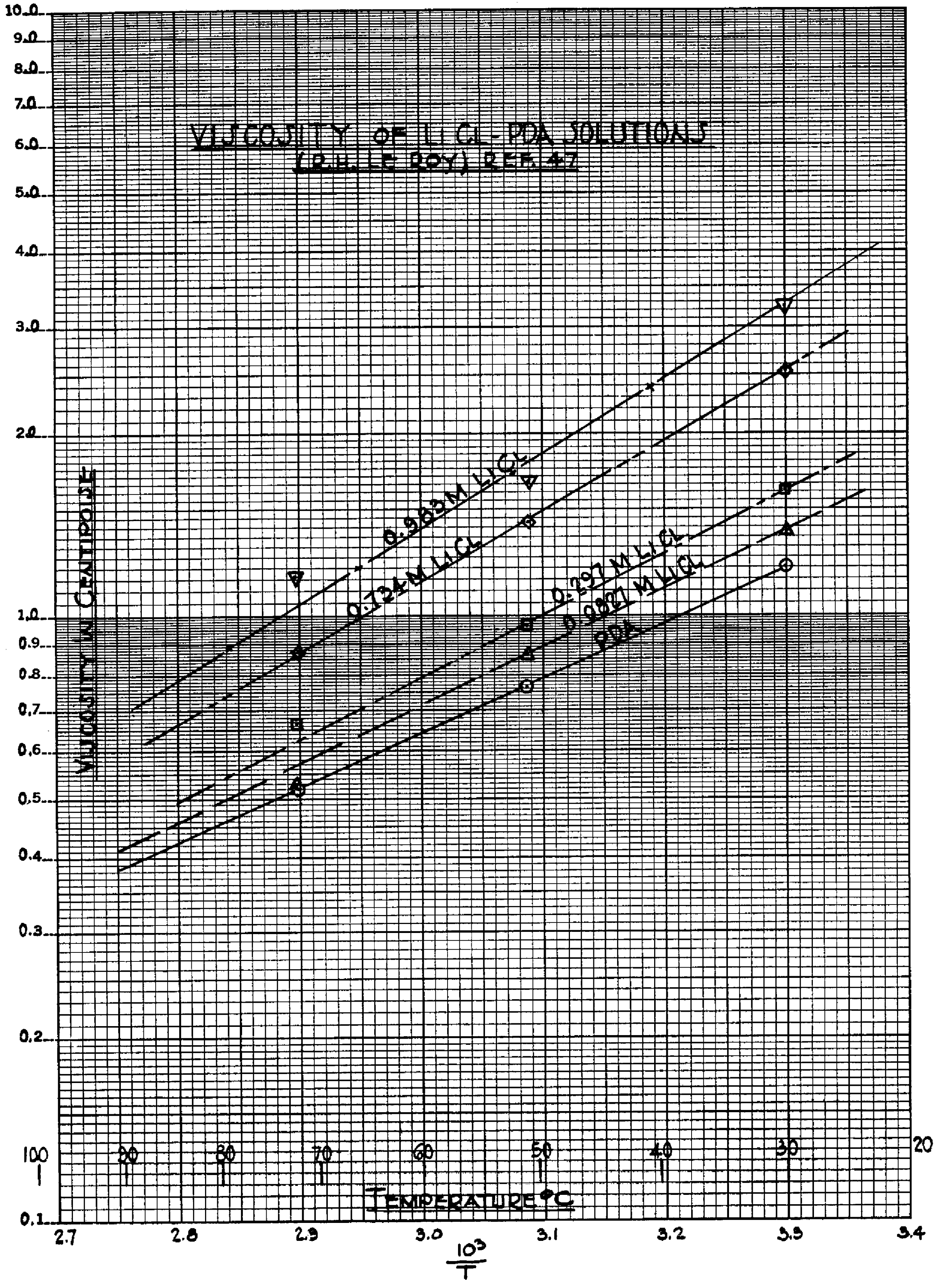
VISCOSITY OF LiCL-PDA SOLUTIONS
(R.H. LE ROY) REF. 47
VISCOSITY IN CENTIPOISE
10.0
9.0
8.0
7.0
6.0
5.0
4.0
3.0
2.0
1.0
0.9
0.8
0.7
0.6
0.5
0.4
0.3
0.2
0.1
0.983M LiCL
0.734M LiCL
0.297 M LiCL
0.0827 M LiCL
PDA
100
90
80
70
60
50
40
30
20
TEMPERATURE °C
2.7
2.8
2.9
3.0
3.1
3.2
3.3
3.4
$\frac{10^3}{T}$

FIGURE 34

VISCOSITY OF Li[redacted]-P[redacted]A SOL'NS

DATA BY R.H. LE ROY REF. 47

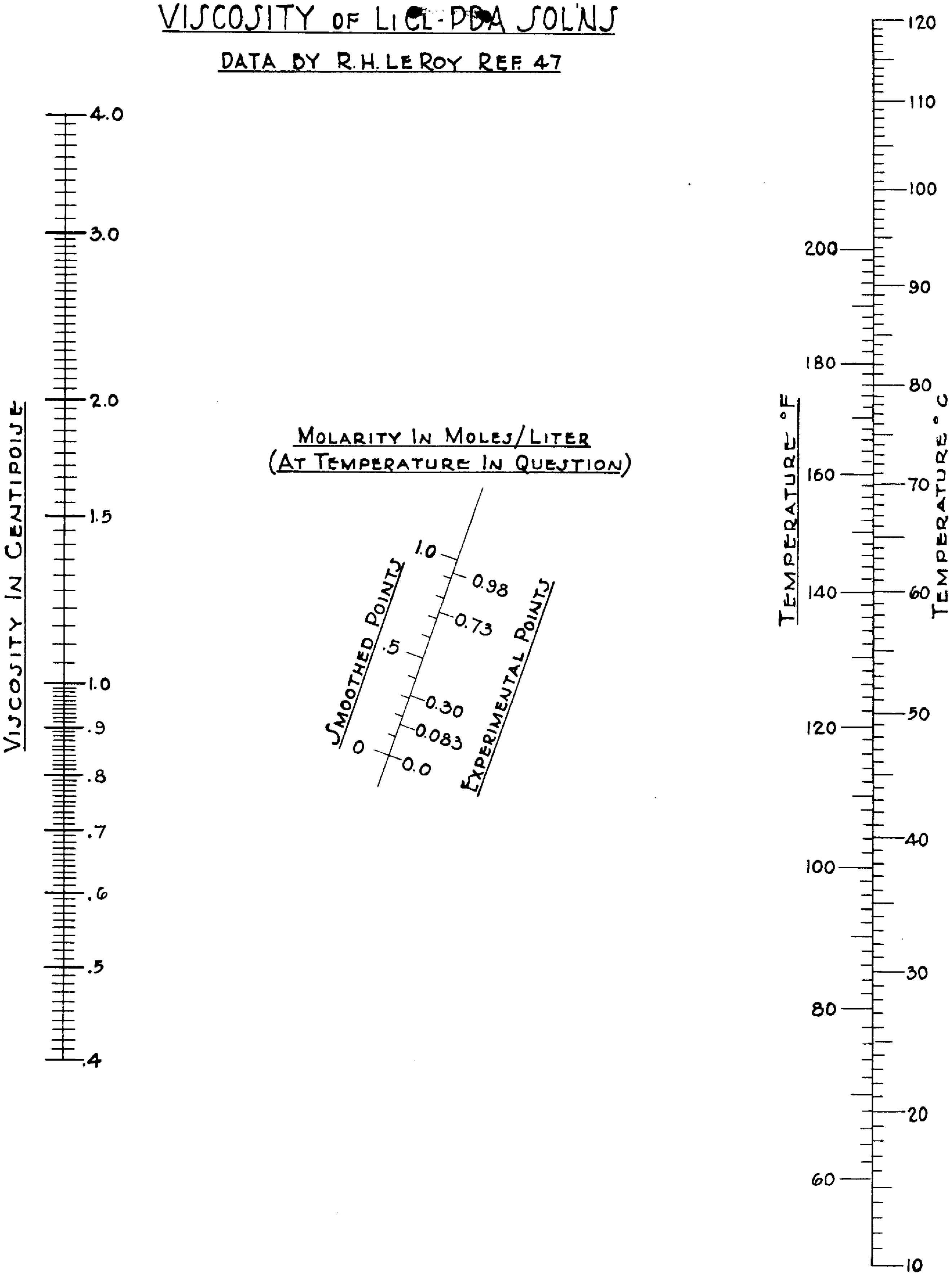

FIGURE 35

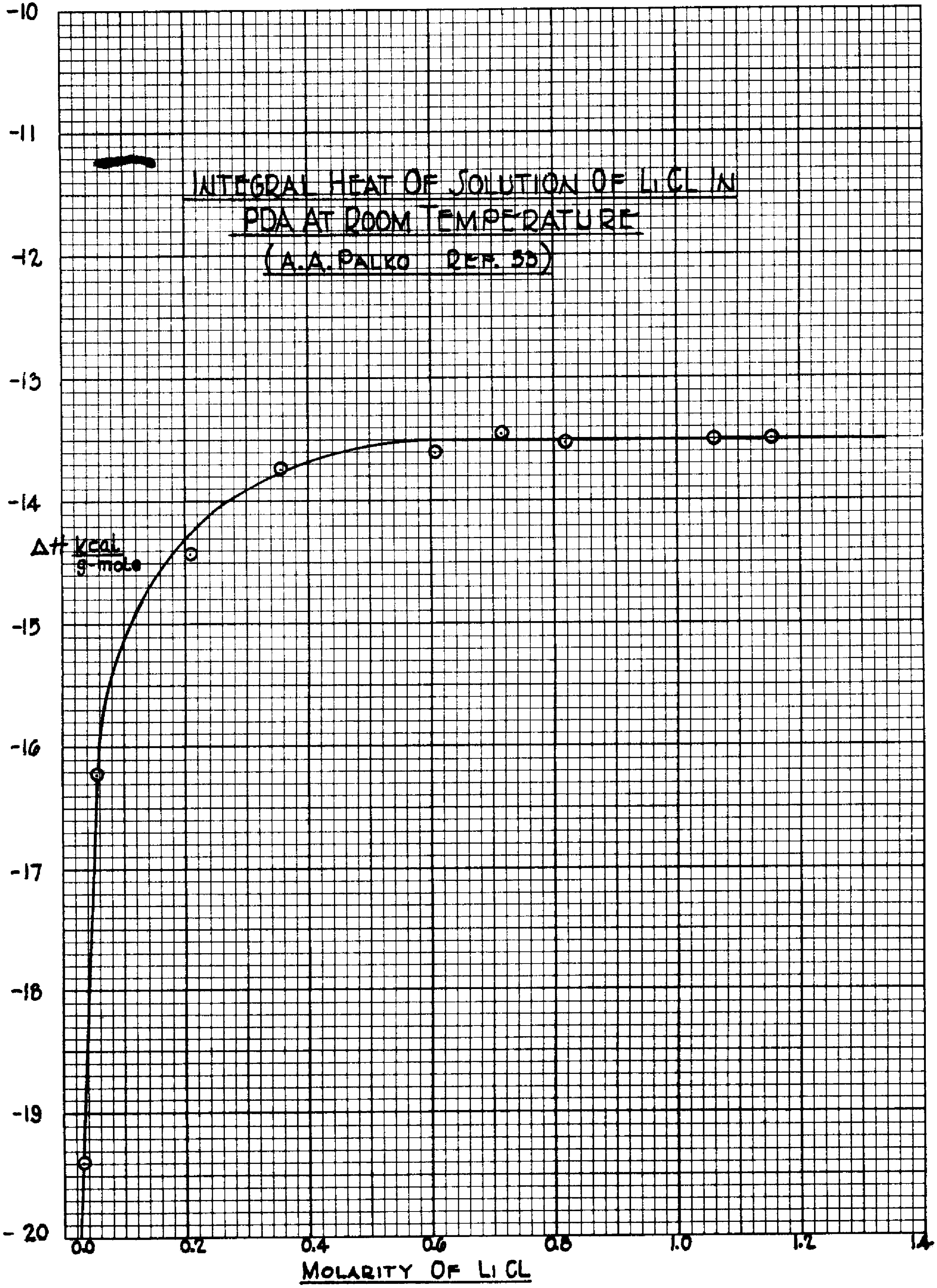

INTEGRAL HEAT OF SOLUTION OF LiCL IN PDA AT ROOM TEMPERATURE

(A.A. PALKO REF. 55)

[redacted]

FIGURE 36

VAPOR PRESSURE OF PDA AND LiCl-PDA SOL'NS.

REF. 51, 86

[redacted]

DWG. 20321

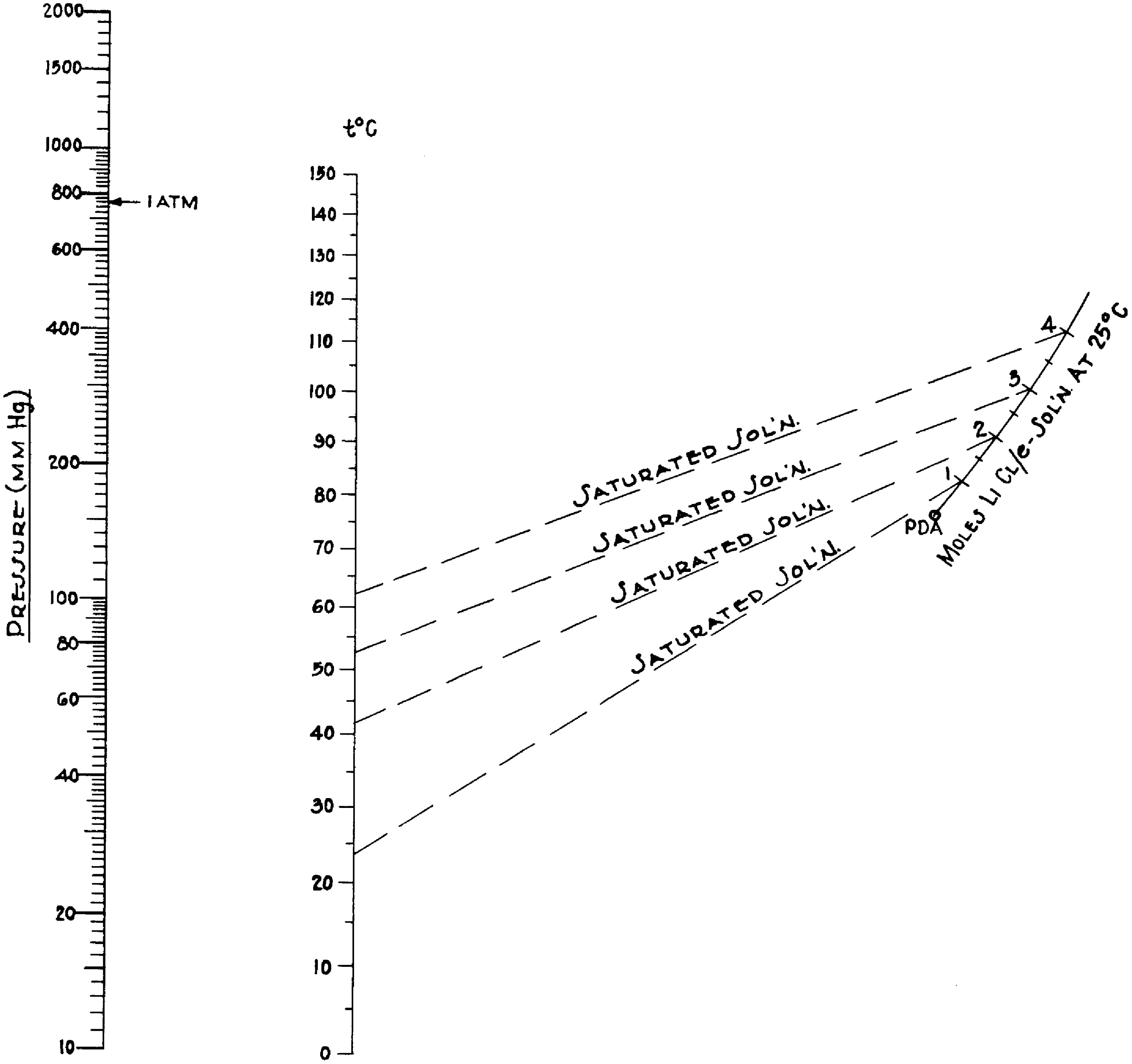

FIGURE 37

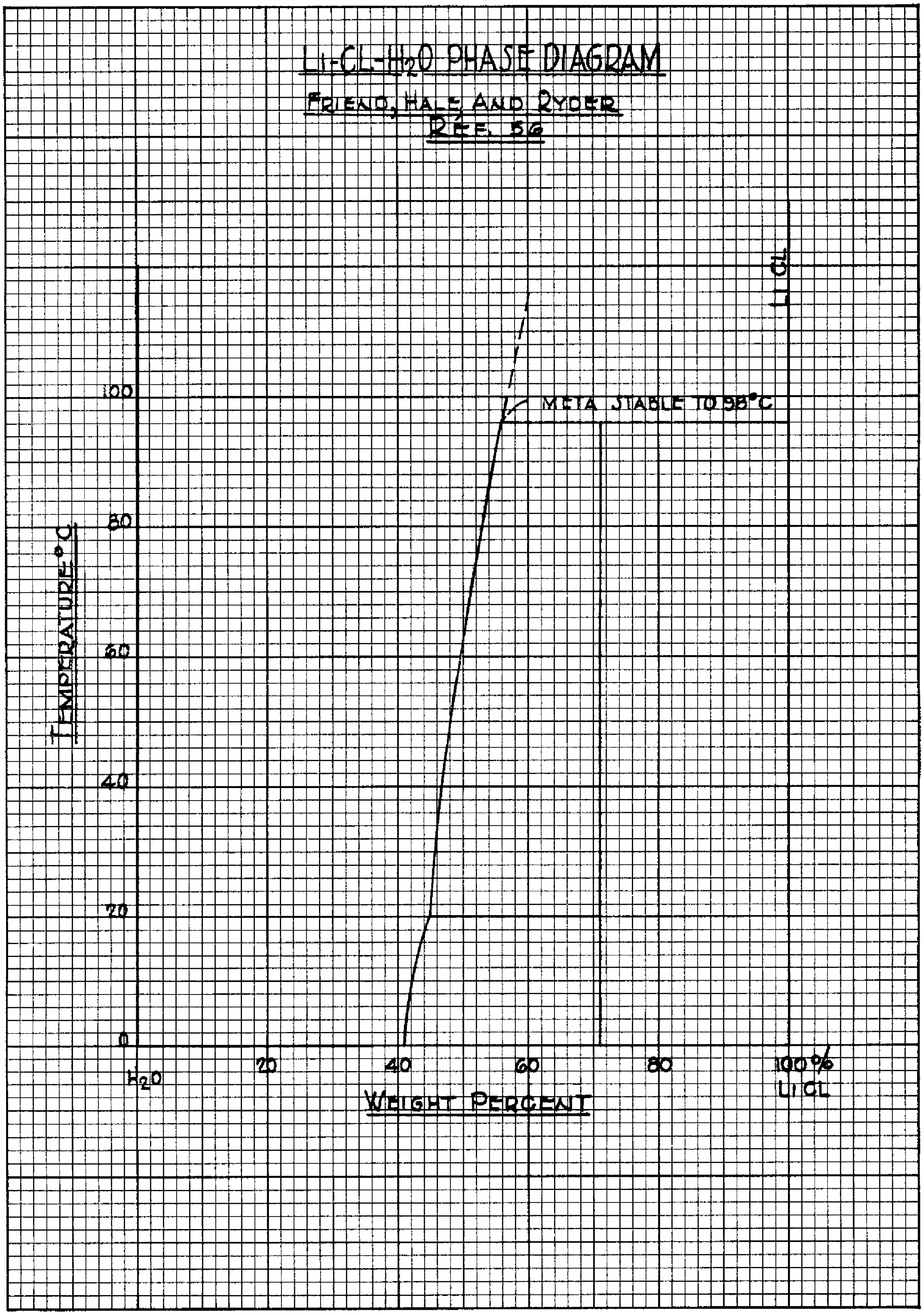

LI-CL-H_2O PHASE DIAGRAM

FRIEND, HALE AND RYDER

REF. 56

Stability	$LiCl\cdot 2H_2O \rightarrow LiCl\cdot H_2O + H_2O$ ~ 20°C	(56)

Lithium Chloride - Ethylenediamine - Propylenediamine

Solubility of LiCl in mixed solvents	% EDA*	Solubility of LiCl mole/liter at room temperature	(40)
	0	1.2	
	10	1.63	
	20	1.55	
	30	1.37	
	40	0.72	
	50	0.72	
	60	0.44	
	70	0.3	
	80	0.3	
	100	0.3	

* % EDA was reported as % of original EDA - PDA mixture prior to addition of excess LiCl.

Lithium Chloride - Sodium Chloride - Ethylenediamine

Solubilities in Solution Saturated with NaCl and LiCl	Solubility moles/liter			(45)
	Temp. °C	NaCl	LiCl	
	26	0.078	0.31	
	60	0.074	0.69	
	80	0.049	2.85	
	101	0.026	4.6	

Lithium Chloride - Magnesium Chloride - Propylenediamine

Phase Diagram	See Figure 38	(57,58)
Solubilities	See Figure 39	(57,58)

Lithium Chloride - Potassium Chloride - Propylenediamine

Solubility of KCl in LiCl-PDA solutions	~0.005 moles KCl/liter of LiCl solution between 24° and 115°C and between 1 and 3.4 molar LiCl	(59)

[redacted]
DWG. 20323

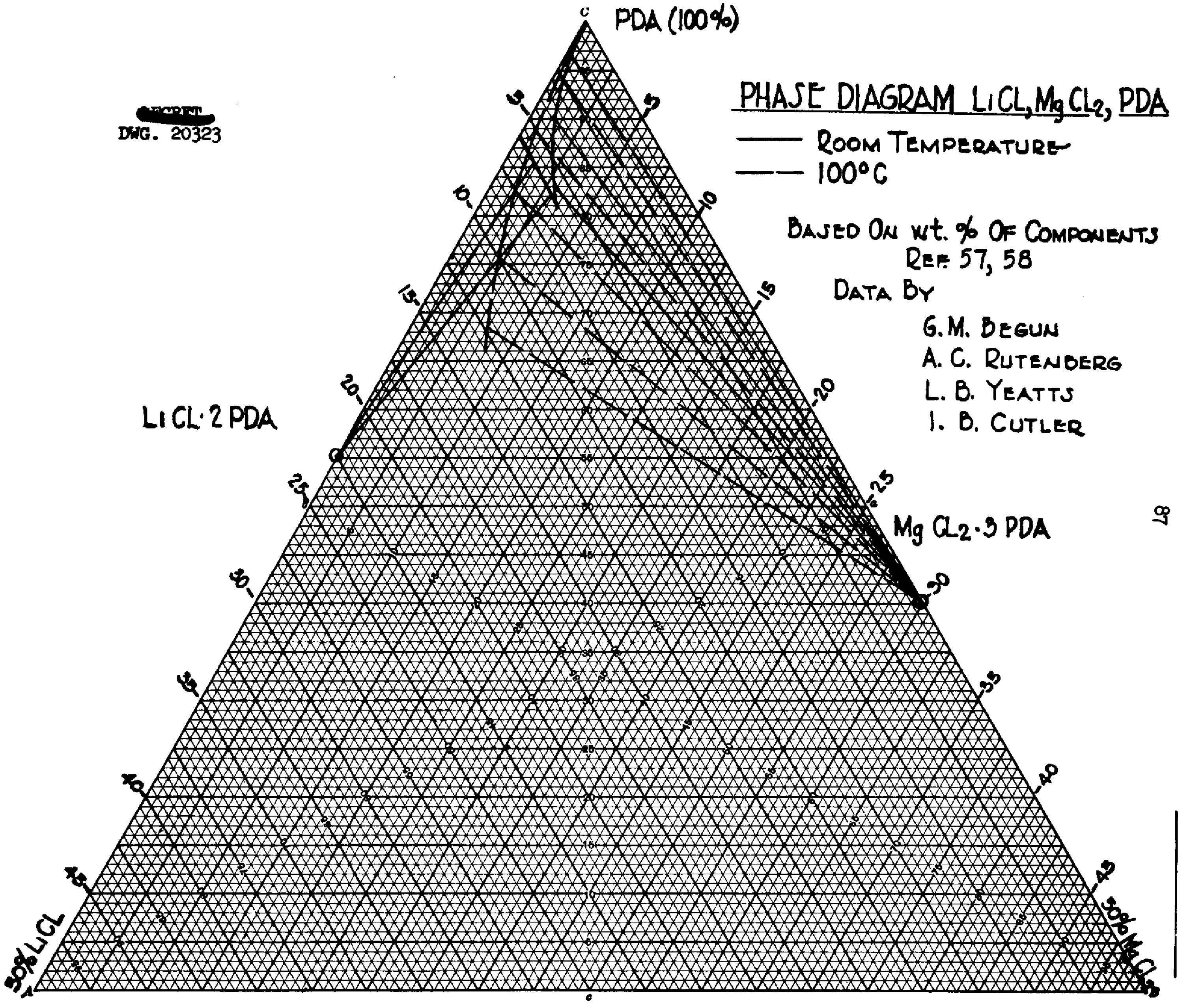

PHASE DIAGRAM LiCL, MgCL$_2$, PDA

—— ROOM TEMPERATURE
— — 100°C

BASED ON wt. % OF COMPONENTS
REF. 57, 58

DATA BY
G. M. BEGUN
A. C. RUTENBERG
L. B. YEATTS
I. B. CUTLER

FIGURE 38

[redacted] DWG. 20324

FIGURE 39

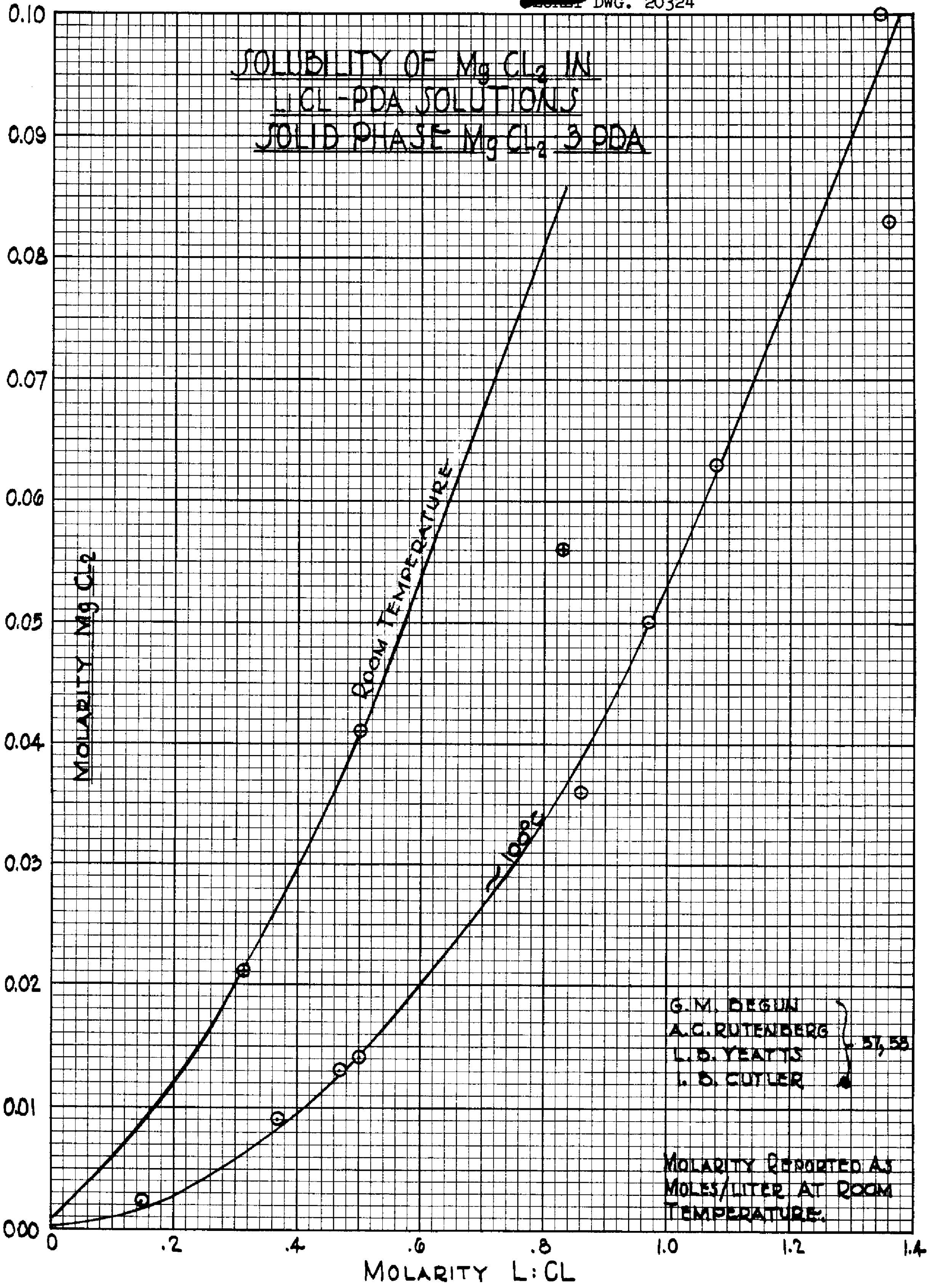

Lithium Chloride - Sodium Chloride - Propylenediamine

		Solubility moles/liter		
	Temp. °C	NaCl	LiCl	
Solubilities in Solution saturated with NaCl and LiCl	30	0.008	0.943	(45)
	72	0.0047	3.31	
	92	0.006	3.73	
	100	0.018(?)	3.97	
	130	0.013(?)	4.28	

Solubilities in Solution saturated with NaCl	See Figure 40	(60)

Lithium Chloride - Propylenediamine - Tetrahydrofuran

	% PDA	Room Temperature Solubility (moles/liter)	
Solubility of LiCl in mixed solvents of PDA and THF	1.4	0.31	(34)
	40.9	0.054	
	87.4	0.77	

Lithium Chloride - Mercury - Water

Chemical Reaction (electrolysis of LiCl)	LiCl (in H_2O solution) + Hg + e $\rightarrow$ Li(Hg) + 1/2 Cl_2 + H_2O	
Effect of PDA impurity	PDA/LiCl $\gtrless$ 0.001 lowers cell efficiency $\gtrless$ 10%. This may be due to two indistinguishable side reactions H_3O + e $\rightarrow$ 1/2H_2 + H_2O and Li(Hg) + H_2O $\rightarrow$ LiOH + 1/2H_2	(62)

Lithium Chloride - Propylenediamine - Water

Phase Diagram	See Figure 41	(61)

Lithium Chloride - Propylenediamine - Magnesium - Mercury

Chemical Reaction	Mg(Hg) + LiCl (in PDA solution) $\rightarrow$ Li(Hg) + $MgCl_2 \cdot 3PDA$ (insoluble) + PDA

FIGURE 40

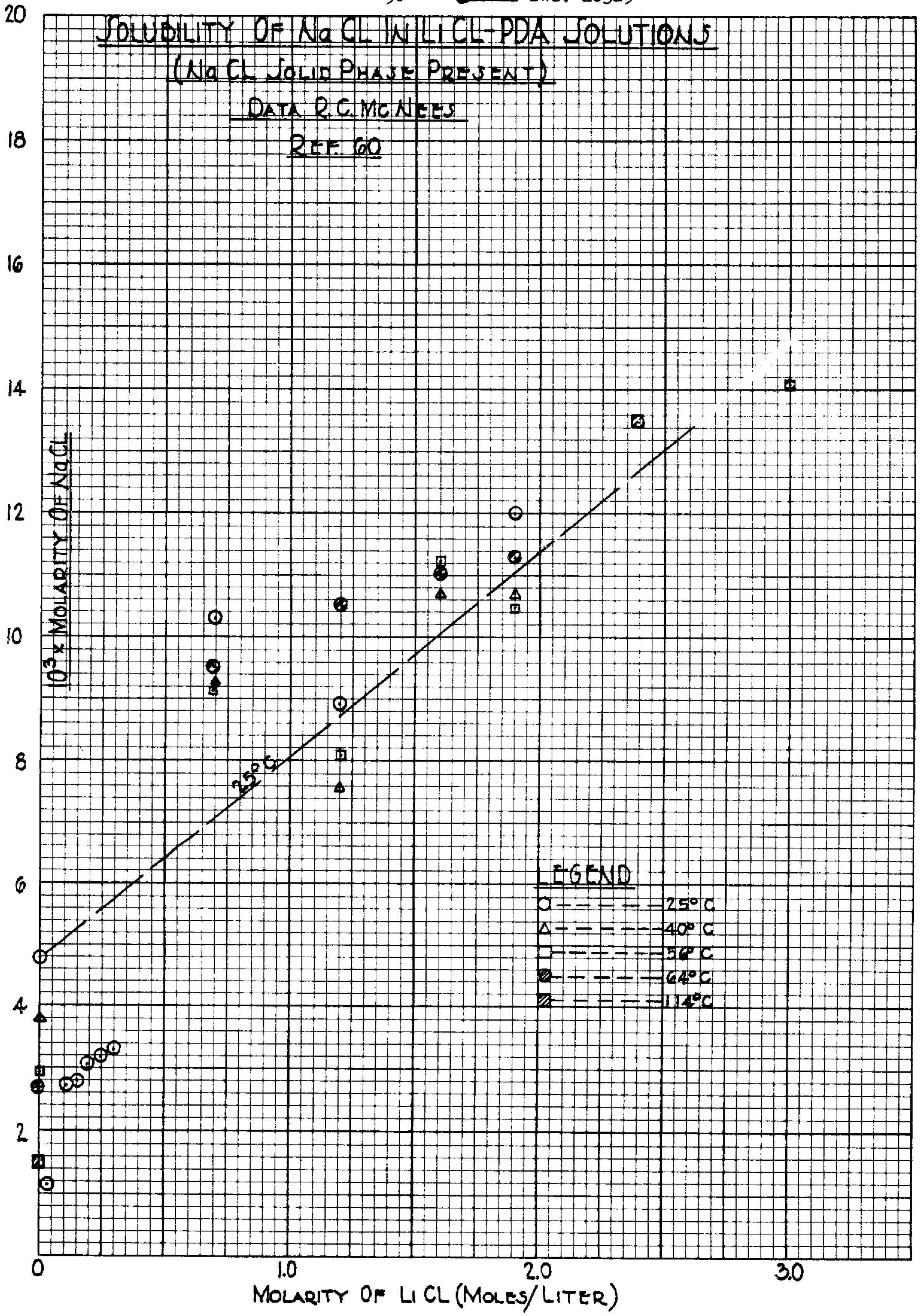

SOLUBILITY OF NaCL IN LiCL-PDA SOLUTIONS
(NaCL SOLID PHASE PRESENT)
DATA R.C. McNEES
REF. 60

$LiCl$-PDA-H_2O PHASE DIAGRAM

1 45.5 g/100g. Sat. Sol. p 912 Seidell Ref 4

2.- 4.6 g/100g. Sat. Sol. Interpolated From
Orex Report YB-30-107
Ref 61

[redacted]
DWG. 20326

Conditions
23 ± 1°C.
Atmospheric Pressure.
All Measurement As
Weight Percent

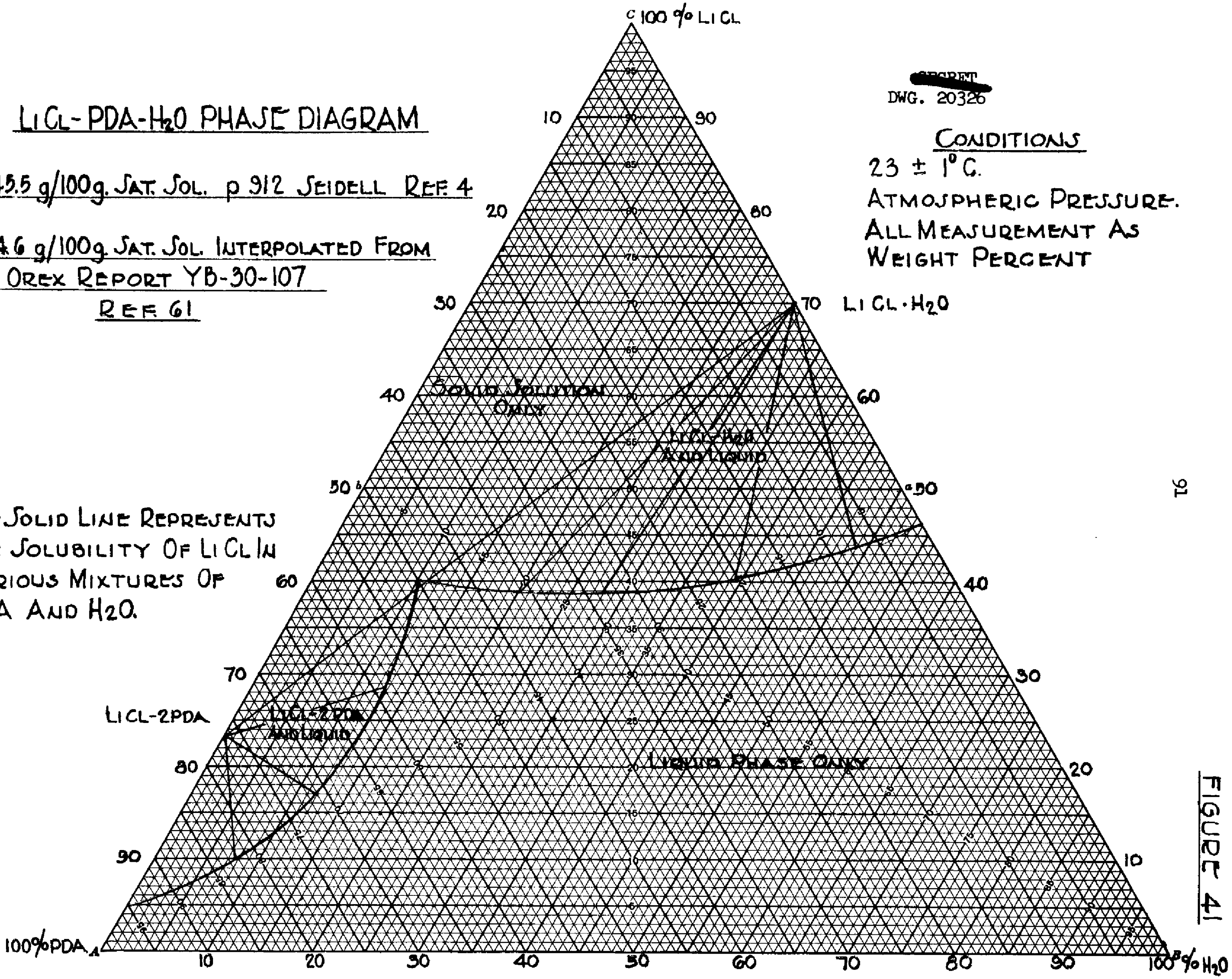

The Solid Line Represents
The Solubility Of LiCl In
Various Mixtures Of
PDA And H_2O.

FIGURE 41

Reaction Kinetics

(1) Reaction Rate appears to be first order with respect to concentration of Mg in the amalgam and independent of the LiCl in the amine phase when LiCl is in stoichiometric excess. (100, 90, 91, 92)

$$-\frac{d(Mg)}{dt} = k(Mg)$$

or:

$$\ln\frac{(Mg)_o}{(Mg)_f} = kt$$

where k is specific rate constant, Mg_o and Mg_f are the initial and final Mg amalgam concentrations, and 't' is the time required to reach a concentration of Mg_f.

(2) Effect of temperature: See Figure 42.

$$\ln k \cong \frac{-2000}{T} + 5.92$$

where T is the absolute temperature (Kelvin)

$k \cong 1.8$ (min.$^{-1}$) when the phases are vigorously contacted at 100°C in a laboratory (Rushton type) contactor.

Equilibrium data

$$K_{eq} = \frac{[Li(Hg)]^2\ [MgCl_2]}{[LiCl]^2\ [Mg(Hg)]} \qquad (57)$$

$K \cong 78$ at 25°C

$K \cong 10.6$ at 60°C

(These data are valid when starting with about 0.4 molar Magnesium - Amalgam and excess LiCl - PDA solution).

FIGURE 42

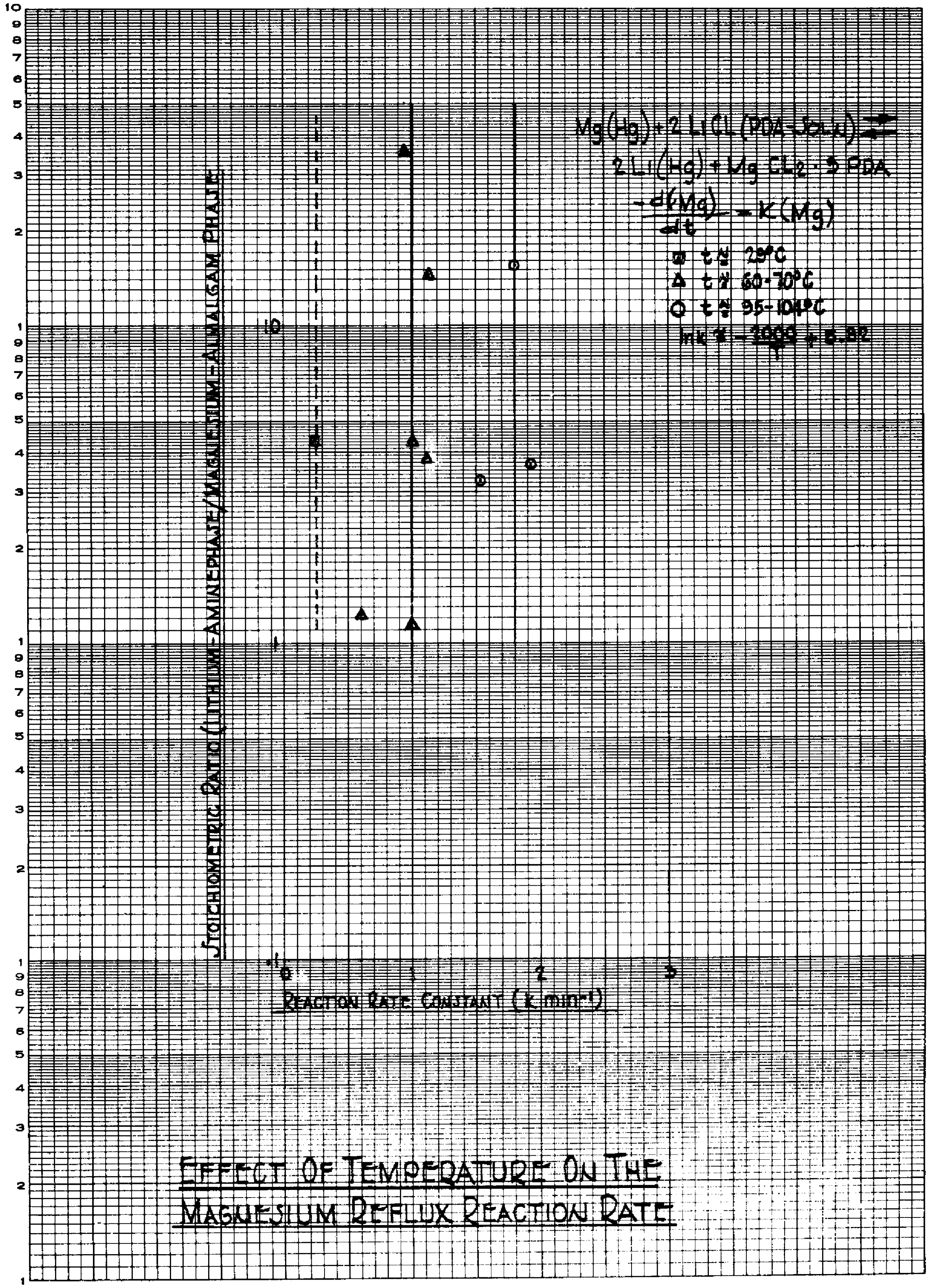

Effect Of Temperature On The Magnesium Reflux Reaction Rate

Lithium Chloride - Propylenediamine - Potassium - Mercury

Chemical Reaction	K(Hg) + LiCl (in PDA solution) $\rightleftharpoons$ Li(Hg) + PDA + KCl (insoluble)	
Reaction Kinetics	Reaction rate is very rapid when phases are well dispersed. Equilibrium was reached in less than 2 minutes in a laboratory mixer column contactor at 100°C. The effect of temperature on the reaction rate has not been investigated.	(101)
Equilibrium Data	See Figures 43, 44, 45	(93,102)

Lithium Chloride - Propylenediamine - Sodium - Mercury (See also Li-Hg-NaCl-PDA)

Chemical Reaction	Na(Hg) + LiCl (in PDA solution) $\rightleftharpoons$ Li(Hg) + PDA + NaCl (insoluble)	
Reaction Kinetics	See page 70 for kinetics of reverse reaction. Rate of forward reaction has not been investigated.	
Equilibrium Data	See Figure 46.	(93)

C. LITHIUM HYDROXIDE

Formula Weight	23.95	
Melting Point	462°C	(5)
	450°C	(2)
	445°C	(3)
Boiling Point	Decomposes 900°C	(63)
Density	1.43 g/ml at 20°C	(3)
	2.54 g/ml at 20°C	(2)

[redacted] DWG. 20328

FIGURE 43

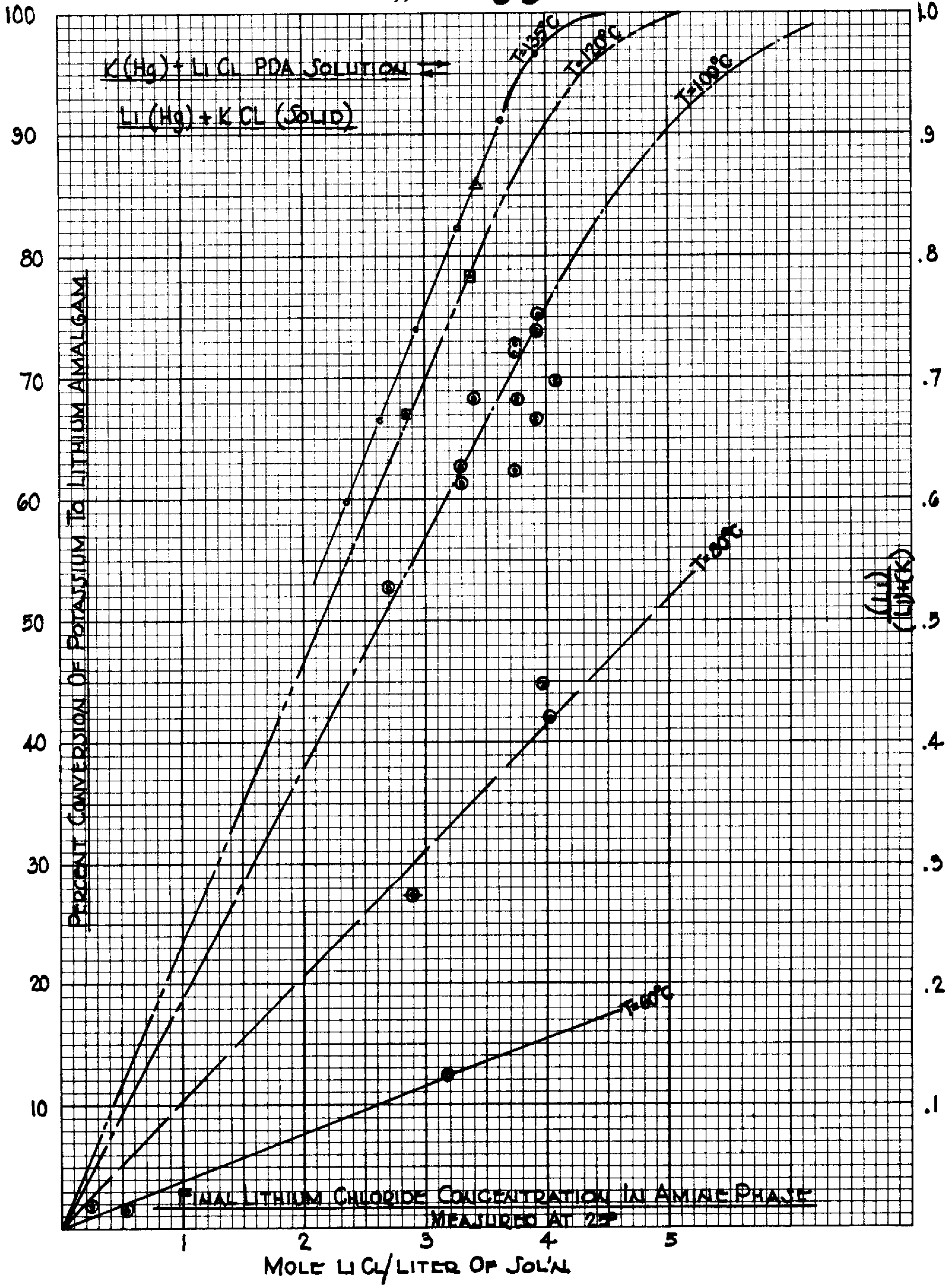

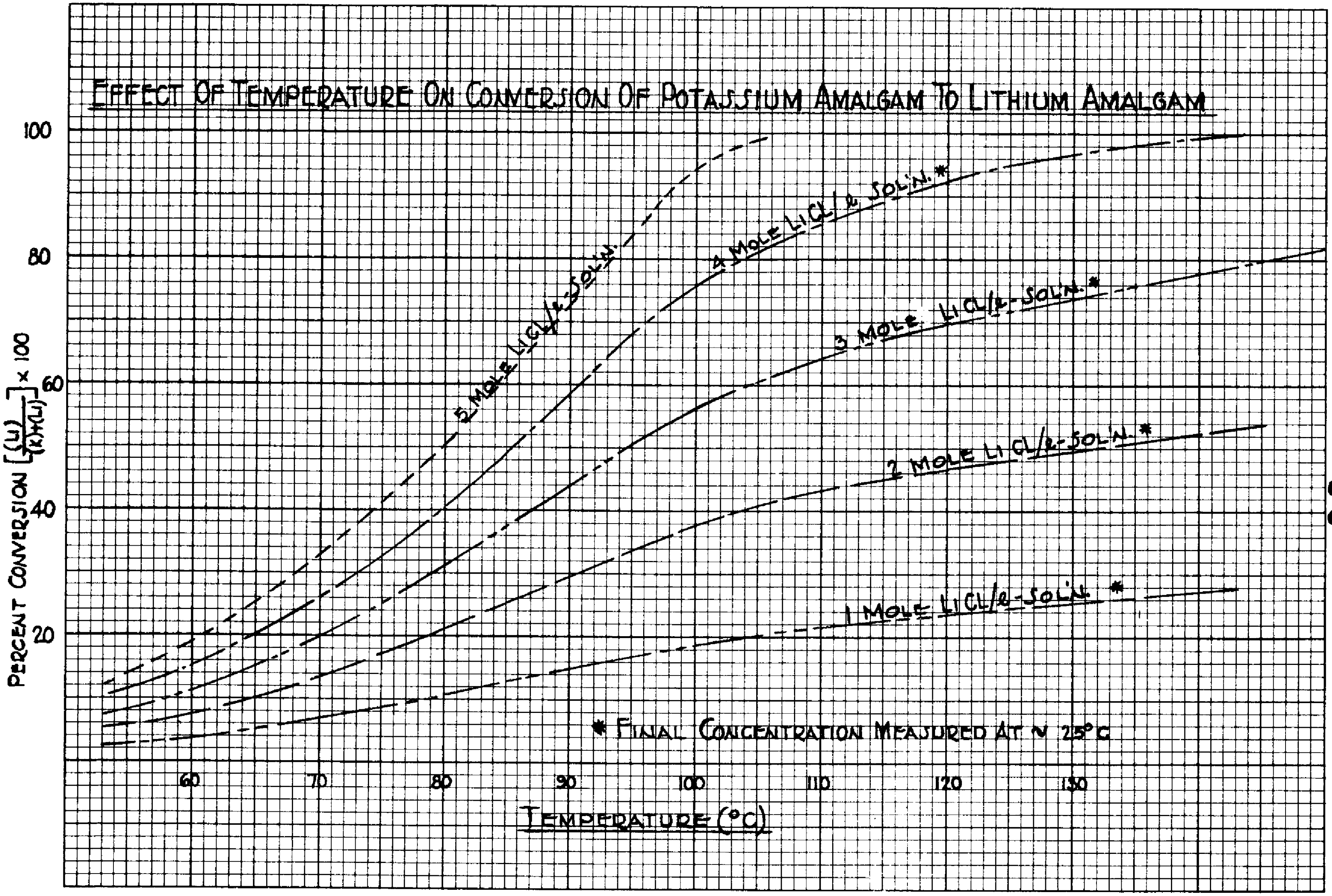

DWG. 20329

FIGURE 44

FIGURE 45

EQUILIBRIUM CONCENTRATION OF [redacted](Hg) FOR CLOSED CYCLE REFLUX AT 100°C

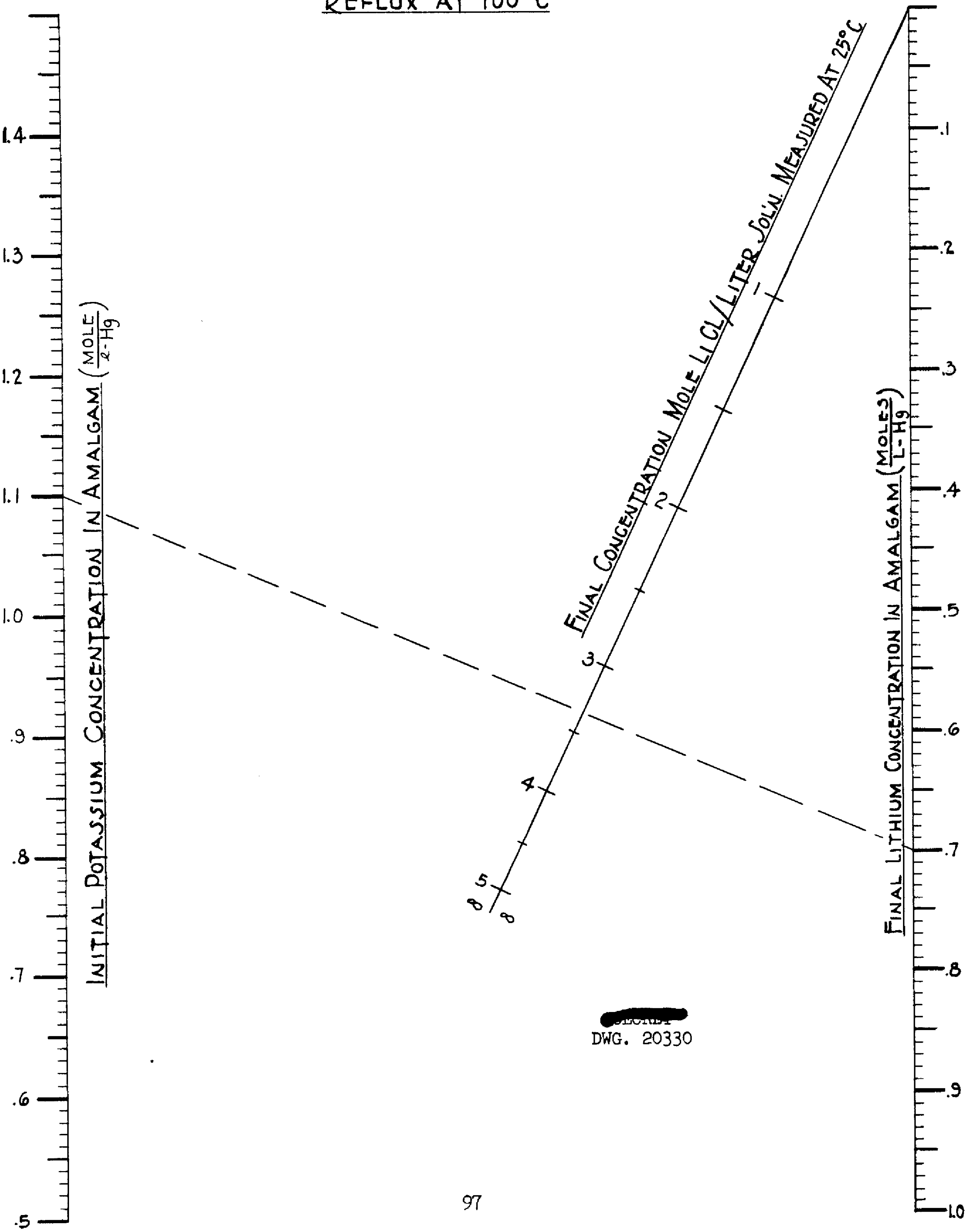

[redacted]
DWG. 20330

[redacted] DWG. 20331

FIGURE 46

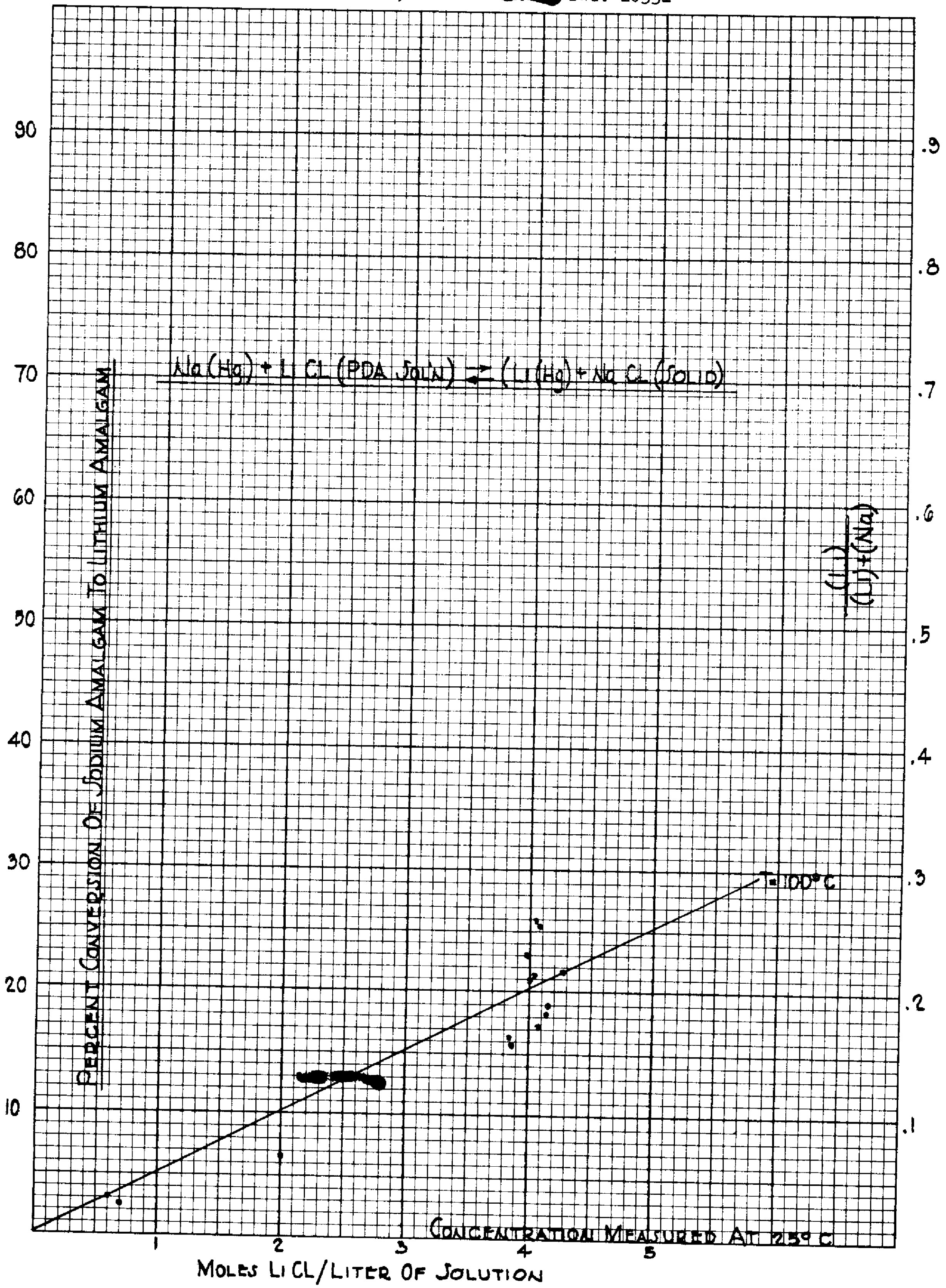

[redacted]

Lithium Hydroxide - Water

Formula Weight ($LiOH \cdot H_2O$)	41.96	
Phase Diagram	See Figure 47	(64)
Solubility of LiOH in H_2O	See Figures 16, 48	(64)
Density of LiOH Solutions	See Figures 49, 50	(9)

Lithium Hydroxide - Sodium Phosphate - Water

Chemical Reaction	LiOH aq. + Na_3PO_4 aq $\longrightarrow$ Li_3PO_4 (insoluble) + NaOH aq.	
Conditions for Filterable Precipitate	Determined by A. A. Palko	(53)

III. MAGNESIUM AND MAGNESIUM COMPOUNDS

A. MAGNESIUM

Atomic Weight	24.36	
Melting Point	651°C, 1204°F	(1)
Boiling Point	1103°C, 2017°F	(1)
Latent Heat of Fusion	82.2 cal/g, 148 Btu/lb, 1990 cal/g mole, 3590 Btu/lb mole	(1)
Latent Heat of Vaporization	1337 cal/g, 2405 Btu/lb, 3250 cal/g mole, 5850 Btu/lb mole	(1)
Vapor Pressure	$\log_{10} P_{mm} = \frac{-7167}{T(^{\circ}K)} + 8.088$	(1)
	Accuracy 10% 1000 - 1400°K 20% 600 - 1450°K	(1)
	See Figure 7	

UNCLASSIFIED DWG. 20332

FIGURE 47

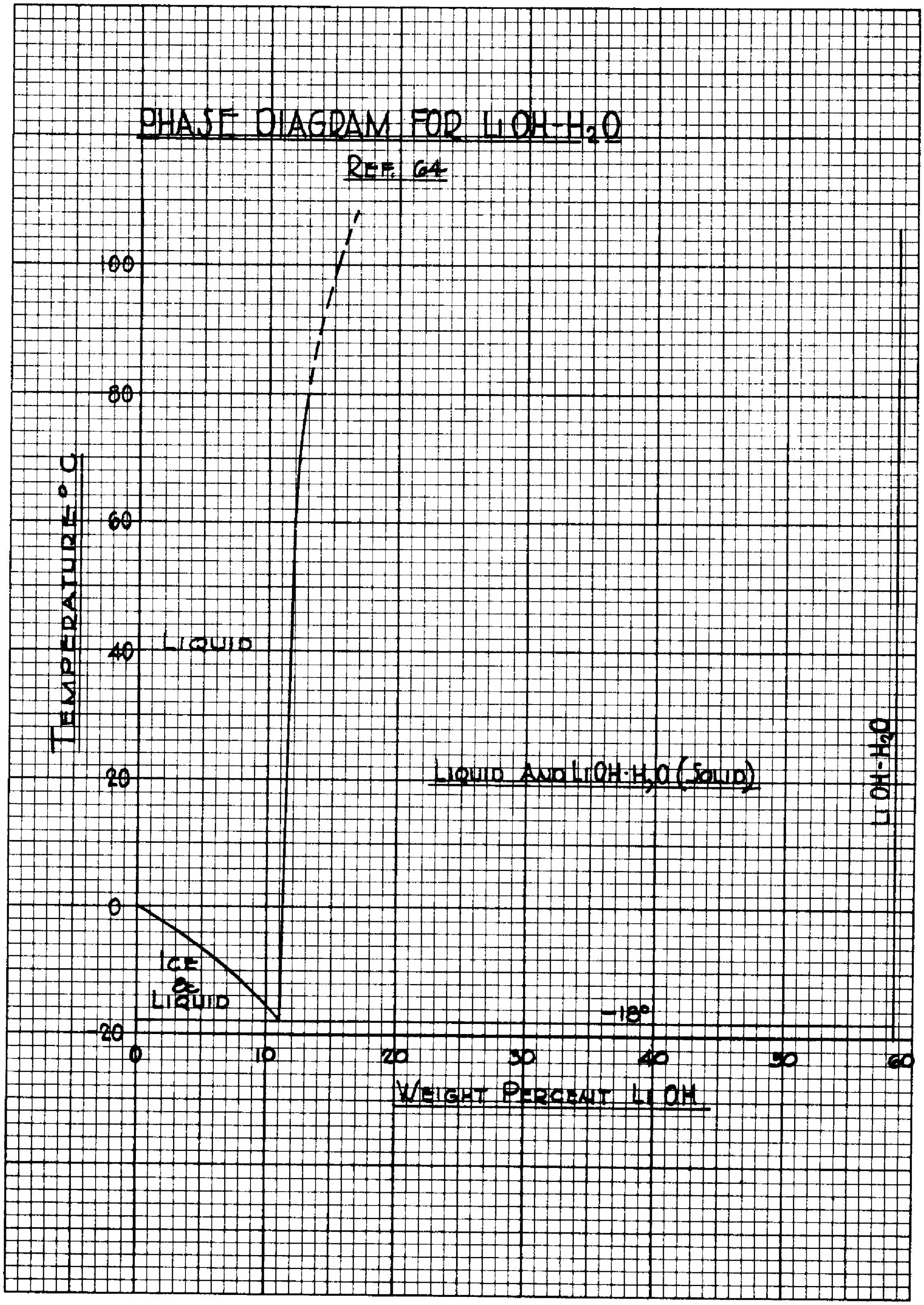

PHASE DIAGRAM FOR $LiOH-H_2O$

REF. 64

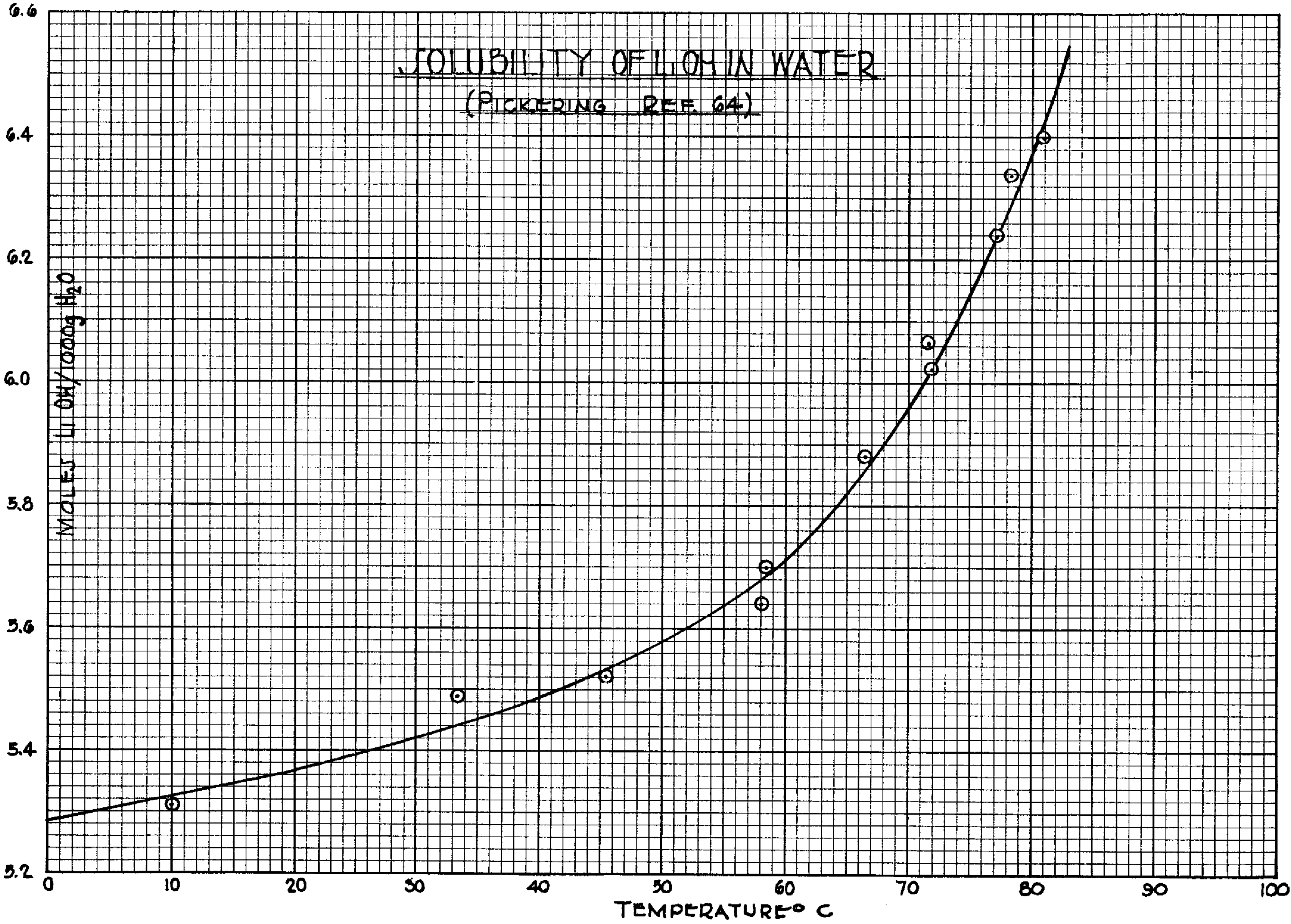

SOLUBILITY OF LiOH IN WATER

(PICKERING REF. 64)

101 UNCLASSIFIED DWG. 20333

FIGURE 48

FIGURE 49

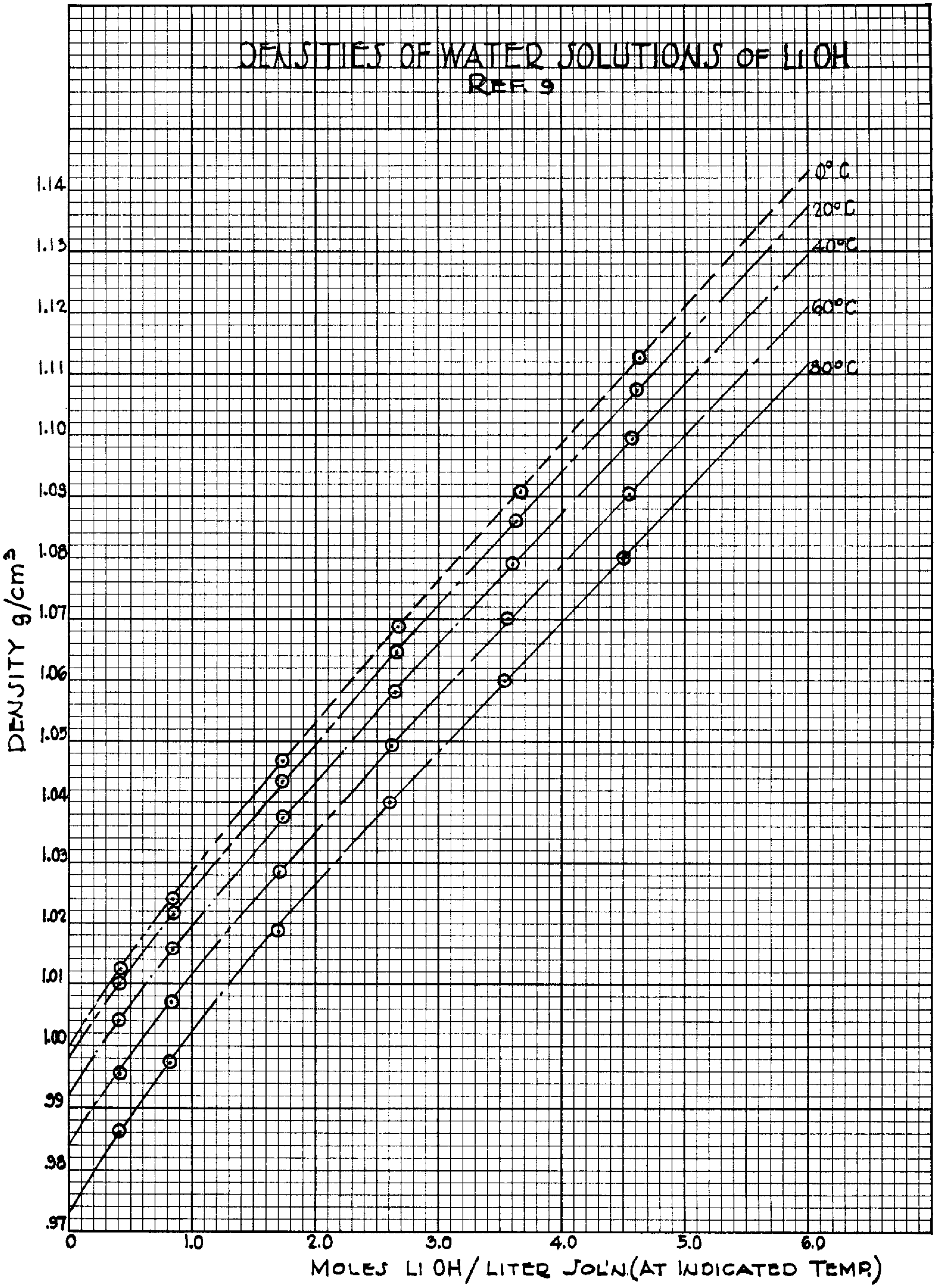
DENSITIES OF WATER SOLUTIONS OF Li OH
REF. 9
0°C
20°C
40°C
60°C
80°C
DENSITY g/cm³
1.14
1.13
1.12
1.11
1.10
1.09
1.08
1.07
1.06
1.05
1.04
1.03
1.02
1.01
1.00
.99
.98
.97
0
1.0
2.0
3.0
4.0
5.0
6.0
MOLES Li OH/LITER SOL'N.(AT INDICATED TEMP.)

DENSITIES OF WATER SOLUTIONS OF Li OH

FIGURE 50

DATA FROM REF. 9

ACCURACY ± 0.001 G/ML FOR TEMP. < 20° C
± 0.002 G/ML FOR MOLARITY 3.5 TO 4.5
± 0.01 G/ML FOR MOLARITY < 3.5, TEMP > 20° C

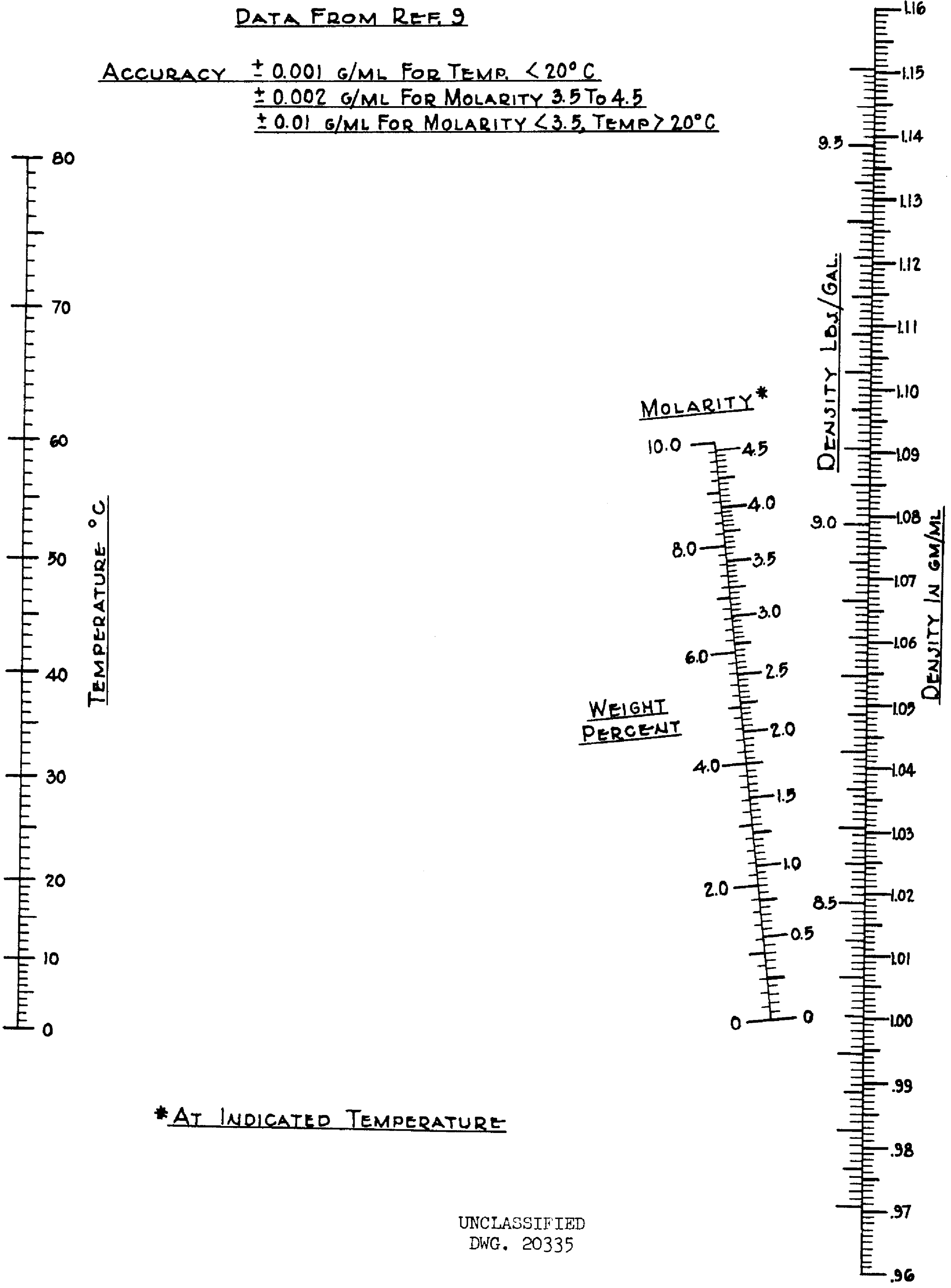

*AT INDICATED TEMPERATURE

UNCLASSIFIED
DWG. 20335

Density	1.74 g/ml at 20°C, 1.536 g/ml at 700°C, 108.5 lbs/ft^3 at 68°F	(3)
Heat Capacity	0.317 cal/g°C at 651°C, 0.342 cal/g°C at 1120°C	(1)
Surface Tension	563 dynes/cm at 681°C, 502 dynes/cm at 894°C	(1)
Volume Change on Fusion (% of sol. volume)	4.2%	(1)

Magnesium - Mercury

Density	$D = 13.55744 - 0.0022656t$ (°C) for 0.8N amalgam $D = 13.4388 - 0.002125t$ (°C) for 3.0N amalgam See Figures 10, 51	(13, 65, 66, 67)
Viscosity	$\log_{10}\eta = -0.2489 + 132.3/T_{(^{o}K)}$ for 0.8N amalgam $\log_{10}\eta = -0.2799 + 148.4/T_{(^{o}K)}$ for 3.0N amalgam See Figure 52	(13, 65, 66, 67)
Surface Tension	See Figure 13	(13,26)
Phase Diagram	See Figure 53	(14,15)
Solubility	See Figures 15, 16	(13,25)
Chemical Reactions with Impurities	No reaction with O_2, H_2O free N_2 has been observed at room temperature. Both O_2 and H_2O impurities in N_2 or He blanketing gases form scums on magnesium amalgams.	(13,67)
Thermodynamics	ΔH mixing = - 17.3 K cal/mole for $Mg + 40.5\,Hg \rightarrow Mg(Hg)_x$ in Hg	(13)

FIGURE 51

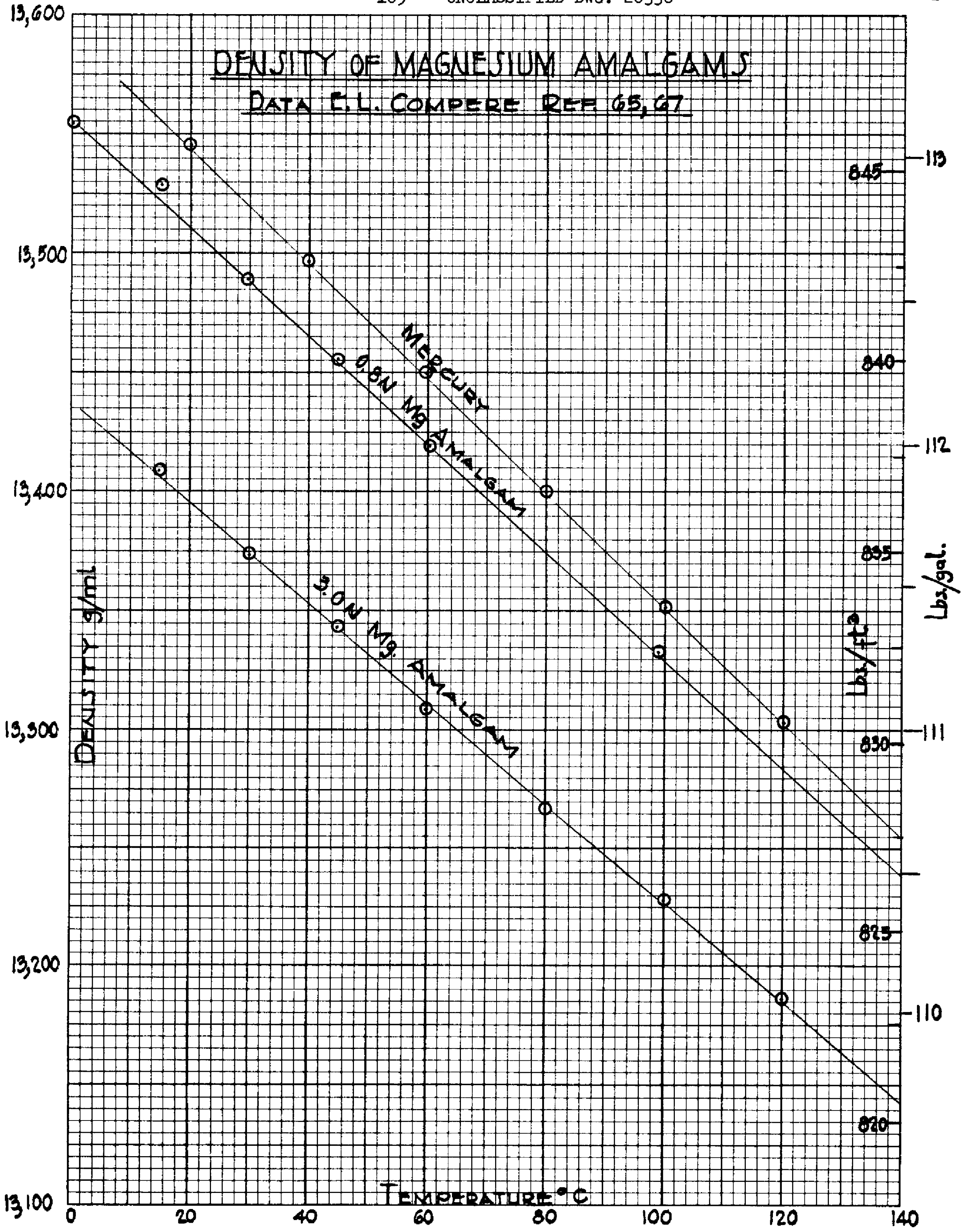
DENSITY OF MAGNESIUM AMALGAMS
DATA E.L. COMPERE REF. 65, 67
MERCURY
0.6N Mg AMALGAM
3.0N Mg AMALGAM
DENSITY g/ml
13,600
13,500
13,400
13,300
13,200
13,100
TEMPERATURE °C
0
20
40
60
80
100
120
140
Lbs/ft³
845
840
835
830
825
820
Lbs/gal.
113
112
111
110

FIGURE 32

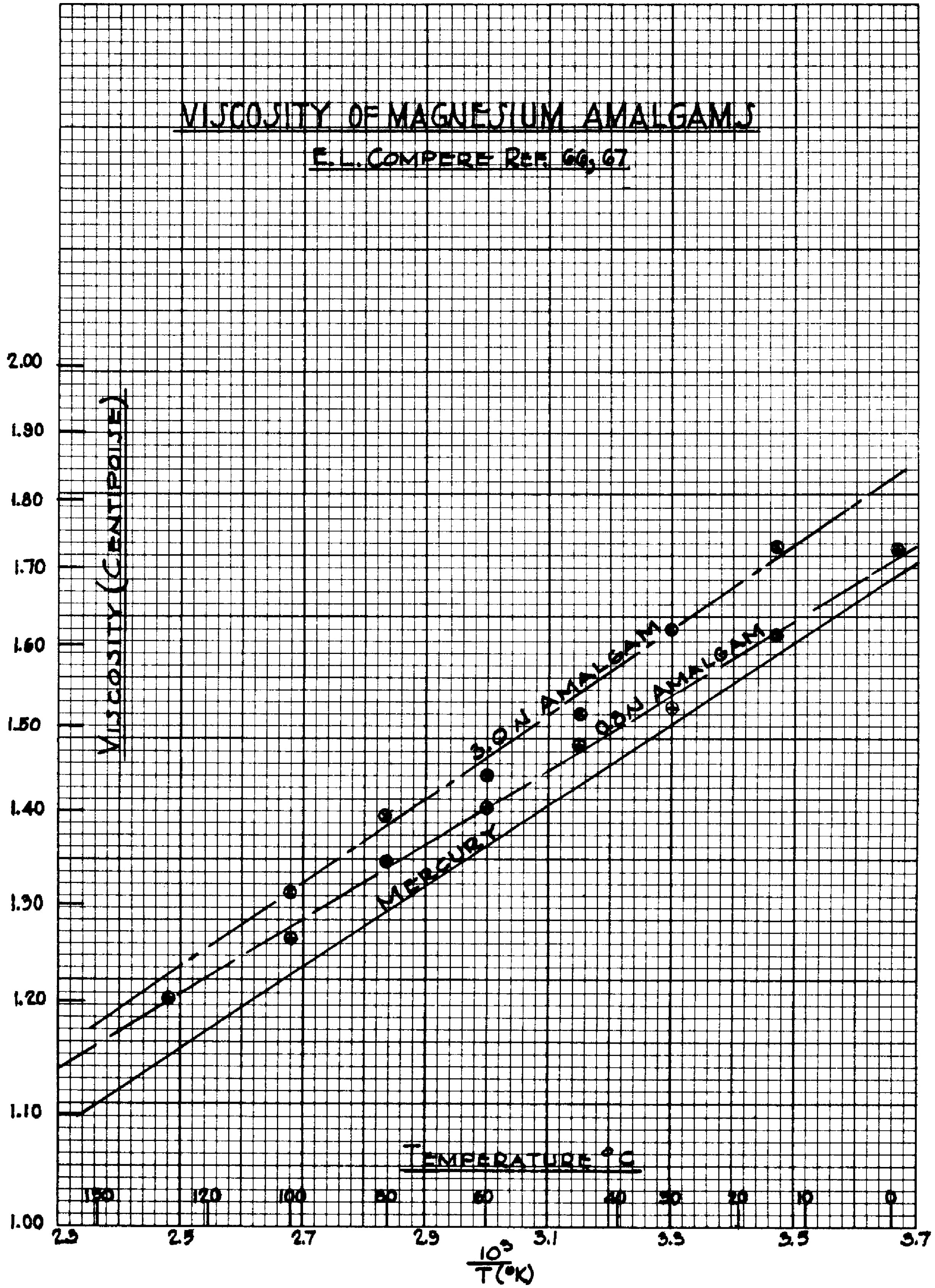
VISCOSITY OF MAGNESIUM AMALGAMS
E. L. COMPERE REF. 66, 67
VISCOSITY (CENTIPOISE)
2.00
1.90
1.80
1.70
1.60
1.50
1.40
1.30
1.20
1.10
1.00
3.0 N AMALGAM
0.9 N AMALGAM
MERCURY
TEMPERATURE °C
130
120
100
80
60
40
30
20
10
0
2.3
2.5
2.7
2.9
3.1
3.3
3.5
3.7
$\frac{10^3}{T(°K)}$

UNCLASSIFIED DWG. 20338

FIGURE 53

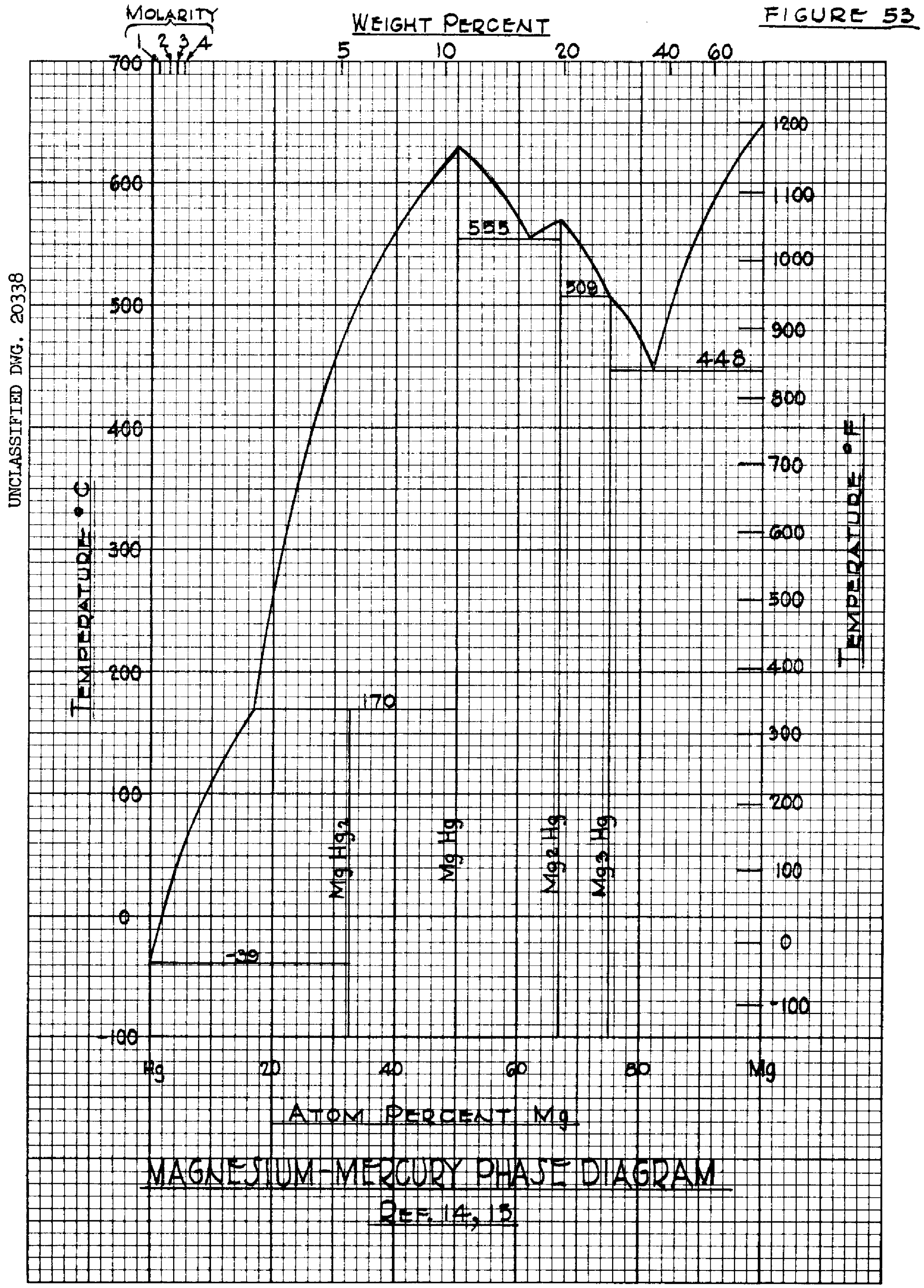

MAGNESIUM-MERCURY PHASE DIAGRAM

REF. 14, 15

B. MAGNESIUM CHLORIDE

Formula Weight	95.23	
Melting Point	714°C, 1317°F	(5,6)
Boiling Point	1418°C, 2584°F	
Heat of Fusion	10,300 cal/g mole, 108 cal/g, 18,500 Btu/lb mole, 194 Btu/lb	(5,6)
Heat of Vaporization	32,700 cal/g mole, 344 cal/g, 58,800 Btu/lb mole, 618 Btu/lb	(5,6)
Vapor Pressure	10^{-3} atm at 763°C, 10^{-2} atm at 907°C	(6)
Density	2.32 g/ml, 145 lbs/ft^3	(2)
Refractive Indicies	1.675, 1.59	(2)
Preparation of Anhydrous Magnesium Chloride	Best method of preparation was found to be that of thermal decomposition of $NH_4Cl \cdot MgCl_2 \cdot 6H_2O$ discussed by Richards, Proc. Amer. Acad. 32 53, (1896).	

Magnesium Chloride - Ammonia

Formula Weights of Compounds:

$MgCl_2 \cdot 6NH_3$	197.41
$MgCl_2 \cdot 4NH_3$	163.35
$MgCl_2 \cdot 2NH_3$	129.29
$MgCl_2 \cdot NH_3$	112.26

Decomposition Temperatures and Heats: (9)

Reaction	Temp°C
$MgCl_2 \cdot 6NH_3 \rightarrow MgCl_2 \cdot 4NH_3 + 2NH_3$	?
$\Delta H = ?$	
$MgCl_2 \cdot 4NH_3 \rightarrow MgCl_2 \cdot 2NH_3 + 2NH_3$	?
$\Delta H = ?$	
$MgCl_2 \cdot 2NH_3 \rightarrow MgCl_2 \cdot NH_3 + NH_3$	272°C
$\Delta H = 17{,}900$ cal/mole	
$MgCl_2 \cdot NH_3 \rightarrow MgCl_2 + NH_3$	365°C
$\Delta H = 20{,}800$ cal/mole	

Vapor Pressure	See Figure 54	(9)

Magnesium Chloride - 2 Ethylhexanol

Solubility of Magnesium Chloride in 2 Ethylhexanol	(0.07 moles $MgCl_2$/liter) (solution at room temp.)	(69)

Magnesium Chloride - Propylenediamine

Chemical Reaction $MgCl_2 + 3PDA \rightarrow MgCl_2 \cdot 3PDA$ (crystalline)

Solubility of $MgCl_2 \cdot 3PDA$ in PDA (43, 55)

Temp.	Solubility mole/liter
27°C	8.5×10^{-4}
60°C	2.1×10^{-3}

Vapor Pressure of PDA over $MgCl_2$ in PDA (70, 71)

Species	Vapor Pressure	Temp.
$MgCl_2 \cdot 3PDA$	30 mm	160°C
$MgCl_2 \cdot 2PDA$	$\sim$ 0.04 mm	162°C
$MgCl_2 \cdot 2PDA$	2.1 mm	200°C
$MgCl_2 \cdot 1PDA$	$<$ 2 mm	400°C

FIGURE 54

UNCLASSIFIED DWG. 20339

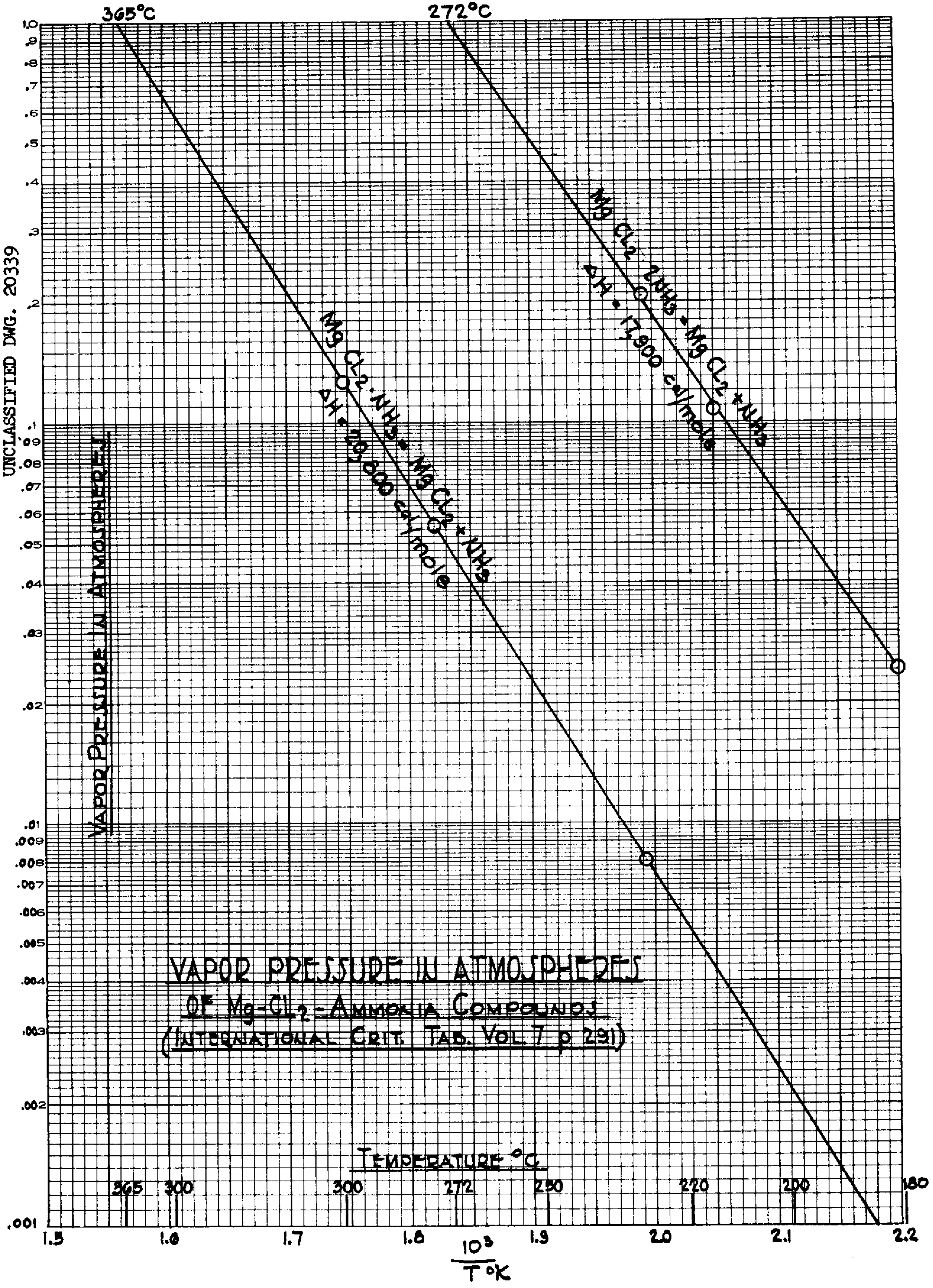
VAPOR PRESSURE IN ATMOSPHERES OF Mg-CL$_2$-AMMONIA COMPOUNDS (INTERNATIONAL CRIT. TAB. VOL. 7 p 291)

Magnesium Chloride - Ammonia - Propylenediamine

Chemical Reaction

$$MgCl_2\cdot 3PDA + 6NH_3 \rightarrow MgCl_2\cdot 6NH_3 + 3PDA$$

	Pressure	Temp.	Starting Mat. PDA/$MgCl_2$	Product (104) PDA/$MgCl_2$
Mole ratio PDA/$MgCl_2$ in washed $MgCl_2\cdot 6NH_3$ precipitate	1 atm	-33°C	∼ 3	0.031
	1 atm	-33°C	∼ 9	.050
	1 atm	-33°C	∼ 9	.053

Magnesium Chloride - Decane - Propylenediamine

Apparent equilibrium PDA/$MgCl_2$ ratio after refluxing and distilling at decane boiling point	0.46, 0.75 PDA/$MgCl_2$ (decane returning to the system upon refluxing carried room temperature saturation of PDA)	(68)

Magnesium Chloride - Dodecane - Propylenediamine

Apparent equilibrium PDA/$MgCl_2$ ratio after refluxing and distilling at dodecane boiling point	1.1, 1.2 PDA/$MgCl_2$ (dodecane returning to the system upon refluxing carried room temperature saturation of PDA)	(72)

Magnesium Chloride - Ethylene glycol - Propylenediamine

Apparent equilibrium PDA/$MgCl_2$ ratio after refluxing and distilling at Ethylene glycol boiling point	0.2 PDA/$MgCl_2$ (Ethylene glycol replaces PDA to some extent in the solvated salt structure)	(73)

Magnesium Chloride - 2 Ethyhexanol - Propylenediamine

Apparent equilibrium PDA/$MgCl_2$ ratio after refluxing and distilling at 2 ethylhexanol boiling point	1.3 PDA/$MgCl_2$	(73)

Magnesium Chloride - Methanol - Propylenediamine

Solubility of $MgCl_2 \cdot 3PDA$ in Methanol-PDA mixtures	See Figure 55	(103)

Magnesium Chloride - Propylenediamine - Water

Chemical Reaction	$MgCl_2 + xs\ H_2O + xs\ PDA \rightarrow Mg(OH)_2 + 2PDA \cdot HCl + H_2O + PDA$	
Solubility of Mg^{++} in H_2O - PDA mixtures	See table below	(60)

Solubility Mg^{++} in moles/liter	% PDA	Temp °C
0.007	90	25
0.033	60	25
0.012	30	25
0.010	60	60
0.003	30	60

Magnesium Chloride - Ammonia - Methanol - Propylenediamine

Chemical Reaction	$MgCl_2 \cdot 3PDA$ (in MeOH sol'n) + $NH_3 \rightarrow MgCl_2 \cdot 6NH$ + 3PDA (in MeOH sol'n)	
Solubility of $MgCl_2 \cdot 6NH_3$ in MeOH in presence of NH_3 and PDA	See Figure 56	(103)
PDA content of $MgCl_2 \cdot 6NH_3$ precipitate	See Figure 57	(103)

IV. POTASSIUM AND POTASSIUM COMPOUNDS

A. POTASSIUM

Atomic Weight	39.096	
Melting Point	63.7°C, 147°F	(1)
Boiling Point	760°C, 1400°F	(1)
Latent Heat of Fusion	14.6 cal/g, 571 cal/g mole, 26.3 Btu/lb, 1027 Btu/lb mole	(1)

SOLUBILITY OF $MgCl_2 \cdot 3PDA$ IN METHANOL FIGURE 55

DATA BY L. B. YEATTS REF. 103

[redacted] DWG. 20340

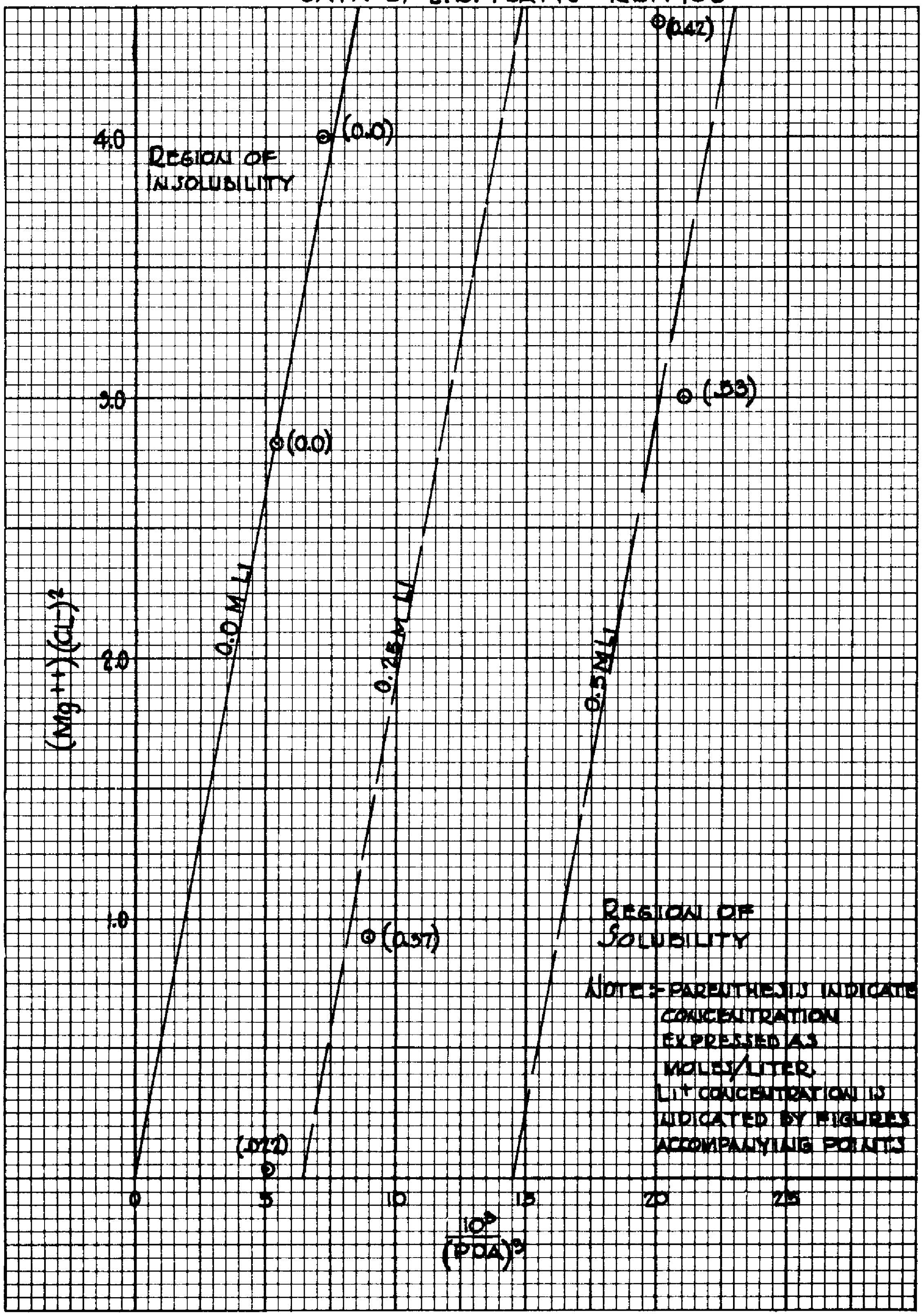

NOTE :- PARENTHESIS INDICATE CONCENTRATION EXPRESSED AS MOLES/LITER. Li^+ CONCENTRATION IS INDICATED BY FIGURES ACCOMPANYING POINTS

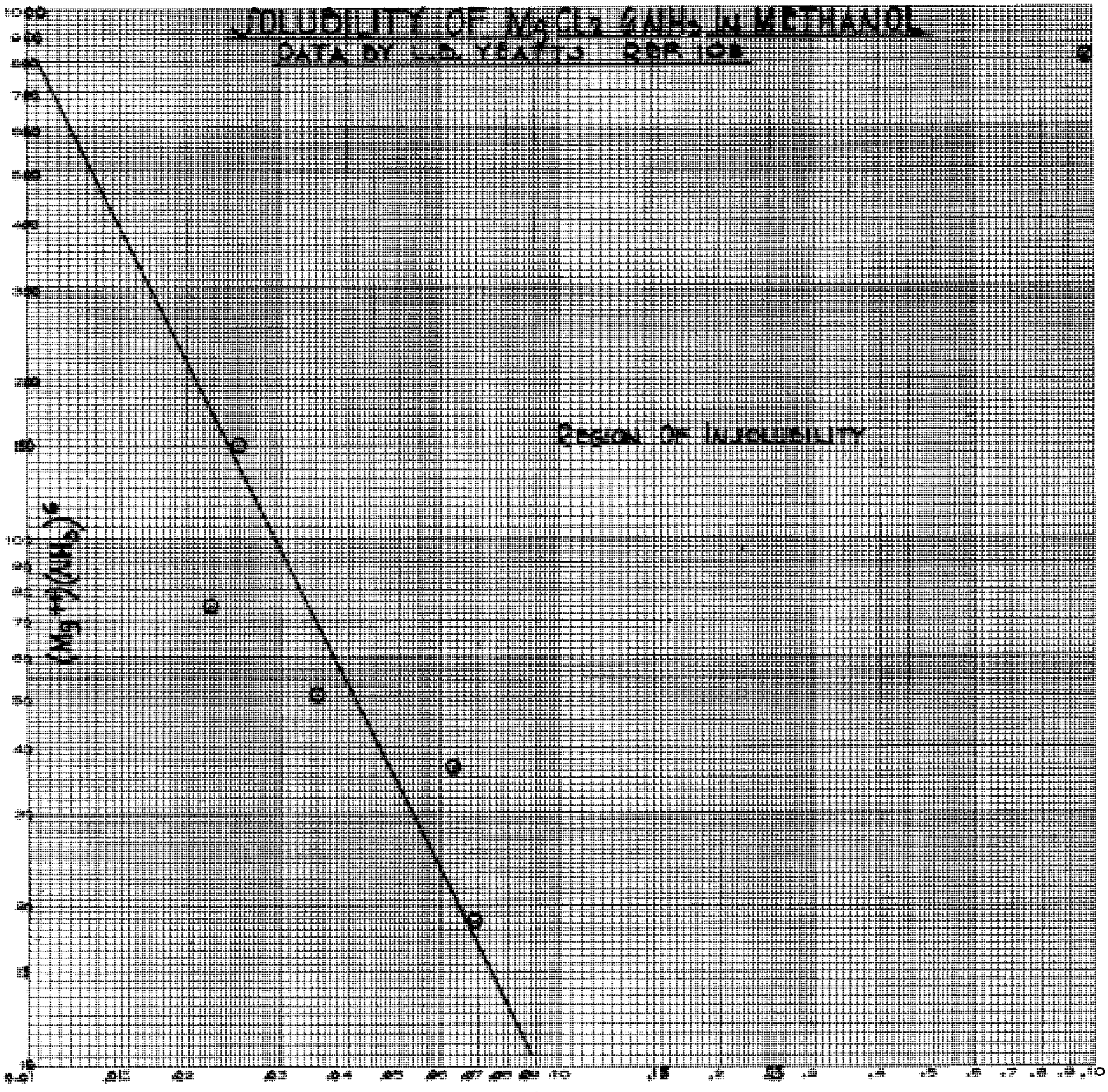
SOLUBILITY OF MgCl2 6NH3 IN METHANOL
DATA BY L.D. YEATTS ORR 108
REGION OF INSOLUBILITY
(Mg++)(NH3)6
(CL-)
1000
900
800
700
600
500
400
300
200
150
100
90
80
70
60
50
40
30
20
15
10
0.01
.015
.02
.03
.04
.05
.06
.07
.08
.09
.10
.15
.2
.25
.3
.4
.5
.6
.7
.8
.9
1.0

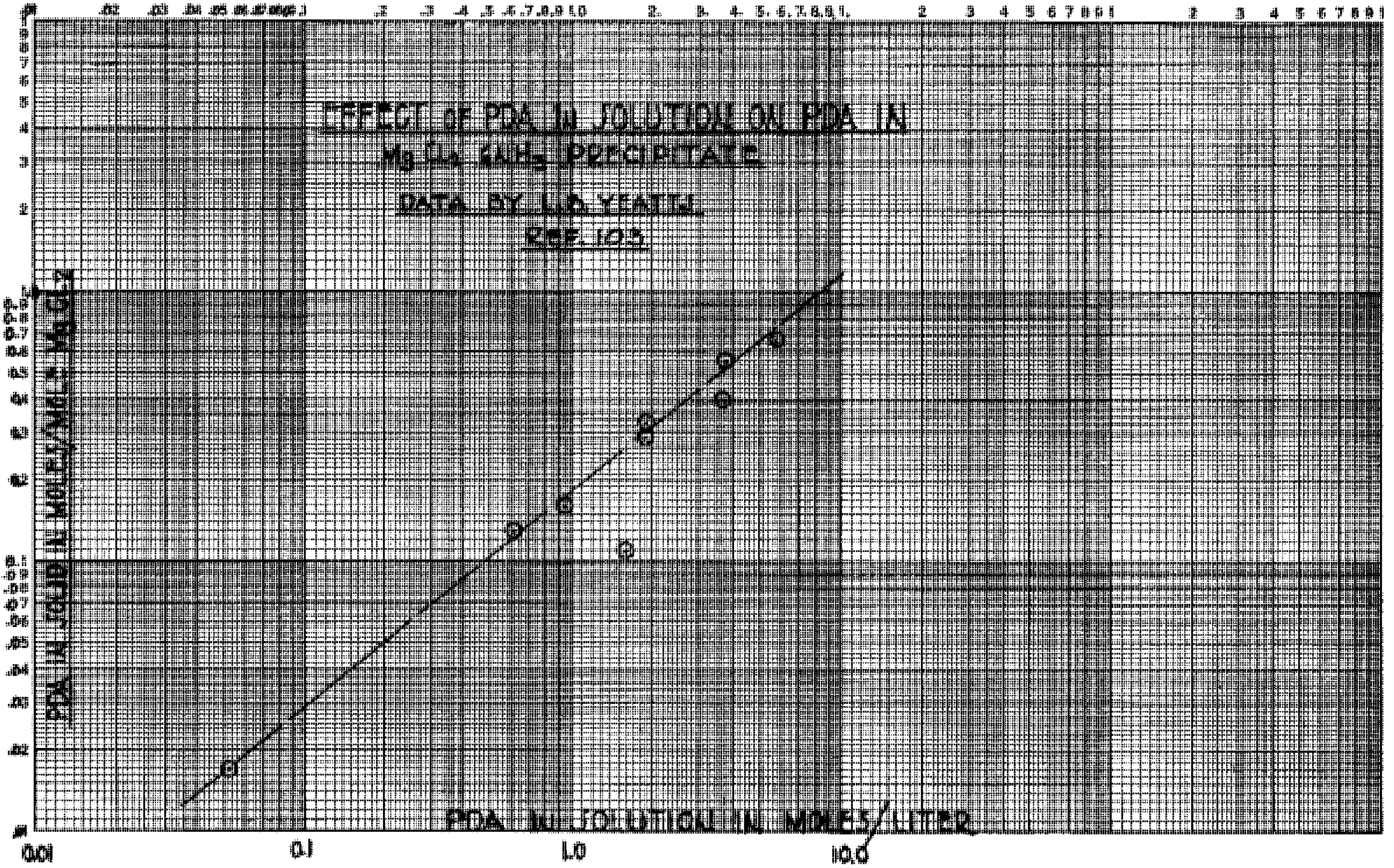

UNCLASSIFIED DWG. 20342

FIGURE 57

Latent Heat of Vaporization	496 cal/g, 1940 cal/g mole, 892 Btu/lb, 3490 Btu/lb mole	(1)
Vapor Pressure	$\log_{10} P_{mm} = -\frac{4552}{T(^{\circ}K)} - 0.5 \log T(^{\circ}K) + 8.793$ Accuracy 5% from 600-1100 °K; 20% 350-1200 °K See Figure 7	(1)
Density	0.86 g/ml at 20°C, 53.6 lbs/ft^3 at 68°F, 0.82 g/ml at 100°C	(1)
Heat Capacity	0.1956 cal/g°C (Btu/lb°F) at 75°C (as a liquid)	(1)
Viscosity	0.515 centipoise at 70°C, 0.331 cp at 167°C See Figure 8	(1)
Thermal Conductivity	0.1073 cal/sec cm°C at 200°C	(1)
Electrical Resistivity	13.16 μ ohms at 64°C	(1)
Surface Tension	86 dynes/cm (100 to 150°C)	(1)
Volume Change on Fusion (% of Sol. Vol.)	2.41%	(1)

Potassium - Mercury

Surface Tension	See Figure 13	(13,26)
Electrical Conductivity	See Figure 12	(13,27)
Density	13.371 g/ml for 0.629 moles K/liter sol'n (0.184 wt %) 12.908* g/ml for 3.14 moles K/liter sol'n (0.950 wt %) both at room temperature	(13, 74)

* must contain KHg_9 crystalline solid

Solubility of K in Hg	See Figures 15, 16	(13,25)
Phase Diagram	See Figure 58	(13,22)
Heat of Solution	$K + 199\ Hg \rightarrow K(Hg)_{199}$ $\Delta H = 26,350$ cal $K + 49\ Hg \rightarrow K(Hg)_{49}$ $\Delta H = 26,120$ cal	
Activity Coefficient	$\log_{10}\gamma = 0.4396\ M$ $(25^{\circ}C)$ where $\gamma =$ activity coefficient and $M =$ g atom K per 13,534 g Hg at $25^{\circ}C$	(54)

Potassium - Sodium

Phase Diagram	See Figure 59	

B. POTASSIUM CHLORIDE

Formula Weight	74.55	
Melting Point	$770^{\circ}C$	(6)
Boiling Point	$1407^{\circ}C$	(6)
Heat of Fusion	6410 cal/g mole	(6)
Heat of Vaporization	38,840 cal/g mole	(6)
Vapor Pressure	10^{-4} atm at $607^{\circ}C$, 10^{-3} atm at $806^{\circ}C$, 10^{-2} atm at $948^{\circ}C$	(6)
Density	1.984 g/ml	(2)
Refractive Index	1.490	(2)

Potassium Chloride - Ethylenediamine

Solubility	0.0017 moles KCl/liter sol'n at room temperature	(11)

FIGURE 58

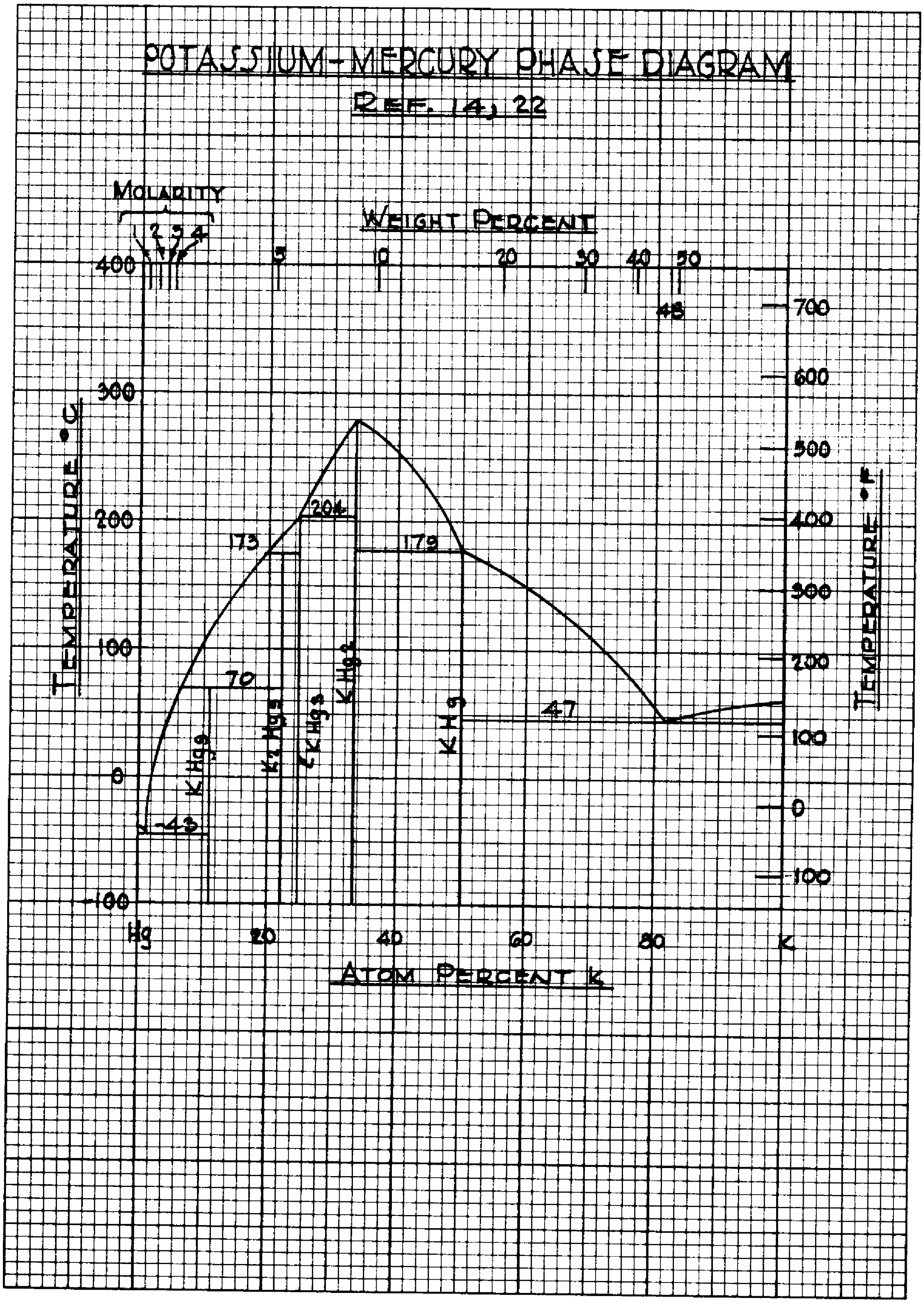
POTASSIUM-MERCURY PHASE DIAGRAM
REF. 14, 22
MOLARITY
1 2 3 4
WEIGHT PERCENT
5
10
20
30
40
50
48
TEMPERATURE °C
400
300
200
100
0
-100
TEMPERATURE °F
700
600
500
400
300
200
100
0
-100
204
173
179
70
47
-43
KHg9
K2Hg9
KHg3
KHg2
KHg
Hg
20
40
60
80
K
ATOM PERCENT K

POTASSIUM-SODIUM PHASE DIAGRAM

REF. 14, 15

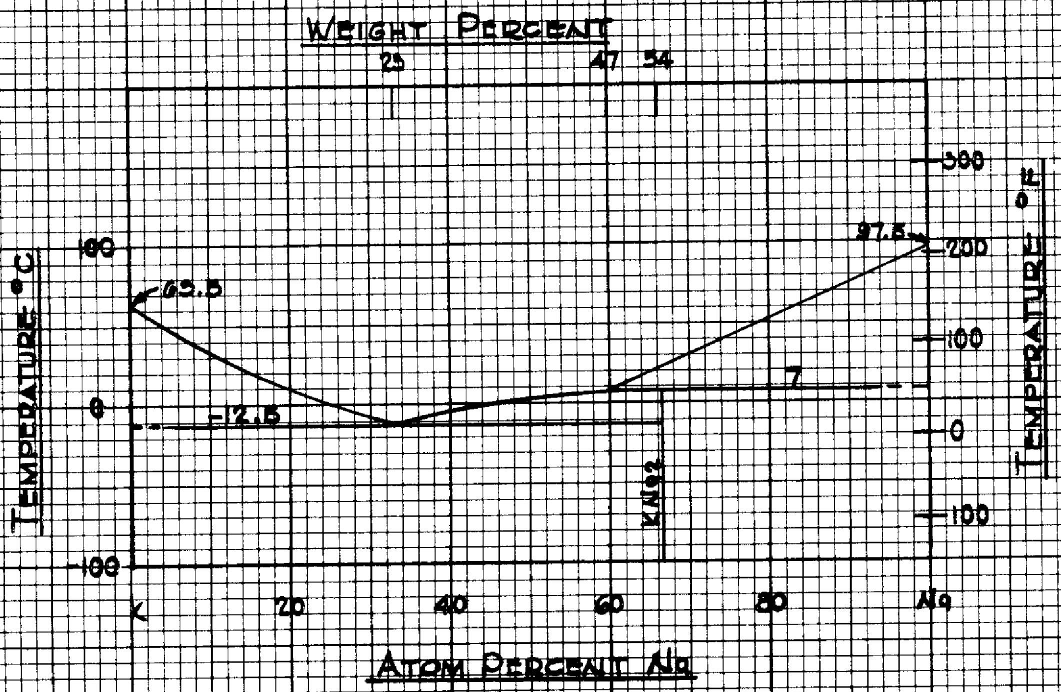

Potassium Chloride - Propylenediamine

Solubility	0.0001 moles KCl/liter sol'n at 20°C 0.0002 moles KCl/liter sol'n at 60°C 0.0004 moles KCl/liter sol'n ave. from 24° to 115°C	(43,55)

V. SODIUM AND SODIUM COMPOUNDS

A. SODIUM

Atomic Weight	22.997	
Melting Point	97.8°C, 208°F	(1)
Boiling Point	883°C, 1621°F	(1)
Latent Heat of Fusion	27.05 cal/g, 622 cal/mole, 48.7 Btu/lb, 1120 Btu/lb mole	(1)
Latent Heat of Vaporization	1005 cal/g, 2315 cal/mole, 1810 Btu/lb, 4160 Btu/lb mole	(1)
Vapor Pressure	$\log_{10} P_{mm} = \frac{-5567}{T} - 0.5 \log_{10} T - 9.235$ $T = {}^{\circ}K$ Accuracy 1200 - 450°K, 5%; 1250 - 370°K, 10% See Figure 7	(1)
Density	0.97 g/ml at 20°C, 0.928 g/ml at 100°C (Liquid) 60.5 lb/ft^3 at 68°F	(1)
Heat Capacity	0.3305 cal/g°C at 100°C (Btu/lb °F) (as a liquid)	(1)

Viscosity	0.686 centipoise at 103.7°C See Figure 8	(1)
Thermal Conductivity	0.2055 cal/sec cm °C at 100°C 49.7 Btu/hr ft °F at 212°F	(1)
Electrical Resistivity	9.65 μ ohms at 100°C	(1)
Surface Tension	206.4 dynes/cm at 100°C	(1)
Volume Change on Fusion (% of sol. vol.)	2.5%	(1)

Sodium - Mercury

Density	13.448 g/ml for 0.601 g atoms Na/liter sol'n (0.103 wt %) 12.965 g/ml for 3.37 g atoms Na/liter sol'n (0.597 wt %) both at room temperature.	(13,74)
Viscosity	1.74 centipoise for 1.95 g atoms Na/liter sol'n at 25°C 2.2 centipoise for saturated sol'n at 25°C	(13)
Surface Tension	See Figure 13	(13,26)
Electrical Conductivity	See Figure 12	(13,27)
Solubility of Na in Hg	See Figure 15, 16	(13,25)
Phase Diagram	See Figure 60	(13,22,14)
Heat of Mixing	$Na + 199\ Hg \rightarrow Na(Hg)_{199}$ $\Delta H = -19{,}930$ cal $Na + 49\ Hg \rightarrow Na(Hg)_{49}$ $\Delta H = -19{,}860$ cal	(13)
Activity Coefficient	$\log_{10} \gamma = 0.2148\ M$ at 25°C where γ = activity coefficient and M = g atom Na per 13,534g Hg at 25°C	(54)

DWG. 20345

FIGURE 60

SODIUM-MERCURY PHASE DIAGRAM

REF. 22, 14

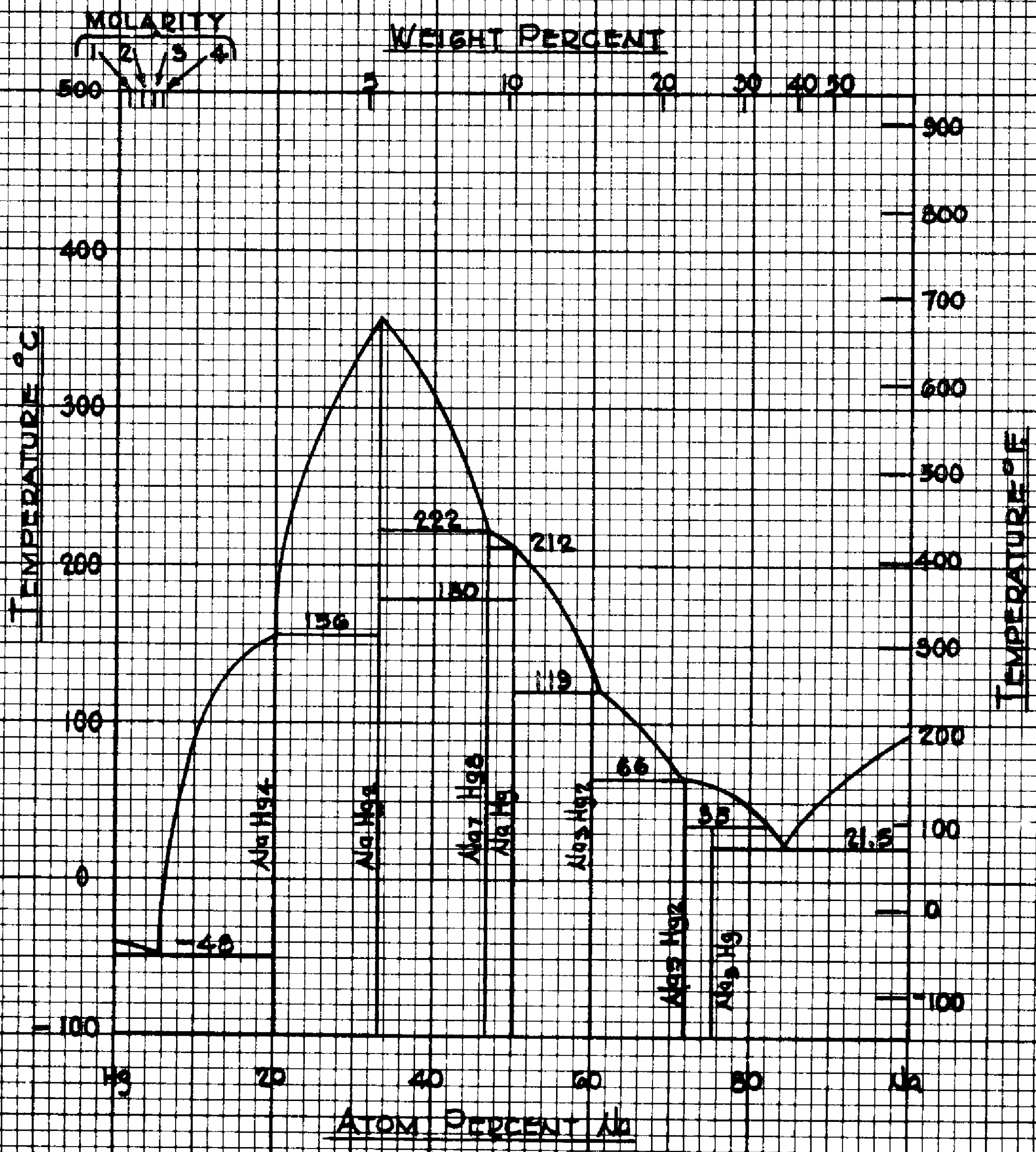

B. SODIUM CHLORIDE

Formula Weight	58.45	
Melting Point	800°C	(6)
Boiling Point	1465°C	(6)
Latent Heat of Fusion	7220 cal/g mole	(6)
Latent Heat of Vaporization	40,808 cal/g mole	(6)
Vapor Pressure	0.01 atm. at 996°C, 0.0001 atm. at 741°C	(6)
Density	2.165 g/ml	(2)
Heat Capacity	11.88 cal/°C mole at 25°C	(5)
Refractive Index	1.5442	(2)

Sodium Chloride - Ethylenediamine

Solubility of NaCl in EDA	See Figures 29, 61	(11)

Sodium Chloride - Propylenediamine

Solubility in NaCl in PDA	See Figure 62	(45,60)

Sodium Chloride - Tetrahydrofuran

Solubility of NaCl in THF	$\sim 2 \times 10^{-4}$ moles NaCl/liter sol'n at 27°C	(31)

FIGURE 61

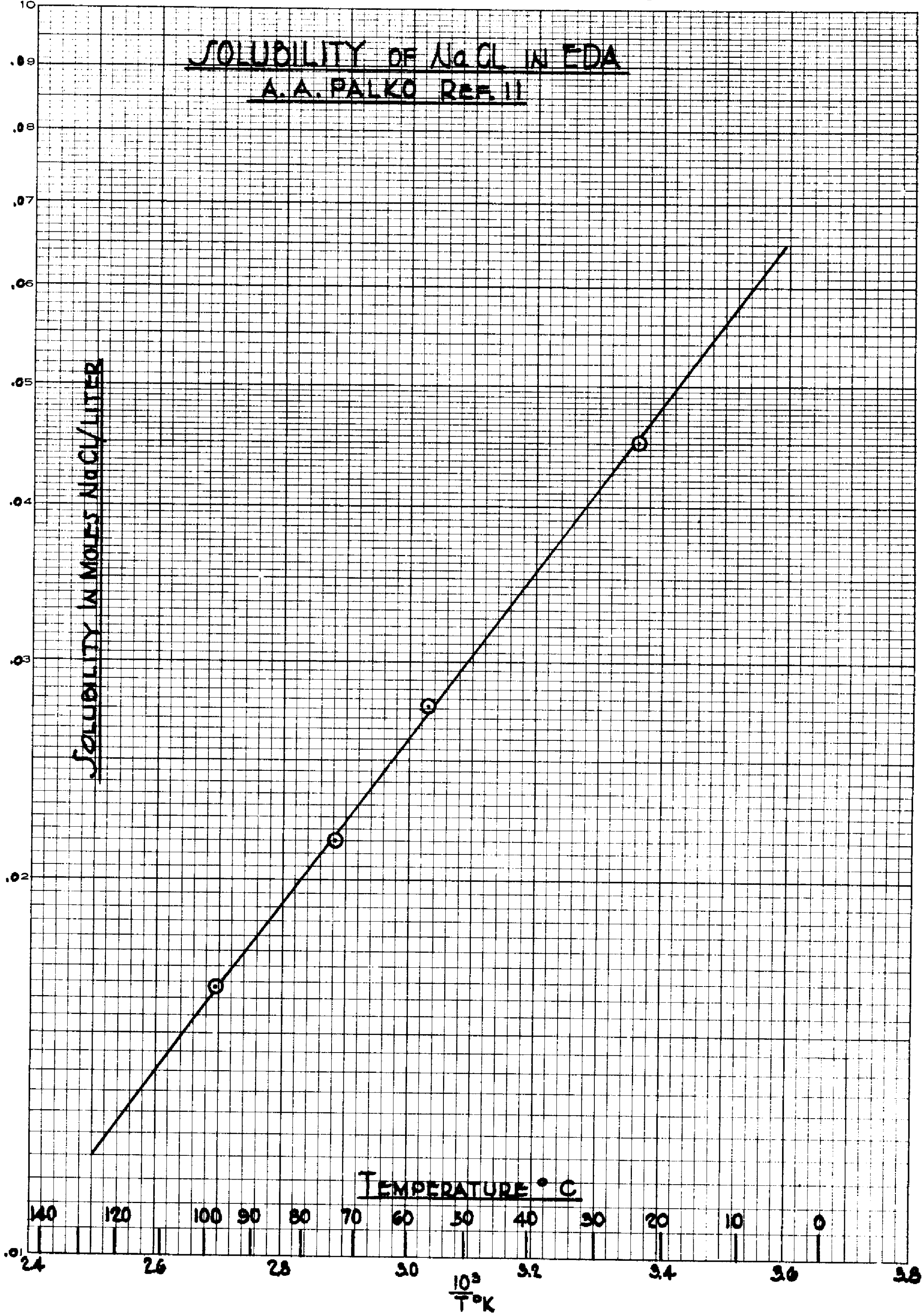
SOLUBILITY OF NaCl IN EDA
A. A. PALKO REF. 11
SOLUBILITY IN MOLES NaCl/LITER
10
.09
.08
.07
.06
.05
.04
.03
.02
.01
TEMPERATURE °C
140
120
100
90
80
70
60
50
40
30
20
10
0
2.4
2.6
2.8
3.0
3.2
3.4
3.6
3.8
$\frac{10^3}{T°K}$

FIGURE 62

UNCLASSIFIED DWG. 20347

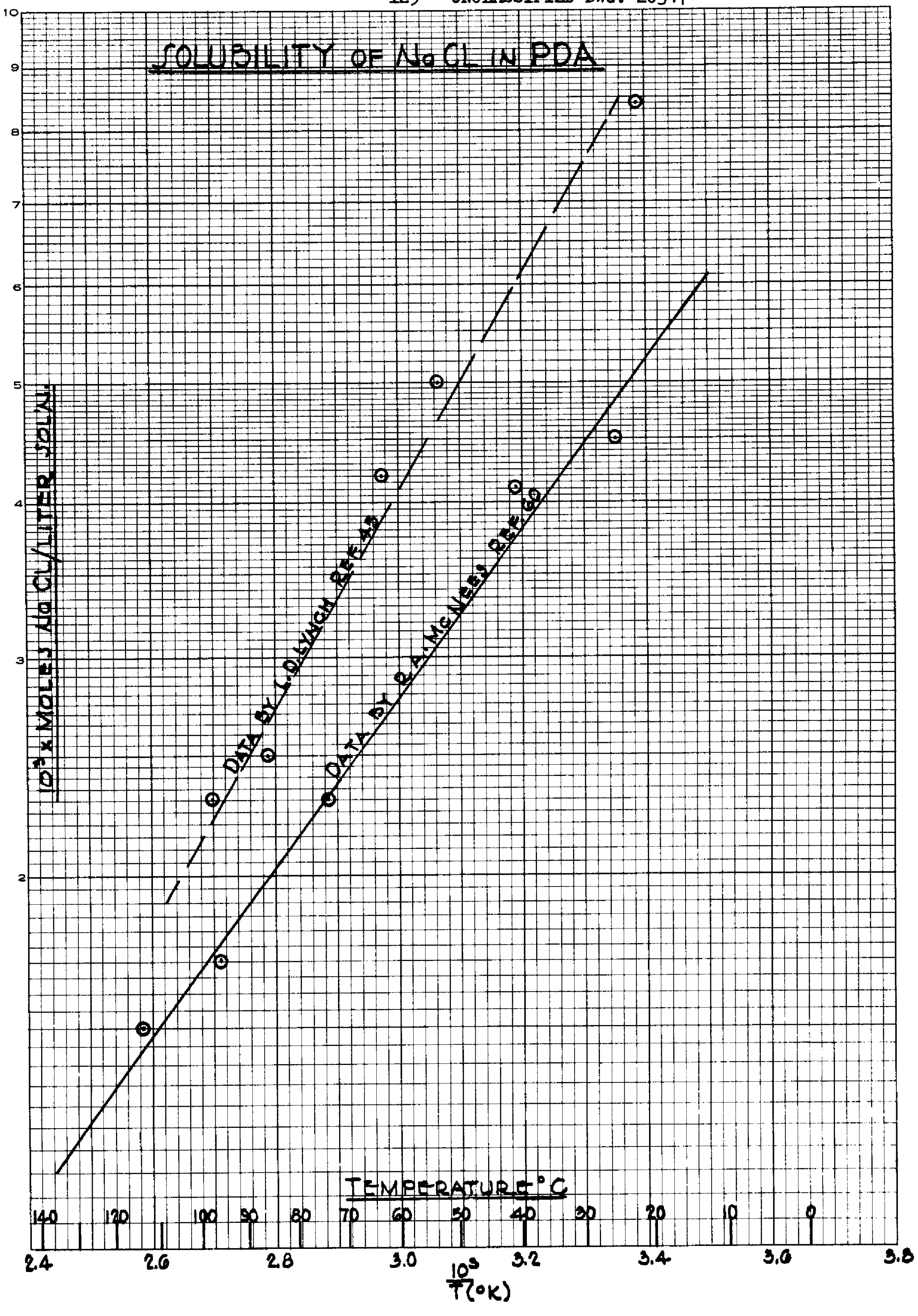

Sodium Chloride - Propylenediamine - Water

		Molarity NaCl/liter sol'n (60)	
	Temp. °C	1% H_2O-99% PDA	2% H_2O-98% PDA
Solubility of NaCl in wet PDA	25	9.4×10^{-3}	15.2×10^{-3}
	40.5	6.8×10^{-3}	11.2×10^{-3}
	56	5.1×10^{-3}	8.6×10^{-3}
	63	5.0×10^{-3}	8.0×10^{-3}
	80	4.3×10^{-3}	6.9×10^{-3}

C. SODIUM HYDROXIDE

Formula Weight	40.01	
Melting Point	320°C	(5)
Boiling Point	1390°C	(2)
Latent Heat of Fusion	1700 cal/g mole	(5)
Density	2.130 g/ml	(2)
Heat Capacity	19.2 cal/°C mole, (Btu/lb°F)	(5)
Refractive Index	1.3576	(2)

Sodium Hydroxide - 2 Ethylhexanol

Solubility	0.51 moles NaOH/liter sol'n at room temperature 0.47 moles NaOH/liter sol'n at 184°C	(79)

Sodium Hydroxide - Propylenediamine

Solubility of NaOH in PDA	~0.0008 moles NaOH/liter sol'n at room temperature < 0.013 mole/liter sol'n at 75°C	(31)

Sodium Hydroxide - Water

Phase Diagram	See Figure 63	(4)

Sodium Hydroxide - Ethylenediamine - Water

Phase Diagram	See Figure 64	(11)

Sodium Hydroxide - Propylenediamine - Water

Phase Diagram	See Figure 65	(75)

D. SODIUM PHOSPHATE

Formula Weight	163.97	
Melting Point	1340°C	(3)
Density	2.537 g/ml at 17.5°C	(3)

Sodium Phosphate - Water

Solubility of Na_3PO_4 in water	See Figure 66	(76)

VI. LIQUID SOLVENTS

A. AMMONIA

Formula Weight	17.03	
Melting Point	- 77.7°C	(16)
Boiling Point	- 33.35°C	(16)
Latent Heat of Fusion	1352 cal/g mole, 79.4 cal/g 83.9 cal/g	(16) (17)

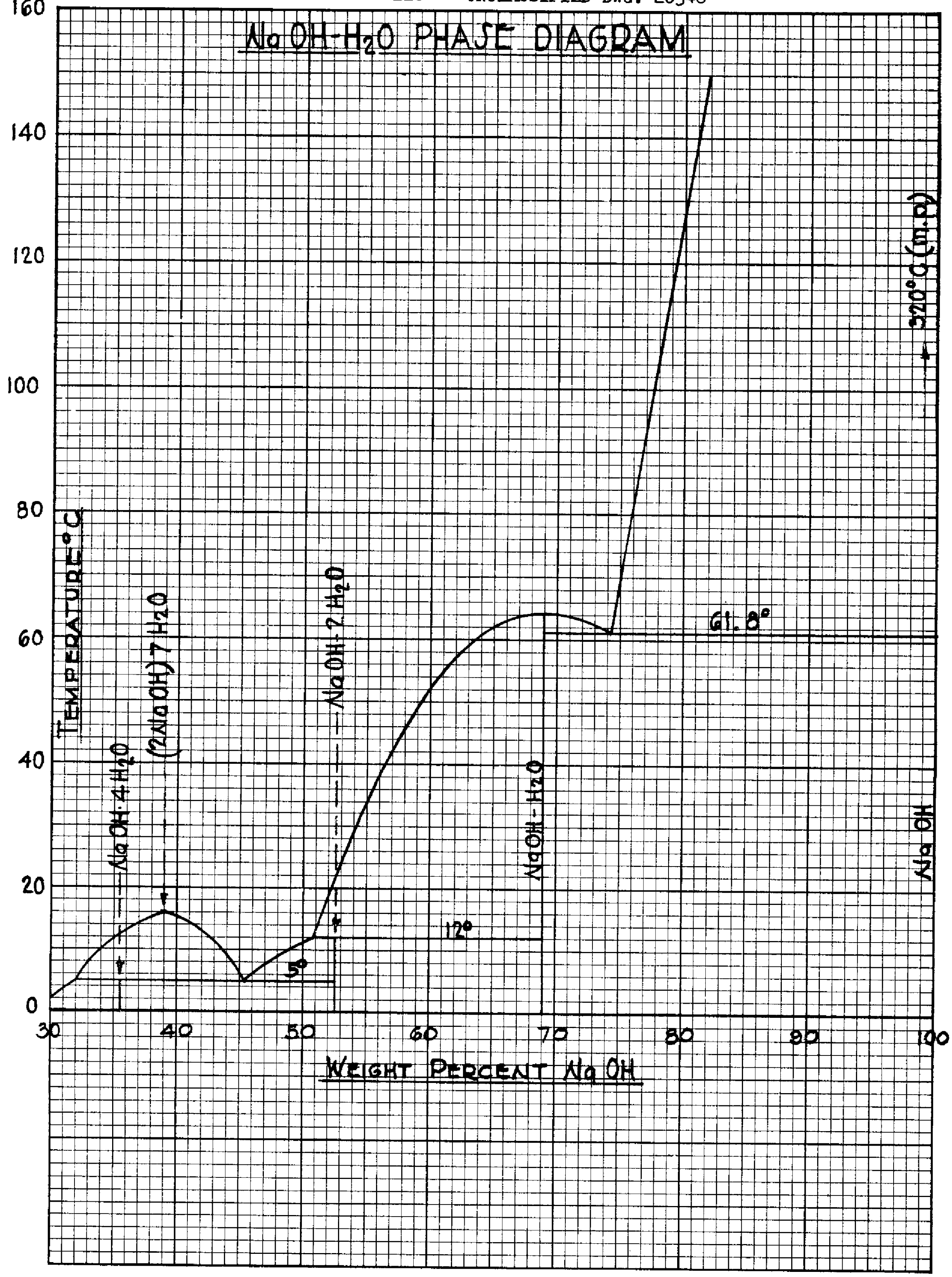
NaOH-H₂O PHASE DIAGRAM
160
140
120
100
80
60
40
20
0
TEMPERATURE °C
NaOH·4H₂O
(2NaOH)7H₂O
NaOH·2H₂O
NaOH·H₂O
NaOH
320°C (m.p)
61.8°
12°
5°
30
40
50
60
70
80
90
100
WEIGHT PERCENT NaOH

MISCIBILITY OF THE SYSTEM EDA-NaOH-H_2O @ 26°C (WT. %)

REF. 11

UNCLASSIFIED
DWG. 20349

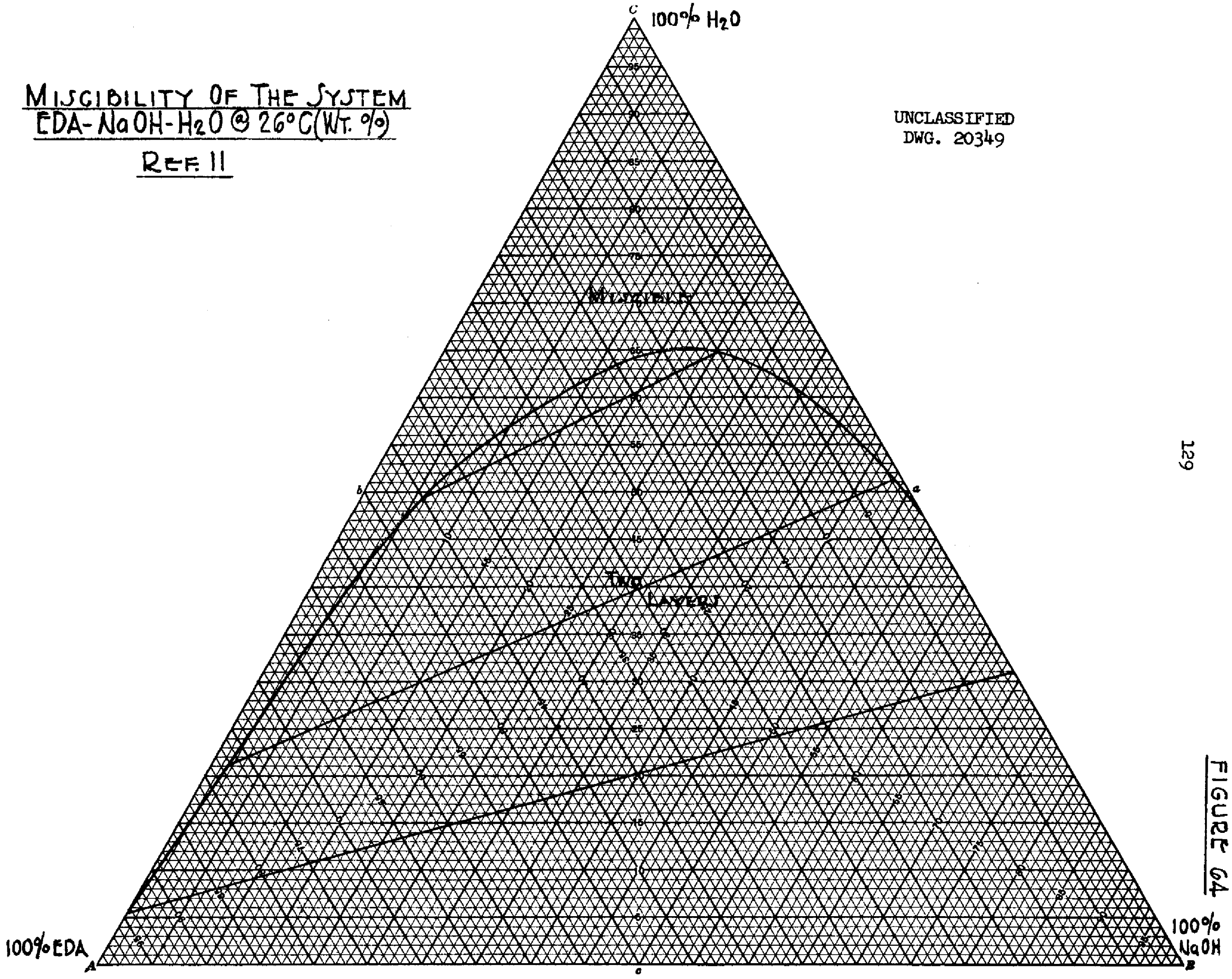

FIGURE 64

MISCIBILITY OF THE SYSTEM PDA-NaOH-H_2O @ 23°C ± 1 (WEIGHT PERCENT
REF. 75

UNCLASSIFIED
DWG. 20350

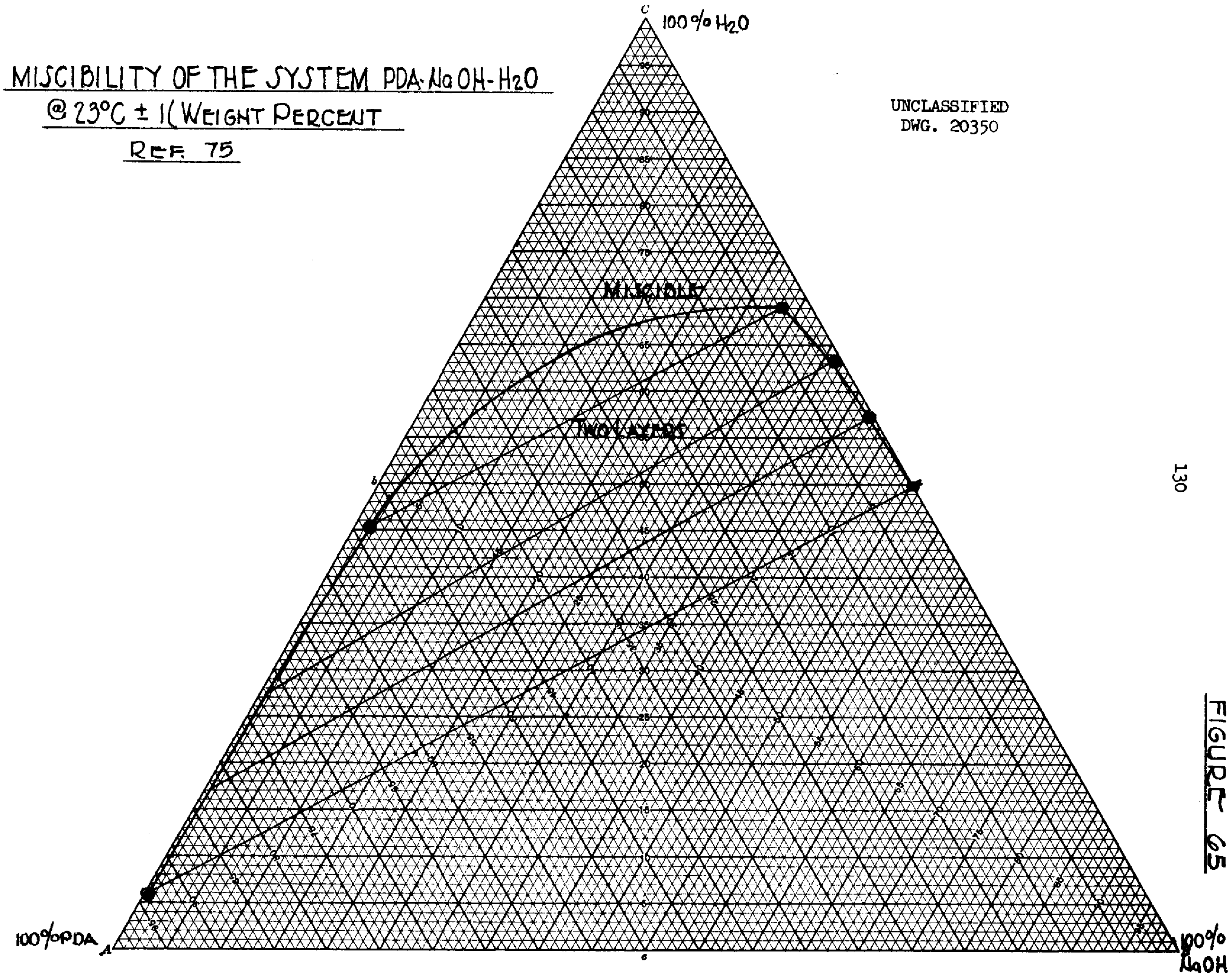

FIGURE 65

FIGURE 66

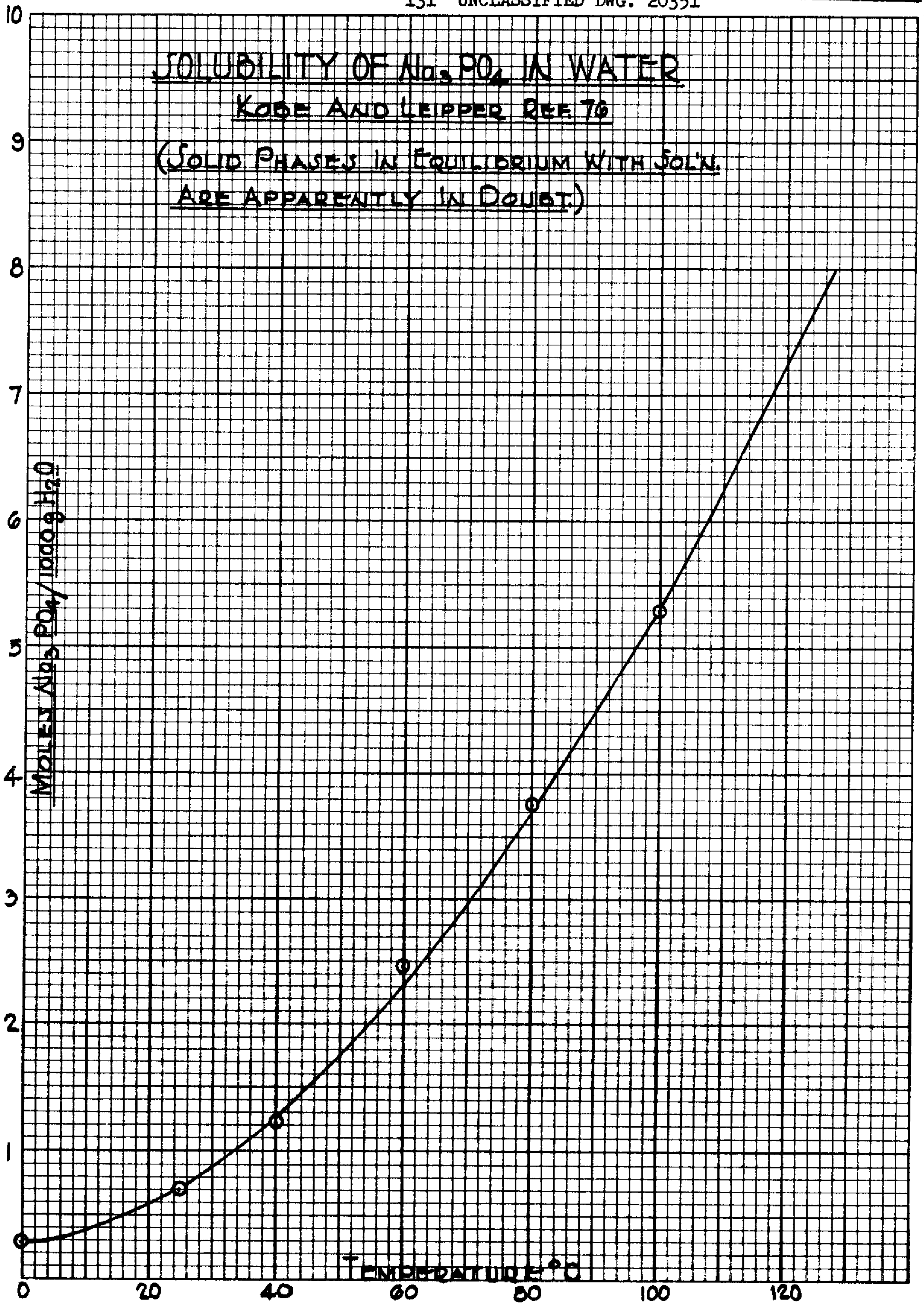

SOLUBILITY OF Na_3PO_4 IN WATER

KOBE AND LEIPPER REF. 76

(SOLID PHASES IN EQUILIBRIUM WITH SOL'N. ARE APPARENTLY IN DOUBT.)

Latent Heat of Vaporization	5581 cal/g mole, 327 cal/g	(16)
Vapor Pressure	$\log_{10}P_{mm} = 12.465400 - \frac{1648.6068}{T} - 0.01638646\ T + 2.403276 \times 10^{-5}T^2 - 1.168708 \times 10^{-8}T^3$ $(183.1^{\circ} < T < 343.1^{\circ}K)$	(16)
Critical Pressure	112.3 atm	(16)
Critical Temperature	133°C	(16)
Density		(16)

Temperature°C	Density g/ml
- 30	0.6777
- 10	0.6520
0	0.6386
20	0.6103

Heat Capacity	1.1 cal/g°C at 0°C	(17)
Viscosity	0.135 centipoise at 25°C	(16)
Dielectric Constant	16.26 at 25°C	(16)
Dipole Moment	1.46×10^{-18} e.s.u.	(16)
Conductivity	5×10^{-11} mho at - 33°C	(17)
Ignition Temperature	651°C, 1204°F	(3)
Limits of Inflammability	>15% and <28% (vol.) NH_3 in dry air at 25°C	(3)
Solubility of Metals in Ammonia		

Metal	Solubility g/100 g NH_3	Temp. °C
Li	10.7	-33.2
Li	11.3	0
Na	24.6	-33
K	49.0	-33

(17)

Solubility of Some Salts in Ammonia

Cation	Solubility g/100 g NH_3 at 0°C		
	Anion		
	Cl	Br	I
Li	1.43	---	---
Na	11.37	39.00	56.88
K	0.132	21.18	64.81
NH_4	39.91	57.96	76.99
Mg	---	0.004	0.156

Ammonia - Methanol

Solubility of NH_3 in Methanol	See Figure 67	(77,4)
Densities of sol'ns of NH_3 in Methanol	See Figure 68	(77)

B. BENZENE

Formula Weight	78.11	
Melting Point	5.5°C, 42°F	(3)
Boiling Point	80.1°C, 176.2°F	(3)
Latent Heat of Fusion	2351 cal/g mole	(2)
Latent Heat of Vaporization	7,353 cal/g mole, 94.14 cal/g, 169.34 Btu/lb	(2)
Vapor Pressure	See Figure 69	(2)
Density	0.874 g/ml, 7.29 lb/gal, 54.5 lb/ft^3 at 25°C	(3)
Heat Capacity (as gas)	19.52 cal/°C g mole at 25°C, 26.74 cal/°C g mole at 127°C	(7)
(as liquid)	0.410 cal/°g at 20°C	(8)
Viscosity	0.7 centipoise at 20°C	(8)
Flash Point	- 11°C, 12°F	(3)

FIGURE 67

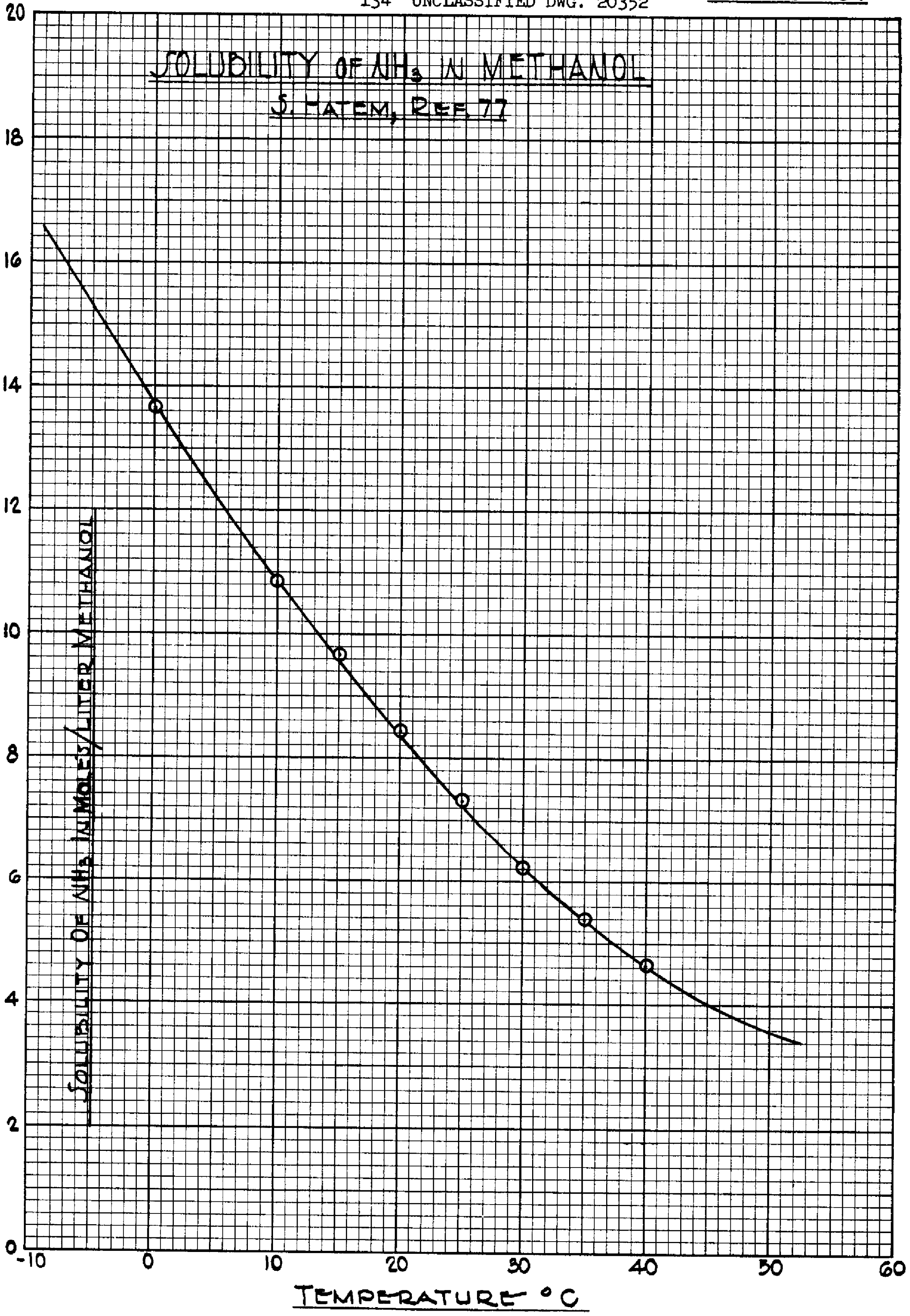
SOLUBILITY OF NH3 IN METHANOL
S. HATEM, REF. 77
SOLUBILITY OF NH3 IN MOLES/LITER METHANOL
TEMPERATURE °C
20
18
16
14
12
10
8
6
4
2
0
-10
0
10
20
30
40
50
60

UNCLASSIFIED DWG. 20353

FIGURE 68

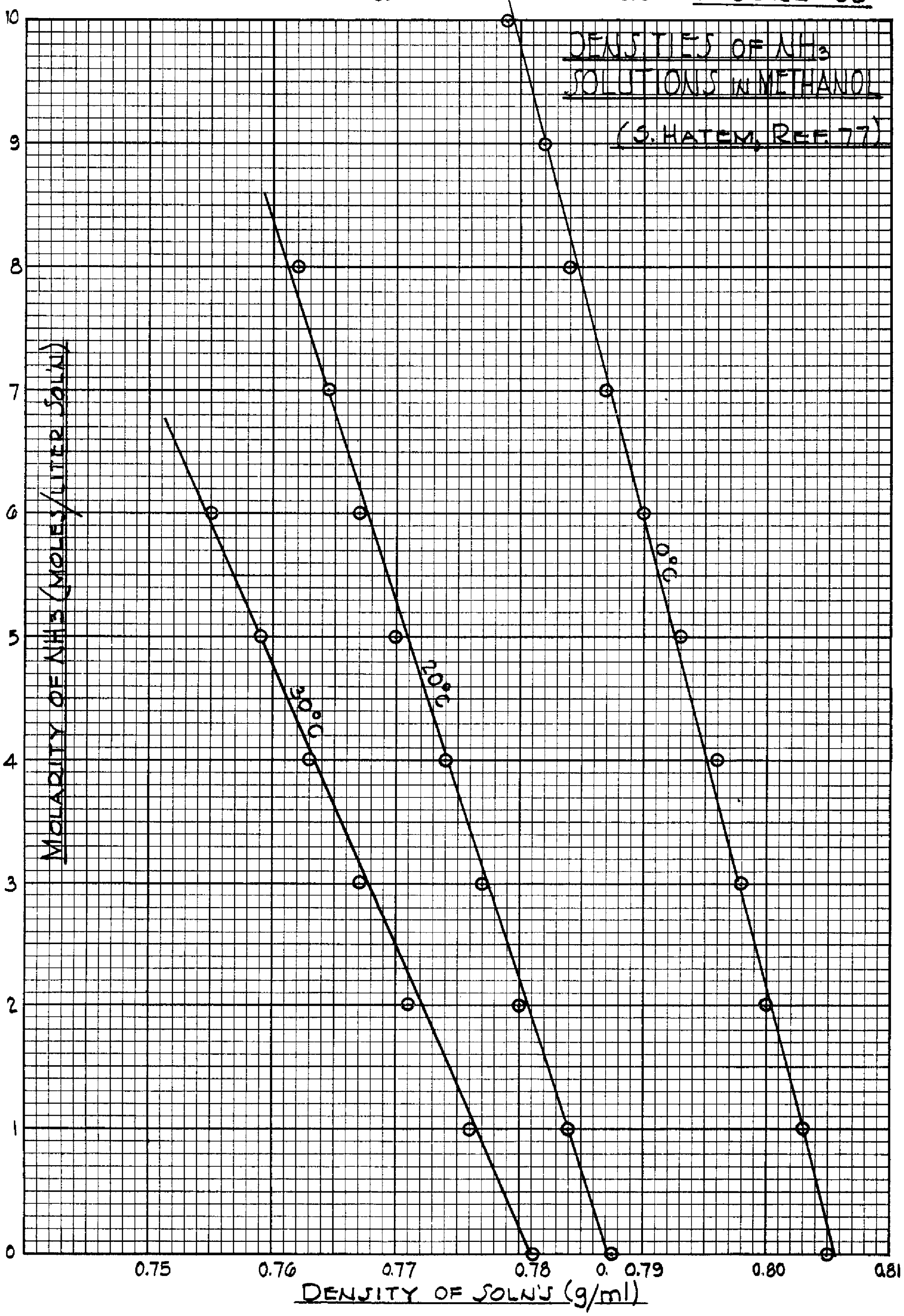

FIGURE 69

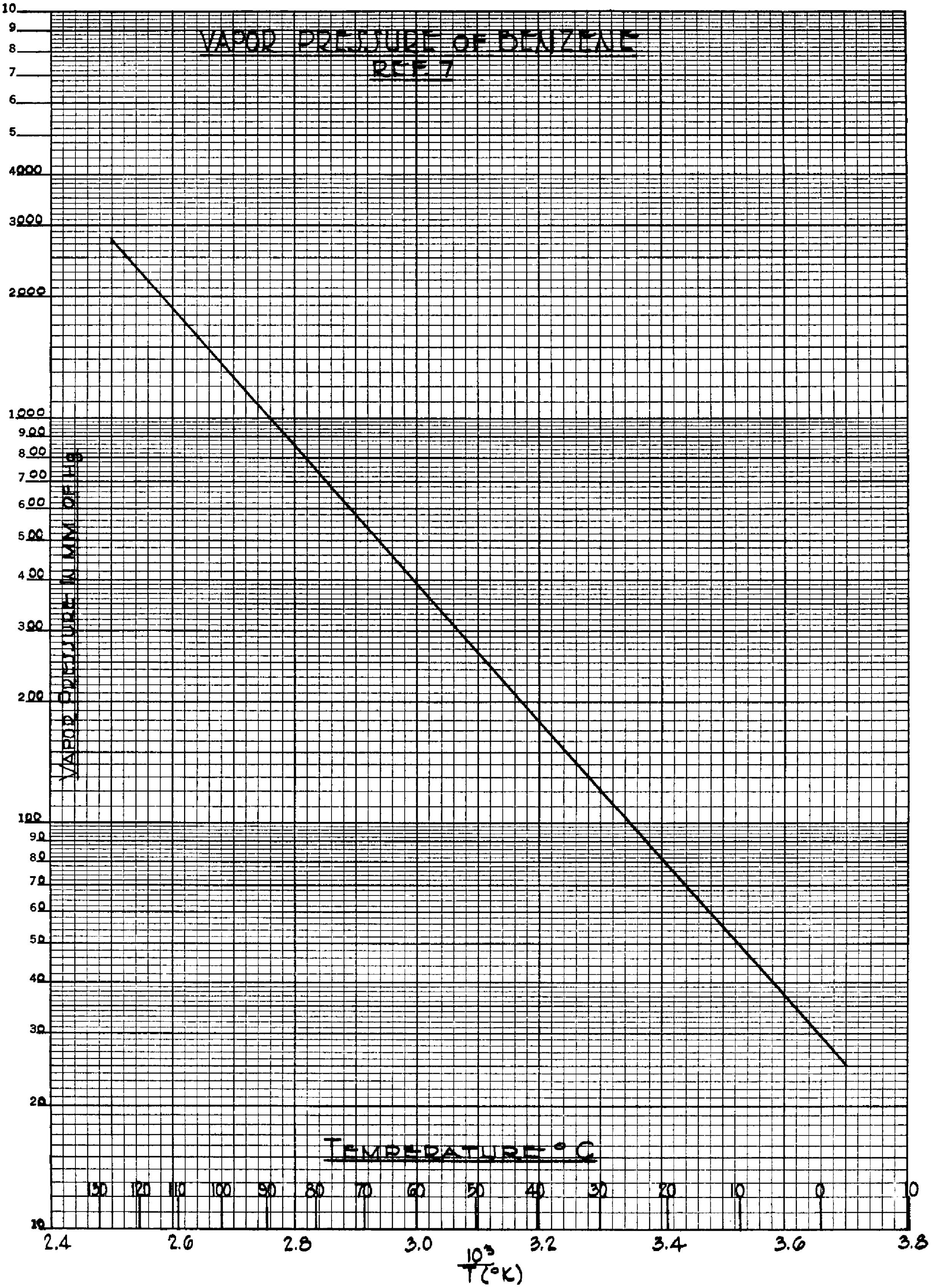
VAPOR PRESSURE OF BENZENE
REF 7
VAPOR PRESSURE IN MM OF Hg
10
9
8
7
6
5
4000
3000
2000
1000
900
800
700
600
500
400
300
200
100
90
80
70
60
50
40
30
20
10
TEMPERATURE °C
150
120
110
100
90
80
70
60
50
40
30
20
10
0
-10
2.4
2.6
2.8
3.0
3.2
3.4
3.6
3.8
$\frac{10^3}{T(°K)}$

Ignition Temperature	580°C, 1076°F	(3)
Limits of Inflammability	$>$1.35% and $<$6.75% (vol.) of C_6H_6 in air	(3)
Refractive Index	1.05011 at 20°C	(8)

Benzene - Ethylenediamine

Phase Diagram	See Figure 70	(78,11)
Vapor Liquid Composition Diagram	See Figure 71	(78)

Benzene - Propylenediamine

Phase Diagram	See Figure 72	(79)
Vapor Liquid Composition Diagram	See Figure 73	(79,80)

C. DECANE

Formula Weight	142.28	
Melting Point	- 29.7°C	(3)
Boiling Point	172.5°C at 762 mm	(81)
Density	0.730 at 20°C	(81)
Heat Capacity	58.10 cal/°C g mole for gas at 25°C	(7)
Viscosity	0.9204 centipoise at 20°C	(7)
Surface Tension	23.7 dynes/cm at 20°C	(81)
Flash Point	46°C	(3)
Ignition Temperature	250°C	(3)
Explosive Limits	0.67 to 2.60% by vol. in air	(3)

UNCLASSIFIED DWG. 20355

FIGURE 70

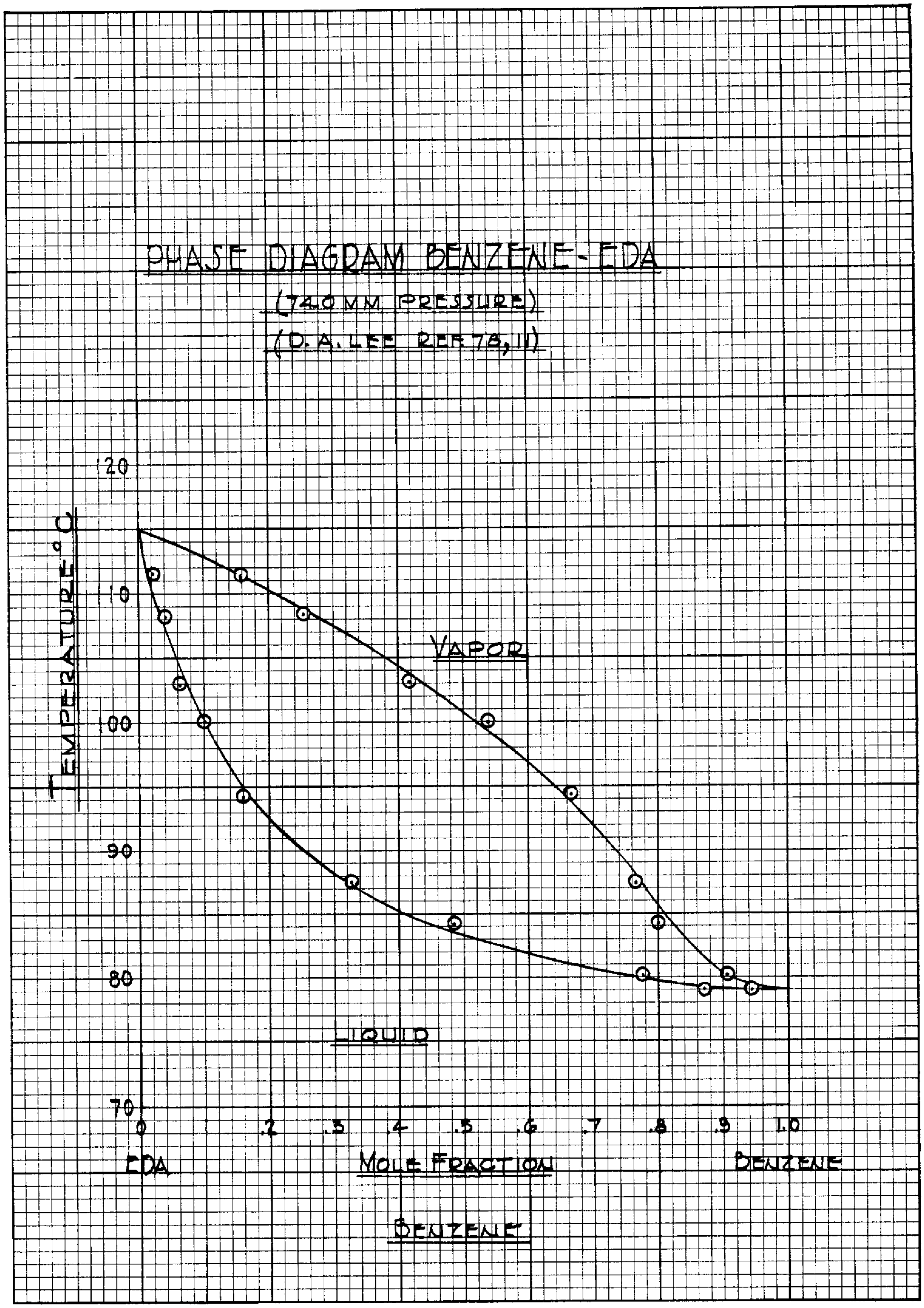

PHASE DIAGRAM BENZENE-EDA

(740 MM PRESSURE)

(D. A. LEE REF 78, 11)

UNCLASSIFIED DWG. 20356

FIGURE 71

VAPOR-LIQUID EQUILIBRIA COMPOSITION DIAGRAM

EDA - BENZENE

(D.A. LEE REF. 78)

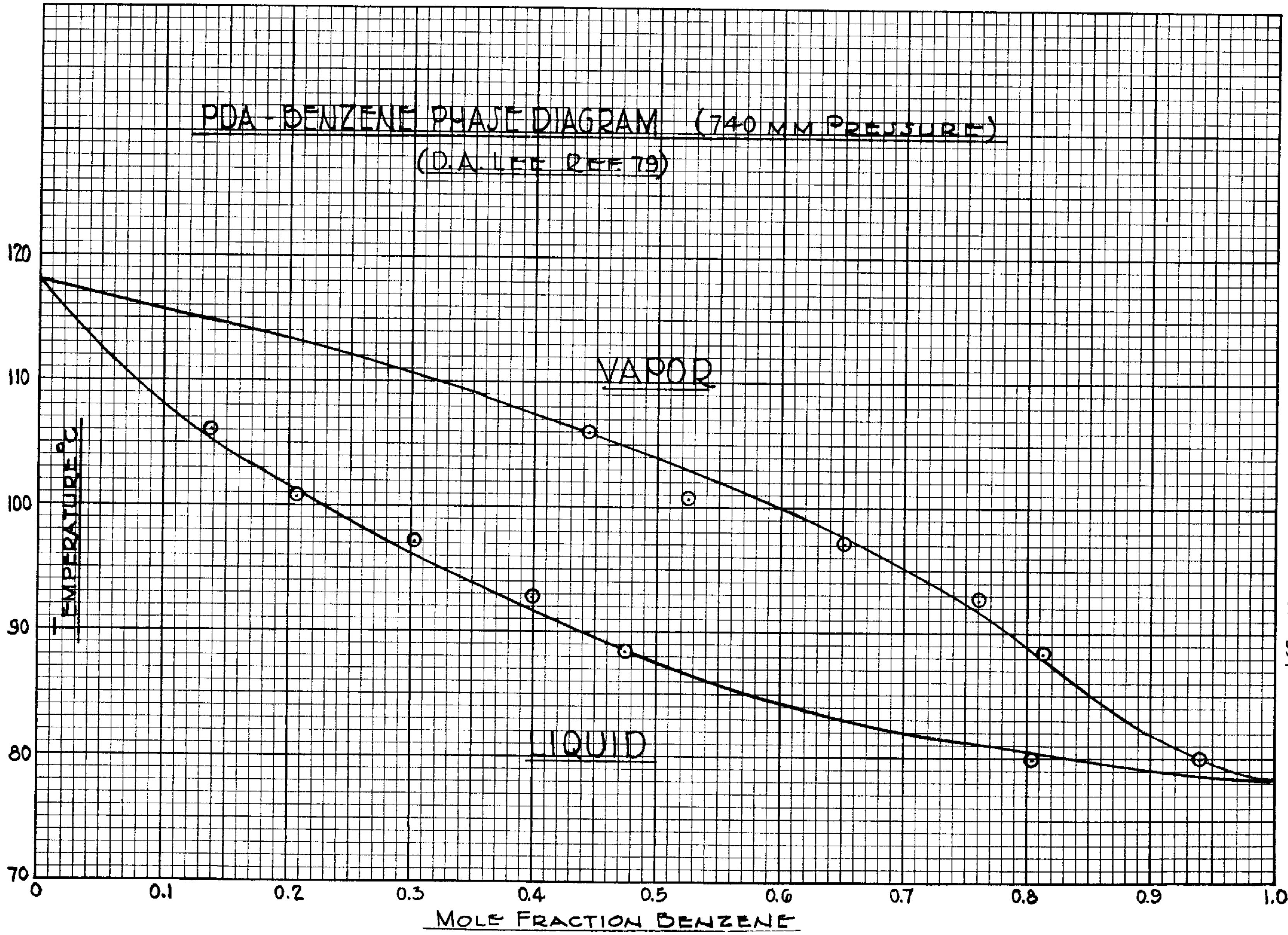

UNCLASSIFIED DWG. 20357

FIGURE 72

UNCLASSIFIED DWG. 20358 FIGURE 73

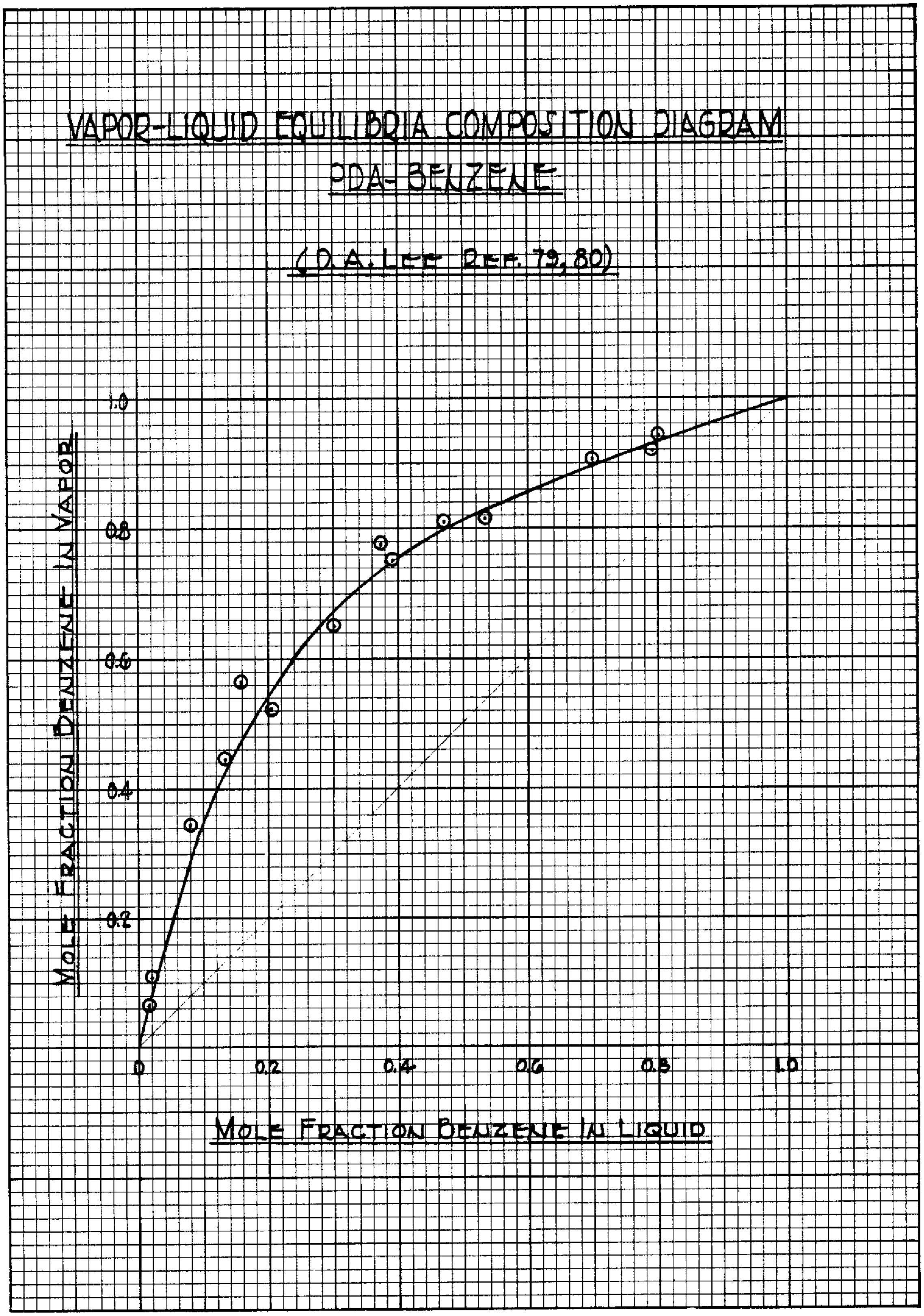

VAPOR-LIQUID EQUILIBRIA COMPOSITION DIAGRAM
PDA-BENZENE
(D.A. LEE REF. 79,80)

Refractive Index	1.41206 at 20°C	(81)

Decane - Propylenediamine

Vapor Liquid Composition Diagram	See Figure 74	(82)
Limits of Solubility Room temperature	0.01 moles PDA soluble per liter decane phase 0.15 mole decane soluble per liter PDA phase	(68)

D. DODECANE

Formula Weight	170.33	
Melting Point	-9.6°C	(3)
Boiling Point	214.5°C	(3)
Density	0.750 g/ml at 20°C	(81)
Heat Capacity	69.62 cal/°C g mole for gas at 25°C	(7)
Viscosity	1.49 centipoise at 20°C	(7)
Surface Tension	25.5 dynes/cm at 20°C	(81)
Flash Point	74°C	(3)
Ignition Temperature	534°C	(3)
Explosive Limits	0.60 to -- % by vol. in air	(3)
Refractive Index	1.42186 at 20°C	(81)

Dodecane - Propylenediamine

Limits of Solubility at room temperature	0.04 moles PDA per liter of dodecane phase 0.01 moles dodecane per liter of PDA phase	(72)

E. ETHYLENEDIAMINE

Formula Weight	60.08	

UNCLASSIFIED DWG. 20359

FIGURE 74

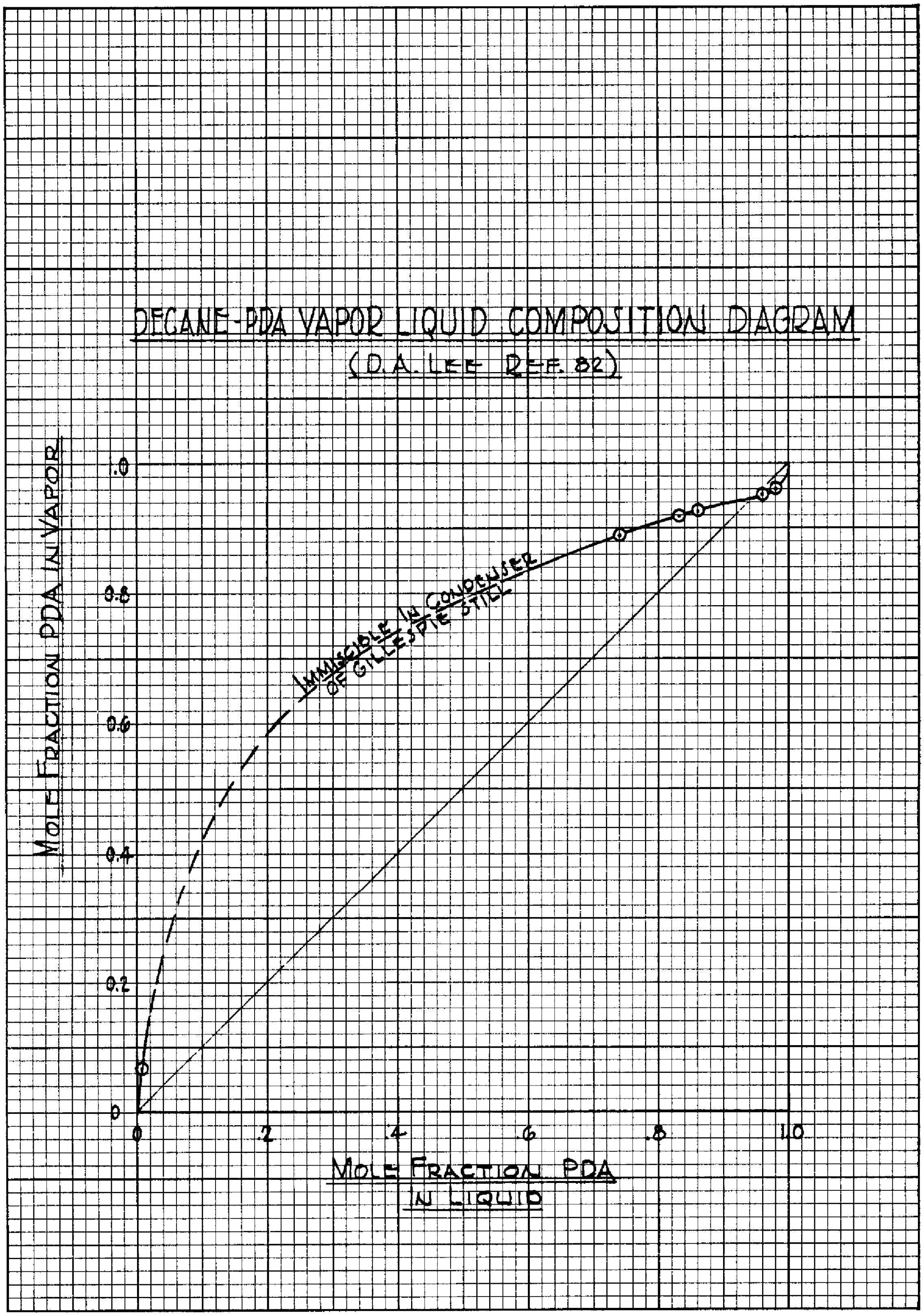

DECANE-PDA VAPOR LIQUID COMPOSITION DIAGRAM

(D.A. LEE REF. 82)

Melting Point	10.8°C	(8)
Boiling Point	116.2°C	(11)
Latent Heat of Fusion	77 cal/g (monohydrate)	(11)
Latent Heat of Vaporization	167 cal/g (monohydrate)	(11)
Vapor Pressure	See Figure 75	(11)
Density	See Figure 76	(11)
Heat Capacity	0.66 cal/g °C (12° - 26°C)	(11)
Thermal Conductivity	0.00060 cal/sec °C cm, 0.145 Btu/hr °F ft	(11)
Viscosity	See Figure 27	(11)
Conductance	9.0 x 10^{-8} mho	(11)
Surface Tension	See Figure 77	(11)
Flash Point	110°F	(8)
Refractive Index	1.4565 at 20°C	(8)
Solubilities of Salts in EDA	See Figures 16,28,29	(11)

Solubilities of Salts in EDA at room temp. (11)

Salt	Solubility moles/liter sol'n
LiF	0.001
LiCl	0.29
LiBr	0.25
LiI	0.37
KCl	0.0017
KBr	0.059
KI	3.44
NaCl	0.05
NaBr	4.09
NaI	1.9
EDA·2HCl	1.70
EDA·H_2SO_4	0.001
EDA·H_2CO_3	1.0

UNCLASSIFIED DWG. 20360

FIGURE 75

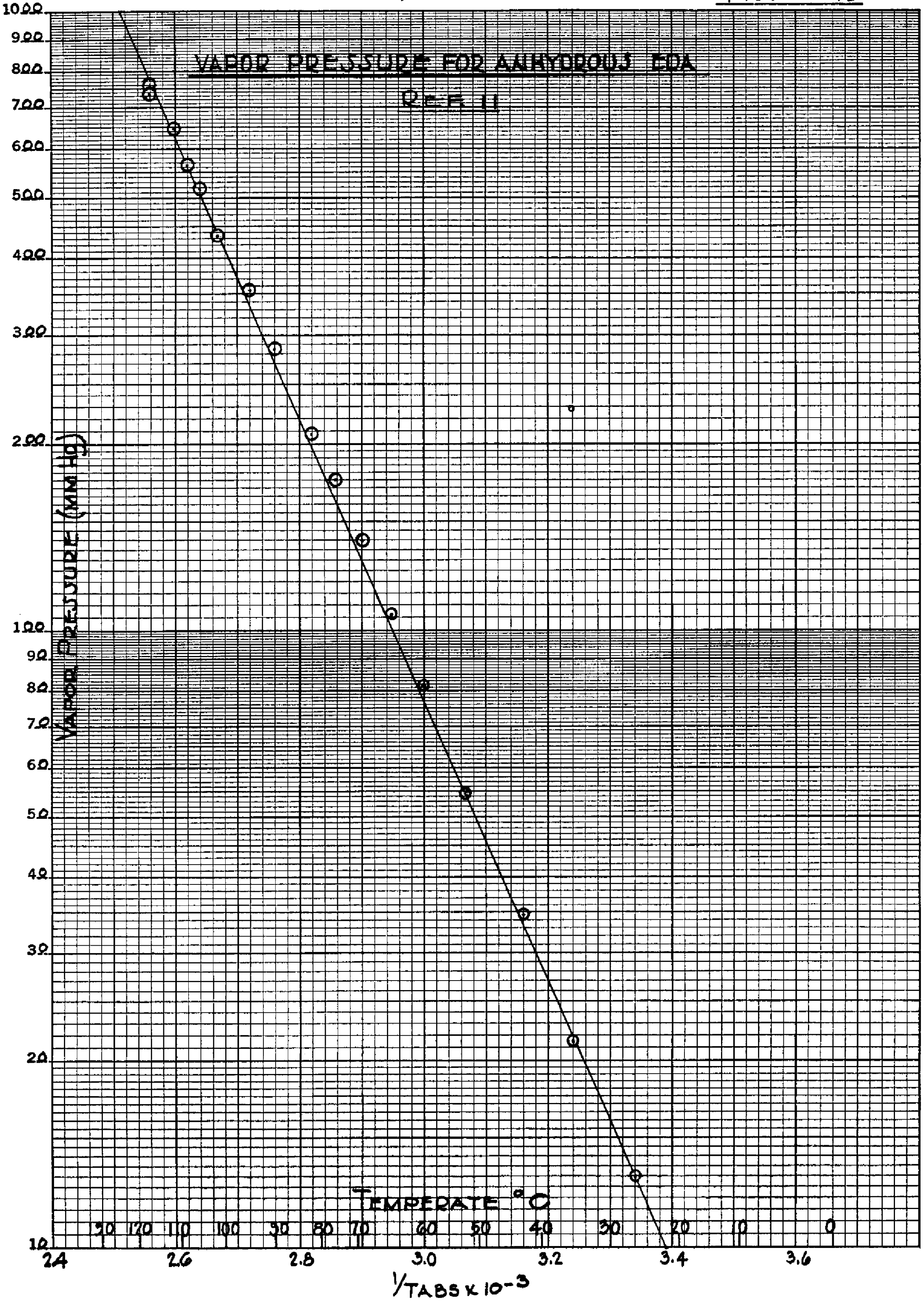

UNCLASSIFIED DWG. 20361

FIGURE 76

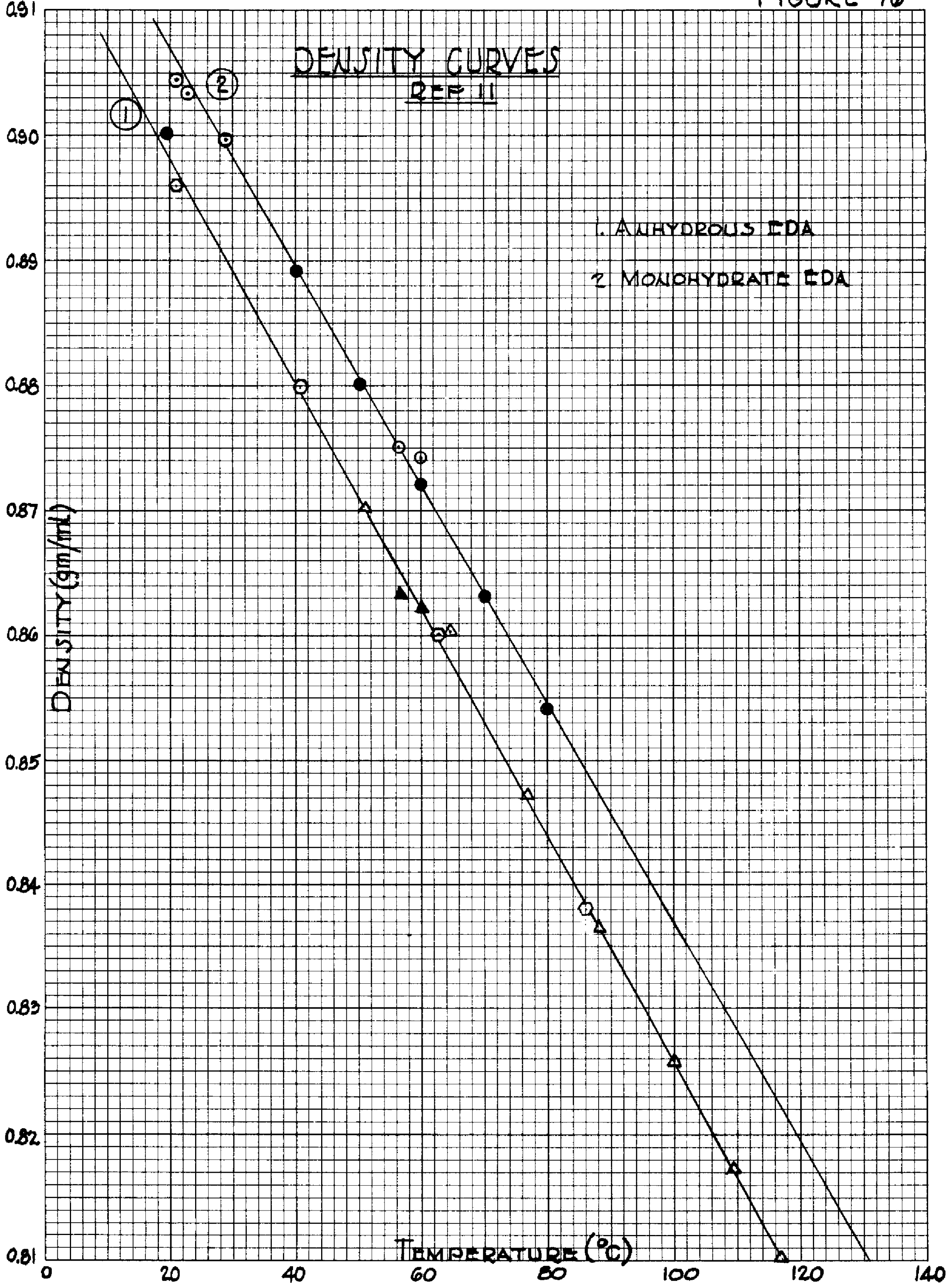

UNCLASSIFIED DWG. 20362

FIGURE 77

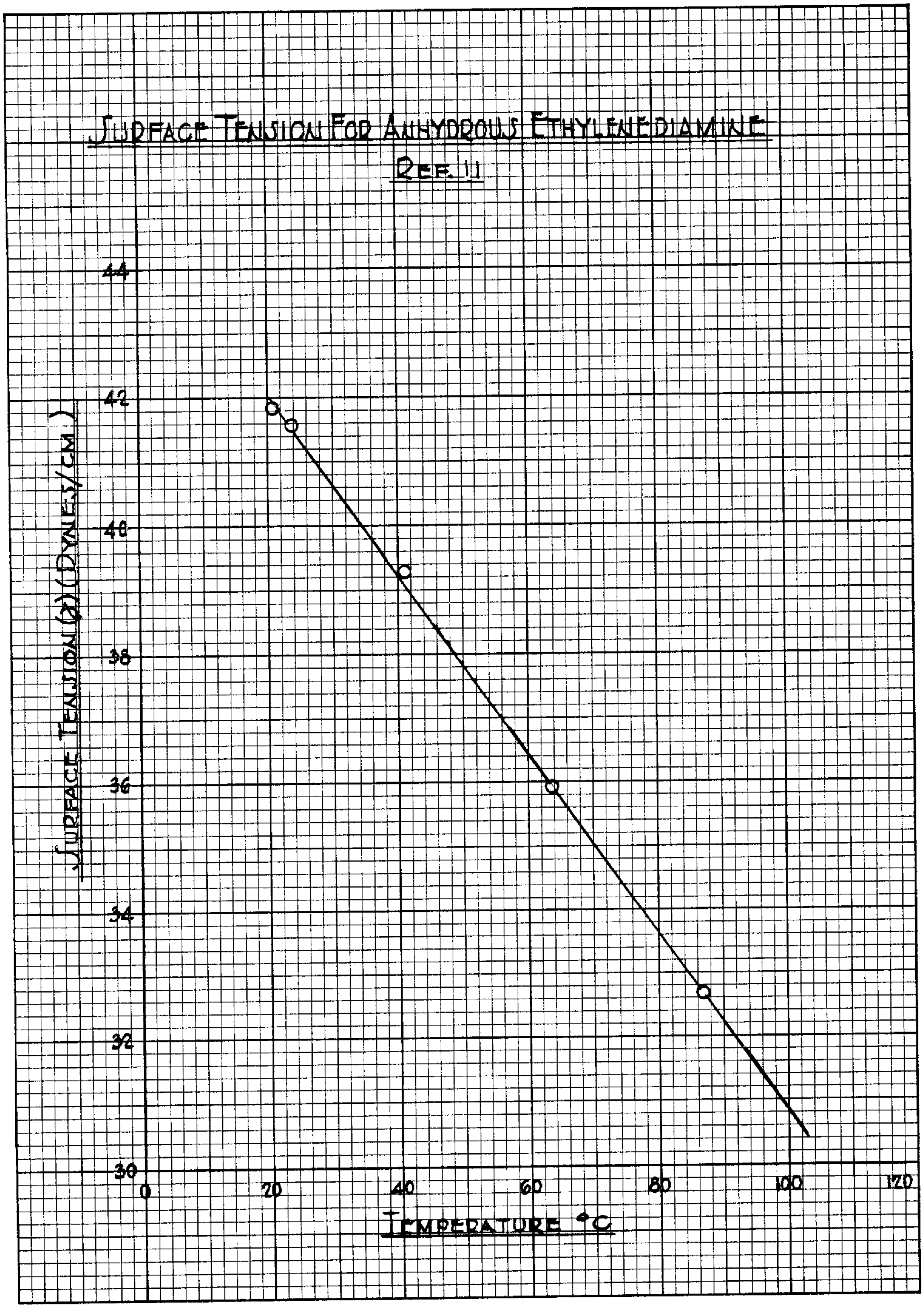

SURFACE TENSION FOR ANHYDROUS ETHYLENEDIAMINE

REF. 11

Ethylenediamine - Water

Phase Diagram	See Figure 78	(11)

F. ETHYLENE GLYCOL

Formula Weight	62.07	
Melting Point	- 13.0°C	(8)
Boiling Point	197.2°C	(8)
Latent Heat of Fusion	44.7 cal/g	(18)
Latent Heat of Vaporization	191 cal/g, 344 Btu/lb	(8)
Vapor Pressure	0.06 mm at 20°C, 10 mm at 89°C, 50 mm at 123°C	(8)
	$\log_{10}P_{mm} = 7.8808 - 1957/(193.8 + t^{\circ}C)$	(18)
Density	1.11336 g/ml at 20°C	(18)
Specific Gravity	1.1154 20/20°C, 9.28 lb/gal at 20°C	(8)
Heat Capacity	0.561 cal/g °C (Btu/lb °F) at 20°C	(8)
	$0.538 + 0.00113t$ °C	(18)
Thermal Conductivity	0.000690 cal/sec cm °C at 20°C	(18)
Viscosity	57.4 cp at 0°C, 20.9 cp at 20°C, 9.5 cp at 40°C	(8)
Conductivity	1.07×10^{-6} mhos	(18)
Surface Tension	48.4 dynes/cm at 20°C, $50.21 - 0.089t$ °C	(18)

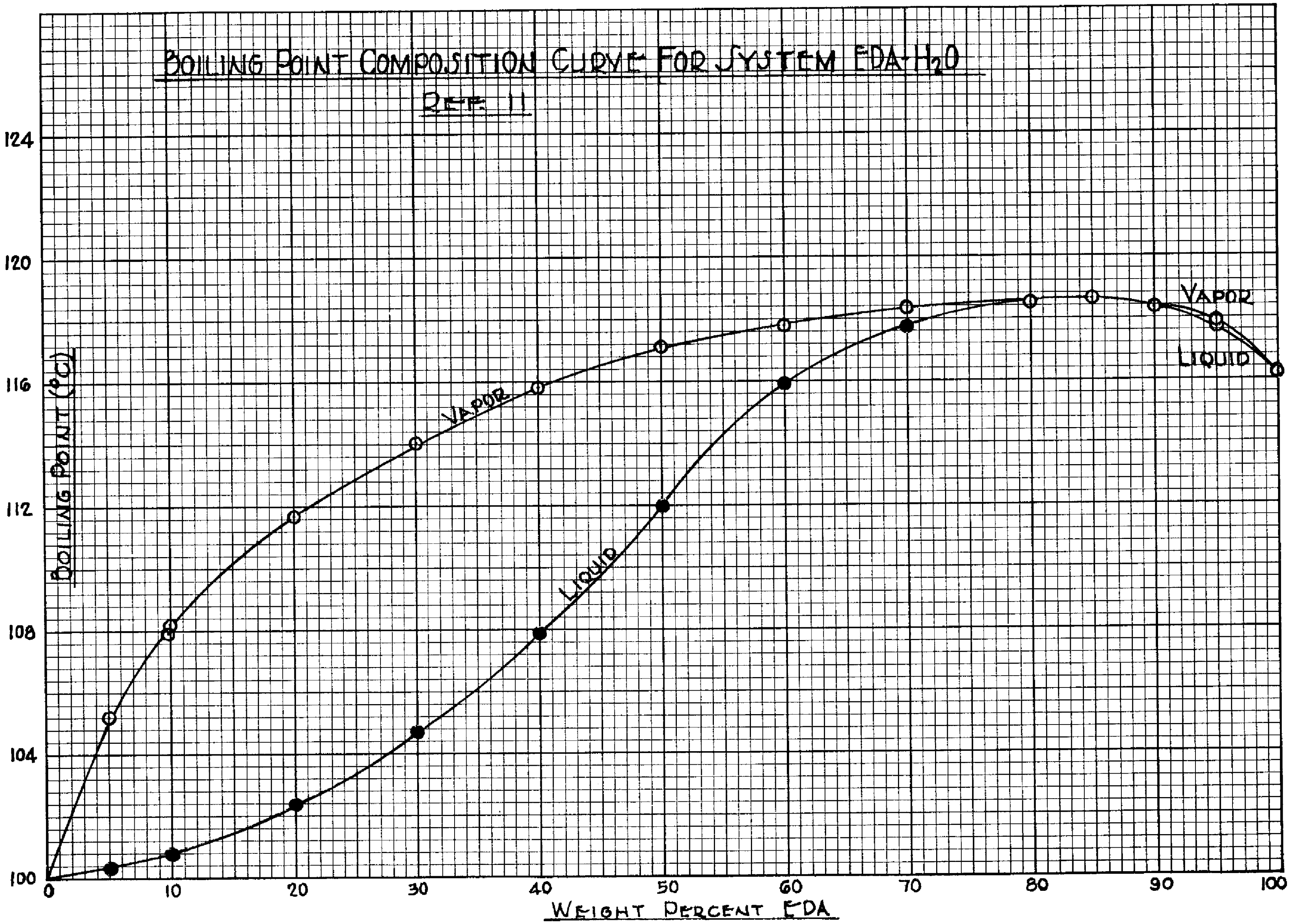

UNCLASSIFIED DWG. 20363

FIGURE 78

Flash Point	111°C, 232°F	(3)
Ignition Temperature	413°C, 775°F	(3)
Refractive Index	1.4316 at 20°C	(8)

Solubility of Salts in Ethylene Glycol

Salt	Solubility g salt / 100 g solvent	moles salt / liter solvent	Temp. °C
LiCl	14.3	3.76	25
LiBr	39.4	5.05	25
KCl	5.18	0.77	25
NaCl	7.15	1.36	25

Ethylene Glycol - Propylenediamine - Water

Vapor - Liquid Composition — For mole ratio PDA/Ethylene Glycol = 0.5 (83)

Mole Fraction H_2O

Vapor	Liquid
.694	.341
.731	.424
.799	.524

G. 2 ETHYLHEXANOL

Formula Weight	130.22	
Melting Point	-76°C	(84)
Boiling Point	184.4°C	(8)
Latent Heat of Vaporization	92.8 cal/g, 167 Btu/lb	(8)
Vapor Pressure	.2 mm at 20°C, 10 mm at 78°C, 50 mm at 109°C	(8)
Specific Gravity	0.8345 20/20°C, 6.94 lbs/gal at 20°C	(8)

Heat Capacity	0.564 cal/g $^{\circ}$C (Btu/lb $^{\circ}$F) at 25°C	(8)
Viscosity	10.0 centipoise at 20°C, 4.0 centipoise at 40°C	(8)
Flash Point	185°F	(8)
Refractive Index	1.4313 at 20°C	(8)
Solubility in Water	0.10 wt % at 20°C	(8)
Solubility of Water in 2-EH	2.6 wt % at 20°C	(8)

2 Ethylhexanol - Propylenediamine

Vapor Liquid Composition Diagram	See Figure 79	(79)

2 Ethylhexanol - Water

Limits of Solubility at Room Temperature	Solubility of H_2O in 2 Ethylhexanol = 2.6% by wt. Solubility of 2 Ethylhexanol in H_2O = 0.1% by wt.	(8)

H. ISOPROPANOL

Formula Weight	60.09	
Melting Point	- 87.8°C	(8)
Boiling Point	82.3°C	(8)
Latent Heat of Vaporization	159 cal/g, 287 Btu/lb	(8)
Vapor Pressure	10 mm at 2°C, 33.0 mm at 20°C, 50 mm at 27°C	(8)
Specific Gravity	0.7868 20/20°C, 6.55 lb/gal. at 20°C	(8)

UNCLASSIFIED DWG. 20364

FIGURE 79

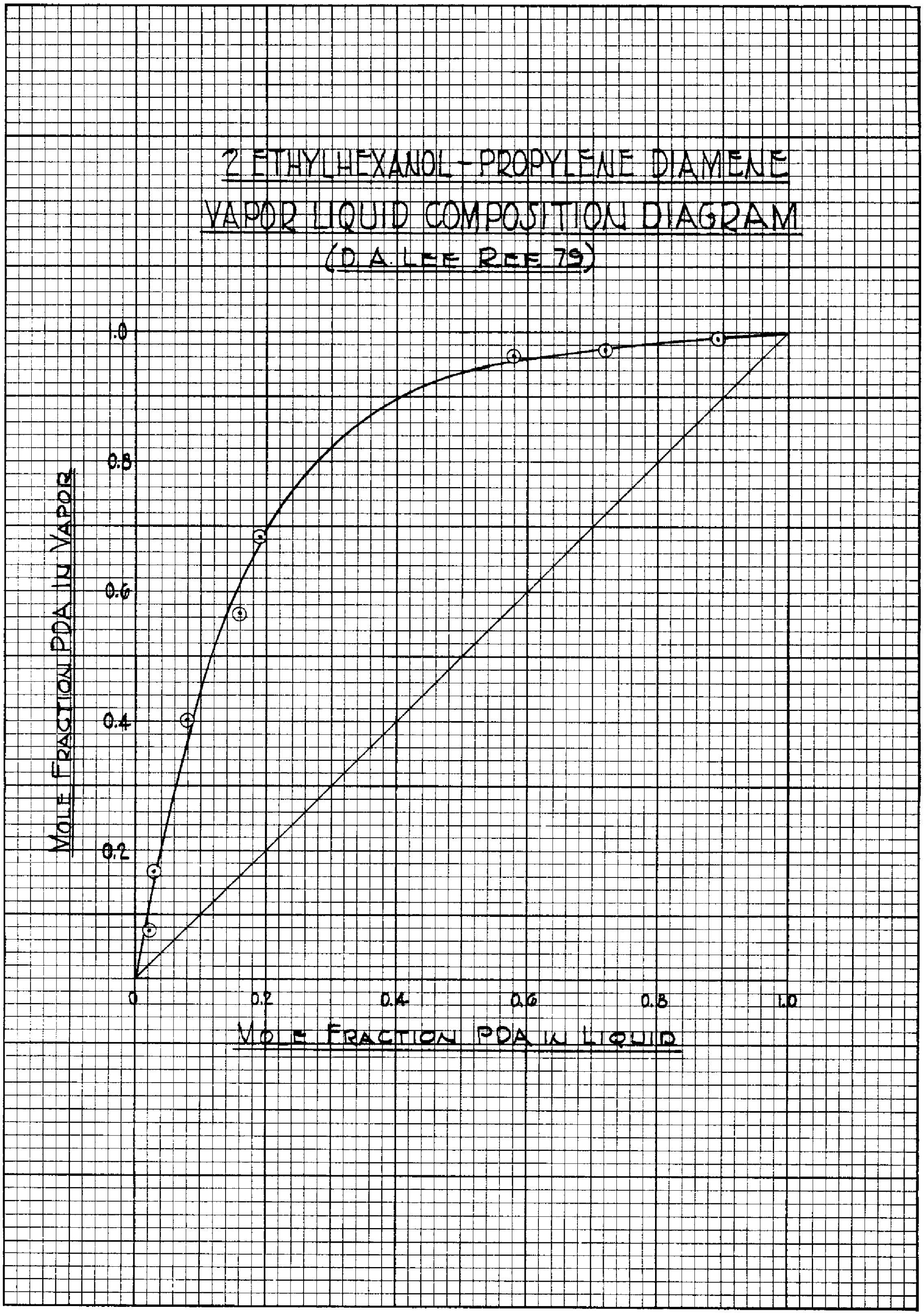

2 ETHYLHEXANOL - PROPYLENE DIAMENE
VAPOR LIQUID COMPOSITION DIAGRAM
(D.A. LEE REF 79)

Heat Capacity	0.596 cal/g °C (Btu/lb °F) at 20°C	(8)
Viscosity	2.4 cp at 20°C	(8)
Flash Point	70°F	(8)
Limit of Inflammability	2.02% by vol. lower limit	(3)
Refractive Index	1.3772 at 20°C	(8)

Isopropanol - Water

Phase Diagram	See Figure 80	(19)

I. METHANOL

Formula Weight	32.04	
Melting Point	- 97.6°C	(8)
Boiling Point	64.5°C	(8)
Latent Heat of Vaporization	263 cal/g, 473 Btu/lb	(8)
Vapor Pressure	10 mm at -17°C, 50 mm at 9°C, 92 mm at 20°C	(8)
Specific Gravity	0.7939 20/20°C, 6.61 lb/gal at 20°C	(8)
Heat Capacity	0.599 cal/g °C (Btu/lb °F) at 20°C	(8)
Viscosity	0.59 cp at 20°C	(8)
Flash Point	11°C, 52°F	(3)
Ignition Temperature	470°C, 878°F	(3)
Limits of Inflammability	6.72 to 36.50% by volume in air	(3)
Refractive Index	1.3285 at 20°C	(8)

FIGURE 80

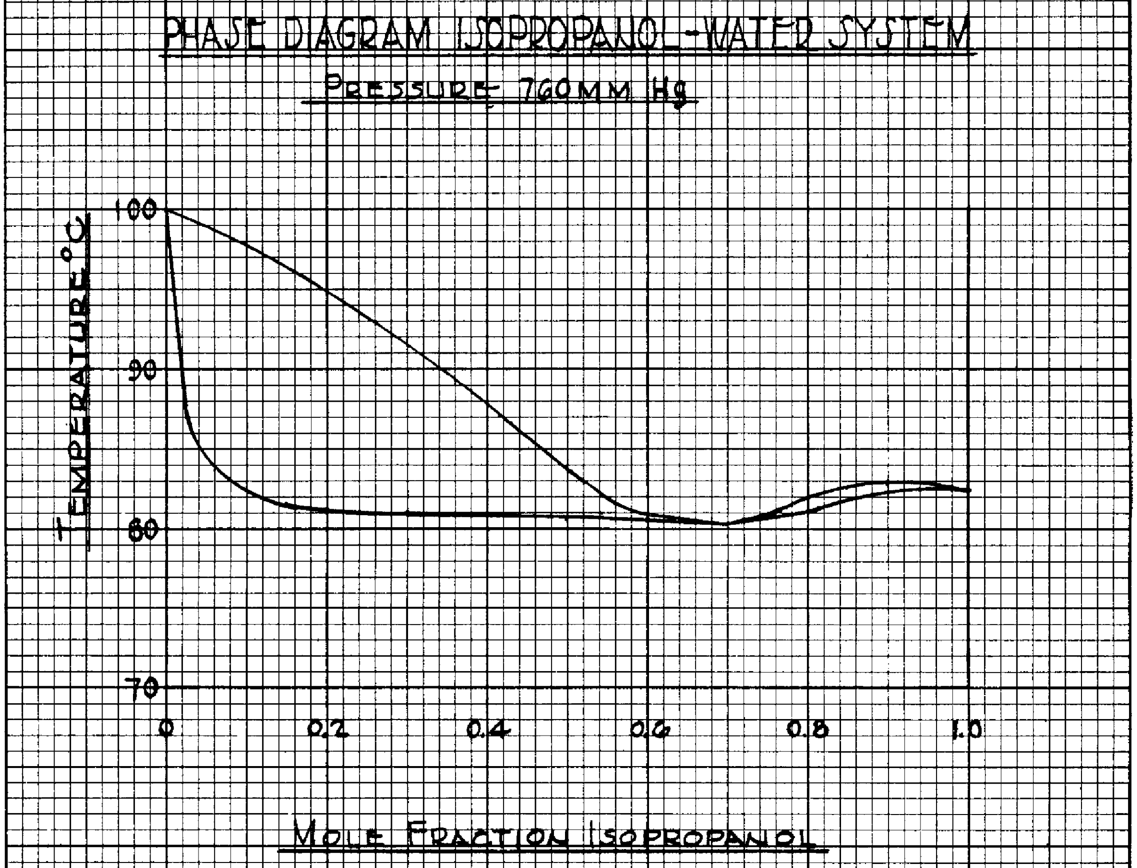
PHASE DIAGRAM ISOPROPANOL-WATER SYSTEM
PRESSURE 760MM Hg
TEMPERATURE °C
100
90
80
70
0
0.2
0.4
0.6
0.8
1.0
MOLE FRACTION ISOPROPANOL

Methanol - Propylenediamine

Phase Diagram	See Figure 81	(79)
Vapor Liquid Composition Diagram	See Figure 83	(85)

Methanol - Water

Phase Diagram	See Figure 82	(19)

J. MERCURY

Atomic Weight	200.61	
Melting Point	- 38.9°C, - 38.0°F	(1)
Boiling Point	357°C, 675°F	(1)
Latent Heat of Fusion	2.8 cal/g, 562 cal/g atom, 5.04 Btu/lb, 1010 Btu/lb atom	(1)
Latent Heat of Vaporization	69.7 cal/g, 1390 cal/g atom, 125.4 Btu/lb, 2500 Btu/lb atom	(1)
Vapor Pressure	$\log_{10} P_{mm} = \frac{-3308}{T} - 0.8 \log T + 10.3735$ Accuracy 2%, 400-800°K; 5%, 234-850°K See Figure 7	(1)
Density	13.546 g/ml at 20°C, 13.352 g/ml at 100°C 845.68 lbs/ft^3, 113.04 lbs/gal at 68°F See Figures 9, 10, 51	(1)
Heat Capacity	0.0332 cal/g $^{\circ}$C (Btu/lb $^{\circ}$F) at 20°C, 0.03279 cal/g $^{\circ}$C at 100°C	(1)

UNCLASSIFIED DWG. 20366

FIGURE 81

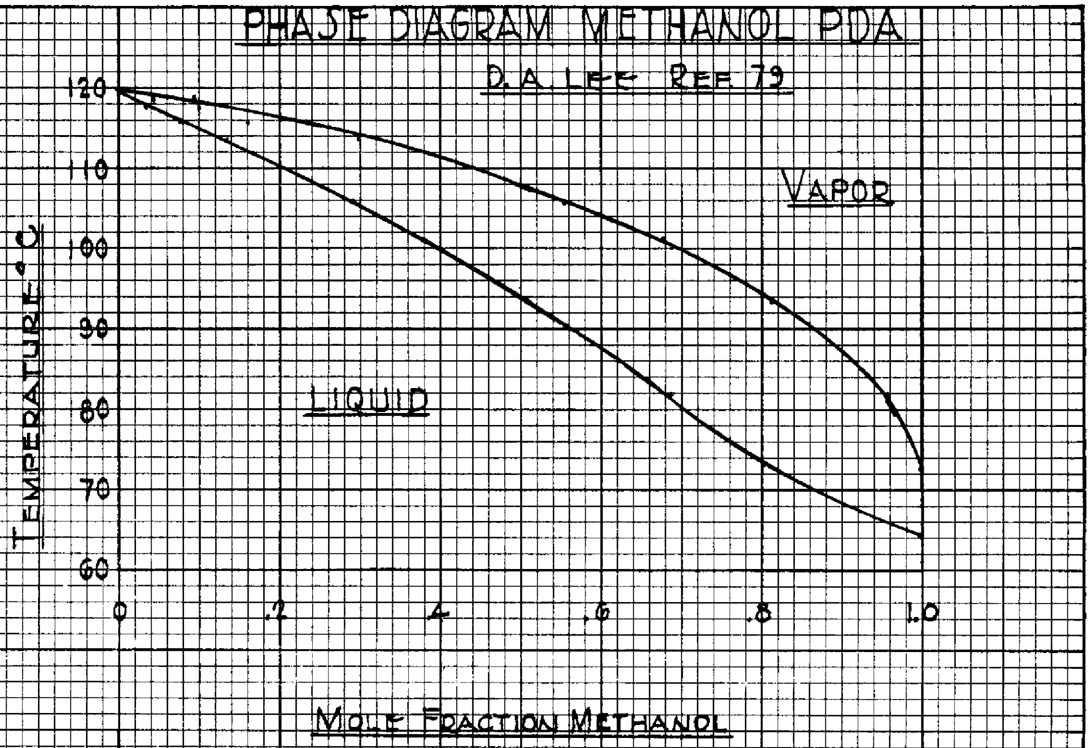

PHASE DIAGRAM METHANOL PDA

D. A. LEE REF 79

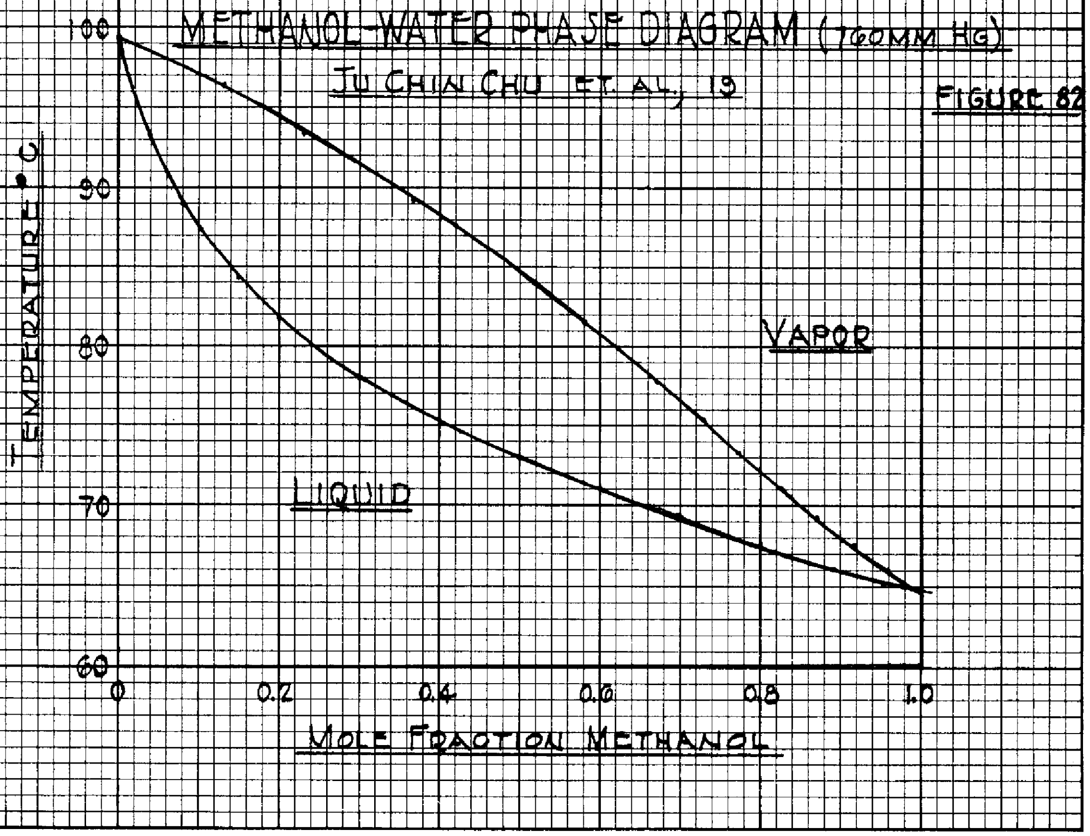

METHANOL-WATER PHASE DIAGRAM (760MM HG)

JU CHIN CHU ET. AL., 19

FIGURE 82

FIGURE 83

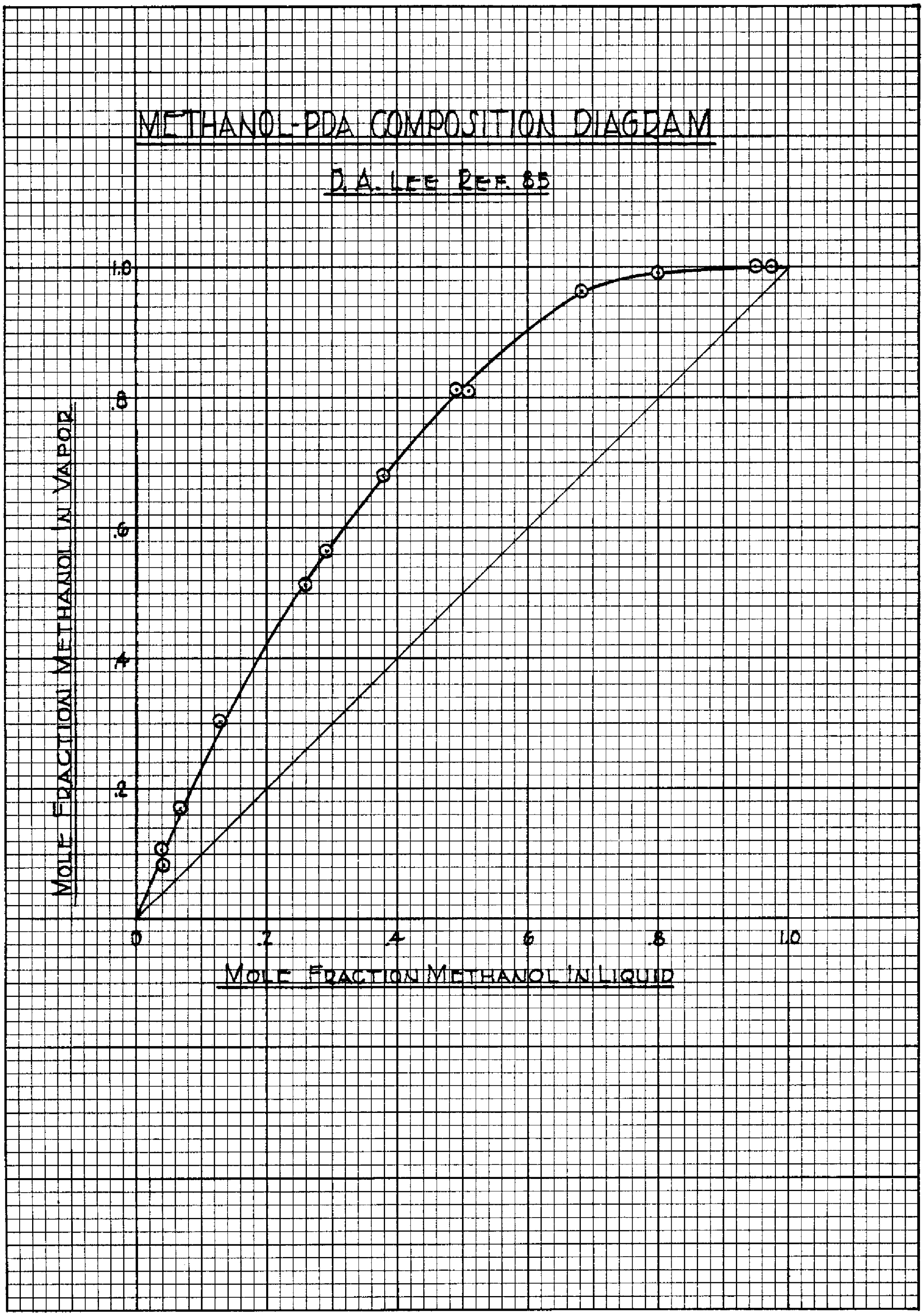
METHANOL-PDA COMPOSITION DIAGRAM
D. A. LEE REF. 85
MOLE FRACTION METHANOL IN VAPOR
MOLE FRACTION METHANOL IN LIQUID
1.0
.8
.6
.4
.2
0
.2
.4
.6
.8
1.0

Viscosity	1.55 centipoise at 20°C See Figures 11, 52, 84	(1)
Thermal Conductivity	0.021 cal/sec cm °C at 20°C, 5.08 Btu/hr ft °F at 68°F 0.026 cal/sec cm °C at 120°C, 6.3 Btu/ft °F at 248°C	(1)
Electrical Resistivity	98.4 μ ohms at 50°C	(1)
Surface Tension	465 dynes/cm at 20°C, 454 dynes/cm at 112°C	(1)

K. PROPYLENEDIAMINE

Formula Weight	74.13	
Melting Point	-38.6°C	(47)
Boiling Point	120.5°C	(86)
Latent Heat of Vaporization	130 cal/gm, 234 Btu/lb	(8)
Vapor Pressure	$\log_{10} P_{mm} = 7.6487 - \frac{1671.2}{t^{\circ}C + 230}$	(86)
Density	See Figures 36, 85	(12)
Heat Capacity	0.65 cal/g °C (Btu/lb °F) at 27°C	(87)
Thermal Conductivity	0.125 Btu/hr °F ft from 95-200°F	(45)
Viscosity	See Figure 33	(47)
Flash Point	160°F	(8)
Refractive Index	1.4492 at 20°C	(8)

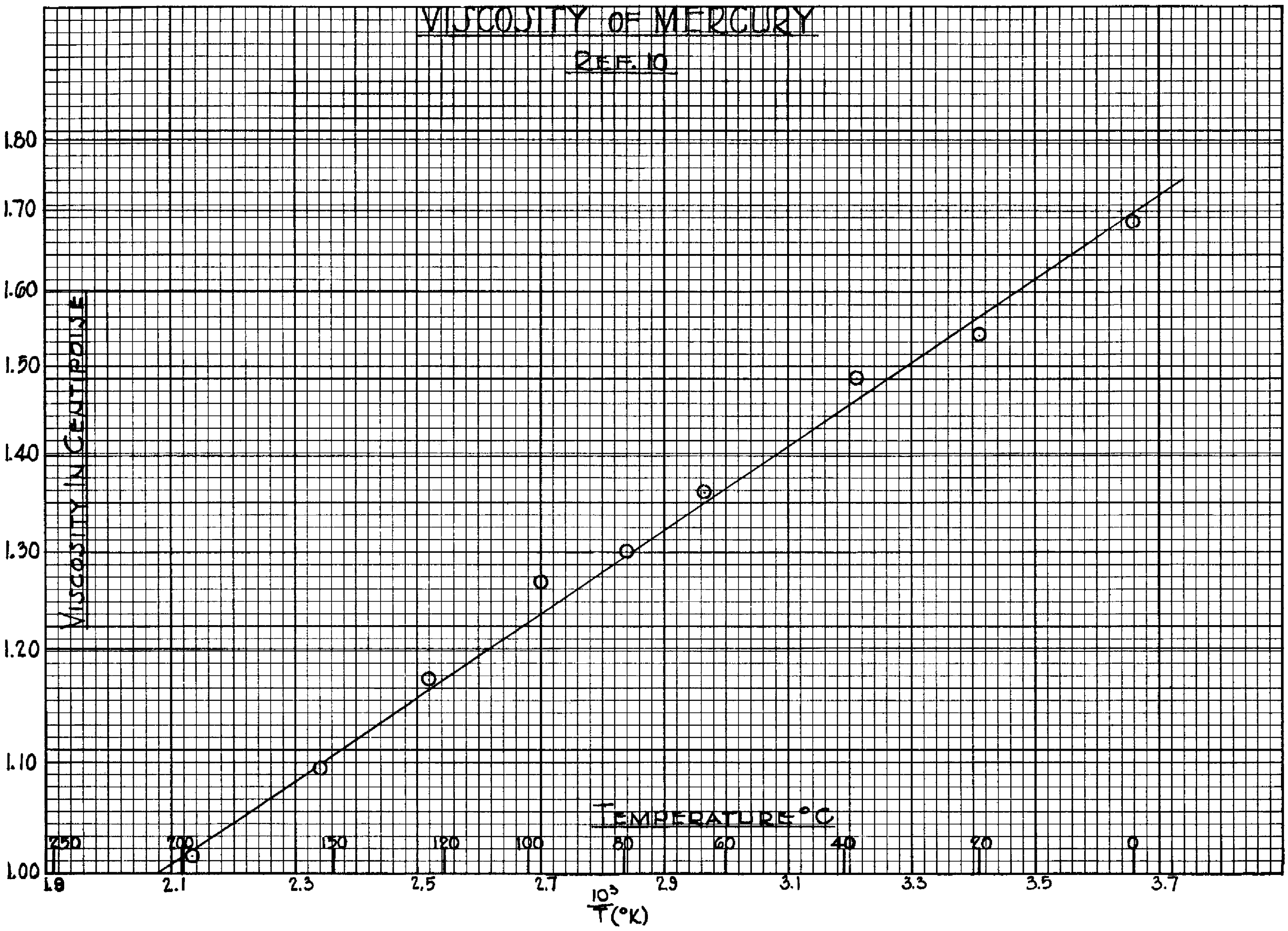

UNCLASSIFIED DWG. 20368

FIGURE 84

UNCLASSIFIED DWG. 20369 FIGURE 85

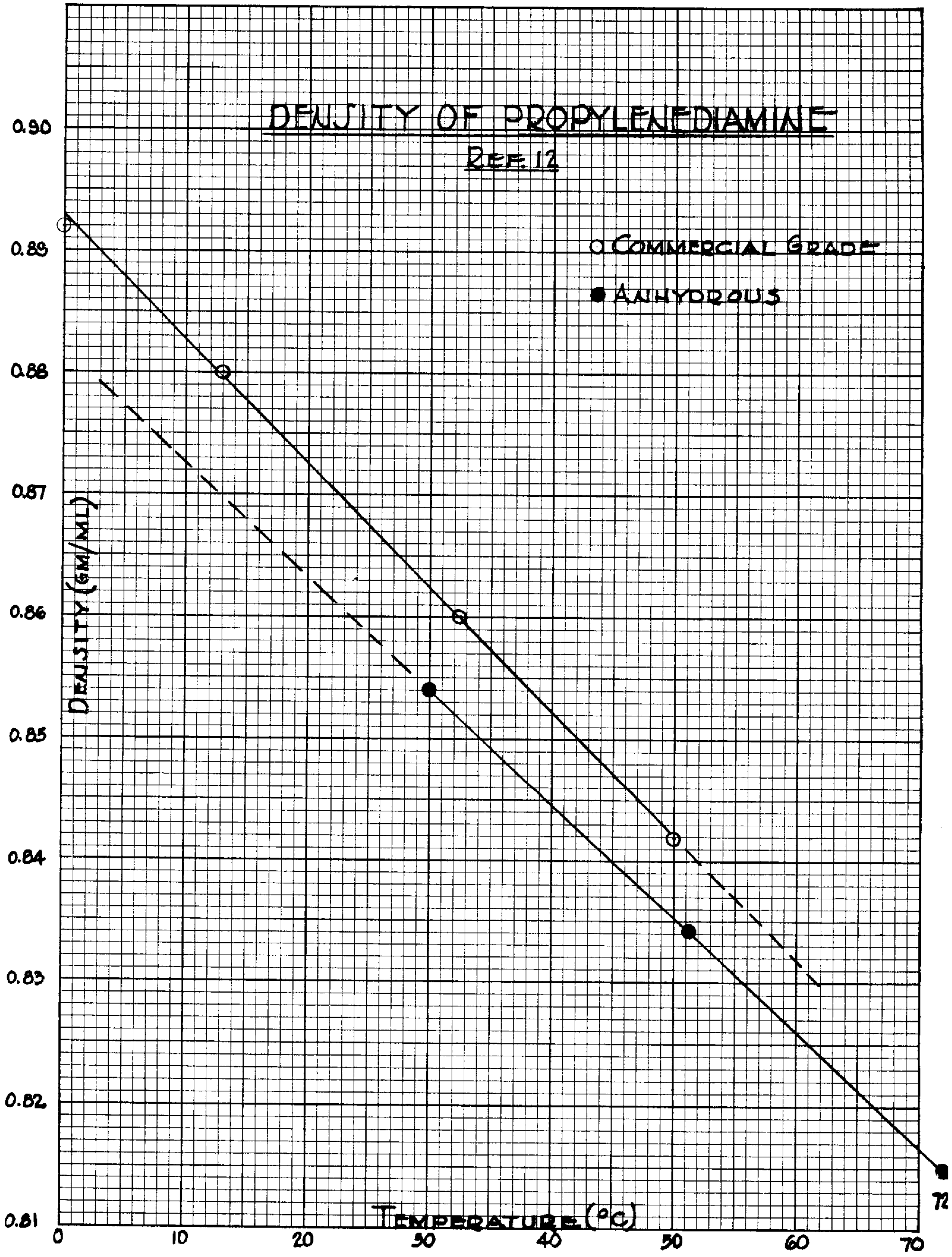

Solubility of Salts in PDA

Salt	Solubility moles/liter sol'n	Temperature °C	
LiCl	1.05	25	(47)
LiBr	1.9	27	(43)
NaCl	0.005	25	(60)
NaBr	2.4	27	(43)
KCl	0.0001	27	(43)
KBr	0.007	25	(59)
KI	1.64	25	(59)
LiOH	0.001	27	(43)

Propylenediamine - Water

Phase Diagrams	See Figure 86	(79)
Vapor-Liquid Composition Diagram	See Figure 87	(78,79)

L. TETRAHYDROFURAN

Formula Weight	72.10	
Melting Point	-108.52°C (-163.3°F)	(88)
Boiling Point	65-67°C (149-152.6°F)	(88)

Vapor Pressure (88)

mm Hg	Temp. °C
114	15
176	25
263	35
385	45
550	55
760	65

Density 0.888 g/ml at 20°C, 7.4 lbs/gal.(88)

FIGURE 86

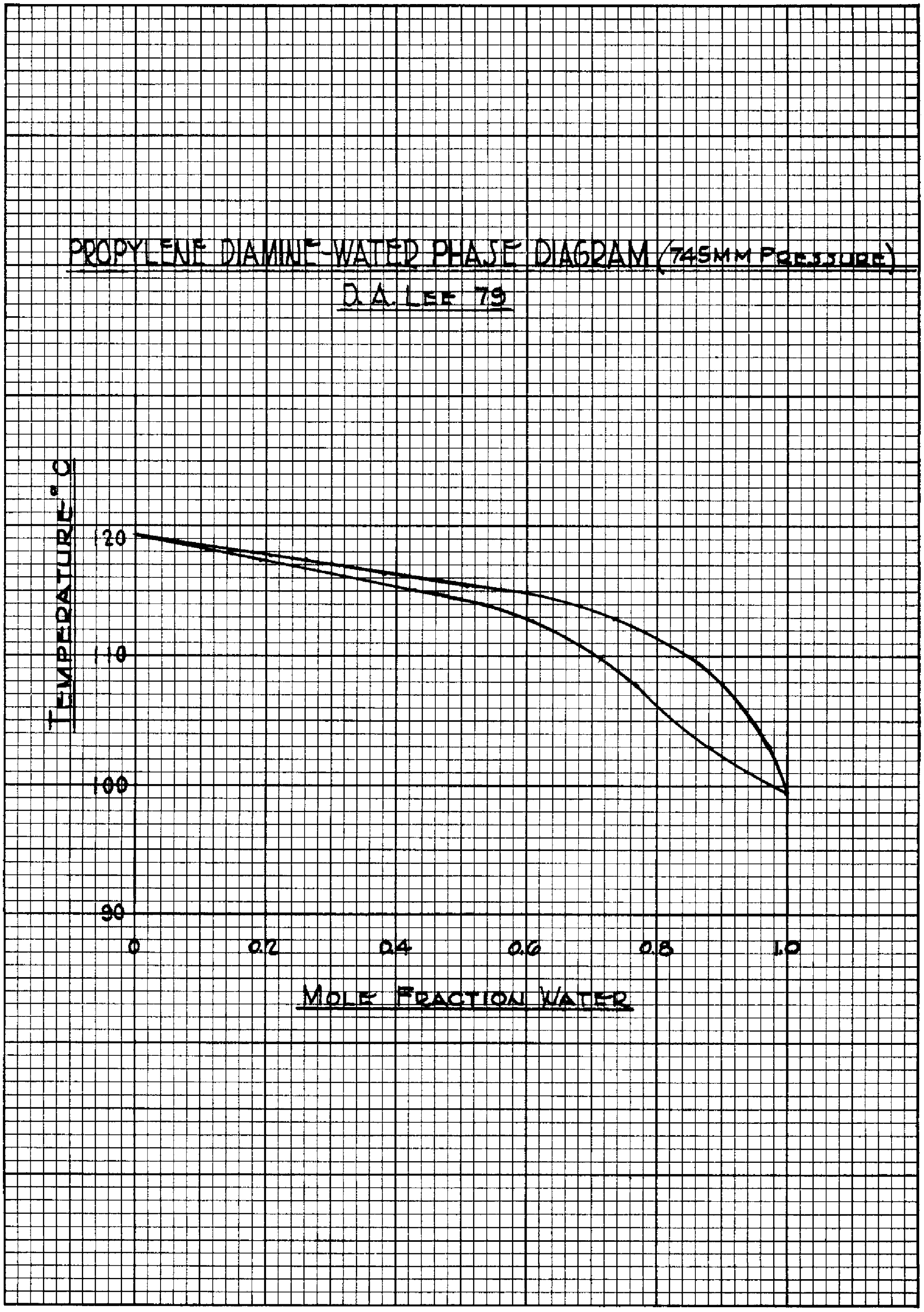

PROPYLENE DIAMINE-WATER PHASE DIAGRAM (745MM PRESSURE)

D.A. LEE 79

UNCLASSIFIED DWG. 20370

FIGURE 87

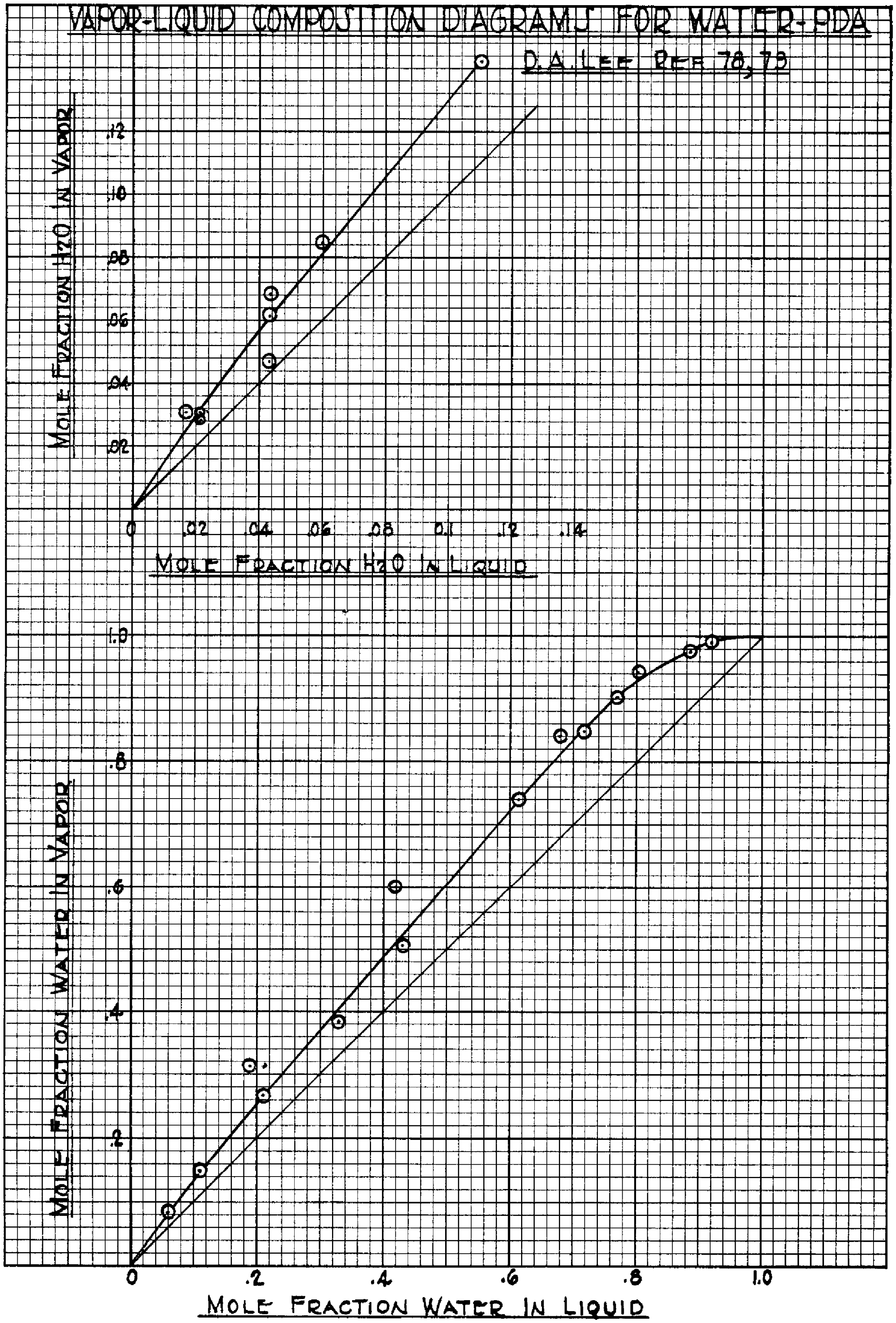

VAPOR-LIQUID COMPOSITION DIAGRAMS FOR WATER-PDA

D.A. LEE REF 78, 79

Viscosity	cp	Temp. °C	(88)
	0.66	0	
	0.55	20	
	0.47	30	
	0.42	40	
Surface Tension	26.4 dynes/cm at 25°C		(88)
Flash Point	- 17°C, 1°F		(88)
Index of Refraction	1.4073 at 20°C		(88)

REFERENCES

1. Lyon, R. N., et. al. "Liquid-Metals Handbook", U. S. Govt. Printing Office, Washington, D. C., 2nd ed., (1952).
2. Hodgman, C. D., et. al. "Handbook of Chemistry and Physics", Chemical Rubber Publishing Company, Cleveland, Ohio, 30th ed., (1947).
3. Perry, John H., et. al. "Chemical Engineer's Handbook", McGraw-Hill Book Co., Inc., New York, 3rd ed., (1950).
4. Seidell, A. "Solubilities of Inorganic and Metal Organic Compounds", D. Van Nostrand Co., Inc., New York, 3rd ed., (1940).
5. Rossini, F. D., et. al. "Selected Values of Chemical Tehrmodynamic Properties:, Nat'l. Bur. Standards Circ. 500, U. S. Govt. Printing Office, Washington, D. C., (1950).
6. Quill, L. L., et. al. "The Chemistry and Metallurgy of Miscellaneous Materials", McGraw-Hill Book Co., Inc., New York, (1950).
7. Rossini, F. D., et. al. "Selected Values of Properties of Hydrocarbons", Nat'l. Bur. Standards Circ. 461, U. S. Govt. Printing Office, Washington, D. C., (1947).
8. Works Laboratory Manual, "Physical Property Tables", Carbide and Carbon Chemical Corp., South Charleston, West Va., Vol. 40, (July 1, 1950).
9. International Critical Tables, McGraw-Hill Book Co., Inc., New York, (1933).
10. Lange, N. A. "Handbook of Chemistry", Handbook Publishers, Sandusky, Ohio, 8th ed., (1952).
11. Palko, A. A. "Handbook on Ethylenediamine", ORNL-1329.
12. Palko, A. A. "Handbook on Propylenediamine", ORNL-1391.
13. Rutenberg, A. C. "Notes on Some Selected Liquid Amalgams", ORNL-1457.
14. Smithells, C. T. "Metal Reference Book", Inter-Science Pub., Inc., New York, (1949).
15. Janecke, E. "Handbook aller Legierungen", Heidelburg, (1949).
16. Yost, D. M. and Russel, H., Jr. "Systematic Inorganic Chemistry", Prentice-Hall, Inc., N. Y., (1944).

17. Audrieth, L. F. and Kleinberg, J. "Non-Aqueous Solvents", John Wiley and Sons, N. Y., (1953).
18. Curme, G. O., et. al. "Glycols", Reinhold Pub. Corp., New York, (1952).
19. Chu, Ju Chin, et. al. "Distillation Equilibrium Data", Reinhold Pub. Corp., New York, (1950).
20. Ditchburn, R. W. and Gilmour, J. C. *Rev. Modern Physics* *13*, 310, (1941).
21. Boyd, C. M. ORNL CF 53-1-298.
22. Grube, G. and Woff, W. *Z. Electrochemic*, 41, 675, (1935).
23. Eaton, G. A. ORNL-1299.
24. Garretson, H. H. ORNL-1457.
25. MacMullin, R. B. *Chem. Eng. Prog.* *46*, 440, (1950).
26. Convers, L. J. *J. Chim. Physique* *36*, 175, (1939).
27. Boohaviwalla, et. al. *Ind. J. Physics* *4*, 147, (1929).
28. Begun, G. M. and Rutenberg, A. C. ORNL-1401.
29. Sklyarenko, S. I. and Sakharov, B. A. *Zhur. Fiz. Khim.* *21*, 97, (1947).
30. Ibid. *Zhur. Obshch. Khim.* 17, 1385, (1947).
31. Rutenberg, A. C. ORNL CF 53-2-174.
32. Begun, G. M. ORNL CF 53-2-174.
33. Dowling, E. J. and Hess, D. N. ORNL CF 53-1-328.
34. Begun, G. M. ORNL CF 53-4-161.
35. Drury, J. S. and Garretson, H. H. ORNL-1238.
36. Drury, J. S. ORNL-1306.
37. Ryon, A. D., Ramsey, J. W. and Weithaup, R. R. ORNL-1306.
38. Eaton, G. A. ORNL-1511.
39. Begun, G. M. ORNL Y-B30-116.
40. Begun, G. M. ORNL CF 53-5-164.
41. Warren, K. S. ORNL CF 53-1-328.
42. Palko, A. A. ORNL CF 53-5-164.
43. Rutenberg, A. C. ORNL Y-B30-116.
44. Begun, G. M. ORNL-1552.
45. Lynch, L. D. ORNL CF 52-11-199.
46. Rutenberg, A. C. ORNL-1306.
47. LeRoy, R. H. ORNL-1388.
48. Begun, G. M., Rutenberg, A. C. and Palko, A. A. ORNL-1238.
49. Johnston, C. P. ORNL Y-B30-116.
50. Harley, P. H. ORNL Y-B35-9.
51. Krohn, N. A. ORNL CF 52-11-199.
52. Hill, W. E. ORNL Y-B30-124.
53. Palko, A. A. ORNL Y-B30-124.
54. Garretson, H. H. "Notes on Activities and Standard Electrode Potentials", ORNL-1457.

55. Rutenberg, A. C. ORNL Y-B30-118.
56. Friend, Hale, Ryder, J. Chem. Soc. (Lond.) 1937, 907.
57. Begun, G. M. and Rutenberg, A. C. ORNL CF 53-4-81.
58. Yeatts, L. B. ORNL CF 53-2-174.
59. Morrison, B. H. ORNL CF 53-2-61.
60. McNees, R. A. ORNL CF 53-1-106.
61. Morrison, B. H. ORNL CF 53-3-85.
62. Friels, J. V. ORNL CF 52-11-199.
63. Huckel, W. "Structural Chemistry of Inorganic Compounds", (Trans. L. H. Long) Elserier Pub. Co., Inc., New York, (1950).
64. Pickering. J. Chem. Soc. (Lond.) 63, 909, (1893).
65. Compere, E. L. ORNL Y-B30-124.
66. Compere, E. L. ORNL CF 53-1-298.
67. Compere, E. L. ORNL CF 53-2-174.
68. Healy, R. M. ORNL Y-B30-124.
69. Healy, R. M. ORNL Y-B30-118.
70. Hill, W. E. ORNL CF 53-4-81.
71. Hill, W. E. ORNL CF 53-4-161.
72. Healy, R. M. ORNL CF 53-1-298.
73. Healy, R. M. ORNL CF 53-4-81.
74. Mellor, J. W. "Comprehensive Treatise on Inorganic and Theoretical Chemistry", Longmans, Green and Co., New York, (1922-1937).
75. Barringer, M. D. ORNL CF 53-2-61.
76. Kobe and Leipper. Ind. and Eng. Chem. 32, 198, (1940).
77. Hafem, S. Bull. Soc. Chim. France, 1949, 337, (1949).
78. Lee, D. A. ORNL-1401.
79. Lee, D. A. ORNL CF 53-5-164.
80. Lee, D. A. ORNL Y-B30-124.
81. Vogel, A. I. "Physical Properties and Chemical Constitution, Part IX, Aliphatic Hydrocarbons", J. Chem. Soc. 1946, 133, (1946).
82. Lee, D. A. ORNL Y-B30-124.
83. Lee, D. A. ORNL CF 53-4-161.
84. Sax, N. I. "Handbook of Dangerous Chemicals", Reinhold Pub. Corp., New York, (1951).
85. Lee, D. A. ORNL CF 53-2-174.
86. Hill, W. E. ORNL Y-B30-116.
87. Weeren, H. O. and Carter, W. L. ORNL CF 52-10-161.
88. Sales Bulletin, E. I. Dupont deNemours and Co.
89. Joseph, E. F. ORNL Y-B35-6.
90. Joseph, E. F. ORNL Y-B35-7.
91. Joseph, E. F. and Buchanan, J. R. ORNL Y-B35-9.
92. [redacted], Sachs, J. W., Decarlo, V. A. and Buchanan, [redacted]35-10.

[redacted]

93. Lynch, L. D. ORNL-1511.
94. Lynch, L. D. ORNL CF 53-5-123.
95. Morrison, B. H. ORNL CF 53-5-123.
96. Morrison, B. H. ORNL-1511.
97. Yeatts, L. B. ORNL CF 53-4-81.
98. Hill, W. E. ORNL CF 53-5-164.
99. Hill, W. E. ORNL CF 53-6-208.
100. Daley, F. L. and Sacks, J. W. ORNL Y-B35-6.
101. Lynch, L. D. ORNL CF 53-4-210.
102. Morrison, B. H. ORNL CF 53-4-210.
103. Yeatts, L. B. ORNL CF 53-5-164.
104. Johnston, C. P. ORNL CF 53-4-81.
105. Dowling, E. J. and Warren, K. S. ORNL CF 53-4-285.
106. Boyd, C. M. Anal. Div. ORNL CF 53-4-161.
107. Clark, W. E. ORNL-1524.
108. Fletcher, F. and Kilpatrick, M. J. Phys. Chem. 42, 113, (1938).
109. Garretson, H. H. ORNL-1299.
110. Lewis, G. N. and McDonald, R. T. "The Separation of Lithium Isotopes", J. Am. Chem. Soc. 58, 2519-24, (1936).
111. Begun, G. M. and Drury, J. S. A Review of Isotopic Separation to be Issued.
112. Johnston, R. J. and Ubbelohde, A. R. "Wedge Effect at Amalgam Electrolyte Surfaces", Proc. Roy. Soc. (London) A206, 275-86, (1951).
113. Bradley, N. C. ORNL Y-B35-6.
114. Spevack, J. S. Columbia Univ. Report A-393.
115. Eidenoff, M. L. "Laboratory Studies for Separation Processes", National Nuclear Energy Series III-4D (1951).
116. Demarcus, W. C. Y-12 Y-887.

[redacted]